





**A study of the role of glycogen in skeletal muscle  
performance and of myosin heavy chain isoform  
expression in amphibian skeletal muscle using the toad**



***Bufo marinus***

Submitted by

Long Thanh Nguyen, MD. (Vietnam), B. Sc. (Hon.)

**A thesis submitted in the total fulfilment of the requirements for the  
degree of  
Doctor of Philosophy**

Muscle Cell Biochemistry Laboratory, School of Life Sciences and Technology,

Footscray Campus, Victoria University of Technology.

GPO. BOX 14428 Melbourne City Mail Centre Victoria, 8001

**AUSTRALIA**

**January 2000**

FTS THESIS

573.754178 NGU

30001005559051

Nguyen. Long Thanh

A Study of the role of  
glycogen in skeletal muscle  
performance and of myosin

# Table of contents

Summary	ix
Declaration	xiv
Acknowledgements	xv
List of publications	xvii
List of abbreviations	xix
List of figures	xxii
List of tables	xxvi
<b>Chapter 1 General Introduction</b>	<b>1</b>
<b>1.1 Basic structure of a skeletal muscle cell</b>	<b>3</b>
1.1.1 Structure of the contractile apparatus	6
1.1.1.1 Structure of the thin filament	7
1.1.1.2 Structure of the thick filament	11
1.1.2 Myosin isoforms	13
1.1.2.1 Myosin heavy chain isoforms expressed in vertebrate skeletal muscles	14
1.1.2.2 Methods for myosin heavy chain isoform analysis	16
<i>(i) Qualitative detection of MHC isoforms by immunohistochemistry</i>	17
<i>(ii) Electrophoretic separation, post-electrophoresis staining and immunoblotting of MHC isoforms</i>	17
<i>(iii) MHC isoform-mRNA detection and measurement in single fibre fragments</i>	18
<b><i>IN SITU-HYBRIDISATION</i></b>	18

	<i>RT-PCR</i>	19
1.1.3	Sarcoplasmic reticulum (SR), transverse-tubular (T-tubular) system and triads	20
1.1.3.1	Structure of the sarcoplasmic reticulum	22
1.1.3.2	Structure of the T-tubular system	25
<b>1.2</b>	<b>Excitation-Contraction-Relaxation cycle</b>	<b>27</b>
1.2.1	Initiation and propagation of action potentials along the sarcolemma and T-system	28
1.2.2	E-C coupling and SR Ca <sup>2+</sup> release	29
1.2.3	Regulation of E-C coupling	31
<b>1.3</b>	<b>Glycogen and skeletal muscle</b>	<b>34</b>
1.3.1	Intracellular location of muscle glycogen	35
1.3.2	Structure of muscle glycogen	35
1.3.3	Muscle glycogen catabolism	39
1.3.4	Methods for determining glycogen contents in skeletal muscle fibres	43
1.3.4.1	Determination of glycogen content in muscle fibres by histochemical PAS-staining method	43
1.3.4.2	Determination of glycogen content in single fibres by the fluorometric method	44
<b>1.4</b>	<b>The aims of this study</b>	<b>47</b>

## **Chapter 2 Development of a rapid microfluorometric method for measuring subpicomole amounts of Glycogen, Glucose and NADPH**

<b>2.1</b>	<b>Introduction</b>	<b>49</b>
<b>2.2</b>	<b>Materials and Methods</b>	<b>51</b>

2.2.1	Chemicals	51
2.2.2	Construction of standard curves for commercial glycogen, glucose and NADPH	51
2.2.2.1	Setting up the microfluorometric system	52
	<i>Stability of the light source</i>	54
	<i>Uniformity of fluorescence in the illuminated sample</i>	54
	<i>Fluorescence intensity of the blank and linearity of the relationship between fluorescence intensity and the concentration of quinine sulfate in the sample</i>	56
2.2.2.2	Preparation of under-oil reagent droplets for microfluorometric determination of known amounts of NADPH, glucose and commercial glycogen	56
2.2.2.3	Transfer of fluid between droplets and from a droplet to the microcell	59
2.2.2.4	Construction of standard curves for commercial glycogen	64
	<i>Composition and stability of the AG reagent</i>	65
	<i>Composition and stability of the GLU reagent</i>	65
2.2.2.5	Construction of standard curves for glucose	67
2.2.2.6	Construction of standard curves for NADPH	68
2.2.3	Statistical analysis	68
<b>2.3</b>	<b>Results</b>	
2.3.1	Optimisation of reaction conditions for glycogen analysis	69
2.3.1.1	AG reaction (step 1)	69
	<i>AG concentration</i>	69
	<i>pH</i>	70
	<i>Time course</i>	70
2.3.1.2	HK/G6PDH reaction (step 2)	74

2.3.2	Construction of standard curves	74
2.3.2.1	Analytical range for NADPH determination	74
2.3.2.2	Analytical range for glucose and glycogen determination	76
2.3.2.3	Verification of the method for glycogen determination	77
<b>2.4</b>	<b>Discussion</b>	<b>82</b>

### **Chapter 3 Microfluorometric analyses of glycogen in freshly dissected, single skeletal muscle fibres of the cane toad using a mechanically skinned fibre preparation**

<b>3.1</b>	<b>Introduction</b>	<b>84</b>
<b>3.2</b>	<b>Materials and Methods</b>	<b>87</b>
3.2.1	Animals and Chemicals	87
3.2.1.1	Animals	87
3.2.1.2	Chemicals	87
3.2.2	Preparation of mechanically skinned single muscle fibre segments	88
3.2.2.1	Muscle dissection	88
	<i>Iliofibularis muscle</i>	91
	<i>Cruralis and sartorius muscles</i>	91
	<i>Pyriiformis muscle</i>	91
3.2.2.2	Muscle handling/storage prior to fibre isolation	93
3.2.2.3	Isolation of single fibre segments	93
3.2.2.4	Measurement of fibre segment dimensions	97
3.2.2.5	Mechanical removal of the plasma membrane (skinning) of fibre segments	98
3.2.3	Glycogen analysis in the mechanically skinned single muscle fibres	100

3.2.3.1	Preparation of under-oil droplets for glycogen analysis in mechanically skinned single fibre segments	101
3.2.3.2	The transfer of a skinned fibre segment from the muscle dissecting-dish to a reaction droplet	103
3.2.3.3	The transfer of a skinned fibre segment between two reagent droplets	104
3.2.3.4	Determination of non-glycogen fluorogenic material ( <b>NGlyc</b> )	105
3.2.3.5	Determination of washable glycogen ( <b>WGlyc</b> )	106
3.2.3.6	Determination of glycogen content in the washed fibre segment ( <b>NWGlyc</b> )	107
3.2.4	Calculations and statistical analyses	108
<b>3.3</b>	<b>Results</b>	
3.3.1	Intracellular pools of fluorogenic material in single muscle fibres	110
3.3.2	Time course of enzymatic reactions in the analytical protocol for glycogen determination	112
3.3.3	Stability of fluorogenic material in toad skeletal muscle	114
3.3.4	Total glycogen content in single fibres from IF, PYR, CRU and SAR muscles of the cane toad	116
<b>3.4</b>	<b>Discussion</b>	122
	<i>The muscle fibre preparation and intracellular pools of fluorogenic material</i>	122
	<i>Inter-fibre and inter-muscle variability of glycogen in the cane toad</i>	125
	<i>Glycogen stability in the toad muscle</i>	126
	<i>The analytical method</i>	127

**Chapter 4 Correlation between glycogen content and responsiveness to Na-depolarisation of mechanically skinned muscle fibres of the cane toad *Bufo marinus***

<b>4.1</b>	<b>Introduction</b>	128
<b>4.2</b>	<b>Materials and Methods</b>	130
4.2.1	Animals	130
4.2.2	The mechanically skinned fibre preparation	130
4.2.3	T-system depolarisation experiments	131
4.2.4	Glycogen analysis	135
4.2.4.1	Glycogen determination in control segments	135
4.2.4.2	Glycogen analysis in fibres mounted in the force recording apparatus	136
4.2.5	Analysis of muscle proteins by sodium dodecyl sulfate-polyacrylamide gel electrophoresis (SDS-PAGE)	136
4.2.6	Data presentation and statistical analyses	139
<b>4.3</b>	<b>Results</b>	
4.3.1	Glycogen stability in mechanically skinned muscle fibre preparation	140
4.3.2	Correlation between fibre responsiveness to T-system depolarisation and glycogen content	147
4.3.3	Protein profile of fibre segments and wash-out/incubation solutions	152
<b>4.4</b>	<b>Discussion</b>	156

**Chapter 5 An electrophoretic study of myosin heavy chain  
expression in skeletal muscles and in single muscle fibres  
of the toad *Bufo marinus***

<b>5.1</b>	<b>Introduction</b>	162
<b>5.2</b>	<b>Materials and Methods</b>	166
5.2.1	Chemicals	166
5.2.2	Animals and muscles	166
5.2.3	Preparation of muscle homogenates and myosin extracts	169
5.2.3.1	Preparation of muscle homogenates	169
5.2.3.2	Preparation of myosin extracts	170
5.2.4	Protein determination in muscle homogenate and myosin extracts	171
5.2.5	Preparation of single muscle fibre segments for electrophoretic analysis of MHC composition	171
5.2.6	Analysis of MHC isoforms by ALANINE-SDS-PAGE	172
5.2.6.1	Sample preparation	172
5.2.6.2	Preparation of ALANINE-SDS-polyacrylamide gel	172
	<i>The separating gel</i>	172
	<i>The stacking gel</i>	173
	<i>The running buffer</i>	174
5.2.7	Data presentation and statistical analyses	175
<b>5.3</b>	<b>Results</b>	
5.3.1	Development of a SDS-PAGE system for separating myosin isoforms in toad skeletal muscle	176
5.3.1.1	Replacement of Glycine with Alanine in SDS-PAGE	176
5.3.1.2	Optimisation of the ALANINE-SDS-PAGE system	182

5.3.1.3	MHC isoform bands detected in myosin extracts of IF, PYR, CRU and SAR muscles are similar to the high molecular weight protein bands detected in whole muscle homogenates	187
5.3.1.4	Identification of the MHC isoforms expressed in IF, PYR, CRU and SAR muscles of the toad <i>Bufo marinus</i>	189
5.3.2	Developmental changes in the MHC composition of IF, PYR, CRU and SAR of the toad <i>Bufo marinus</i>	195
5.3.3	MHC isoform composition of single muscle fibre segments isolated from <i>Rectus abdominis</i>	198
<b>5.4</b>	<b>Discussion</b>	204
5.4.1	<i>Separation of MHC isoforms in toad skeletal muscles by a novel ALANINE-SDS-PAGE method</i>	204
5.4.2	<i>Identification of MHC isoforms expressed in IF, PYR, CRU and SAR muscles</i>	205
5.4.3	<i>Developmental changes in the MHC composition of IF, PYR, CRU and SAR muscles</i>	207
5.4.4	<i>MHC isoform composition of single muscle fibre segments</i>	208
	<b>Concluding remarks</b>	211
	<b>Bibliography</b>	213

## Summary

The overall aim of this study was to contribute knowledge to two areas of inquiry in muscle research: one concerned with the molecular mechanism(s) underlying the positive correlation between intracellular glycogen content and skeletal muscle performance and the other with the MHC isoform composition in amphibian skeletal muscle and single muscle fibres. To achieve this aim it was important to develop a rapid and reproducible microfluorometric method for glycogen determination in segments of freshly dissected, single muscle fibres, and a SDS-PAGE method that allows effective separation and visualisation of MHC isoforms in amphibian skeletal muscle preparations. The organism used throughout this study was the cane toad *Bufo marinus*. The information generated in the present work can be summarised as follows:

(1) The microfluorometric glycogen assay developed in this study is based on the enzymatic breakdown of glycogen by *amyloglucosidase* (AG) and the stoichiometric production of NADPH in two coupled reactions catalysed by *hexokinase* (HK) and *glucose-6-phosphate dehydrogenase* (G6PDH). Several parameters were evaluated and optimised with respect to glycogen determination in solutions of commercial (rabbit liver) glycogen and in single muscle fibre segments. These parameters include: (i) the concentration of AG, (ii) the time course of the AG reaction with commercial glycogen or with glycogen associated with mechanically skinned fibre preparations, (iii) the time course of the coupled reactions catalysed by HK/G6PDH, and (iv) the effect of the washing buffer and time of washing of a skinned fibre

segment on the relative proportion of various glycogen and non-glycogen pools of fluorogenic material. The method described in this study is able to detect subpicomole amounts of glycogen (as glucosyl units), glucose, NADH and NADPH with a detection limit of 0.16-0.17 pmol in a 25 nl sample.

(2) The microfluorometric method developed in the study was used to examine the range of glycogen concentrations in single fibres from iliofibularis (IF), pyriformis (PYR), cruralis (CRU) and sartorius (SAR) muscles of adult toads and the stability of fibre glycogen when the muscle from which they were dissected was stored at different temperatures. Prior to the AG step, mechanically skinned fibre segments were washed to remove the non-glycogen fluorogenic material. The ranges of glycogen concentrations (mmol glucosyl units/l fibre volume) found in toad skeletal muscle fibres were 25.8-369.0 (IF,  $n = 129$ ), 33.7-194.5 (PYR,  $n = 36$ ), 46.1-383.5 (CRU,  $n = 36$ ) and 45.1-367.2 (SAR,  $n = 36$ ). The glycogen content appeared to vary markedly not only between fibres originating from different muscles of the same type, but also between individual fibres dissected from the same muscle. Substantial differences in glycogen content were also found between single IF muscle fibres originating from toads collected in different seasons. Interestingly, the total amount of glycogen in single muscle fibres of the toad did not decrease significantly when the tissue was stored under oil at 19-25°C for up to 6 hrs or at 4°C for up to 24 hrs. This is indicative of a relatively high stability of amphibian muscle glycogen.

(3) The use of freshly dissected, mechanically skinned muscle fibres for glycogen determination allowed the separation of two intracellular glycogen pools: the first, amounting to 15-26% of fibre glycogen, was washed within 5 min when the skinned

fibre segment was incubated in a washing solution (100 mM acetate buffer, pH 5.0-7.0 or 75 mM HDTA/KOH, pH 5.0-7.0), while the other, amounting to 74-85% of fibre glycogen, remained associated with the washed skinned fibre, even after 40 min exposure of the skinned fibre preparation to the aqueous environment. The retention of most glycogen in the fibre preparation after mechanical removal of the plasma membrane and extensive washing indicates that the largest proportion of glycogen in toad skeletal muscle fibres is tightly bound to intracellular structures.

(4) The glycogen pool associated with skinned muscle fibres was found to decrease gradually at a rate of  $0.59 \pm 0.20\% \text{ min}^{-1}$  in a relaxing solution ( $[\text{Ca}^{2+}] = 200\text{nM}$ ), at a considerably higher rate when the preparations were exposed to  $30\mu\text{M} [\text{Ca}^{2+}]$  ( $2.66 \pm 0.38\% \text{ min}^{-1}$ ) and even at a greater rate ( $> 40\% \text{ min}^{-1}$ ) in fibres undergoing contractions induced by T-system depolarisation. Since no glycogenolytic enzymes were added to the system, these data suggest that (i) the loss of fibre glycogen in the presence of added  $\text{Ca}^{2+}$ , or  $\text{Ca}^{2+}$  released from the SR, was caused by endogenous glycogenolytic processes and (ii) the mechanically skinned fibre preparation is well suited to study the regulation of endogenous glycogenolytic enzymes. Silver-stained SDS gels of components eluted into the relaxing solution from single skinned fibres revealed a rapid (2min) loss of parvalbumin (an endogenous  $\text{Ca}^{2+}$  binding protein) and at least 10 other proteins varying in molecular weight between 10 and 80kD, but there was essentially no loss of myosin heavy and light chains or of actin. Subsequent elution for a further 30 min in either relaxing or maximally  $\text{Ca}^{2+}$ -activating solution did not result in any further detectable loss of fibre protein.

(5) An important finding of this study was that depletion of fibre glycogen was associated with loss of fibre ability to respond to T-system depolarisation even though the bathing solutions contained high levels of ATP (8mM) and creatine phosphate (10mM). Furthermore, the capacity of a mechanically skinned fibre to respond to T-system depolarisation was highly positively correlated ( $P < 0.0001$ ) with initial fibre glycogen concentration. Taken together these results indicate that: (i) the capacity of skeletal muscle to respond to T-system depolarisation is related (directly or indirectly) to the non-washable glycogen pool in fibres and (ii) this relationship holds for conditions where glycogen is not required as a source of energy.

(6) Several modifications were made to the Laemmli SDS-PAGE system to achieve the separation of the four myosin heavy chain (MHC) isoform bands that were expected to be found in muscle preparations from the cane toad. These modifications included: (i) replacement of glycine with alanine in the running buffer, (ii) inclusion of alanine in the separating gel and (iii) the use of glycerol in the separating gel. The four MHC isoforms, namely BmHC1, BmHC2, BmHC3 and BmHCT, found to be expressed in all four muscle types examined (IF, PYR, CRU and SAR) were identified, based on the previously reported fibre type composition of IF and SAR muscles in the toad and of PYR muscle in the frog. The ALANINE-SDS electrophoretic method was used to examine changes in the MHC isoform composition of IF, PYR, CRU and SAR muscles with the ontogenetic growth of the toad from post-natal life (body weight  $< 1$  g) to late adulthood (body weight 200-450 g). The results show that the developmental changes in the MHC isoform composition of the toad IF muscle observed in this study are in very good agreement with those reported in the literature for the fibre type composition changes in the

developing IF muscle. When used to analyse the MHC isoform composition in a population of single fibres isolated from *Rectus abdominis* (RA) muscle of the cane toad, the ALANINE-SDS-PAGE method detected ten discrete groups of fibre types, some expressing only one MHC isoform, other co-expressing two or even three MHC isoforms.

## Declaration

This thesis contains no material which has been presented or accepted for the award of any other degree or diploma in this or any other university. Except where specifically indicated in the text, the data presented herein is the result of work of the author, and to the best of my knowledge and belief, has not been previously written or published by any other person.



Long Thanh Nguyen

## Acknowledgements

I would like to express my gratitude to my supervisor Associate Professor Gabriela M. M. Stephenson who enabled me to work in her laboratory and who provided me with endless patience, encouragement and support throughout this work. She has proved to me that she is not only a supervisor but also a friend and a teacher. Now and forever I owe her a special debt of thanks for her enthusiasm to help me to discover myself.

I would like to thank Professor G. D. Stephenson who guided me into the 'world of mechanically skinned, single muscle fibres' and who provided very crucial input into the study on the correlation between glycogen content and T-system depolarisation.

My special thanks go to Dr. Michael Patterson who was very kind to read and criticise the first draft of this thesis during his annual holidays.

I must also thank Professor J. Lawrence (University of Virginia, USA) who provided me with the opportunity to visit to his laboratory in Charlottesville (VA) and in St. Louis (MO).

I would like to thank Ms. Jill Manchester (former Lowry's laboratory, Dept of Molecular Pharmacology, Medicine School, Washington University at St. Louis, MO, USA) who taught me the oil-well technique, the method of ultrasensitive microanalysis and how to make a fishpole balance.

I should also like to thank a number of people who have supported me directly or indirectly throughout my studies: Associate Professor G. J. Hamilton who always encouraged me to 'hang on there' until the day I submitted my thesis, Ian Sullivan for supplying me with chemicals at the right time, Min Nguyen for provided much needed laboratory glassware supply, Craig Goodman for generously giving me many of his precious articles that proved to be very helpful for my literature review, Susan K. Bortolotto for her help in densitometry and very useful discussion about the gel's problems and *Dominica Trifilo* for her assistance in gel preparation.

Finally, I would like to send very special thanks to my mother, my brother, my sisters, my sister-in-law and my four nephews and nieces who are still living in Vietnam, for their much needed support financially and spiritually in the past four years. Without their encouragement and support, I do not think I could have gone this far.

## List of publications

**LONG THANH NGUYEN & GABRIELA M. M. STEPHENSON** (1999) An electrophoretic study of myosin heavy chain expression in skeletal muscles of the toad *Bufo marinus*. *J. Muscle. Res. Cell. Motility*. **20**(7), 687-95.

**STEPHENSON, D. G., NGUYEN, L. T., STEPHENSON, G. M. M.** (1999) Glycogen content and excitation-contraction coupling in mechanically skinned muscle fibres of the cane toad. *J. Physiol.* **519**(1), 177-87.

**NGUYEN, L. T., STEPHENSON, D. G., STEPHENSON, G. M. M.** (1998) A direct microfluorometric method for measuring subpicomole amounts of Nicotinamide Adenine Dinucleotide Phosphate, Glucose and Glycogen. *Anal. Biochem.* **259**, 274-8.

**NGUYEN, L. T., STEPHENSON, D. G., STEPHENSON, G. M. M.** (1998) Microfluorometric analyses of glycogen in freshly dissected, single skeletal muscle fibres of the cane toad using a mechanically skinned fibre preparation. *J. Muscle. Res. Cell. Motility*. **19**, 631-38.

**NGUYEN, L. T., STEPHENSON, D. G., STEPHENSON, G. M. M.** (1997) Correlation between the ability to respond to T-system depolarisation and the glycogen content of mechanically skinned fibres of the cane toad. *J. Physiol.* **505**.P, 89P.

**NGUYEN, L. T., STEPHENSON, G. M. M.** (1997) Electrophoretic analyses of myosin heavy chain expression in skeletal muscle of the cane toad *Bufo marinus*. *Australian Electrophoresis Society* 4<sup>th</sup> annual conference. Melbourne, Victoria, Australia.

**NGUYEN, L. T., STEPHENSON, G. M. M. (1997)** Myosin heavy chain expression and glycogen content in single skeletal muscle fibres of the cane toad. *Proc. Australian Soc. Biochem. Mol. Biol.* **29**, P. B1-53.

**NGUYEN, L. T., STEPHENSON, G. M. M. (1996)** A novel microfluorometric method for glycogen determination in mechanically skinned skeletal muscle fibres. *Proc. Australian Physiol. Pharmacol. Soc.* **27**(2), 161P.

## List of abbreviations

ADP	Adenosine Diphosphate
AG	<i>amyl<math>\alpha</math>-1,4-<math>\alpha</math>-1,6-glucosidase</i>
AT	Anterior tibialis
ATP	Adenosine Triphosphate
<i>Bis</i>	<i>N,N'</i> -methylene bisacrylamide
BSA	Bovine Serum Albumin
Ca <sup>2+</sup>	Calcium ion
CP	Creatine phosphate
CRU	Cruralis muscle
DHPR	Dihydropyridine receptor (or L-type Ca <sup>2+</sup> channel)
Dry wt	Dry weight
DTT	Dithiothreitol
E-C	Excitation-Contraction
E-C-R	Excitation-Contraction-Relaxation
EDL	Extensor digitorum longus muscle
EGTA	Ethyleneglycol[bis( $\beta$ -aminoethyl ether)]- <i>N,N,N',N'</i> -tetraacetic acid
EM	Electron micrograph
G-6-P	Glucose-6-phosphate
G6PDH	<i>Glucose-6-phosphate dehydrogenase</i>
HDTA	Hexamethalenediamine <i>N,N,N',N'</i> -tetraacetic acid
HEPES	<i>N</i> -(2-Hydroxyethyl)piperazine- <i>N'</i> -(2-ethanesulfonic acid)
HK	<i>Hexokinase</i>
IF	Iliofibularis muscle

$K^+$	Potassium ion
$KH_2PO_4$	Potassium phosphate monobasic
$K_2HPO_4$	Potassium phosphate dibasic
KOH	Potassium hydroxide
MF	Myofibril
$Mg^{2+}$	Magnesium ion
$MgCl_2$	Magnesium chloride
MgO	Magnesium Oxide
MHC	Myosin heavy chain
MLC	Myosin light chain
$Na^+$	Sodium ion
NADH	Nicotine adenine dinucleotide (reduced form)
$NAD^+$	Nicotine adenine dinucleotide (oxidised form)
NADPH	Nicotine adenine dinucleotide phosphate (reduced form)
$NADP^+$	Nicotine adenine dinucleotide phosphate (oxidised form)
$NaN_3$	Sodium azide
NGlyc	Non-glycogen fluorogenic materials
NWGlyc	Non-washable glycogen
PAS	Periodic acid Schiff
Pi	Inorganic phosphate
PMSF	Phenylmethylsulfonyl fluoride
PYR	Pyrimiformis muscle
RA	Rectus abdominis muscle
RyR	Ryanodine receptor

RT	Room temperature (19-25°C)
SAR	Sartorius muscle
SOL	Soleus muscle
SDS-PAGE	Sodium dodecyl sulphate polyacrylamide gel electrophoresis
SR	Sarcoplasmic reticulum
TC	Terminal cisternae
TCA	Trichloric acid
TEMED	<i>N,N,N',N''</i> -tetramethylethylenediamine
TFluo	Total fluorogenic material present in a single fibre segment
Tris	Tris(hydroxymethyl)methylamine
T-system	Transverse tubular system
VO <sub>2</sub> max	Maximum rate of oxygen uptake
Wet wt	Wet weight
WGlyc	Washable glycogen
WFluo	Washable fluorogenic material

## List of figures

Figure No.	Figure title	Page
1.1A	Electron micrograph showing the basic structure of an amphibian skeletal muscle cell	4
1.1B	Schematic diagram showing the change in the relative position of thick and thin filaments at rest and during contraction	8
1.2	Schematic representation of the thin filament	10
1.3	Electron micrograph and schematic representations of the thick filament and myosin molecule	12
1.4	The triad as seen in a quick frozen, freeze-substituted and in a schematic representation	21
1.5	Schematic representation of proteins believed to participate in events that take place at the level of the triad	23
1.6	Diagrammatic representation of glycogen structure and an electron micrograph of a glycogen particle from rat skeletal muscle	37
1.7	Glycogenolytic and glycolytic pathways	41
2.1	Microfluorometric system used in this study	53
2.2	Brass frame custom-designed to hold 22 microcells	55
2.3	Arrangement of reagent droplets used for constructing glycogen standard curves	58
2.4	Strategy used to form reagent droplets under oil, on the bottom of the petri dish	60
2.5	Strategy used to withdraw solution from a reagent droplet located on the bottom of a petri dish, under a layer of oil	62
2.6	Sample transfer, by capillarity, from the microtip into the microcell	63
2.7	The relationship between the concentration of AG and the	

	intensity of fluorescence signals	71
2.8	The relationship between the intensity of fluorescence signals and the pH of step-1 reaction solution	72
2.9	The time course of the AG reaction with commercial glycogen as substrate	73
2.10	The time course of the HK/G6PDH reactions (step 2)	75
2.11A	The standard calibration curve for NADPH	78
2.11B	Comparison of the fluorescence signals produced by a series of equivalent amounts of glycogen and glucose	79
2.11C	Comparison of the fluorescence signals produced by a series of equivalent amounts of glucose and NADPH	80
2.11D	The standard calibration curve for commercial glycogen	81
3.1A	A dorsal view of frog muscles	89
3.1B	A ventral view of frog muscles	90
3.2	Dissection of the IF muscle of the cane toad	92
3.3	Procedure used to dissect, under oil, single fibres from skeletal muscle of the toad	95
3.4	Strategy used when skinning mechanically a single muscle fibre	99
3.5	Arrangement of reagent droplets used for glycogen analysis in mechanically skinned, single muscle fibres	102
3.6	The time course of endogenous fibre glycogen hydrolysis by exogenous AG	113
3.7	The effect of storage conditions on the total amount of endogenous fluorogenic material in single fibres from IF muscle	115
3.8	Histogram of total glycogen concentration values of mechanically skinned single fibres dissected from one each of IF, PYR, CRU and SAR muscles	117
3.9	Histogram of the total glycogen concentration values in 129 single	

	fibres from IF muscles	120
3.10	Comparison of glycogen concentrations in single muscle fibres obtained from winter and summer toads	121
4.1	The run-down of force responses induced by the depolarisation of the sealed T-system in a mechanically skinned muscle fibre segment	133
4.2	Fraction of total glycogen remaining in mechanically skinned fibres after exposure to a rigor solution containing 100 mM sodium acetate at pH 7.0	141
4.3	Time course of fibre glycogen loss from mechanically skinned fibre segments exposed to a relaxing or a maximally $\text{Ca}^{2+}$ -activating solution	143
4.4	Correlation between fibre capacity to respond to T-system depolarisation and initial glycogen concentration in the fibre	150
4.5	Electrophoretogram of muscle proteins from segments of single muscle fibres and from the solutions to which single fibre segments were exposed for various lengths of time	154
5.1	Electrophoretogram of whole tissue homogenates prepared from IF, PYR, CRU and SAR muscles of young adult cane toads and of a complete rat marker using a modified <b>Laemmli</b> gel protocol	177
5.2A	Electrophoretogram of whole tissue homogenates prepared from IF, PYR, CRU and SAR muscles of young adult cane toads and of a complete rat marker using a modified <b>Talmadge &amp; Roy</b> gel protocol	178
5.2B	Electrophoretogram of whole tissue homogenates prepared from cane toad IF and rat EDL muscles using Glycine-SDS-PAGE	179
5.2C	Electrophoretogram of whole tissue homogenates prepared from cane toad IF and rat EDL muscles using ALANINE-SDS-PAGE	181
5.3A	Electrophoretic profile of MHC isoforms in PYR muscle homogenate at different concentrations of alanine in the separating gel	183

5.3B	Electrophoretic profile of MHC isoforms in PYR muscle homogenate at different concentrations of alanine in the running buffer	185
5.3C	Electrophoretic profile of MHC isoforms in a PYR muscle homogenate at different concentration of glycerol in the separating gel	186
5.4	Alanine-SDS-PAGE analysis of adult toad IF, PYR, CRU and SAR: (A) muscle homogenates; (B) myosin extract	188
5.5A	Representative electrophoretic profile of MHC isoforms detected in SAR muscle homogenates from junior and old adult toads	191
5.5B	Representative electrophoretic profile of MHC isoforms detected in IF muscle homogenates from juvenile and young adult toads	192
5.5C	Representative electrophoretic profile of MHC isoforms detected in PYR muscle homogenate from young adult toads	194
5.6	Bar graph illustrating the relative proportion of MHC isoforms in IF, PYR, CRU and SAR muscle of the cane toads at different stages of ontogenetic growth	197
5.7	Representative electrophoretic profile of MHC isoforms detected in RA muscle homogenates from juvenile and old adult toads	200
5.8	Representative electrophoretic profile of MHC isoforms in 10 discrete populations found in 136 fibres of RA muscles	201
5.9	Electrophoretogram of MHC isoform composition expressed in t2+t3 hybrid fibres	202
5.10	Bar graph illustrating the relative proportion of 10 different fibre type populations classified based on MHC isoform composition	203

## List of tables

Table No.	Table title	Page
2.1	Composition of standard solutions in step 1	67
3.1	Effect of washing buffer and time of fibre washing on the relative proportion of different fluorescent pools	111
3.2	Ranges of glycogen concentration values measured in single fibres prepared from one each of IF, PYR, CRU and SAR muscles	119
4.1	Composition of solutions used in T-system depolarisation experiments	132
4.2	Recipe for preparing the separating gels in the Glycine-SDS-PAGE system used in analyses of low molecular weight muscle proteins	137
4.3	Recipe for preparing the stacking gels used in the Glycine-SDS-PAGE system	138
5.1	Age/size related classification and physical characteristics of the toads used in the study of MHC expression in IF, PYR, CRU and SAR muscles	167
5.2	Recipe for preparing the separating gels used in the Alanine-SDS-PAGE method	173
5.3	Recipe for preparing the stacking gels used in the Alanine-SDS-PAGE method	174
5.4	The MHC isoform composition of each fibre type group in a populations of RA muscle fibres	199

# CHAPTER 1

## General Introduction

Studies of amphibian muscle have allowed us to gain a better insight into the anatomical construction, molecular organisation and contractile function of skeletal muscle. For example, frog skeletal muscle was used as a model by Huxley and colleagues to develop the current theories of muscle contraction (for review see Huxley, 1974) and by Ebashi's laboratory and other groups for physiological investigations of  $\text{Ca}^{2+}$  release (for review see Ogawa *et al.*, 1999).

Skeletal muscle is classified as a type of striated muscle because, when the tissue is examined under a microscope, alternating light and dark band-like structures (striations) are observed. As suggested by the name, skeletal muscles are attached primarily to bones and move parts of the skeleton; however, in some cases, a skeletal muscle can be found to be attached to the skin, to other muscles, or to *deep fascia* i.e. to a sheet of connective tissue wrapped around the muscle to hold it in place.

Regardless whether originating from an amphibian or mammalian organism, skeletal muscles are built up from numerous elongated, multinucleated, cylindrical cells, *skeletal muscle cells/fibres*, which can be viewed microscopically when the tissue is teased apart. Skeletal muscles are referred to as *voluntary* muscles as they can be caused to contract or relax by conscious control (Tortora & Anagnostakos, 1990).

The major function of skeletal muscles is to generate movement and force in a specific direction at the expense of metabolic energy. This function is reflected in their highly ordered structure, from macro-anatomical construction down to molecular organisation (Craig, 1994). Skeletal muscle (both amphibian and mammalian) is an extremely heterogenous tissue comprising a variety of different fibre types which can be distinguished based on structural, metabolic and contractile characteristics. For example, data produced by a number of studies on mammalian muscles indicate that there is a great variation in glycogen content among different fibres types (Brown, 1994). Thus, it is the complex combination of individual fibres that ultimately determines the properties of the whole muscle.

Not only is skeletal muscle a heterogenous tissue, but each muscle appears to be unique with regard to its fibre type composition (for review see Pette *et al.*, 1999). For example, it has been reported that amphibian skeletal muscle contains at least four different fibre types (Lutz *et al.*, 1998b; Hoh *et al.*, 1994) and that the relative proportion of these fibre types varies between jumping and non-jumping hindlimb muscles (Lutz *et al.*, 1998a). Based on the high degree of heterogeneity of skeletal muscle tissue, it is now widely accepted that studies using whole muscle preparations provide limited information on the metabolic and contractile characteristics of skeletal muscle fibres and that details of molecular events underlying muscle contractility can be obtained only from single fibre analyses.

## 1.1 BASIC STRUCTURE OF A SKELETAL MUSCLE CELL

Skeletal muscle fibres lie parallel to one another and, in small- to medium-sized mammals, range typically from 10 to 100  $\mu\text{m}$  in diameter and up to several centimetres in length (Bagshaw, 1993).

Each muscle fibre is enveloped by a membrane called the *sarcolemma* (Fig. 1.1A), which surrounds the intracellular fluid or cytoplasm, also referred to as the *sarcoplasm*, and the contractile apparatus. In mature skeletal muscles, there are no gap junctions or tight junctions (and therefore no electrical communication) between individual fibres. The plasma membrane of a myocell contains ion pumps, such as the  $\text{Na}^+/\text{K}^+$ -pump ( $\text{Na}^+$ ,  $\text{K}^+$ -ATPase), that maintain ionic gradients across the cellular membrane by actively transporting ions in both directions. The density of the  $\text{Na}^+$ ,  $\text{K}^+$ -pumps was found to vary between 1000 to 3500 per  $\mu\text{m}^2$  (Clausen, 1996). The sarcolemma is in continuation with another major membrane compartment of the muscle cell, the transverse tubular system (T-system) and together, the sarcolemma and the T-system facilitate the transmission of a stimulus as a wave of depolarisation, from the surface of the fibre, inwards, into the muscle cell (Despopoulos and Silbernagl, 1991; see also section 1.2.1 for details).



**Figure 1.1A** Electron micrograph showing the basic structure of an amphibian skeletal muscle cell (slightly modified from Tortora & Anagnostakos, 1990). Note that  $\text{Na}^+/\text{K}^+$  pumps are also present in the T-tubular system. MF: myofibril.

In some fibres, the wave of depolarisation is an all-or-nothing event, triggered by a stimulus higher than a certain level (called *threshold*), that propagates without decrement along the entire length of the fibre (action potential). Fibres that respond to a stimulus with an action potential produce a brief contraction, a *twitch*, and hence they are referred to as *twitch* fibres. In each twitch fibre, usually only one *motor end plate* (the neuromuscular junction between the motor neuron and the muscle fibre) innervates the sarcolemma from a large motor neuron axon, where the action potential is triggered. (Luff & Proske, 1976; Birks *et al.*, 1960; Hess, 1960; Gray, 1957).

In other muscle fibres, the wave of depolarisation is graded depending on the intensity of the stimulus and propagates with decrement over short distances. Such fibres, known as *slow/tonic fibres* (see Hess, 1970 for review), are found particularly in amphibia, reptiles and also in a very limited number of mammalian muscles (extraocular and tensor tympani muscles). In these fibres, nerve terminal contacts are distributed all over the muscle fibre membrane with a 'grape-cluster' appearance ('en grappe' or grape-like ending) (Luff & Proske, 1976; Birks *et al.*, 1960; Hess, 1960; Gray, 1957; Kuffler & Vaughan Williams, 1953; Kuffler & Gerard, 1947; Tasaki & Mizutani, 1944). In contrast to the twitch fibres, these fibres produce a graded contractile response.

As will be described in section 1.2, the contractile activity of a muscle cell involves the complex communication between a number of intracellular compartments which include: the contractile apparatus, consisting of thin and thick filaments, the intracellular store of the contraction activator  $\text{Ca}^{2+}$  (the *sarcoplasmic reticulum*; *SR*),

the T-system and the sarcolemma. The structure and function of these compartments is described in the next sections.

### 1.1.1 STRUCTURE OF THE CONTRACTILE APPARATUS

Within the muscle fibre, there are packed numerous highly organised protein structures, running parallel to the fibre axis, the *myofibrils* (see Fig. 1.1A), which occupy up to 80% of the myofibre volume and are responsible for muscle contraction (Craig, 1994). Mitochondria and glycogen granules are sandwiched between the myofibrils. Myofibrils, about 1 to 3  $\mu\text{m}$  in diameter, ranging in number from several hundred to several thousand, are organised in register, thus producing a striated appearance in the fibre as a whole (Tortora & Anagnostakos, 1990). Molecular examination of the cross section of a myofibril reveals two kinds of interacting protein filaments: thick and thin filaments. The thick filaments have diameters of about 15 nm, whereas the thin filaments have diameters of about 8 nm (Craig, 1994). Each thin filament has three neighbouring thick filaments and each thick filament is encircled by six thin filaments.

The striation pattern of the myofibrils is repeated with a periodicity of about 2 – 3  $\mu\text{m}$ . The repeating unit, known as *sarcomere*, is regarded as the fundamental contractile unit of a striated muscle (Craig, 1994; Rüegg, 1992). As shown in Fig. 1.1A, sarcomeres are separated from one another by narrow zones ( $\sim 0.1 \mu\text{m}$ ) of dense material called *Z lines disks*. Each Z line bisects a light band (*I band*; isotropic in polarised light),  $\sim 1 \mu\text{m}$  long, which is shared between adjacent sarcomeres. At the

centre of the sarcomere, there is a dark band (*A band*, *anisotropic* in polarised light), about 1.6  $\mu\text{m}$ -long, representing the length of the thick filament. The A band itself is bisected by a less dense *H zone*. In the middle of the A band there is a still lighter region often called the *H zone* (Fig. 1.1B), and this contains a region of higher density called the *M line* (Fig. 1.1B), a series of fine fibres that appears to connect the middle parts of adjacent thick myofilaments. The I band consists of *thin filaments* only, whereas only *thick filaments* are found in the H zone of the A band (see also Fig. 1.1B). Also shown in Fig. 1.1B, the sides of the A band appear darker because of the overlapping of thick and thin myofilaments. The length of the sarcomere (i.e. the distance between two adjacent Z lines) depends on the extent of filament overlapping, which in turn depends on the degree of contraction.

The thin filaments contain *actin*, *tropomyosin* and the *troponin complex* while the thick filaments are composed primarily of *myosin*. Actin and myosin together account for more than 70% of myofibrillar protein, where 20% is actin and 54% is myosin (Craig, 1994).

#### 1.1.1.1 STRUCTURE OF THE THIN FILAMENT

In vertebrate striated muscles, thin filaments run from the Z line to the edge of the H zone (Fig. 1.1A & B). There is evidence to suggest that thin filaments are joined together by the protein  *$\alpha$ -actinin*, which was found to be a major component of the Z line (Craig, 1994).

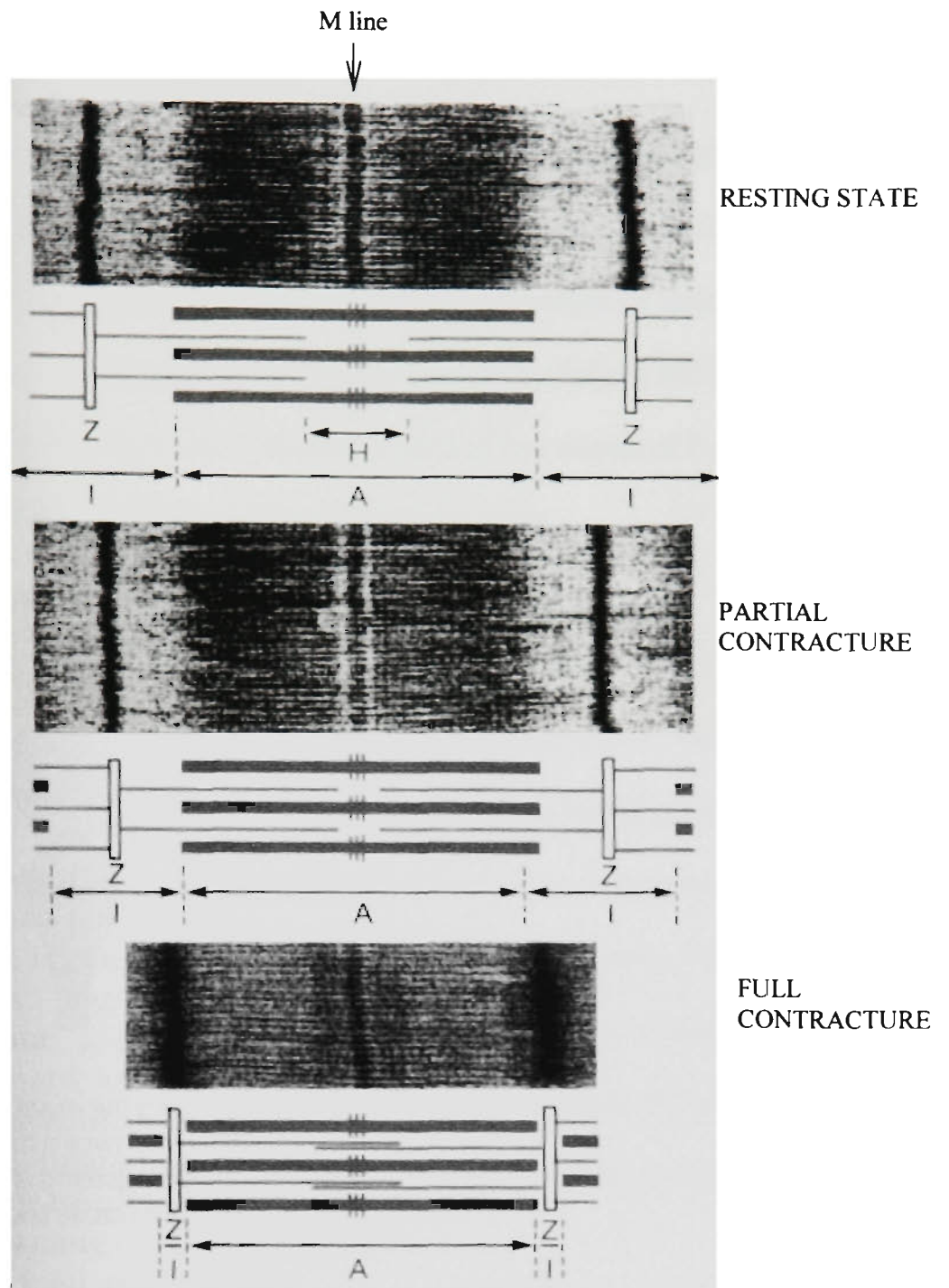


**Figure 1.1B** Schematic diagram showing the change in the relative position of thick and thin filaments at rest and during contraction (reproduced from Voet *et al.*, 1999).

Z: Z line; I: I band; A: A band; H: H zone.

The thin filament is composed mostly of *G-actin*, a globular protein with a molecular weight of about 42 kDa. Each G-actin molecule contains a *myosin-binding site* that interacts with a specific site on the myosin molecule. In vertebrate skeletal muscle cells, actin exists in a polymeric form (F-actin) composed of about 360 G-actin molecules per strand. The F-actin filament consists of two strands of F-actin that entwine to form a helical structure (Fig. 1.2) (Craig, 1994).

The thin filament contains also other protein molecules, such as *Tropomyosin* and *Troponin*, that are involved in the regulation of muscle contraction. Tropomyosin is a long, two-stranded  $\alpha$ -helical molecule, which follows the helical grooves formed by actin. Troponin is located at regular intervals on the surface of tropomyosin and is made up of three subunits: *Troponin T*, which binds to tropomyosin, *Troponin I*, which binds to actin and *Troponin C*, the putative calcium sensor which binds  $\text{Ca}^{2+}$  ions. Together, tropomyosin and troponin (referred to as the *tropomyosin-troponin complex*) act as inhibitors of actin-myosin interaction in a resting muscle (Stryer, 1995; Craig, 1994).

In addition to actin and the *tropomyosin-troponin complex*, the thin filament contains the myofibrillar protein *nebulin* and certain glycolytic enzymes, which may be bound to the filaments in vivo (Craig, 1994).

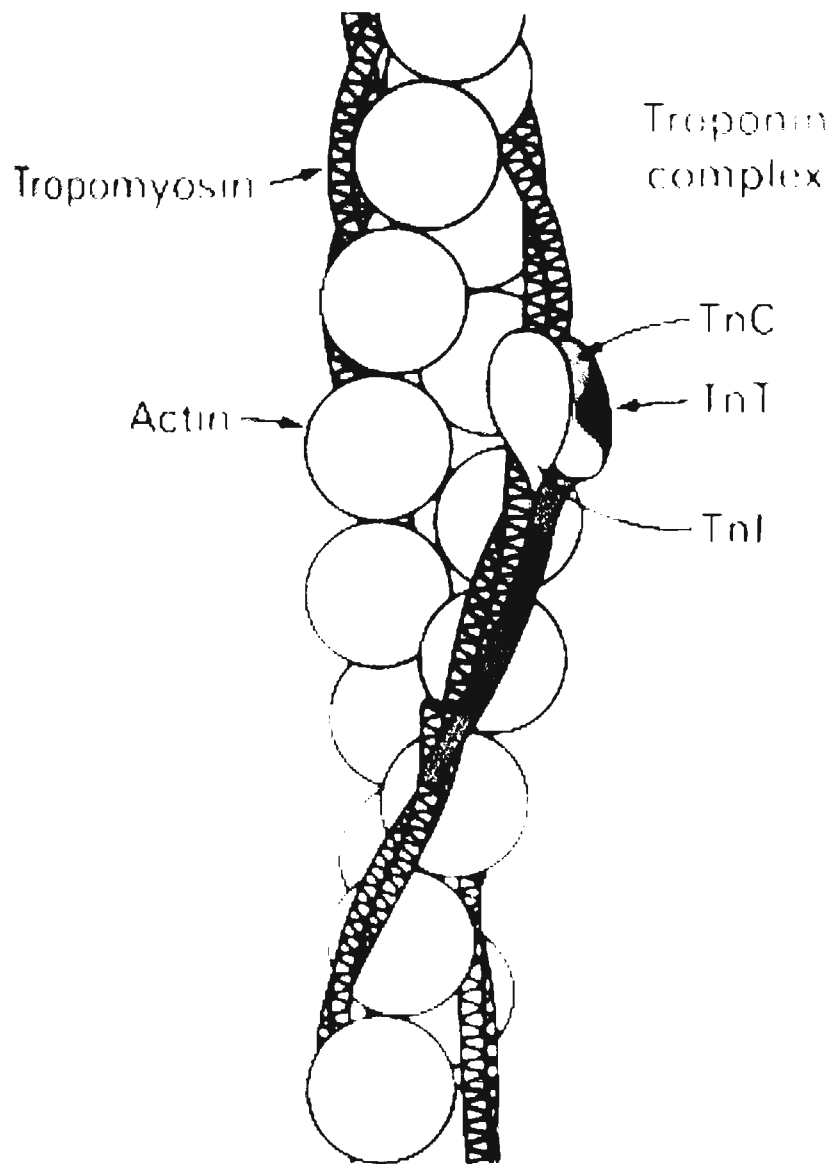


**Figure 1.2** Schematic representation of the thin filament (reproduced from Stryer, 1995).

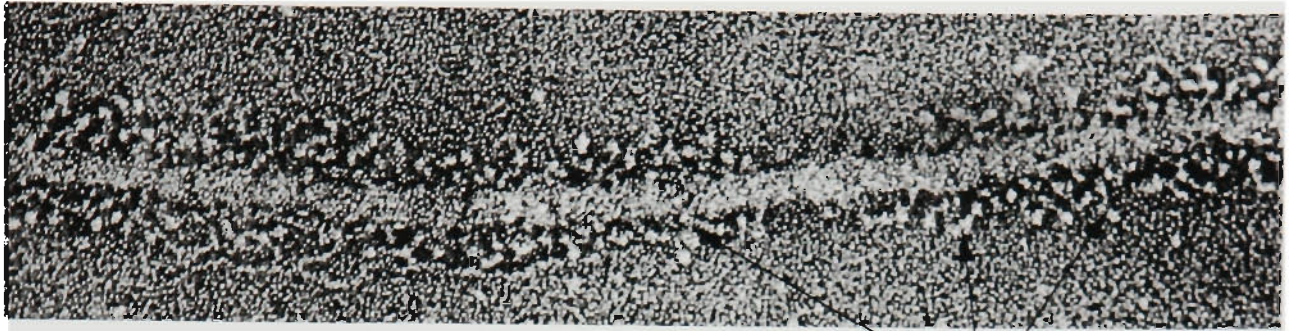
TnC: Troponin C; TnT: Troponin T; TnI: Troponin I.

### 1.1.1.2 STRUCTURE OF THE THICK FILAMENT

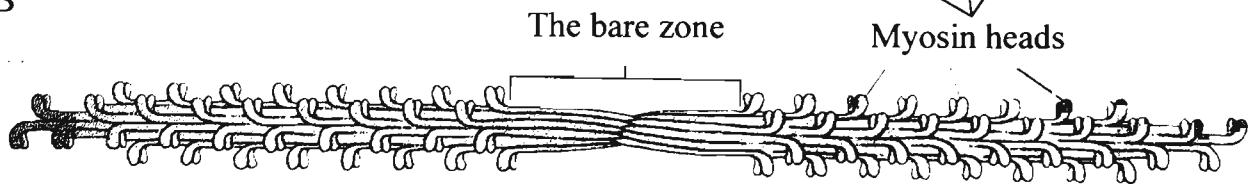
When dissociated from the muscle by high ionic strength (0.5 M KCl) extraction, the thick filament has a length of about 1.5  $\mu\text{m}$  (Bagshaw, 1993). Thick myofilaments are composed chiefly of *myosin*, a multi-subunit protein that consists of six polypeptide chains: two heavy chains (MHCs; MW approximately 220 kDa) and two pairs of different light chains (MLCs), the so called *essential* light chains (ELC; MLC1 and MLC3) and *regulatory* light chains (RLC, MLC2). The MLCs vary in size between 15 and 22 kDa depending on their source. As shown in Fig. 1.3C, a myosin molecule appears in electron micrographs as a fibrous entity with a tail and two globular heads. The tails of individual myosin molecules are arranged in parallel to each other, forming the shaft of the thick myofilament, while the heads of the myosin molecules project outward from and are arranged spirally on the surface of the shaft (see panels A and B in Fig. 1.3). The myosin projecting head contains an *actin-binding site* and an *ATP binding site* and is referred to as a *cross-bridge*.

In addition to myosin, the thick filaments of vertebrate striated muscle contain small quantities of non-myosin proteins. These include C protein, H protein and X protein, which are present in the middle third of each half of the thick filaments, AMP deaminase located at the tips of the filaments and myomesin, M protein and creatine kinase, located in the M line. The thick filaments are also associated along their length with the giant protein *titin*, which extends through the I band as far as the Z line (Craig, 1994).

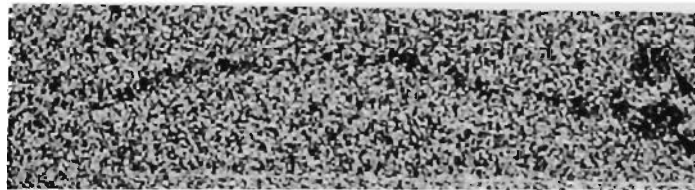
A



B



C



D

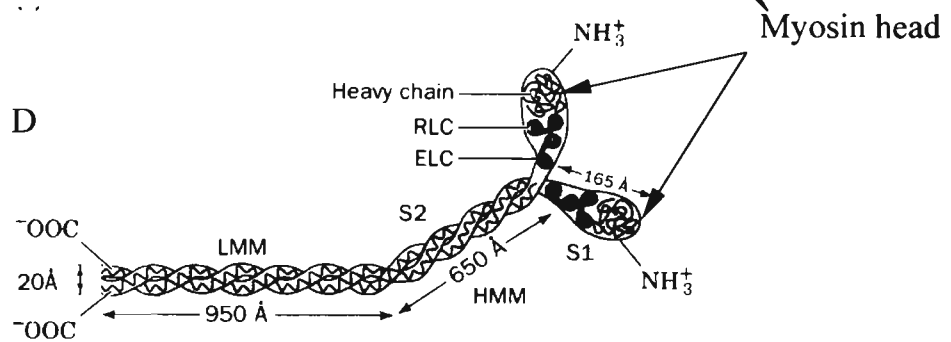


**Figure 1.3 Electron micrograph (EM) and schematic representations of the thick filament and myosin molecule** (reproduced from Voet & Voet, 1995).

(A) EM of the thick filament, (B) schematic representation of the thick filament (C) EM of a myosin molecule (D) schematic diagram of the myosin molecule. RLC: regulatory light chain (MLC2), ELC: essential light chain (MLC1 or MLC3). HMM: heavy meromyosin; LMM: light meromyosin. HMM and LMM are myosin fragments generated by limited trypsin digestion of the myosin molecule.

### 1.1.2 MYOSIN ISOFORMS

Thick filaments comprise about 300 myosin molecules, each having a molecular weight about 520 kDa. It is now well established that each of the protein subunits making up a myosin molecule (MHC, MLC1, MLC2 and/or MLC3) exists in multiple molecular forms (isoforms), which are expressed in a fibre-type specific manner. Many other muscle proteins have been found to exist as isoforms (including some protein components of the sarcotubular system), but the complexity of myosin isoforms is apparently much greater than that of other components of a muscle fibre (Schiaffino & Salviati, 1998).

MHC isoform composition is rapidly becoming the parameter of choice for distinguishing between skeletal muscle fibre types. Furthermore, there is increasing evidence that molecular differences between MHC isoforms are related to fibre differences in parameters of contractile performance, such as maximum shortening velocity and ATPase activity. The study of MHC isoforms is thus essential in gaining a better understanding of skeletal muscle heterogeneity and of the molecular basis of muscle contractility (Schiaffino & Reggiani, 1996; Moss *et al.*, 1995; Pette & Staron, 1990).

### 1.1.2.1 MYOSIN HEAVY CHAIN ISOFORMS EXPRESSED IN VERTEBRATE SKELETAL MUSCLES

An early study of Bárány (1967) indicated indirectly that skeletal muscles contain only two MHC isoforms-fast and slow. From 1967 to the present time, as many as ten MHC isoforms, all belonging to the so called *myosin gene II family*, have been found in myofibrils of mammalian striated muscles (Weiss & Leinwand, 1996; Moss *et al.*, 1995; Kelly & Rubinstein, 1994) and rat is probably the most widely used animal model in studies concerned with the physiological implications of MHC diversity in mammalian muscle (Moss *et al.*, 1995).

MHC isoforms are encoded by a highly conserved multigene family (Weiss & Leinwand, 1996; Moss *et al.*, 1995; Schiaffino & Reggiani, 1994 for review). All isoforms identified to date have been established at both protein and *mRNA* levels (Schiaffino & Salviati, 1998). Two of these isoforms, MHC $\alpha$  and MHC $\beta$ , were found in the cardiac muscle: MHC $\alpha$  is predominantly present in the atrial muscle of most mammals, while MHC $\beta$  is a major isoform of ventricle tissue in large mammals with low resting heart rates (Reiser & Kline, 1998). A third MHC isoform, the slow-tonic isoform is expressed only in certain intrafusal fibres and in extraocular and tensor tympani muscles, whereas the slow-twitch MHC isoform (MHC $\gamma$ ), which is identical to MHC $\beta$  of the cardiac muscle, is the major component of slow twitch muscles such as the soleus (SOL) muscle of the rat. Embryonic (MHC $\text{emb}$ ) and neonatal MHC isoforms (MHC $\text{neo}$ ) are found in a large proportion of developing muscle fibres and are also detected in the extraocular muscle of adult mammals (Kelly

& Rubinstein, 1994). In the 'super fast' extraocular and branchial muscle fibres (with the exception of human muscles) are expressed two MHC isoforms known as MHCIIeom and MHCIIIm. Finally, and most widely expressed in muscles throughout the body, are the three distinct fast-twitch isoforms: MHCIIa, MHCIIb and MHCIIId/x.

A fibre that expresses only one type of MHC isoform is referred to as a *pure fibre*, while a fibre that expresses more than one MHC isoform is known as a *hybrid fibre*. Based on analysis of MHC isoform composition in single fibres of mammalian skeletal muscles, Pette and Staron (1990) established a nomenclature system for pure fibres and for MHC isoforms. According to this system, type I fibres contain the MHCI isoform, type IIA fibres contain the MHCIIa isoform, type IIB fibres contain the MHCIIb isoform and type IID/X fibres contain the MHCIIId/x isoform. Pette and Staron's nomenclature (1990) has been used throughout this study when referring to rat muscles.

There is increasing evidence that in mammalian skeletal muscle MHC isoform expression and fibre type composition change in parallel with the maturation of animals, with variations in neural stimuli or hormonal activity and under conditions of mechanical stress (Schiaffino & Salviati, 1998; Pette & Staron, 1997; Moss *et al.*, 1995). The plasticity of a skeletal muscle has been used in a large number of studies concerned with the correlation between the contractile properties of a muscle fibre type and its MHC isoform phenotype.

As will be discussed at length in Chapter 5, in contrast to a wealth of available information on the MHC isoform expression in mammalian striated muscles, little is known to date about the MHC isoform composition of amphibian skeletal muscles. Our currently limited knowledge of MHC expression in amphibian muscle comes indirectly from studies of fibre types in frog and toad skeletal muscles ( Hoh *et al.*, 1994; Rowleson & Spurway, 1988; Lännergren & Hoh, 1984; Smith & Ovalle, 1973) and from the recently published data on MHC expression in skeletal muscles of the frog *Rana pipiens* (Lutz *et al.*, 1998 a&b). It is interesting to note that in one study concerned with contractile properties of single, amphibian muscle fibres, Edman *et al.* (1988) found that segmental differences in contractile properties along the length of single fibres isolated from the anterior tibialis (AT) muscle of *Rana temporaria* were accompanied by variations of MHC composition. This finding brings a new dimension to the story of the diversity of MHC expression in vertebrate skeletal muscle fibres and also confirms that there is a close association between MHC isoform composition and muscle contractility.

#### 1.1.2.2 METHODS FOR ANALYSIS OF MYOSIN HEAVY CHAIN ISOFORMS

Currently, MHC isoform analyses can be carried out by one or a combination of direct methods, such as (i) qualitative detection of MHC isoforms by immunohistochemistry (ii) electrophoretic separation, post-electrophoresis staining and immunological identification of MHC isoforms and (iii) MHC isoform-*mRNA* detection by *in situ* hybridisation and measurement of MHC isoform-*mRNA* in single fibre fragments by *RT-PCR*.

(i) *Qualitative detection of MHC isoforms by immunohistochemistry.* MHC isoform expression has been determined immunohistochemically, in whole muscles or single muscle fibres, by incubating serial transverse cryosections ( $\sim 10 \mu\text{m}$ ) of frozen muscle or single fibre preparations in immuno-reactive solutions, containing a panel of monoclonal MHC antibodies, at appropriate pH. For example, Lutz *et al.* (1998b) detected the MHC isoforms expressed in type 1, 2, 3 and tonic fibres in AT muscle of *Rana pipiens* using a combination of 4 antibodies raised against mammalian (rat) and avian (chicken) skeletal muscles.

Currently, immunohistochemistry is regarded as the best available morphological method for mapping the distribution of MHC isoforms within a certain cross-section of a given muscle and along the length of a single fibre (Schiaffino & Salviati, 1998). However, the method has major problems related to (1) the limited availability of specific antibodies against certain isoforms; (2) its inability to quantify MHC isoforms and to identify hybrid fibres, and (3) the cross-reactivity of antibodies.

(ii) *Electrophoretic separation, post-electrophoresis staining and immunoblotting of MHC isoforms.* Electrophoretic separation in polyacrylamide gels in the presence of sodium dodecyl sulphate (SDS) is currently one of the most common methods used for analysing proteins. The basic method (Laemmli, 1970) involves:

- degradation of the protein sample in a buffer containing SDS and the reducing agent  $\beta$ -mercaptoethanol
- preparation of a discontinuous gel system comprising two polyacrylamide gels (stacking gel and separating gel) of different porosity and pH

- applying the protein sample to be analysed on top of the stacking gel, under the running buffer
- running the sample in an electric field for a predetermined length of time
- fixing and staining the protein bands in the gel
- quantitative evaluation of the relative proportion of proteins in the mixture by scanning densitometry
- identification of protein bands by immunoblotting

Due to its low cost, its convenience, high sensitivity, ability to quantify relative proportion of proteins, and unique ability to distinguish hybrid fibres, electrophoretic analysis of MHC and other muscle protein isoforms has become the method of choice in biochemical studies of single muscle fibres. SDS-PAGE was used in generating some of the data in Chapter 4, and all data in Chapter 5.

*(iii) MHC isoform-mRNA detection and measurement in single fibre fragments*

Currently, MHC isoform-*mRNA* detection and quantification of MHC isoform-*mRNA* are carried out by *in situ-hybridisation* and *RT-PCR*, respectively.

*IN SITU-HYBRIDISATION.* The *in situ*-hybridisation assay involves the use of specific cRNA probes for unique regions of each MHC isoform-specific *mRNA*. These probes are prepared by cloning the sequences corresponding to the 5' and 3'

untranslated regions of the transcript, which are highly specific for each isoform even when the coding regions are highly homologous. (Schiaffino & Salviati, 1998). The prepared probes can be radioactive or non-radioactive, but non-radioactive probes are preferred because they allow the hybridisation transcripts to be detected by microphotometry and because they provide better resolution of *mRNA* locations in the intrafibre space (Pette *et al.*, 1999). *In situ*-hybridisation is carried out in several steps, which include:

- Fixation of a muscle cryosection in a mixture of 4% paraformaldehyde and phosphate-buffer saline (PBS) for 30 min; adequate fixation of the sample is required for the optimisation of visual resolution (Schiaffino & Salviati, 1998).
- Removal of paraformaldehyde from the sample by washing in PBS
- Exposure of sample to protease pre-treatment and acetylation
- Incubation of the muscle section with the labeled probe for hybridisation, followed by washing and visualisation of the probe (Schiaffino & Salviati, 1998).

*RT-PCR*. This method allows amplification of selected regions of MHC isoform-specific *mRNA* (for example, near the 3'-end of the gene). The method involves total *mRNA* isolation, reverse transcription (RT) using specific pairs of short oligonucleotide primers to generate cDNA, and amplification of this cDNA by polymerase chain reaction (PCR) (Schiaffino & Salviati, 1998). *RT-PCR* is a highly sensitive method, allowing the determination of MHC *mRNA* isoforms in freeze-dried dissected single fibre segments as small as 20 – 50 ng dry wt (Pette *et al.*, 1999).

Even though *RT-PCR* is a very powerful tool for detecting the distribution of MHC

*mRNA* isoforms in fibre segments, the method cannot measure precisely the amplification products because of variations known to occur both in the reverse transcriptase and polymerase chain reactions (Schiaffino & Salviati, 1998).

### 1.1.3 SARCOPLASMIC RETICULUM, TRANSVERSE-TUBULAR SYSTEM AND TRIADS

*Sarcoplasmic reticulum* is a collective term describing the network of membrane-enclosed, longitudinally lying tubules surrounding each myofibril. The SR, which is comparable to the smooth endoplasmic reticulum in a non-muscle cell, acts as the major store of calcium in skeletal muscle cells. Dilated endings of longitudinal SR containing  $\text{Ca}^{2+}$  and the low affinity  $\text{Ca}^{2+}$  binding protein *calsequestrin*, form ringlike tubes around the myofibrils. These blind-endings are known as *terminal cisternae* (TC). TCs are closely apposed to the *transverse tubular system*, which runs transversely through the fibre and perpendicularly to the SR.

The structure formed by a T tubule and two neighbouring TCs on either side, is known as a *triad* (Porter & Palade, 1957); the two facing membranes in a triad (i.e. the SR membrane and the T-tubule membrane) are separated by a junctional gap of 10-15 nm (see Fig. 1.4). The number of triads per sarcomere appears to be related to the speed of shortening of a fibre. For example, chicken fast-twitch muscle fibres contain up to eight triads per sarcomere, while in tonic fibres of frogs only every sixth sarcomere contains a triad (Page, 1965).

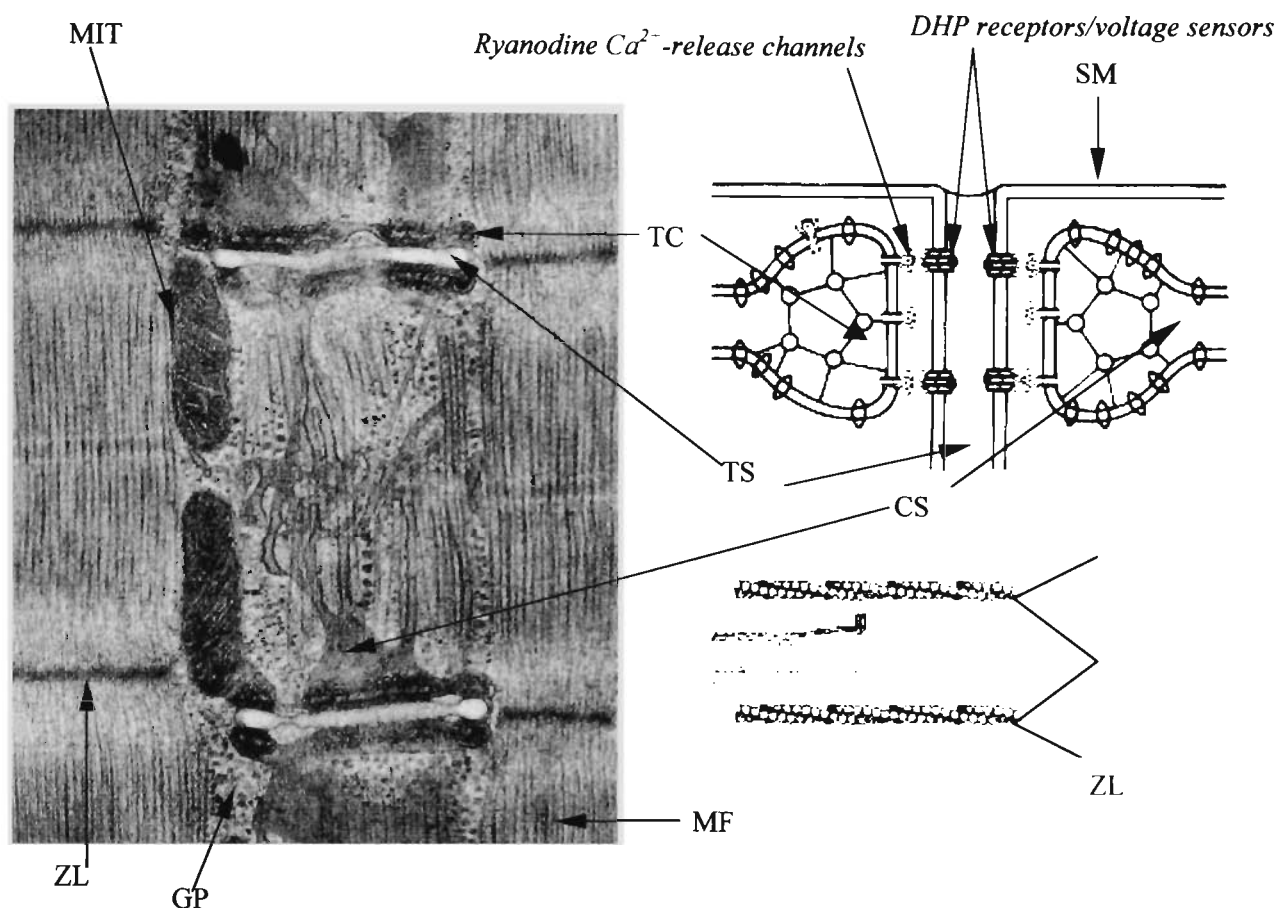


**Figure 1.4** The triad as seen in a quick frozen, freeze-substituted frog muscle (left panel, reproduced from Franzini-Armstrong, 1994) and in a schematic representation (right panel, reproduced from Stephenson, 1996).

SM: sarcolemma; TS: T-system; TC: terminal cisterna; CS: calsequestrin; GP: glycogen particles; MF: myofilaments; MIT: mitochondria; ZL: Z line. Note the location of the triad at the level of the Z line which is characteristic of amphibian skeletal muscle.

### 1.1.3.1 STRUCTURE OF THE SARCOPLASMIC RETICULUM

The major functions of the SR are to pump  $\text{Ca}^{2+}$  from the myoplasmic into the luminal space, against a steep concentration gradient, to maintain a relatively large total internal  $[\text{Ca}^{2+}]$  and to release  $\text{Ca}^{2+}$  rapidly into the myoplasm when required. In all types of muscle fibres, SR membranes include *fenestrated*, *tubular* and *junctional* regions. The fenestrated regions of the SR display perforations that allow direct communication between the luminal and myoplasmic sides of the SR membranes. The level of fenestration is low in amphibian muscles and the disposition of fenestrated regions is relatively constant in an individual type of muscle fibre (Franzini-Amstrong, 1994). The margins of the fenestrated regions of the SR are continuous with tubular regions, where the SR forms individual parallel tubules, usually oriented longitudinally. These tubular components, referred to as *longitudinal* SR, contain the sites of rapid calcium uptake during relaxation (Ebashi & Endo, 1968). Finally, the *junctional* regions of the SR (the *terminal cisternae*) form junctions with the T-tubules at the level of triads; they have one flat or regularly scalloped junctional surface which is covered by small periodically arranged electron dense structure named the *junctional feet* (Franzini-Amstrong, 1994).

It is now known that the junctional feet are homotetrameric (~560 kDa/subunit) protein structures, with each of the four subunits having several transmembrane segments at the C-terminus and a large cytoplasmic domain. These proteins are known as *junction-spanning foot proteins*, *ryanodine receptors (RyR)*, or *SR- $\text{Ca}^{2+}$ -release channels* (see diagrams in Figs. 1.4 and 1.5) because of their location in the

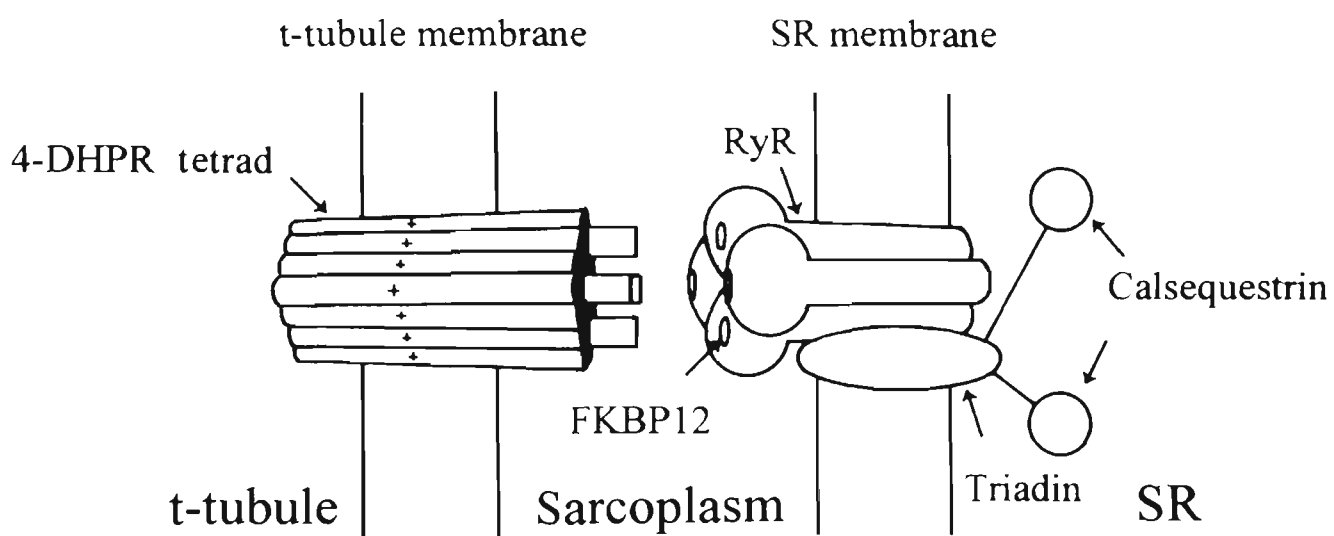


**Figure 1.5** Schematic representation of proteins believed to participate in events that take place at the level of the triad.

4-DHPR tetrad: protein complex containing DHP receptors; RyR: ryanodine receptor; FKBP12: a 12 kDa protein that binds the immuno-suppressant drug FK506; triadin: a 37 kDa glycoprotein assumed to be involved in SR function; calsequestrin: calcium binding protein (reproduced from Stephenson, 1996).

junctional region, their high affinity for the plant alkaloid *ryanodine* and their physiological role.

Associated with each  $\text{Ca}^{2+}$  release channel, are four molecules of a small protein which is referred to as FKBP12 because it binds the immunosuppressant drug FK 506 and has a molecular weight of about 12 kDa. The junctional SR membrane also contains *triadin*, a protein believed to provide a link between the SR  $\text{Ca}^{2+}$  release channels and the luminal  $\text{Ca}^{2+}$  binding protein calsequestrin. The SR- $\text{Ca}^{2+}$ -release channels can be activated by  $\text{Ca}^{2+}$  (RyR activation by  $\text{Ca}^{2+}$  is referred to as *calcium induced calcium release* or *CICR*), caffeine and ATP, and inhibited by  $\text{Mg}^{2+}$  and ruthenium red (Stephenson *et al.*, 1998; Leong & MacLennan, 1998) (see also section 1.2.3).

Studies of mammalian muscles have revealed three different isoforms of ryanodine receptors, Ryr1 (the main RyR isoform in rabbit skeletal muscle), Ryr2 and Ryr3, which are coded for by three different genes (Ogawa *et al.*, 1999; Leong & MacLennan, 1998). In frog skeletal muscle, there are two RyR isoforms:  $\alpha$ -RyR and  $\beta$ -RyR, which are homologous to Ryr1 and Ryr3 isoforms in mammals, respectively, and coexist in similar amounts. The  $\alpha$ - and  $\beta$ -RyR are believed to contribute independently to SR activities and, in an isotonic medium, they show very similar properties with respect to [ $^3\text{H}$ ]ryanodine binding and to activation by adenine nucleotides, caffeine and  $\text{Ca}^{2+}$  (Ogawa *et al.*, 1999).

It is interesting to note that the SR membranes are associated with glycogen particles (Goldstein *et al.*, 1985; see also in Fig. 1.4) and also contain, or are associated with, the entire chain of glycogenolytic and glycolytic enzymes. Furthermore, there is overwhelming evidence that  $\text{Ca}^{2+}$  enhances glycogenolysis by activating glycogen phosphorylase kinase (Heilmeyer *et al.*, 1970). Taken together, these findings have led to the conclusion that the ATP generated in reactions catalysed by SR-associated glycolytic enzymes may play an important role in excitation-contraction (E-C) coupling (Xu & Becker, 1998; Nogues, 1996; Xu *et al.*, 1995; Cuenda *et al.*, 1993; Montero-Lomelí & Meis, 1992; Han *et al.*, 1992). The role of glycogen in skeletal muscle contractility is discussed also in section 1.3 and in Chapter 4.

#### 1.1.3.2 STRUCTURE OF THE T-TUBULAR SYSTEM

The T-system occupies about 0.5% of the fibre volume and has evolved from invaginations of the sarcolemma (Schiaffino & Margreth, 1969). These tubules, 30-80 nm in diameter, enter the fibre near the border line at A-I junction in mammalian skeletal muscle or, as previously mentioned, near the Z-disc in amphibian skeletal muscle. Earlier it was observed that transverse tubules communicate with the extracellular environment by forming intricate ramifications and caveolae which open to the outer-cellular surface (Peachey, 1968; Huxley HE, 1964). This led to the conclusion that the T-tubular system is just an extension of the sarcolemma. The continuity between the T-system and sarcolemma, which has been used to explain the unusually high capacitance of the muscle cell membrane, has major functional significance, because it allows the rapid conduction of excitatory signals from the

outer membrane to the interior of the muscle fibre via the T- system (Hodgkin & Nakajima, 1972).

The size of the T-system appears to be dependent on fibre type. For example, in a frog sartorius twitch muscle fibre, the total surface area of the T-system has been estimated to be 5-7 times larger than the outer surface of the fibre (Peachey, 1968; Falk & Fatt, 1964). In a frog tonic/slow fibre, on the other hand, the total surface area of the T-system was found to be only about twice as large as the outer surface of the fibre (Peachey, 1968).

On the myoplasmic side of the T-tubular membrane and opposing alternate junctional feet are groups of four particles called tetrads (Franzini-Amstrong & Jorgensen, 1994). These particles, which consist of four supra-molecular complexes known as the *dihydropyridine (DHP) receptors* or *L-type  $Ca^{2+}$  channels* (see Fig. 1.5), have been recently shown to serve as voltage sensors and to be responsible for asymmetric charge movements within the T-tubular membrane. Asymmetric charge movements have been suggested to play a role in the coupling of transverse tubular depolarisation to SR calcium release (for review see Stephenson *et al.*, 1995; Horowicz, 1994).

Each DHP receptor is an oligomer consisting of five subunits:  $\alpha_1$  (185 kDa),  $\alpha_2$  (143 kDa),  $\beta$  (54 kDa),  $\gamma$  (26 kDa),  $\delta$  (30 kDa) in which the  $\alpha_1$ -subunit is the channel-forming and DHP-binding portion of the molecule (see Stephenson *et al.*, 1995; Horowicz, 1994; Franzini-Amstrong & Jorgensen, 1994; for review). The structure of the  $\alpha_1$  subunit resembles that of the  $Na^+$ -channels with four 'repeats' (I-IV), each

consisting of at least 6 T-tubular membrane-spanning segments (S1-S6). Five of these segments (S1, S2, S3, S5 and S6) are hydrophobic, but the fourth segment (S4) in each of the four 'repeats' is positively charged. The positively charged S4 segments are believed to be the voltage-sensitive elements of the DHP receptors and to be responsible for the asymmetric charge movement in muscle. The cytoplasmic loop between 'repeats' II and III of the skeletal muscle DHP receptor appears to be essential for signal transmission to the SR. The  $\beta$ -subunit of the DHP receptor plays also a regulatory role in the  $\text{Ca}^{2+}$ -channel function and interacts with the  $\alpha_1$  subunit through the loop between 'repeats' I and II. Both  $\alpha_1$ - and  $\beta$ -subunits of the DHP receptor contain multiple sites for phosphorylation that may be critical during muscle activity (for review see Favero, 1999). The functions of the other subunits ( $\alpha_2$ ,  $\gamma$ , and  $\delta$ ) of the DHP receptor are not yet fully understood.

## 1.2 EXCITATION-CONTRACTION-RELAXATION CYCLE

The term excitation-contraction-relaxation (E-C-R) cycle refers to a series of reactions that occurs in a twitch skeletal muscle fibre from the time when the sarcolemma is stimulated to the time when the fibre relaxes. Regardless of fibre type characteristics, the main events of the E-C-R cycle in amphibian and mammalian twitch muscle fibres include: (i) initiation and propagation of an action potential along the sarcolemma and T-tubular system; (ii) detection of the T-system depolarisation signal and signal transmission from the T-tubules to the SR membrane; (iii)  $\text{Ca}^{2+}$  release from the SR, (iv) transient rise of myoplasmic  $[\text{Ca}^{2+}]$ ; (v) transient activation of the  $\text{Ca}^{2+}$  regulatory system and of the contractile apparatus and (vi)  $\text{Ca}^{2+}$  reuptake by the SR  $\text{Ca}^{2+}$  pump

and  $\text{Ca}^{2+}$  binding to myoplasmic sites (Stephenson *et al.*, 1998). In the present review, attention will be focused on the molecular events that take place between the depolarisation of the sarcolemma and  $\text{Ca}^{2+}$  release from the SR and particular emphasis will be put on the communication between the DHP voltage sensor and the RyR receptor/ $\text{Ca}^{2+}$  release channel, at the triadic junction.

### 1.2.1 INITIATION AND PROPAGATION OF ACTION POTENTIALS ALONG THE SARCOLEMMA AND T-SYSTEM

There are considerable differences between the outside and inside of a muscle fibre with respect to concentrations of several ionic species. Thus, the sarcoplasm contains a high concentration of potassium ( $\text{K}^+$ ) and low concentration of sodium ( $\text{Na}^+$ ) ions, while the opposite is true for the extracellular environment. The difference in  $\text{K}^+$  and  $\text{Na}^+$  concentrations on either side of the membrane is maintained by the *Na<sup>+</sup> K<sup>+</sup> pump* (see Fig. 1.1A). Also, trapped in the cell are large, negatively-charged, non-diffusible ions, such as organic phosphate and protein anions. The uneven distribution of ions on either side of the sarcolemma and the different permeability of the membrane for various ions are responsible for the generation of an electrical potential across the sarcolemma which is known as the *membrane potential*. When a muscle fibre is at rest, its membrane potential is around  $-90$  mV, i.e. the inside of the fibre is more negative than the outside (Rüegg, 1992).

When a nerve impulse (nerve action potential) reaches the synaptic vesicles of an axon terminal, a small amount of  $\text{Ca}^{2+}$  enters the synaptic end bulb, causing the

vesicles to release the neurotransmitter *acetylcholine* into the synaptic cleft. Binding of the neurotransmitter to its receptors in the *motor end plate* region of the muscle fibre is accompanied by the activation of neighbouring non-selective cationic channels, which in turn brings about a local depolarisation of the sarcolemma from  $-90$  mV toward more positive values. This depolarisation activates *voltage-sensitive*  $Na^+$  and  $K^+$  channels, which causes the inward movement of  $Na^+$  ions and further depolarisation. As already mentioned in section 1.1, this wave of depolarisation that travels along the sarcolemma and then into the T-tubular system represents the *muscle action potential*. During an action potential, the membrane potential is reversed so that, for a brief moment, the inside of the muscle cell becomes positively charged with respect to outside. Within a few milliseconds, however, the initial negativity of the interior is restored. An action potential is short lived primarily due to the inactivation of the voltage sensitive  $Na^+$  channels and to the delayed activation of the  $K^+$  channels (Clausen, 1996; Nielsen & Overgaard, 1996).

### 1.2.2 E-C COUPLING AND SR $Ca^{2+}$ RELEASE

In skeletal muscle, when an action potential reaches the T-tubules close to the SR,  $Ca^{2+}$  ions are released from the *terminal cisternae* (junctional membrane) of the SR into the sarcoplasm surrounding the myofibrils (see also sections 1.1.3.1 and 1.1.3.2). While this indicates that a certain type of communication takes place between the T-system and SR, it gives no information of the molecular mechanism of signal transmission, which is far from being understood. Currently, a number of models

have been proposed to explain the mechanism of signal transmission between T-tubule and *terminal cisternae* in the SR.

According to one theory, for example, the coupling of T-system depolarisation to SR calcium release is related to membrane charge movements, which originate in the *DHP receptor* proteins and are triggered by the depolarisation of the T-tubules. (see Ríos & Stern, 1997; Schneider, 1994; Meissner, 1994; Franzini-Amstrong & Jorgensen, 1994; for review). The relationship between charge movements in the T-system membranes and  $\text{Ca}^{2+}$ -release from SR vesicles is a complex process and may involve mechanical, electrical and chemical messengers.

More recently, Lamb & Stephenson (1991 & 1990) proposed a mechanism for signal transmission from the DHP receptors to the  $\text{Ca}^{2+}$ -release channels in twitch muscle fibres that involves  $\text{Mg}^{2+}$ . According to this model, under resting conditions, when present in concentrations of about 1 mM,  $\text{Mg}^{2+}$  ions bind tightly to and inhibit the  $\text{Ca}^{2+}$ -release channels, which are essentially closed. Upon signal transmission from the DHP receptors, via the cytoplasmic loops, the affinity of  $\text{Mg}^{2+}$  for the  $\text{Ca}^{2+}$ -release channels is decreased, the inhibition of the channels by  $\text{Mg}^{2+}$  is removed (see also review by Stephenson *et al.*, 1998) and  $\text{Ca}^{2+}$  is released into the sarcoplasm in the vicinity of the contractile/regulatory system. When myoplasmic  $[\text{Ca}^{2+}]$  increases from resting levels of less than  $10^{-7}$  M to about  $10^{-6}$  M,  $\text{Ca}^{2+}$  binds to Troponin C, the structure of the thin filament changes, the cyclic interaction between actin and myosin is facilitated and contractile tension develops.

### 1.2.3 REGULATION OF E-C COUPLING

E-C coupling can be regulated at different levels by various factors (for review see Stephenson *et al.*, 1998). For example it has been reported that the transmission of the signal from the T-tubules to the SR is depressed in the presence of oxidising agents, when  $[Mg^{2+}]$  is increased over 1 mM, when  $[MgATP]$  is reduced or when the myoplasmic  $[Ca^{2+}]$  is raised above 10  $\mu M$  (see Stephenson *et al.*, 1998, for review). In this section, the regulation of events involved in SR  $Ca^{2+}$  release is discussed using primarily the mammalian twitch skeletal muscle as a model. No major differences in the regulation of the mammalian and amphibian RyR isoforms have been reported so far.

It is generally accepted that if the conductance of the RyR is constant, then the rate of SR- $Ca^{2+}$  release depends on channel density, probability of channel opening and electrochemical gradient of  $Ca^{2+}$  across the SR junctional membrane (for review see Stephenson *et al.*, 1998). It is now known that the average open time of SR- $Ca^{2+}$  release channels can be modulated by many endogenous factors. Thus, acidic pH, calmodulin at micromolar concentrations of myoplasmic  $[Ca^{2+}]$  and protein phosphorylation of specific groups decrease the average open time of SR- $Ca^{2+}$  release channels, while adenine nucleotides, a rise in myoplasmic  $[Ca^{2+}]$  within the micromolar range, myoplasmic Pi, lipid metabolites or protein phosphorylation at different sites increase the average open time of SR- $Ca^{2+}$  release channels (for reviews see Stephenson *et al.*, 1998; Ríos & Stern, 1997; Schneider, 1994; Meissner, 1994; Franzini-Amstrong & Jorgensen, 1994).

Regarding modulation of the electrochemical gradient of  $\text{Ca}^{2+}$  across the SR junctional membrane, it is worth noting a recent theory proposed by Stephenson *et al.* (1998), that in intense muscle activity,  $[\text{Pi}]$  in the SR rises above 10 mM and causes calcium phosphate precipitation in the SR lumen. According to Stephenson *et al.* (1998), this leads to a decrease in free  $[\text{Ca}^{2+}]$  within the SR, a subsequent reduction in the concentration gradient of  $\text{Ca}^{2+}$  across the SR membrane and therefore a decrease in SR- $\text{Ca}^{2+}$  release. Interestingly, the immuno-suppressant drug FK506-binding protein (FKBP) appears to stabilise the full conductance state of the RyR receptor and, as such, may play a vital role in enabling the voltage sensors to activate RyR/ $\text{Ca}^{2+}$  release channels in fast-twitch mammalian fibres (for review see Stephenson *et al.*, 1998).

In the last decade, a large amount of information regarding the regulation of E-C coupling events has been obtained from studies using mechanically skinned muscle fibre preparations in which the T-system reseals and can be depolarised chemically (for review see Stephenson *et al.*, 1998). In these studies, the plasma membrane of a fibre, freshly dissected under oil, is carefully removed/damaged, under the microscope, with two pairs of fine tweezers (details of the skinning procedure are given in section 3.2.2.5) in a manner that allows T-system membranes to reseal. Chemical depolarisation of the resealed T-tubules is subsequently achieved by exposing the fibre preparation to a 'depolarising solution' in which  $\text{K}^+$  is replaced with  $\text{Na}^+$ , and E-C coupling is monitored by using force responses as an indicator of  $\text{Ca}^{2+}$  release from the SR. This experimental strategy has been used extensively in Chapter 4.

As described in the section 1.1.3.1, the entire chain of glycolytic enzymes as well as glycogen particles are closely associated with the SR membrane in the triadic region. Isolated skeletal muscle triads have been found to synthesise ATP in the vicinity of T-tubular membrane/SR membrane junctions (Han *et al.*, 1992). These locally produced-ATP molecules are not readily exchangeable with the bulk myoplasmic ATP (for review see Meissner, 1994). It is conceivable, therefore, that within the restricted space of the T-tubular/SR junction, an alteration in local [ATP], an increase in the local concentration of by-products of ATP hydrolysis or the degradation of glycogen particles, brought about by a change in the metabolic state of the muscle fibre, may modulate the activity of RyR/Ca<sup>2+</sup> release channels.

As discussed in detail in section 1.3.1, glycogen particles are present not only in triadic junctions but are also sandwiched in intrafibre spaces between myofibrils. Why are glycogen particles located so closely to these major sites of action in the E-C-R cycle? One explanation is that events taking place at the level of triads or myofibrils produce energetic needs that have to be rapidly satisfied by the local ATP generated as a result of glycogen breakdown. Alternatively, the glycogen moiety may sequester kinases and phosphatases that are essential in events of the E-C-R cycle. This latter possibility is discussed in more detail in section 1.3 and Chapter 4.

Although there is a wealth of information regarding the metabolism of muscle glycogen, the physiological significance of this biopolymer in skeletal muscle contractility is not yet fully understood.

### 1.3 GLYCOGEN AND SKELETAL MUSCLE

Glycogen is the major form of storage polysaccharide in animals. Muscle glycogen, which accounts for 1 – 2% of the tissue mass, is present in the sarcoplasm, within granular structures (10-40 nm) that also contain enzymes of glycogen synthesis, as well as glycogenolytic and glycolytic pathways (Garrett & Grisham, 1995; Stryer, 1995; DiMauro *et al.*, 1971).

Exercise testing of normal muscles has shown that, during 60 min of intermittent heavy exercise ( $> 60\%$   $\text{VO}_2$  max, where  $\text{VO}_2$  max is the maximal rate of  $\text{O}_2$  consumption) most of the required energy is derived from the breakdown of glycogen even when the blood glucose level is very high (Brown, 1994; Bergström *et al.*, 1967). This clearly indicates that endogenous glycogen is the preferred fuel molecule during intermittent, intense exercise. This preferential use of glycogen has been attributed to various factors such as (i) the fast rate of glycogen mobilisation, (ii) the biological need for preservation of blood glucose for use by the brain, (iii) the higher power output and the more rapid acceleration to maximal power output produced by glycogen, and (iv) the higher molar ratio of ATP production/ $\text{O}_2$  consumption associated with glycogen oxidative degradation (Brown, 1994).

At work loads between 65-85%  $\text{VO}_2$  max, it appears that glycogen plays also a protective role against fatigue. Indeed, after 2-3 hours exercise at this load, when the endogenous glycogen store is depleted, muscle performance decreases dramatically,

even though the ATP pool is largely unaffected (Fitts, 1994). Current opinions regarding the role of glycogen in muscle fatigue are discussed in detail in Chapter 4.

### **1.3.1 INTRACELLULAR LOCATION OF MUSCLE GLYCOGEN**

Using electron microscopy, Fridén *et al.* (1989) found that within human skeletal muscle, glycogen particles are present (i) as deposits in the subsarcolemmal space, especially in the vicinity of mitochondria, (ii) in the intermyofibrillar space particularly around the region of the I band and (iii) as longitudinal rows between actin filaments on either side of the Z line or in the H zone (only for fast glycolytic fibres). Recently, glycogen particles were also found to be tightly associated with junctional SR membranes or located in the restricted space of the intrajunctional triadic region (Connett & Sahlin, 1996; see also Fig. 1.4).

The relationships between different myoplasmic glycogen pools or between glycogen particles and the function of the adjacent subcellular organelles/compartments are not understood.

### **1.3.2 STRUCTURE OF MUSCLE GLYCOGEN**

Glycogen is a highly branched homopolysaccharide containing only D-glucosyl units (Stetten & Stetten, 1960). It is formed as chains of 13 glucose residues linked by *amylo- $\alpha$ -1,4-glycosidic bonds*. Half of the chains in a glycogen molecule (see below)

have two branching points. The branches are linked to the chain of origin by *amylo- $\alpha$ -1,6-glycosidic bonds*.

Glycogen molecules have been found to contain both branched chains (B-chains) and non-branched chains (A-chains) (see Fig. 1.6). Each B-chain and A-chain contains 13 glucose residues. Every B-chain has two branches on it that create further A- or B-chains. There are four glucose residues between branches and in the tail after the second branch in the B-chains (Meléndez-Hevia *et al.*, 1993). Glycogen phosphorylase can react only with A-chains, since the tail of the B-chains is too short (about 4 glucose residues, which is at the limit of phosphorylase action) (Meléndez-Hevia *et al.*, 1993).

As shown in Fig. 1.6, the glycogen molecule has a spherical shape (21 nm radius) and is organised in concentric tiers. A full glycogen molecule has 12 tiers, each tier being about 1.9 nm in length. Only A chains are in the outermost tier (Meléndez *et al.*, 1998 & 1997; Meléndez-Hevia *et al.*, 1993).

Because the degree of branching is 2, the number of chains in any tier is twice as high as that in the previous one and is equal to the total number of chains of all other previous tiers. Using these data, Meléndez-Hevia *et al.* (1993) deduced that, independent of size and number of tiers of the glycogen particle (i) the number of A-chains (all of them in the last tier) is equal to that of the B-chains and (ii) the amount of glucose directly available to be released by glycogen phosphorylase is 34.6% of the total amount of glucose residues.

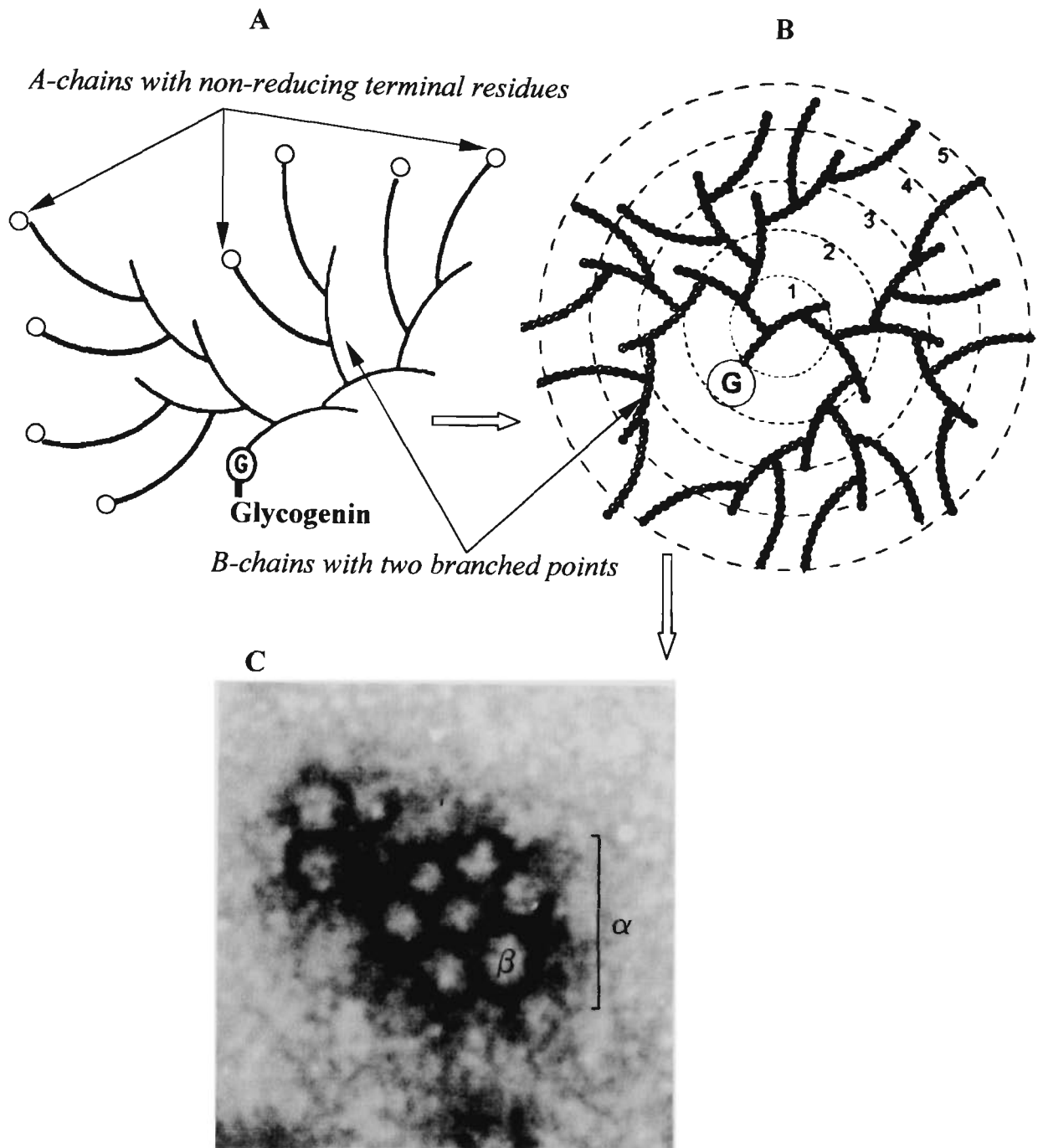


**Figure 1.6** Diagrammatic representation of glycogen structure (A & B; reproduced from Meléndez *et al.*, 1997 and Meléndez *et al.*, 1998) and the electron micrograph of a glycogen particle (C) from rat skeletal muscle (reproduced from Voet *et al.*, 1999). (A) part of glycogen molecule displaying A-chains and B-chains (with two branched points); (B) a spherical glycogen molecule in which the chains are organised into tiers (note that a full glycogen molecule contains 12 tiers); (C) several spherical glycogen molecules ( $\beta$ ) and associated protein form a glycogen granule/particle (labeled  $\alpha$ ).

The spherical, highly branched structure of the glycogen molecule is believed to be physiologically significant, as it allows the rapid degradation of glycogen through the simultaneous release of glucose units at the end of every A-chain. This may explain the roles of glycogen as a major energy store and preferred fuel in intense exercise.

It has been found that, unlike most other important compounds in the animal body that have a fixed molecular weight, glycogen is a highly polydisperse polysaccharide of molecular weight ranging between  $1 \times 10^6$  and  $1 \times 10^8$  (Stetten & Stetten, 1960) or between  $1 \times 10^6$  and  $1 \times 10^9$  (Geddes & Chow, 1994), depending upon the method of isolation and purification.

Early in the 1990s, the Whelan group (Miami, Florida, USA) proved the existence of a low molecular weight form of glycogen in rabbit skeletal muscle (subsequently named *proglycogen*) that co-existed with the traditional large molecular weight form glycogen species ( $1-100 \times 10^7$  Da) called *macroglycogen* (Alonso *et al.*, 1995; Lomako *et al.*, 1993 & 1991). Proglycogen was found to have a molecular weight of ~400 000 Da and contain, in addition to carbohydrate, a protein moiety (~10% w/w) of 37 kDa molecular weight, referred to as *glycogenin*. In contrast to proglycogen, macroglycogen was found to contain only 0.35% protein. Because of its relatively high protein content (about 10%), proglycogen is precipitated in trichloroacetic acid (TCA, 5%) while macroglycogen, containing a small proportion of protein, is acid soluble (Adamo & Graham, 1998; Huang *et al.*, 1996). As discussed in detail in Chapter 3, this relatively recent evidence of two molecular forms of cellular glycogen

that differ by their molecular weight confirms an earlier report of two populations of mammalian glycogen by Stetten *et al.* (1958).

The finding of these two pools of glycogen with different molecular weights was explained by a 2-stage mechanism of glycogen synthesis (Meléndez *et al.*, 1997; Alonso *et al.*, 1995). According to this mechanism, in the first stage of glycogen synthesis, an intermediate molecule of glycogen with 8 tiers and a molecular weight of  $\sim 400\,000\text{Da}$  (proglycogen) is formed via a series of reactions in which *glycogenin* acts as a primer or precursor. In the second stage of glycogen synthesis, proglycogen is built up further to a full molecule with 12 tiers and a molecular weight of  $\sim 10^7\text{ Da}$  (macroglycogen) (Alonso *et al.*, 1995).

There is also evidence to suggest that macroglycogen and proglycogen are metabolised with different rates and that proglycogen contributes a greater proportion of carbohydrates to the early phase of glycogen degradation (Shearer *et al.*, 1998). The physiological significance of these two pools of glycogen is not fully understood.

### 1.3.3 MUSCLE GLYCOGEN CATABOLISM

The process of glycogen mobilisation (glycogen breakdown or *glycogenolysis*) involves sequential cleavages of  $\alpha$ -1,4-glucosidic bonds, catalysed by *glycogen phosphorylase*. This enzymatic reaction always begins at the A-chains in the outermost tier (normally tier No. 12) of the glycogen molecule (see section 1.3.2) when the glycogenolytic pathway is initiated by the sequential removal of glucose

units from the *non-reducing ends* (ends with free C<sub>4</sub>-OH group) of glucan chains (Stryer, 1995; Meléndez-Hevia *et al.*, 1993).

The  $\alpha(1 \rightarrow 4)$  linkage between the C<sub>1</sub>-OH group of the terminal residue and the C<sub>4</sub>-OH of the adjacent glucose residue is cleaved by orthophosphate (Pi) (in presence of phosphorylase) to yield a phosphorylated sugar, glucose-1-phosphate (G1P) (Stryer, 1995). The phosphorolytic cleavage of glycogen is energetically advantageous because the released sugar is phosphorylated. In contrast, a hydrolytic cleavage would yield glucose, which would have to be phosphorylated at the expense of an ATP molecule to enter the glycolytic pathway. An additional advantage of phosphorolytic cleavage for muscle cells is that G1P, ionised under physiological conditions, cannot diffuse out of the cells, whereas glucose can (Stryer, 1995).

Glycogen is degraded to a limited extent by phosphorylase alone which stops its  $\alpha(1 \rightarrow 4)$ -linkage cleavage action at four glucose residues away from a branching point. The debranching enzyme,  $\alpha(1,4 \rightarrow 1,4)$ -glucantransferase, thus, is needed to convert the branch structure into a linear structure, which paves the way for further cleavage by phosphorylase (Stryer, 1995). The debranching enzyme carries out two reactions: first, it removes three of the four remaining glucose residues from the branch chain, and second, it transfers this intact trisaccharide moiety to the end of some other outer A-chain. The glucose residue that is still attached to the chain by an  $\alpha(1 \rightarrow 6)$  linkage is split by  $\alpha$ -1,6-glucosidase (Stryer, 1995). The newly formed (straight) A-chain is ready for further degradation by phosphorylase.

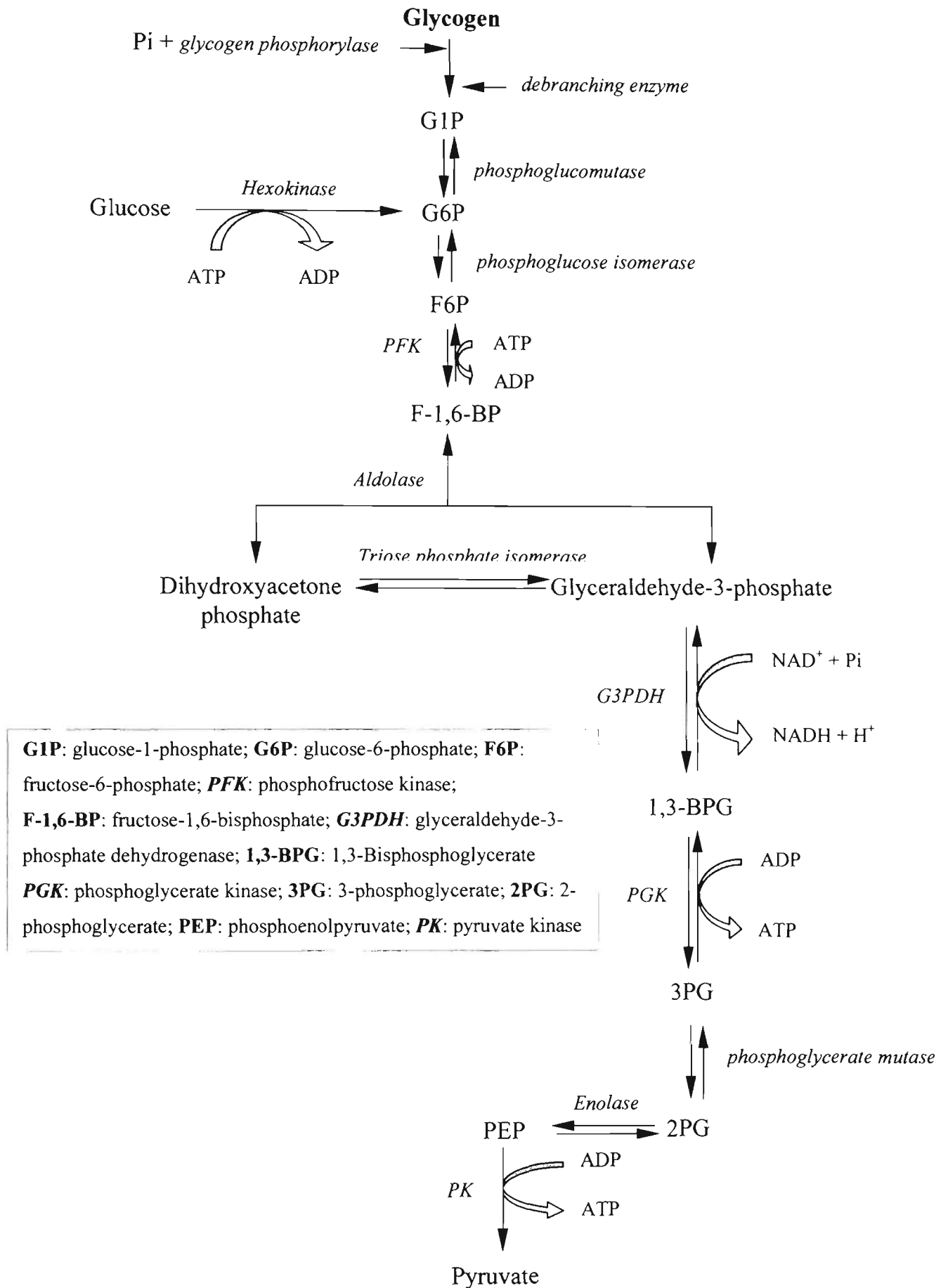


**Figure 1.7** Glycogenolytic and glycolytic pathway (Voet *et al.*, 1999; Stryer, 1995)

The G1P formed in the phosphorolytic cleavage of glycogen is then converted into glucose-6-phosphate (G6P) which enters the glycolytic pathway. This phosphoryl-shift is catalysed by *phosphoglucomutase*. From the stage of formation of G6P, the glycogenolytic and glycolytic pathways have the same stream of reactions - known as *glycolysis* - which is illustrated in Fig. 1.7.

Muscle glycogen represents an important reservoir of potential energy and the reactions involved in its degradation are carefully controlled and regulated. As shown in previous sections, the first reaction in the glycogenolytic pathway which produces G1P is catalysed by *glycogen phosphorylase*. This enzyme is activated by *phosphorylase kinase*, whose activity has been known for a long time to be stimulated by  $\text{Ca}^{2+}$  ions (Stryer, 1995). At pH 6.8, the  $K_m$  value of phosphorylase kinase for  $\text{Ca}^{2+}$  is 0.5  $\mu\text{M}$  (Brown, 1994).

*Phosphorylase kinase* is composed of four subunits,  $\alpha$ ,  $\beta$ ,  $\gamma$  and  $\delta$ , where the  $\delta$  subunit is *calmodulin*, a ubiquitous  $\text{Ca}^{2+}$ -binding peptide (Brown, 1994). It has been established that the conversion of *phosphorylase b* to *phosphorylase a* (the active form of phosphorylase) in skeletal muscle occurs immediately after and as a consequence of electrical stimulation and is closely related to  $\text{Ca}^{2+}$  release from the SR. Thus,  $\text{Ca}^{2+}$  released from the SR not only initiates contraction, but also stimulates *phosphorylase kinase* to catalyse the phosphorylation of *phosphorylase b* by ATP (Danforth & Helmreich, 1964). The activation of *phosphorylase kinase* by  $\text{Ca}^{2+}$  results from a 10 fold (Heilmeyer *et al.*, 1970) to 20-fold increase (Brown, 1994) in its affinity for its substrate *phosphorylase b* upon  $\text{Ca}^{2+}$  binding.

### 1.3.4 METHODS FOR DETERMINING GLYCOGEN CONTENT IN SKELETAL MUSCLE FIBRES

So far, two methods have been used for glycogen analysis in skeletal muscle fibres: one based on glycogen staining by a histochemical method, the other based on a system of enzymatic reactions in which glycogen breakdown is stoichiometrically coupled with the formation of fluorochromes. A brief description of the principle and application of each of these methods is presented in the following sections.

#### 1.3.4.1.DETERMINATION OF GLYCOGEN CONTENT IN MUSCLE FIBRES BY HISTOCHEMICAL *PAS*-STAINING METHOD

This method, which allows glycogen determination in muscle fibres visualised in serial cross sections of a whole muscle (Halkjaer-Kristensen & Ingemann-Hansen, 1979), is a modified version of the Periodic Acid Schiff (*PAS*) staining procedure. The main advantage of periodic acid in glycogen determination by *PAS* is that it reacts only with glucose residues within non-degraded glycogen molecules and not with glucose residues in short carbohydrate chains generated by the degradation of glycogen. After the periodic acid treatment, samples containing glycogen (cryostat serial sections of a muscle, air-dried at room temperature) are treated with Schiff's aldehyde reagent to form a coloured product.

The intensity of *PAS* staining (expressed as absorbance at 510 nm;  $A_{510}$ ) is measured on each single cell by spot measurements using a computerised Zeiss Scanning

Microphotometer (Zeiss SMP, PDP 12A), which has a circular measuring diaphragm with a diameter of 39  $\mu\text{m}$ . The histochemically-determined mean glycogen concentration in each fibre is calculated from the mean value of  $A_{510}$  divided by the thickness of the *PAS*-stained section and is expressed in arbitrary units ( $A_{510}/\mu\text{m}$ ) (Halkjaer-Kristensen & Ingemann-Hansen, 1979).

The *PAS* method is regarded as useful in establishing the pattern of glycogen depletion in different fibre types, when a muscle is subjected to different regimens of mechanical activity (Conlee, 1987). However, its usefulness for glycogen measurement in isolated, single muscle fibres is rather limited.

#### 1.3.4.2 DETERMINATION OF GLYCOGEN CONTENT IN SINGLE FIBRES BY THE FLUOROMETRIC METHOD

Over the last four decades, Lowry's laboratory has developed, refined and successfully applied the fluorometric method based on the *pyridine nucleotide system* for quantifying metabolic enzyme activities and endogenous metabolites in a range of biological preparations.

The use of NAD and NADP for analytical purposes depends on some of their unusual properties (Passonneau and Lowry, 1993):

- (i) They serve as the natural oxidising and reducing agents in a wide variety of specific enzyme systems in which one or more auxiliary enzymes are used.

Almost all metabolic intermediates can be specifically oxidised or reduced with an appropriate enzyme as catalyst.

- (ii) The reduced forms of the nucleotides (NADH and NADPH), absorb near UV light, and are fluorescent, whereas the oxidised forms (NAD<sup>+</sup> and NADP<sup>+</sup>) are not.
- (iii) NADH and NADPH can be totally destroyed in acid without affecting the oxidised forms. Conversely, NAD<sup>+</sup> and NADP<sup>+</sup> can be completely eliminated in alkali without influencing the reduced forms. Therefore, at the end of a reaction, the excess pyridine nucleotide in the reagent can be removed leaving the fraction that has been oxidised or reduced intact for subsequent measurement by procedures that enhance their native fluorescence.

Using appropriate enzymes, NAD or NADP, and properly processed biological samples, Lowry's group could determine 44 different metabolite intermediates at very low concentrations (Passonneau and Lowry, 1993).

The method developed by Lowry's group for determining glycogen in single muscle fibres involves the use of freeze-dried fibre segments, extraction of glycogen with 1 M HCl, enzymatic breakdown of glycogen, conversion of glucose to G6P, oxidation of G6P and reduction of NADP to NADPH. When all reactions proceed to completion, there is 1:1 stoichiometry between glucose and NADPH (Passonneau & Lowry, 1993; Passonneau & Lauderdale, 1974). The fluorescence intensity of the NADPH solution generated is measured fluorometrically at 465 nm wavelength.

Through measurement of NADPH, the concentration of glucose and hence glycogen can be determined and expressed as mmol glucosyl units per weight of either dry or wet tissue (Michel *et al.*, 1994; Hintz *et al.*, 1982 & 1980; Lust *et al.*, 1981 & 1975; Nassar-Gentina, 1978; Lowry *et al.*, 1978).

To increase the sensitivity of fluorometric methods for metabolite determination, Lowry's group introduced a step of analyte amplification by enzymatic cycling. In a cycling system for nicotinamide adenine dinucleotide or nicotinamide adenine dinucleotide phosphate (NAD or NADP cycle), the pyridine nucleotide is alternately oxidised by one enzyme, then reduced back again by another in a cyclic fashion. After a sufficient number of cycles (pre-calculated based on the amount of enzymes used), the reaction is heat stopped (normally by incubation at 95°C for 5 min) and one of the products is measured. Cycling systems for pyridine nucleotides are useful, not so much for measuring nucleotides *per se*, but as means of measuring a host of metabolites or enzymes activities (Kato *et al.*, 1973). With enzymatic amplification, Lowry group's method of glycogen determination operated in the range of 1 to 10 pmol glucosyl units (see Chapter 3 for further discussion).

Glycogen content (expressed as mmol of glucosyl units) in single fibres of human, frog and rat skeletal muscles has been investigated by several laboratories using Lowry's method with or without analyte amplification, depending on the size of the fibre preparation. For example, Essen and Henriksson (1974) reported average values for human fast and slow twitch fibres of 124 and 118 mmol glucosyl units/kg wet wt, respectively. In semitendinosus muscle fibres of *Rana pipiens*, the glycogen values found in two different experiments were  $328 \pm 37$  nmol/mg protein ( $n = 12$ ) and  $323 \pm$

43 nmol/mg protein ( $n = 6$ ) (Nassar-Gentina *et al.*, 1978), which are equivalent to  $69.9 \pm 8.0$  mmol/kg wet wt and  $68.8 \pm 9.2$  mmol/kg wet weight, if one assumes that 1 g wet wt of frog (sartorius) muscle contains 0.213 g solid and 0.662 g intracellular water (Desmedt, 1953). Finally, Hintz *et al.* (1982) found that fast fibres from rat plantaris muscle contained 34 – 40 mmol glucosyl units/kg wet wt while slow fibres from the same muscle contained only 30 mmol glucosyl units /kg wet wt.

As already mentioned, the use of freeze-dried preparations and analyte amplification represent two of the major features of the method developed and refined by Lowry and colleagues for determining glycogen in single muscle fibres. This precludes the use of the Passonneau & Lowry protocol when trying to correlate glycogen content with parameters of E-C coupling because (i) freeze dried muscle fibre preparations cannot be used for determining E-C coupling characteristics and (ii) the Passonneau & Lowry procedure is lengthy and laborious. This prompted the development in this study of a novel microfluorometric method for glycogen determination in segments of freshly dissected and mechanically skinned muscle fibre segments (see Chapter 3).

#### **1.4. THE AIMS OF THIS STUDY**

The overall aim of this study was to contribute knowledge to two areas of inquiry in muscle research: one concerned with the molecular mechanism(s) underlying the positive correlation between intracellular glycogen content and muscle performance and the other with the MHC isoform composition in amphibian skeletal muscle and skeletal muscle fibres. More specifically, this study has addressed the following major research questions:

- (i) does a mechanically skinned fibre preparation retain some or all of its intracellular glycogen after incubation in aqueous solutions? If it does:
- (ii) is the ability of a skinned fibre preparation to respond to T-system depolarisation correlated with its glycogen content, when the depolarising solution contains an excess of ATP and creatine phosphate?
- (iii) what happens to the glycogen associated with a mechanically skinned fibre preparation when the fibre is activated by T-system depolarisation or by exposure to  $\text{Ca}^{2+}$ -containing solutions?
- (iv) can one visualise and identify all MHC isoforms expected (on the basis of its fibre type composition) to be present in an amphibian muscle?
- (v) can one observe the age-related plasticity reported previously for two skeletal muscles of cane toad using SDS-PAGE analysis of MHC isoforms?
- (vi) do amphibian skeletal muscles contain hybrid fibres?

To answer these and other related questions, two novel methods were developed: (1) a microfluorometric method for rapid determination of glycogen in mechanically skinned, single fibre segments and (2) an ALANINE-based SDS-PAGE method for MHC isoform analysis in whole muscle homogenates, MHC extracts and single fibres isolated from toad muscles. The muscle preparations used throughout the study were obtained from cane toads (*Bufo marinus*).

## Chapter 2

# Development of a rapid microfluorometric method for measuring subpicomole amounts of Glycogen, Glucose and NADPH

### 2.1 INTRODUCTION

The method of metabolite analysis based on fluorogenic properties of pyridine nucleotides involves coupled reactions in which enzymatic transformation of the compound of interest is stoichiometrically related to the formation of the reduced/oxidised form of a pyridine nucleotide (NADH/NAD<sup>+</sup>; NADPH/NADP<sup>+</sup>; for further detail see section 1.3.4.2). In its earlier versions, the method allowed determination of analyte concentrations in the range 0.1-10  $\mu\text{M}$ , equivalent to 0.1-10 nmol/ml when a 1 ml-cuvette was used (Passonneau and Lowry, 1993). Following further refinement which included the use of more sophisticated fluorometers, the analytical range of the method was increased to cover the pmol range (e.g. 1-10 pmoles for glycogen) (Passonneau and Lowry, 1993). Two major factors that contributed to the improvement in the sensitivity of the method were (i) the use of an oil-well technique, which allowed analytical reactions to be carried out in smaller volumes ( $\leq 2 \mu\text{l}$ ) and (ii) analyte amplification by enzymatic cycling of the oxidised

forms of pyridine nucleotides. Passonneau and Lowry's ultra-sensitive fluorometric procedure for glycogen determination involves 6 steps:

*Step 1* (30 min): destruction of glucose by heating the sample in 0.02 M NaOH at 90°

*Step 2.* (120 min): glycogen hydrolysis

*Step 3* (20 min): glucose phosphorylation, G6P oxidation and reduction of  $\text{NADP}^-$  to NADPH

*Step 4* (20 min): destruction of  $\text{NADP}^-$  by 0.25 M NaOH at 80° C

*Step 5* (2-12 hours): enzymatic cycling of NADPH using *glutamate dehydrogenase* (GDH) and G6PDH.

For any given experiment involving determination of small amount (pmoles) of glycogen, the whole analytical procedure would require no less than 6 hours for completion, without including the time spent to prepare the biological sample.

The major objective of the work presented in this chapter was to develop an accurate and reproducible microfluorometric pyridine nucleotide method for measuring subpicomole amounts of NADPH, glucose and glycogen, which does not involve chemical or enzymatic fluorochrome amplification and takes no longer than 2.5 hr. As described in Chapters 3 and 4, the method was used to measure the glycogen content of segments of freshly dissected and mechanically skinned, single fibres from skeletal muscles of the cane toad *Bufo marinus*.

## 2.2 MATERIALS AND METHODS

### 2.2.1 CHEMICALS

*Amylo- $\alpha$ -1,4- $\alpha$ -1,6-glucosidase (AG)*, *hexokinase (HK)* and *glucose-6-phosphate dehydrogenase (G6PDH)* were purchased from Boehringer-Mannheim (Germany). NADP<sup>+</sup>, NADPH (nicotinamide adenine dinucleotide phosphate, oxidised form and reduced form, respectively), ATP (adenosine triphosphate), DTT (dithiothreitol),  $\alpha$ -D-glucose, glycogen (rabbit liver), quinine sulfate (Sigma ultra grade), *n*-hexadecane, light and heavy mineral oil were obtained from Sigma-Aldrich (St. Louis, MO, USA). Paraffin oil (Ajax Chemicals), sodium acetate and acetic acid (BDH, Merck, Germany) and other chemicals were analytical grade.

### 2.2.2 CONSTRUCTION OF STANDARD CURVES FOR COMMERCIAL GLYCOGEN, GLUCOSE AND NADPH

The microfluorometric strategy used for determining subpicomole amounts of NADPH, glucose and commercially purified glycogen involves four stages: (i) setting up the microfluorometric system, (ii) preparation of under-oil reagent droplets for microfluorometric determination of known amounts of NADPH, glucose and commercial glycogen, (iii) transfer of fluid between droplets and from a droplet to a microcell, (iv) measurement of the fluorescence signals produced by samples, and (v)

determination of the range in which the fluorescence intensity is directly proportional to the concentration of analyte in the standards.

#### 2.2.2.1 SETTING UP THE MICROFLUOROMETRIC SYSTEM

Fluorescence signals were measured, in a dark room, with an inverted Epi-Fluorescence microscope (Axiovert 100TV, Zeiss, Germany) equipped with a bialkali photomultiplier (Thorn EMI, USA) and a chart recorder (Activon, USA) (Fig. 2.1). A Xenon lamp (XBO 75W) was used as the light source. The Zeiss filter system included an excitation filter (G 365), a beamsplitter (FT 425), and an emission filter (LP 420). For microfluorometric measurements, samples were introduced by capillarity into rectangular borosilicate glass microcells/microslides with dimensions of  $0.05 \times 0.5 \times 50$  mm (Vitro Dynamics Inc., USA), which could contain up to  $1.25 \mu\text{l}$  sample. The microcells were placed on the wider side in the grooves ( $1.5 \times 1.5 \times 2$  mm) of a custom-designed brass frame ( $3 \times 30 \times 75$  mm, Fig. 2.2) which could carry 22 microcells.

At the start of each set of fluorometric readings, several adjustments were carried out after placing the microcell-loaded brass frame on the stage. These included centralisation of the microcells in the light field and focusing on a small region of the sample. To minimise the bleaching of sample signals during these adjustments (which could take up to 5 min), the microcell placed in the first groove of the frame was empty and all adjustments were made with this microcell positioned in the illuminated field. The arrangement of microcells on the frame was such that the

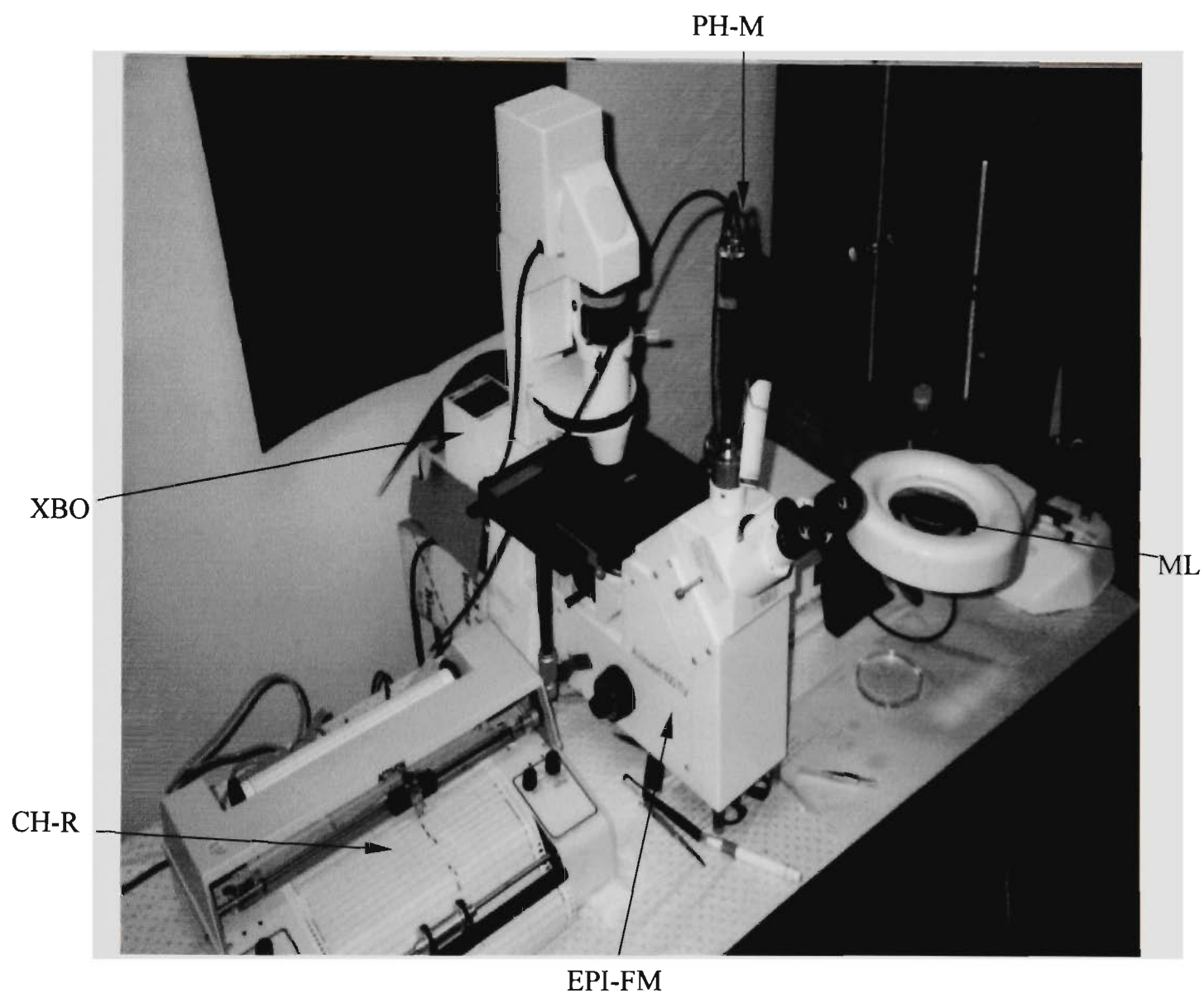


**Figure 2.1** Microfluorometric system used in this study. CH-R: chart recorder; EPI-FM: Epi-Fluorescent microscope; ML: magnifying lens; PH-M: photomultiplier; XBO: Xenon lamp.

empty microcell was followed by three blanks (controls) and then by sample-containing microcells. Fluorescence signals were generated when a 1 mm section of the microcell (equivalent to 25 nl of sample) was illuminated. Signals were recorded over 10-15 s exposure of the sample microcell to UV radiation. No significant bleaching (decrease of signal) was observed during such measurements.

The measuring system was checked for stability of the light source, uniformity of fluorescence signals recorded at different points along the microcell, fluorescence intensity of the blank and linearity of the relationship between fluorescence intensity and the concentration of analyte in the sample.

*Stability of the light source.* The lamp was turned on and allowed to warm up for about one hour. The stability of the light source over the period of experimentation was tested by comparing the fluorescence signals produced by a given concentration of quinine sulfate (9  $\mu\text{M}$ ) at different times during the experiment. This test was carried out more frequently towards the end of the life-span of the lamp (after 300 hours of use). During the period recommended (400 hours) by the manufacturer (Zeiss, Germany), no change in the fluorescence signal produced by the test sample was observed between the beginning and the end of an experimental run (2-8 hours).

*Uniformity of fluorescence in the illuminated sample.* As seen in Fig. 2.2, signals emitted by the fluorogenic sample could be recorded from any point along the 24-mm section of the microcell/microslide which could be exposed to the exciting light. The uniformity of the fluorescence signals produced by the quinine sulfate sample

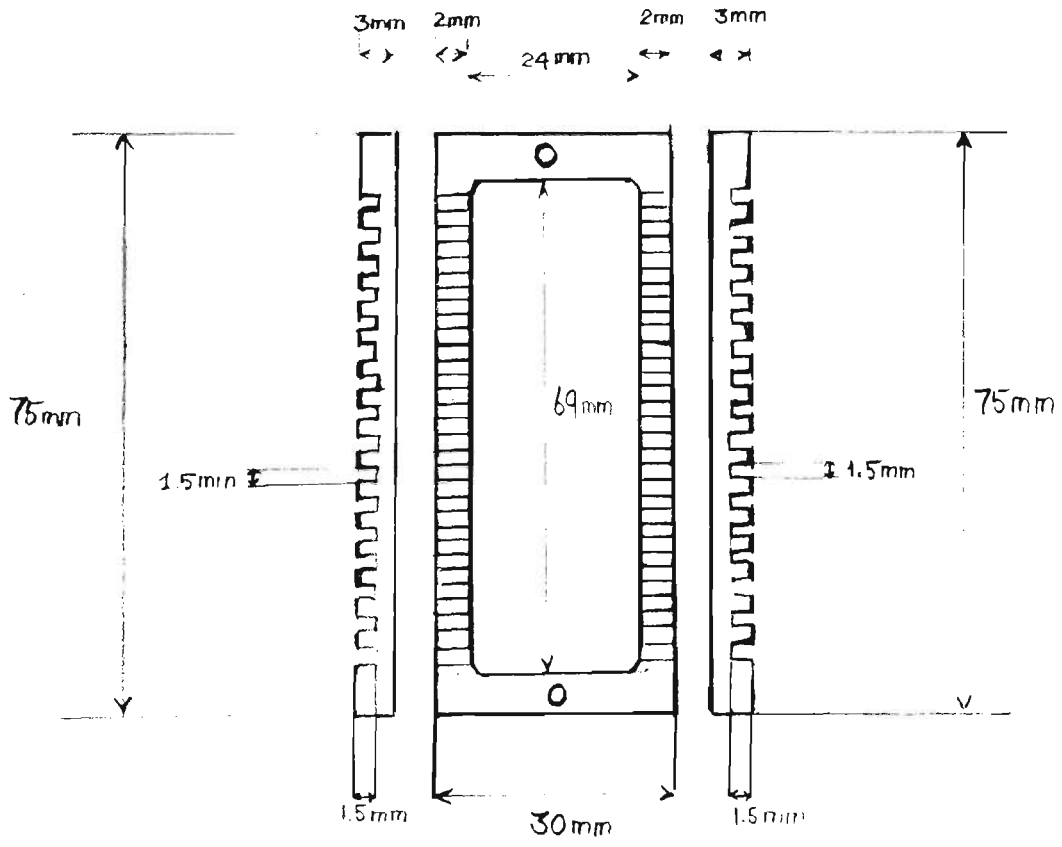


Figure 2.2 Brass frame custom-designed to hold 22 microcells.

contained in the microcell was confirmed in an experiment in which the fluorescence signals were continuously recorded while the microcell, positioned in the centre of the illuminated field, was slowly moved along its length.

*Fluorescence intensity of the blank and linearity of the relationship between fluorescence intensity and the concentration of quinine sulfate in the sample.* Under the conditions used in this study, the fluorescence intensity was directly proportional ( $r^2 \geq 0.998$ ;  $n = 6$ ) to the fluorochrome concentration in a series of solutions containing 0, 3, 6, 9, 12 and 15  $\mu\text{M}$  quinine sulfate (equivalent to 0, 100, 200, 300, 400 and 500 mM NADPH; Lowry & Passonneau, 1993). The quinine sulfate standards were prepared in 5 mM sulfuric acid. The intensity of the light source was adjusted such that the blank (5 mM sulfuric solution) signal was minimal and the signal produced by the highest standard (15  $\mu\text{M}$ ) reached the top of the chart paper.

#### 2.2.2.2 PREPARATION OF UNDER-OIL REAGENT DROPLETS FOR MICROFLUOROMETRIC DETERMINATION OF KNOWN AMOUNTS OF NADPH, GLUCOSE AND COMMERCIAL GLYCOGEN

In the microfluorometric method described here, all reactions were carried out in reagent droplets (0.25 to 10  $\mu\text{l}$ ), placed under oil, on the bottom of a glass petri dish. The viscosity of the oil and the thickness of the oil layer were chosen to minimise reagent evaporation while maintaining the spherical shape of the droplets. A 1.5-2 mm layer of oil mixture containing 30% *n*-hexadecane (Sigma-ultra grade) and 70% light mineral oil (Sigma-ultra grade) satisfied all the above requirements. A similar

mixture was used in the oil-well technique of Lowry's group (Passonneau and Lowry, 1993) for determining small amounts of metabolic analytes.

Before use, all petri dishes (size: 20 x 100 mm, Schott and Gen Mainz, Germany) were rinsed with drum acetone, washed with detergent and tap water using a soft sponge, rinsed with 6 M KOH/ethanol to remove any remaining traces of biological materials, rinsed about four times with hot tap water and carefully rinsed six times with deionised water. Finally, the petri dishes were placed up-side down on a tray and dried in an oven at 60°C overnight or left at ambient temperature for several days until the bottom surface was completely dry. One day before analysis, the bottom surface of the petri dish was gently cleaned with soft tissue paper and immediately covered by a 1.5-2 mm thick layer of analytical oil mixture. This treatment was found to accelerate and facilitate the adhesion of reagent droplets to the bottom surface of the petri dish, and was a critical factor, because small droplets ( $\leq 1\mu\text{l}$ ) had a tendency to float on top of the oil layer if they did not adhere very quickly to the bottom. In addition, the pre-treatment of petri dishes contributed to the maintenance of the shape (dome-like with a small base) of the droplets. The shape of the reagent droplet was also important with respect to the transferral of fluid from one droplet to another or from a droplet to the microcell (see section 2.2.2.3).

The reagent droplets were dispensed in a pre-defined pattern using an adjustable 2.5- or 20- $\mu\text{l}$  pipette (Eppendorf, Germany) (see Fig. 2.3). For example, when constructing a standard curve for glycogen, the droplets containing the reaction

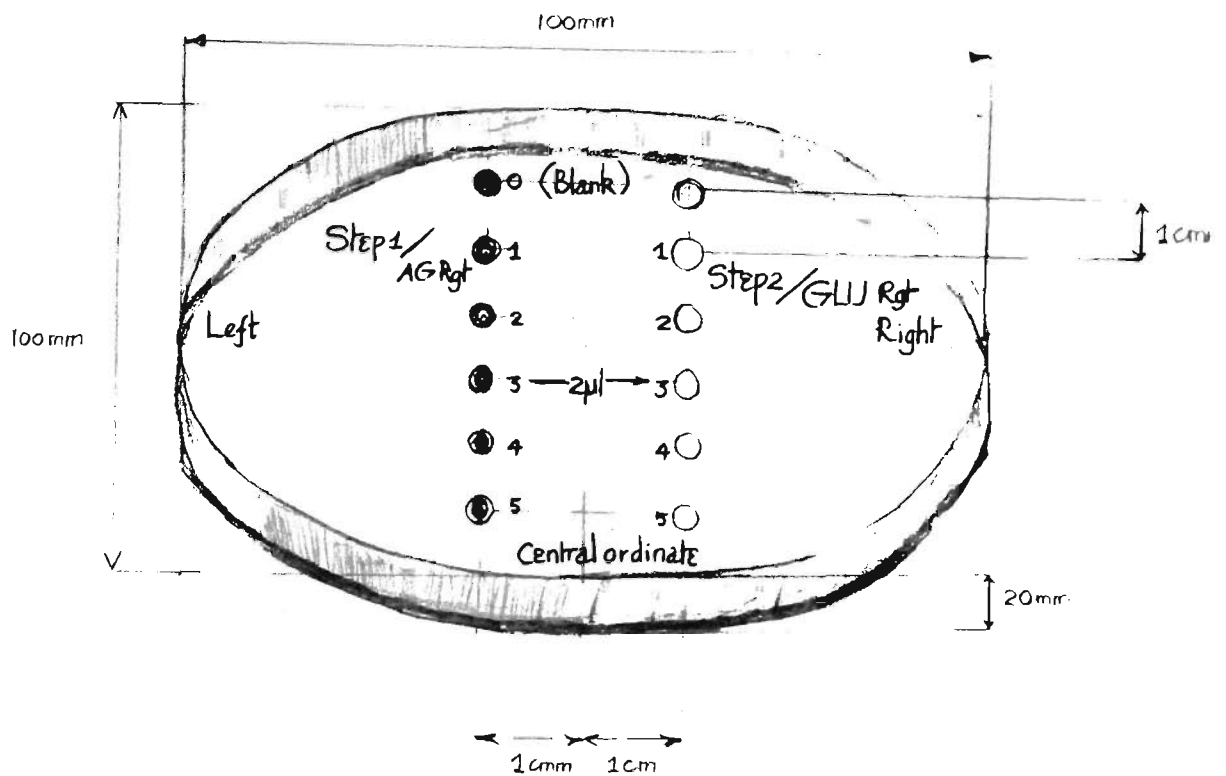


**Figure 2.3** Arrangement of reagent droplets on the bottom of a Petri dish, under a layer of oil. The droplets were used for constructing glycogen standard curves as described in section 2.2.2.2.

mixture for blank and glycogen standards in *Step 1* (AG reagent) and *Step 2* (GLU reagent) of the reaction (described in detail in section 2.2.2.4) were aligned at an equal distance (about 1 cm) from the axis of symmetry of the petri dish as illustrated in Fig. 2.3.

The strategy used to form reagent droplets under oil is described in Fig. 2.4. Briefly, this strategy involved the following steps: (i) the petri dish was placed on the stage of a dissecting microscope in such a way that the region intended for loading the droplet was located in the centre of the viewing field, (ii) the microtip containing the sample was inserted through oil at an angle of  $\sim 80^\circ$  (with reference to the plane of the petri dish) until it touched the bottom of the dish and a small fraction of the reaction solution was released slowly and gently until the fluid made contact with the dish, (iii) when the first tiny fraction of solution adhered to the bottom of the petri dish, the angle of the microtip was adjusted to  $\sim 45^\circ$  (this facilitated the formation of the droplet in the dome-shape) and the rest of the solution was delivered slowly until an air bubble was released from the tip. It is important to note that while the solution was delivered, the contact point between the microtip and the bottom of the petri dish was kept fixed to minimise the possibility of droplet spreading.

### 2.2.2.3 TRANSFER OF FLUID BETWEEN DROPLETS AND FROM A DROPLET TO THE MICROCELL

The transfer of minute volumes of solution between droplets involved two major steps: the withdrawal of fluid from one droplet and its delivery to another droplet.

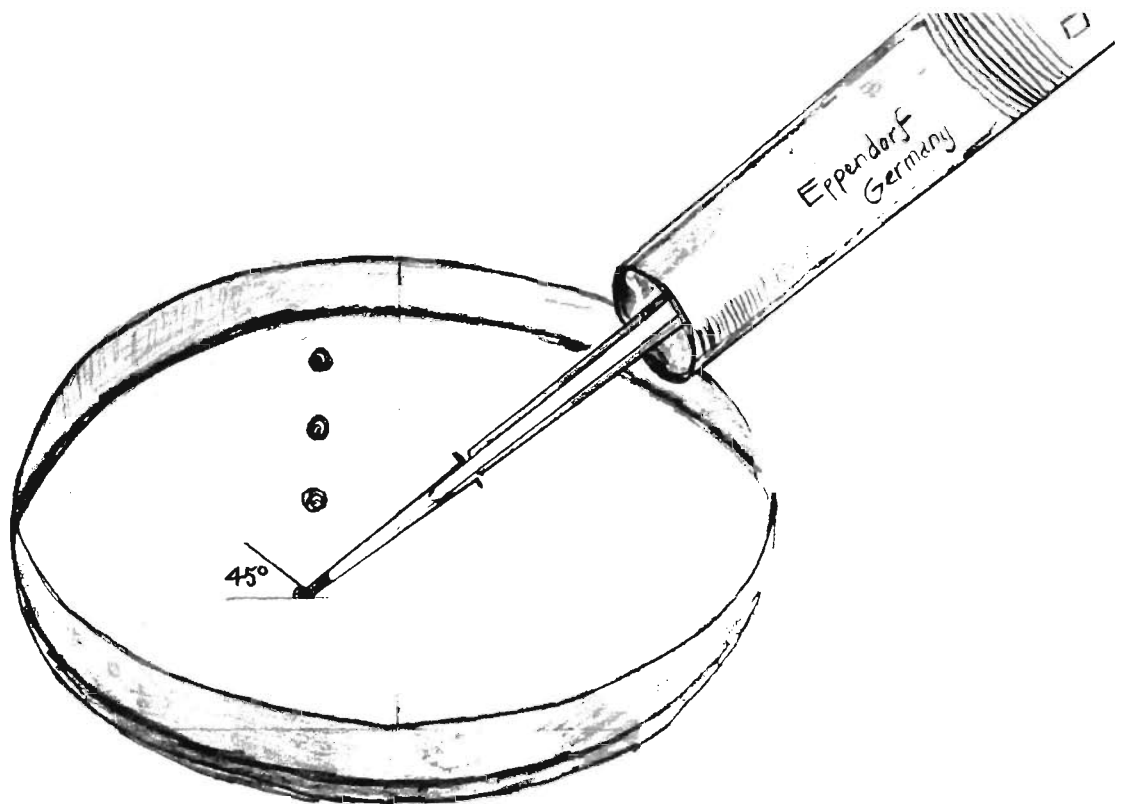


**Figure 2.4** Strategy used to form reagent droplets under oil, on the bottom of a petri dish. For details of the procedure refer to section 2.2.2.2. Note that the 45° angle refers to the angle between the plane of the dish and the plane of the tip opening.

The first step was carried out as follows (see Fig.2.5): (i) the micropipette with piston depressed and held at an angle of  $\sim 45^\circ$ , was brought into contact with the edge of the droplet, when the opening of the microtip touched the droplet a small fraction of solution was automatically drawn into the tip, and (ii) the piston of the pipette was slowly released while changing the angle of the microtip from  $45$  to  $\sim 80^\circ$ . Note that when withdrawing fluid from a droplet, the angle of the microtip was changed in the reverse direction to that used when forming the droplet. To avoid withdrawal of oil in the microtip, great care was taken to keep the microtip in continuous contact with the aqueous solution. The second step involved approaching the spherical surface of the receiving droplet with the microtip held at  $\sim 45^\circ$ . The point at which the microtip touched the droplet was indicated by the automatic withdrawal of a small fraction of solution from the receiving droplet into the microtip, at that point the piston of the micro-pipette was pressed very slowly to deliver the solution from microtip to the receiving droplet. Potential errors occurring at this stage included (i) disturbance of the dome of the receiving droplet if too much pressure was applied from the micro-pipette and (ii) the formation of another droplet in the oil phase if the microtip did not touch the receiving droplet and the fluid was delivered into the oil layer.

The sample ( $0.5-1.5 \mu\text{l}$ ) was transferred from the reaction droplet to the microcell using the micro-pipette. The first step in the transfer protocol i.e withdrawal of the sample from the reagent droplet was carried out as described in the previous paragraph. It was always observed that after the sample was withdrawn, a drop of oil remained attached to the microtip. This drop was removed by very careful wiping of

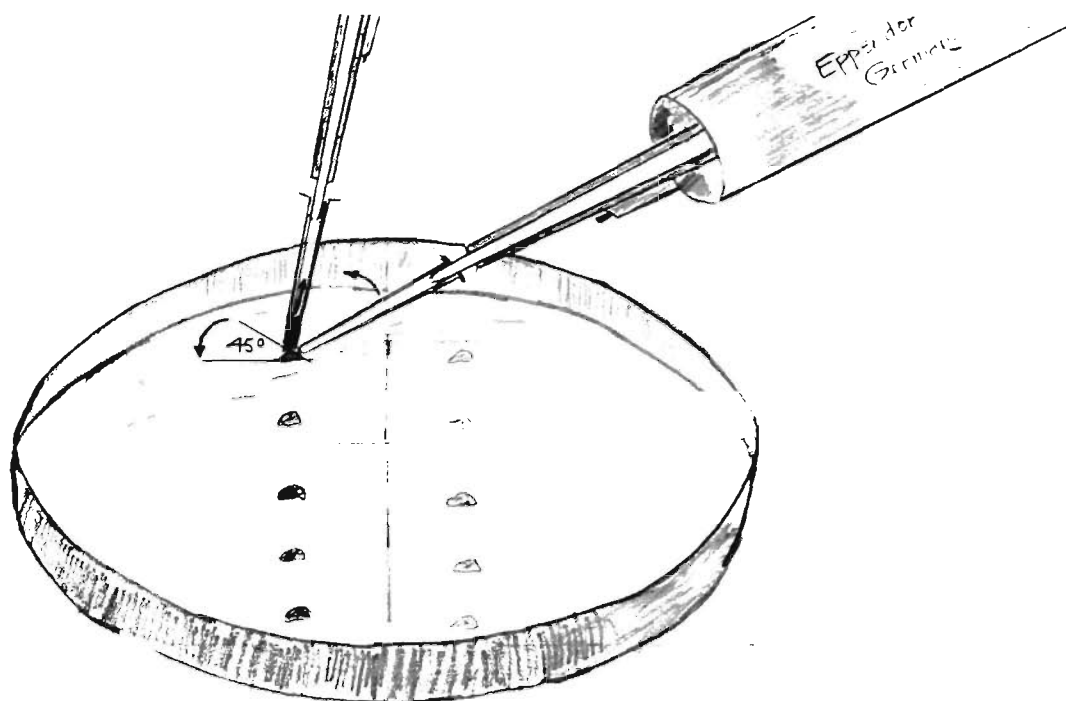


**Figure 2.5** The strategy used to withdraw solution from a reagent droplet located on the bottom of a petri dish, under a layer of oil. Details of the strategy are given in section 2.2.2.3. Note that the  $45^\circ$  angle refers to the angle between the plane of the dish and the plane of the tip opening.

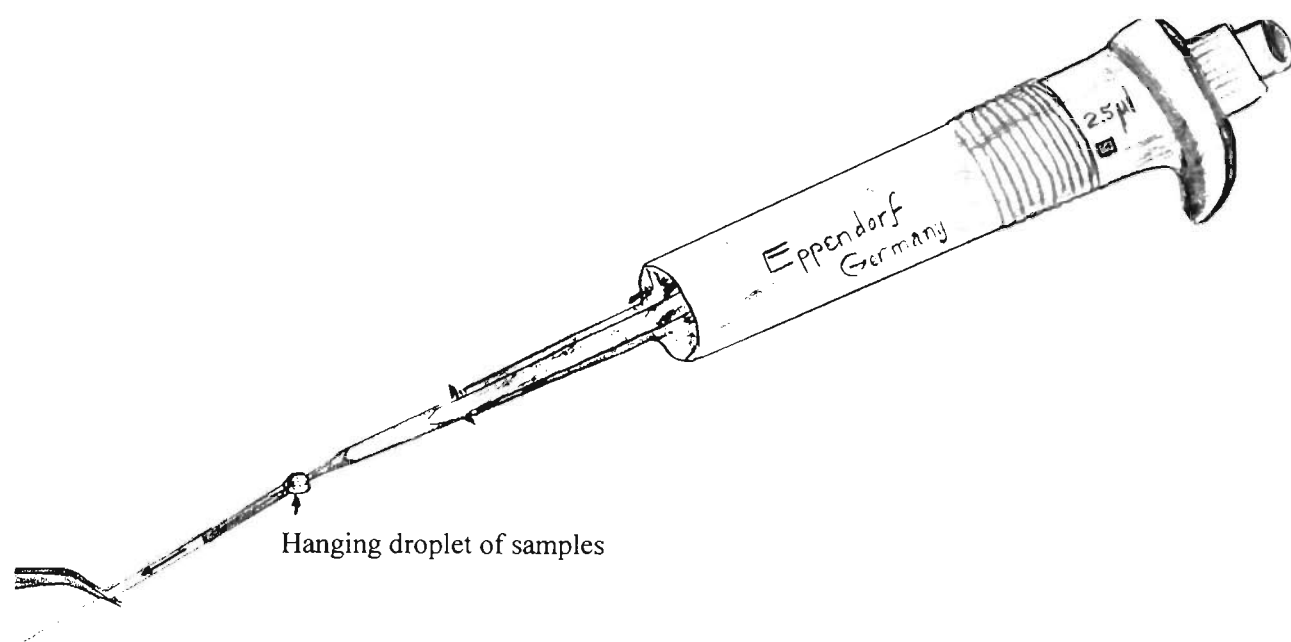


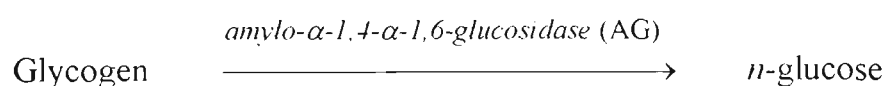
**Figure 2.6** Sample transfer, by capillarity, from the microtip into the microcell. See section 2.2.2.3 for details.

the microtip with an absorbing tissue such that the paper did not touch the opening of the tip at any time. The transfer of fluid between the microtip and microcell involved the release of a minute amount of sample which hung onto the microtip opening: the fluid in the tip was aspirated into the microcell by capillarity when the microcell was brought into contact with the droplet attached to tip (see Fig. 2.6).

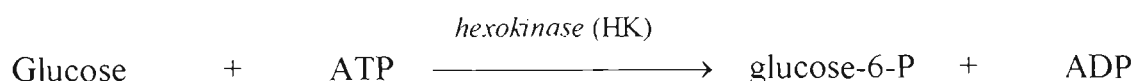
#### 2.2.2.4 CONSTRUCTION OF STANDARD CURVES FOR COMMERCIAL GLYCOGEN

Except when stated otherwise, the glycogen assay was carried out in two steps according to the analytical protocol of Passonneau and Lowry (1993):

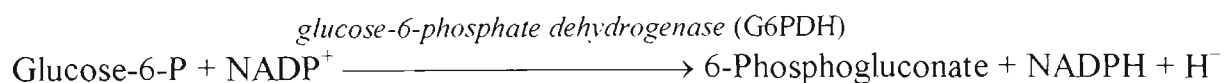
Step 1 / reaction 1.



Step 2 / reaction 2



Step 2 / reaction 3



All reactions were conducted at RT (19-25°C) in droplets formed under oil as described in detail in section 2.2.2.2.

These two reaction steps had to be conducted separately because (i) AG works best at a mild acidic pH (4.7-5.0), (ii) HK and G6PDH work best at neutral or slightly alkali pH (8.1-8.8) and (iii) NADPH is stable in alkali pH (8.1-9.0) (Passonneau and Lauderdale, 1974; Passonneau and Lowry, 1993).

*Composition and stability of the AG reagent.* Glycogen hydrolysis was carried out in a reaction cocktail containing 100 mM sodium acetate buffer, pH 5.0, 2.5 mM Tris (optional; see later), 0.002% BSA (optional; see later) and 0.14 U/ml (10 µg/ml) *amyl $\alpha$ -1,4- $\alpha$ -1,6-glucosidase* (AG reagent). The enzyme was added as a 10 × stock solution [100 mM sodium acetate buffer, pH 5.0, and 1.4 U/ml (100 µg/ml) *amyl $\alpha$ -1,4- $\alpha$ -1,6-glucosidase*]; the stock solution was prepared and stored for up to three weeks at 4°C or was prepared freshly on the day of the experiment. In the former case the enzyme stock solution also included 25.0 mM Tris and 0.02% BSA, because these compounds have been shown to maintain the AG activity upon long storage times (Passonneau and Lauderdale, 1974).

It is important to note that when kept at RT the AG reagent was stable for up to 24 hours. This allowed the author of this study to prepare AG reagent droplets, under oil, several hours prior to use.

*Composition and stability of the GLU reagent.* The GLU reagent contained 676 mM Tris-HCl, pH 8.8, 5 mM MgCl<sub>2</sub>, 0.1 mM DTT, 0.8 mM NADP<sup>+</sup>, 0.8 mM ATP, 0.34 U/ml (2.4 µg/ml) hexokinase and 0.64 U/ml (1.6 µg/ml) glucose-6-phosphate dehydrogenase. The GLU reagent, prepared from a number of stock solutions, was

stored at 4°C and used within one week. The stock solutions included: 1M Tris-HCl, pH 8.8; 50 mM MgCl<sub>2</sub> (stored at 4°C), 0.2M DTT (stored at -20°C); 10 mM NADP<sup>-</sup> and 10 mM ATP (both stored at -85°C). The enzymes were added to the reaction cocktail, directly from commercial bottles, on the day of the experiment.

The standard curve for commercial glycogen was constructed as follows:

*Step 1 (AG reaction)* In this step, reactions were carried out in 10 µl droplets, under oil, as described in section 2.2.2.2. Solutions were added in the following order: sodium acetate buffer, glycogen stock and enzyme stock; the volumes used are summarised in Table 2.1. The droplets were incubated at RT for 120 min.

*Step 2 (HK/G6PDH reaction)* Five minutes before stopping the AG reaction, six 8 µl-droplets of GLU reagent were lined up in parallel with the AG reagent droplets. Then 2 µl samples were transferred from each of the AG reaction droplets into the corresponding HK/G6PDH reaction droplets as described in section 2.2.2.3.

The two solutions in the droplets were mixed by slowly and carefully aspirating/releasing the fluid into/from the microtip until the opaque solutions transferred from the step 1-droplets appeared to be totally dispersed into the GLU reagent. The petri dish containing these droplets was incubated at RT for a further 20 min. At the end of this period, blank and standard solutions were aspirated into microcells as illustrated in Fig. 2.6. The fluorescence signals of blank and standards

were measured immediately using the instrumental set up and the procedures described in section 2.2.2.1.

**Table 2.1. Composition of standard solutions in step 1**

Amount of Glycogen in 25 nl (pmol)	Na-acetate buffer (100 mM), $\mu$ l	Glycogen stock solution (10 mM), $\mu$ l	Enzyme stock solution, $\mu$ l
0	9	0	1.0
2.5	8.5	0.5	1.0
5.0	8.0	1.0	1.0
7.5	7.5	1.5	1.0
10.0	7.0	2.0	1.0
12.5	6.5	2.5	1.0

#### 2.2.2.5 CONSTRUCTION OF STANDARD CURVES FOR GLUCOSE

Glucose standard curves were constructed to verify the completion of glycogen hydrolysis by AG in reaction step 1. The reactions employed in constructing these curves were carried out using exactly the same protocol as that described for commercial glycogen. Thus, in *Step 1*, 5 – 25 nmol of glucose were mixed with AG reagent (final volume 10  $\mu$ l) without incubation; in *Step 2*, 2  $\mu$ l aliquots of the step-1 mixture were transferred to 8  $\mu$ l GLU reagent droplets and incubated at RT for 20 min. At the end of *Step 2*, samples were processed as described in the section concerned with the construction of glycogen standard curves (see section 2.2.2.4).

#### 2.2.2.6 CONSTRUCTION OF STANDARD CURVES FOR NADPH

The completion of the HK/G6PDH reactions in the analytical protocol for glycogen determination was checked by comparing the slopes of glucose and NADPH standard curves. Experiments for constructing NADPH standard curves were carried out at RT, in the instrument room illuminated only by the microscope lamp to minimise the bleaching of NADPH fluorescence. Briefly, 5 – 25 nmol of NADPH were quickly mixed, without incubation, with AG reagent (final volume 10  $\mu$ l) (*Step 1*). In *Step 2*, 2  $\mu$ l aliquots of NADPH/AG reagent mixtures were rapidly transferred to 8  $\mu$ l GLU reagent droplets. The final solutions were quickly aspirated into microcells and their fluorescence signals were immediately recorded as described in section 2.2.2.4.

#### 2.2.3 STATISTICAL ANALYSIS

All fluorescence measurements were performed in triplicate. Unless otherwise stated, the data were expressed as means  $\pm$  SE. Student's *t*-test was used to compare two groups of data and one-way Anova (Bonferoni post-test) was used to compare several groups of data.

## 2.3 RESULTS

### 2.3.1 OPTIMISATION OF REACTION CONDITIONS FOR GLYCOGEN ANALYSIS

#### 2.3.1.1 AG REACTION

The reaction conditions for Step 1 were optimised with respect to: (i) enzyme (AG) concentration, (ii) pH and (iii) time.

*AG concentration.* In their original protocol, Passonneau and Lauderdale (1974) used 0.4 µg/ml (0.0056 U/ml) to break down glycogen in the range 0 to 10 nmoles. More specifically, these authors used 50 ng of AG to breakdown 0 to 10 nmoles glycogen (i.e. a minimum of 5 ng AG/nmol glycogen) in 130 µl reaction cocktail.

In the microfluorometric method developed in this study, the amount of glycogen used to construct the standard curve ranged between 0 and 25 nmoles and the reaction was carried out in volumes  $\leq 10$  µl. In order to find the optimal AG concentration for this range of glycogen amounts, 25 nmoles of glycogen were incubated with varying amounts of AG (in the range 0.4 - 10 ng/nmol glycogen) in 100 mM acetate buffer, pH 4.7 (final volume 10 µl) for 150 min at RT. At the end of the incubation period, a 2 µl aliquot of AG/glycogen mixture was transferred to 8 µl of GLU reagent and incubated for a further 20 min at RT. The final mixture was immediately aspirated into a microcell and fluorescence signals were recorded.

In Fig. 2.7 are shown the data from 9 independent experiments. The intensity of fluorescence signals (indicative of the amount of glycogen broken down) produced by the sample containing different amounts of AG increased gradually up to 4 ng AG/nmol glycogen (10  $\mu\text{g/ml}$  or 0.14 U/ml) and remained constant thereafter.

*pH.* The effect of  $[\text{H}^+]$  on the AG reaction was investigated by varying the pH of the reaction cocktail over the range 4.7 to 6.1. Commercial glycogen (25 nmoles) was incubated for 150 min at RT in 10  $\mu\text{l}$  reaction cocktail containing 100 mM Na-acetate buffer (pH 4.7 - 6.1) and 100 ng *amyl $\alpha$ -1,4- $\alpha$ -1,6-glucosidase*. At the end of the 150 min-incubation period, a 2  $\mu\text{l}$  aliquot of Step 1 mixture was transferred to 4 volumes (8  $\mu\text{l}$ ) of GLU reagent and incubated for another 20 min at RT. As shown in Fig. 2.8, the intensity of fluorescence signals produced by the glycogen sample at different pHs did not vary significantly between pH 4.7 and pH 5.3 but decreased significantly at  $\text{pH} \geq 5.6$ .

*Time course.* The time course of the AG reaction was studied by incubating 25 nmol commercial glycogen with 100 ng *amyl $\alpha$ -1,4- $\alpha$ -1,6-glucosidase* (4 ng AG/nmol of glycogen) in 100 mM Na-acetate, pH 5.0 (final volume 10 $\mu\text{l}$ ) for 15 to 150 min. All incubations were carried out at RT. At the end of each incubation period, a 2  $\mu\text{l}$  aliquot of the reaction mixture was transferred to 8  $\mu\text{l}$  GLU reagent and incubated for another 20 min at RT. Results obtained from 9 independent experiments show (see Fig. 2.9) that an increase in the incubation time from 15 to 120 min was accompanied by a gradual increase in the fluorescence signal produced by the sample. No further increase was observed when the incubation time was extended from 120 to 150 min.

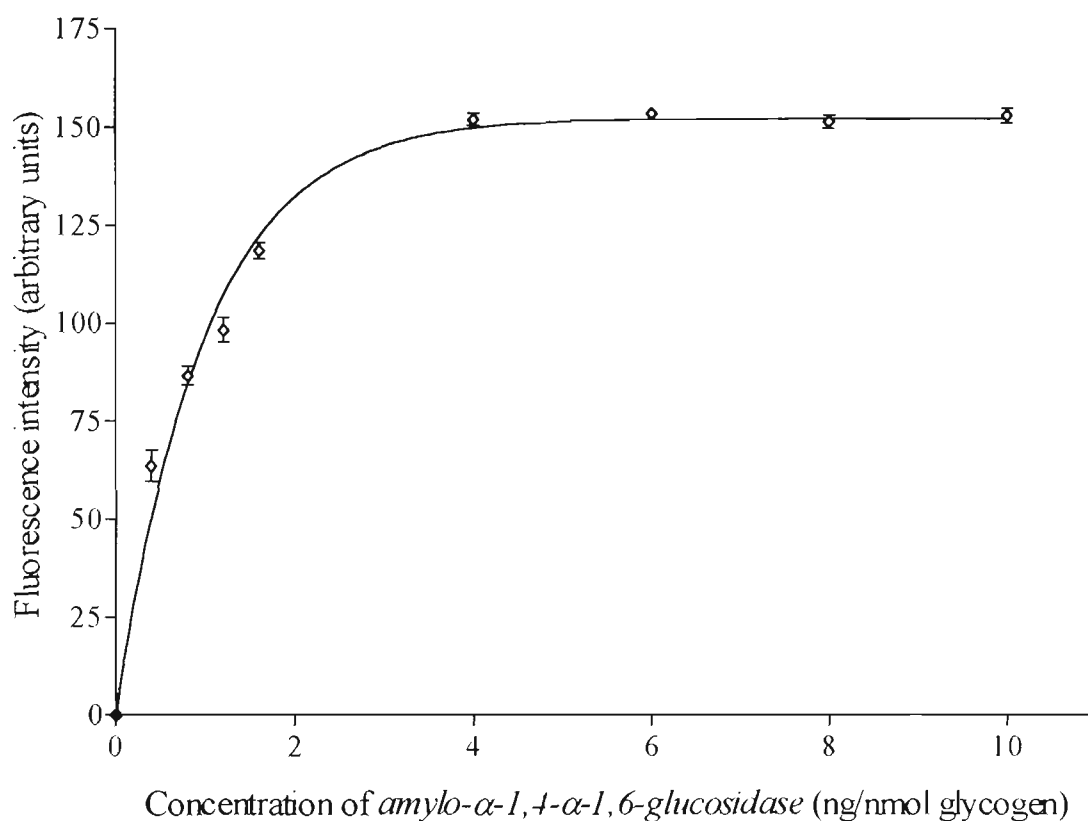


**Figure 2.7.** The relationship between the concentration of *amylo- $\alpha$ -1,4- $\alpha$ -1,6-glucosidase (AG)* and the intensity of fluorescence signals.

The sample contained 25 nmol glycogen. The amount of AG was varied from 10 to 250 ng (0.4 to 10 ng per nmol of glycogen) equivalent with 1 to 25  $\mu\text{g/ml}$  of AG or 0.014 to 0.35 U/ml of AG. Glycogen was incubated in AG reagent at pH 4.7 for 150 min at RT. Data were mean  $\pm$  SE obtained from 9 independent experiments and error bars represent 95% confidence intervals for 9 replicates. The curve was fitted to measured data by one phase exponential association:  $y = 153.1(1 - e^{-Kx})$ , where  $K = 1.005$ . Goodness of fit:  $R^2 = 0.9714$ .  $S_{y \cdot x} = 8.635$ .

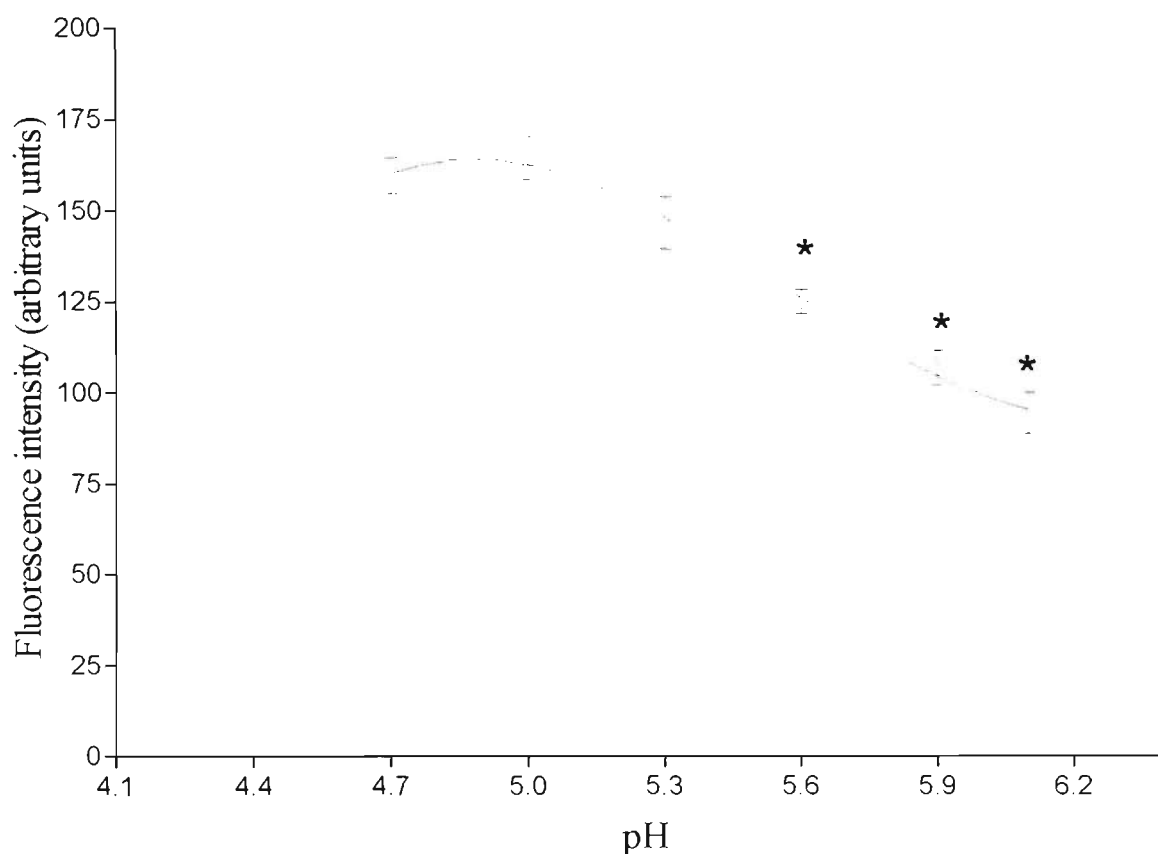


**Figure 2.8.** The relationship between the intensity of fluorescence signals and the pH of *step 1*-reaction solution. Data were collected from nine independent experiments in which 25 nmol of commercial glycogen was incubated in the reagent containing 100 mM Na-acetate, 100 ng of *amyl $\alpha$ -1,4- $\alpha$ -1,6-glucosidase*, and the pH of solution was varied from 4.7 to 6.1. The mixture was incubated at RT for 150 min. An aliquot of 2  $\mu$ l was then transferred into 8  $\mu$ l of GLU reagent and the fluorescence signals were recorded after 20 min at RT. The results show mean  $\pm$  SE, the error bars represent 95% confidence intervals for 9 replicates. The curve was fitted with measured data by polynomial – third order:  $y = -8904 + 5022x - 915.8x^2 + 54.83x^3$ ,  $R^2 = 0.7377$ ,  $S_{y \cdot x} = 16.14$ . \*: significant difference from the first three data point ( $P < 0.05$ ).

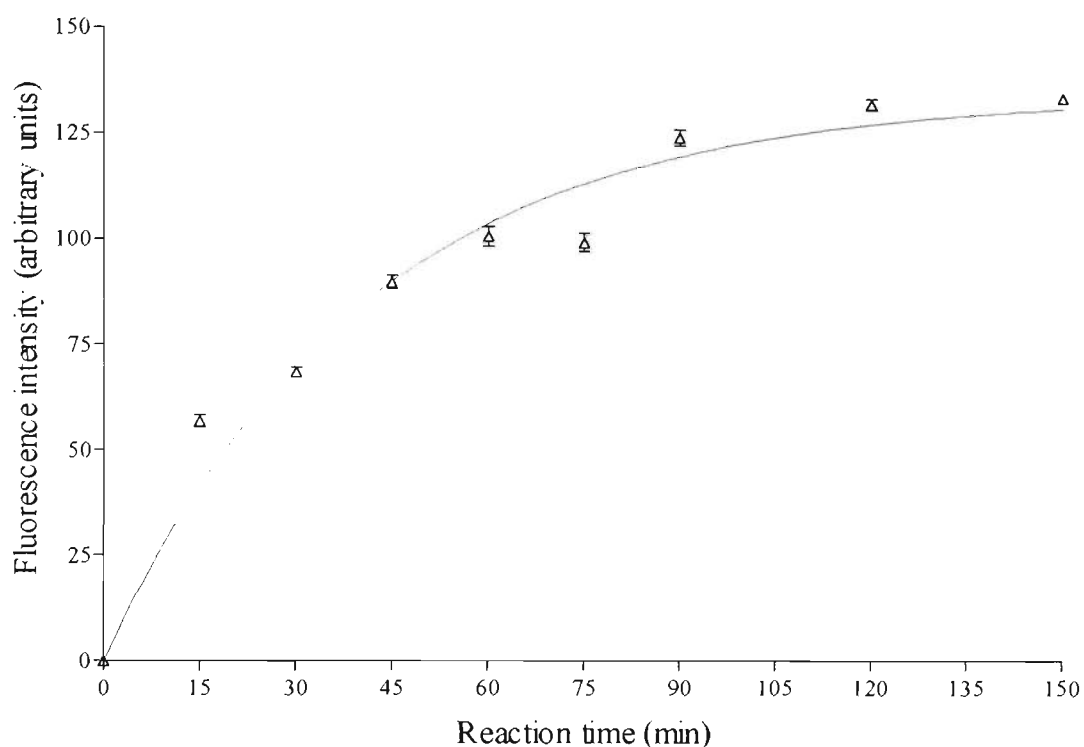


**Figure 2.9** The time course of the glucosidase reaction with commercial glycogen as substrate.

A 25 nmol sample of commercial glycogen (rabbit liver) was incubated at RT in 10  $\mu$ l of AG reagent containing: Na-acetate, 100 mM, pH 5.0; 100 ng *amyl $\alpha$ -1,4- $\alpha$ -1,6-glucosidase*, for a specified period of time, from 15 to 150 min. At the end of each period of incubation, 2  $\mu$ l of the step 1 mixture was transferred into 8  $\mu$ l of GLU reagent and incubated for a further 20 min. Results show means  $\pm$  SE collected from 9 independent experiments. Error bars represent 95% confidence intervals for 9 replicates. The curve was fitted with measured data by one phase exponential association:  $y = 2.586(1 - e^{-Kx})$  where  $K = 0.0247$ . Goodness of fit:  $R^2 = 0.9548$ ,  $S_{y,x} = 8.748$ .

### 2.3.1.2 HK/G6PDH REACTIONS (STEP 2)

The time course of *hexokinase/glucose-6-phosphate dehydrogenase* reactions was examined by using commercial glucose as the substrate. An aliquot of 2  $\mu$ l of glucose solution containing 5 nmoles glucose was transferred to 8  $\mu$ l of GLU reagent (see Methods and Materials for composition) and incubated at RT for 10 - 50 min. Results collected from nine independent experiments show (see Fig. 2.10) that the fluorescence signal produced by the sample (indicative of the amount of NADPH generated in Step 2) reached maximum intensity by 20 min. Since sample fluorescence did not increase beyond 20 min, it was concluded that at 20 min, the two reactions occurring in Step 2 were completed.

## 2.3.2 CONSTRUCTION OF STANDARD CURVES

### 2.3.2.1 ANALYTICAL RANGE FOR NADPH DETERMINATION

The standard calibration curve for NADPH shown in Fig. 2.11A was generated, using the protocol described under Materials and Methods, from data collected in six independent sets of measurements when a 1-mm section of the microcell, corresponding to a volume of 25 nl, was illuminated. The values on the abscissa are picomoles NADPH in the illuminated volume. The fluorescence signal is directly proportional to the amount of NADPH ( $r^2 = 0.998$ ,  $S_{y,x} = 2.995$ ) in the range 0 to 12.5 pmol. The detection limit, defined as the amount of NADPH corresponding to 3 SD of the blank value (Bergmeyer *et al.*, 1983), is 0.17 pmol in the illuminated volume (25 nl).

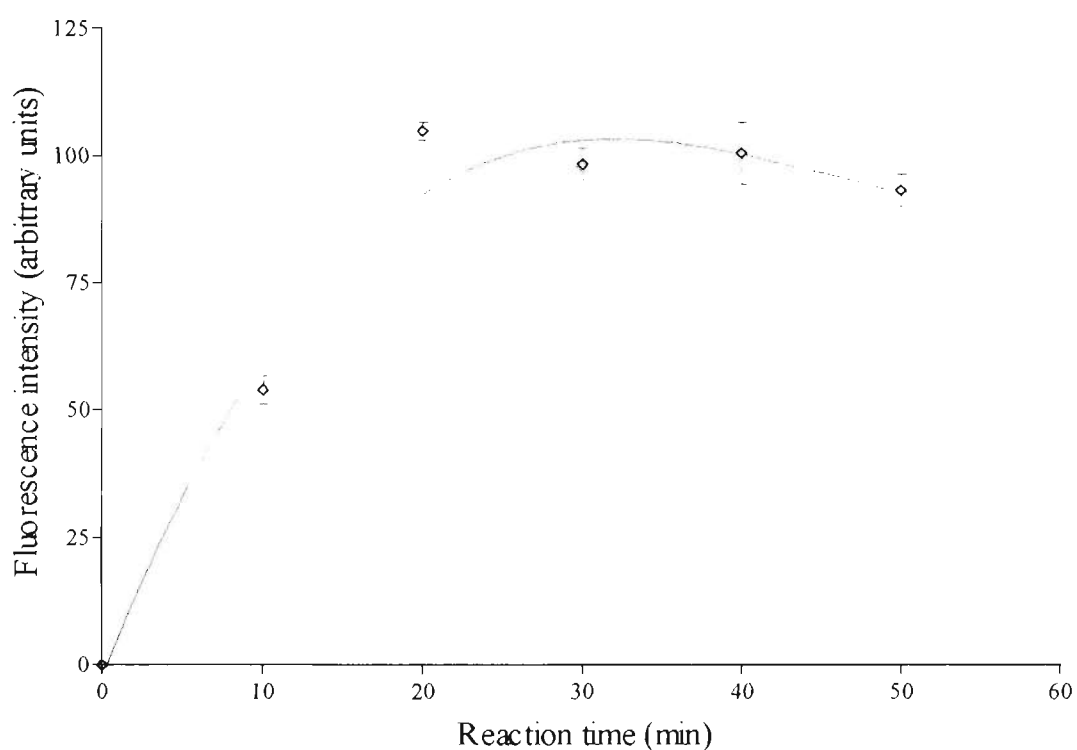


**Figure 2.10** The time course of the hexokinase/glucose-6-phosphate dehydrogenase reactions (Step 2) with glucose as substrate. A 2.5 mM solution was prepared in AG solution and 2  $\mu$ l aliquot (25 nmol glucose) of this mixture was incubated with four volumes (8  $\mu$ l) of GLU reagent at RT (19-25°C) in specified period of time. Data (mean  $\pm$  SE) were collected from nine independent experiments. Error bars represent 95% confidence intervals for 9 replicates. The curve was fitted with measured data by polynomial – third order:  $y = -2.454 + 8.061x - 0.1929x^2 + 0.0014x^3$ . Goodness of fit:  $R^2 = 0.8409$ ,  $S_{y,x} = 15.32$ .

### 2.3.2.2 ANALYTICAL RANGE FOR GLUCOSE AND GLYCOGEN DETERMINATION

As described in Materials and Methods, all reactions leading to the enzymatic transformation of standard commercial glycogen and the stoichiometric production of NADPH were carried out in small volumes ( $\leq 10 \mu\text{l}$ ) of enzyme reagent reactions. This strategy minimises metabolite dilution and reduces the need for additional fluorochrome amplification steps.

To ensure the complete conversion of glycogen to glucose over the range of interest (2.5 to 12.5 pmol), it was necessary to incubate the glycogen sample with 10  $\mu\text{l}$  AG reagent for 120 min. The fluorescence signals produced by glycogen after being subjected to the two reaction steps compared with the fluorescence signals produced by a series of equivalent amounts of glucose subjected to reaction step 2 only (Fig. 2.11B), indicates that the two sets of fluorescence signals are almost identical. This confirms the completion of glycogen hydrolysis by AG under the conditions employed in this study.

From the time course of the reaction in step 2 (see section 2.3.1.2) it was estimated that, under the conditions described, the complete conversion of a given amount of glucose (2.5 nmol in a 10- $\mu\text{l}$  reaction mixture) to NADPH was achieved after 20 min incubation with HK and G6PDH. Again, this was confirmed by the high degree of similarity between the fluorescence signal values produced by a series of glucose

solutions (2.5 – 12.5 pmol) after incubation with the HK/G6PDH mixture and by a series of equivalent amounts of NADPH (Fig. 2.11C).

The calibration curve for glycogen which was generated from data collected in three (range, 0 – 2 pmol) and nine (range, 2.5 – 12.5 pmol) independent experiments, using commercial glycogen and the protocol described in Materials and Methods, is shown in Fig. 2.11D. The fluorescence signals are proportional to the amount of glycogen in the 0 – 12.5 pmol range (in the final sample). The detection limit for glycogen, defined as the amount of glycogen corresponding to 3 SD of the blank value, was estimated to be 0.16 pmol in 25 nl, a value which is essentially the same as that determined for NADPH.

### 2.3.2.3 VERIFICATION OF THE MICROFLUOROMETRIC METHOD FOR GLYCOGEN DETERMINATION

To verify the accuracy of the microfluorometric method for glycogen determination described in this study, the glycogen concentration in crude extracts prepared from whole muscles was determined using both the microfluorometric method and a conventional fluorometric method. The value of the ratio of glycogen concentration determined by the two methods ( $[\text{glycogen}]_{\text{microfluoro}}/[\text{glycogen}]_{\text{fluoro}}$ ) was  $0.937 \pm 0.029$  (mean  $\pm$  SE;  $n = 4$ ). This value is not statistically different from 1 ( $P > 0.05$ ; two-tail  $t$  test), indicating a high degree of similarity between the two sets of values and thus validating the accuracy of the microfluorometric method.

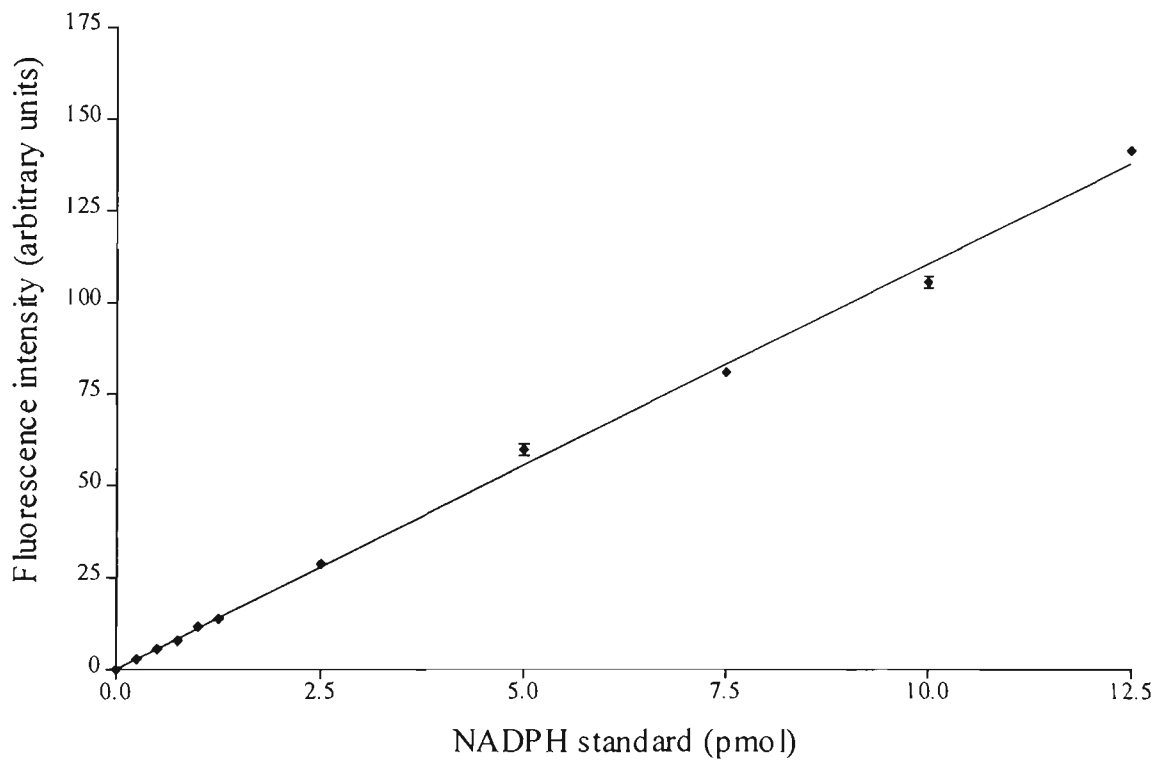


**Figure 2.11A Standard calibration curve for NADPH** illustrates the linear relationship between the fluorescence intensity and the amount of NADPH (pmol) in a 1-mm section of the microcell corresponding to a volume of 25 nl ( $r^2 = 0.998$ ,  $S_{y.x} = 2.995$ , slope = 10.69). Results are means  $\pm$  SE of six separate determinations. Error bars represent 95% confidence intervals for 6 replicates.

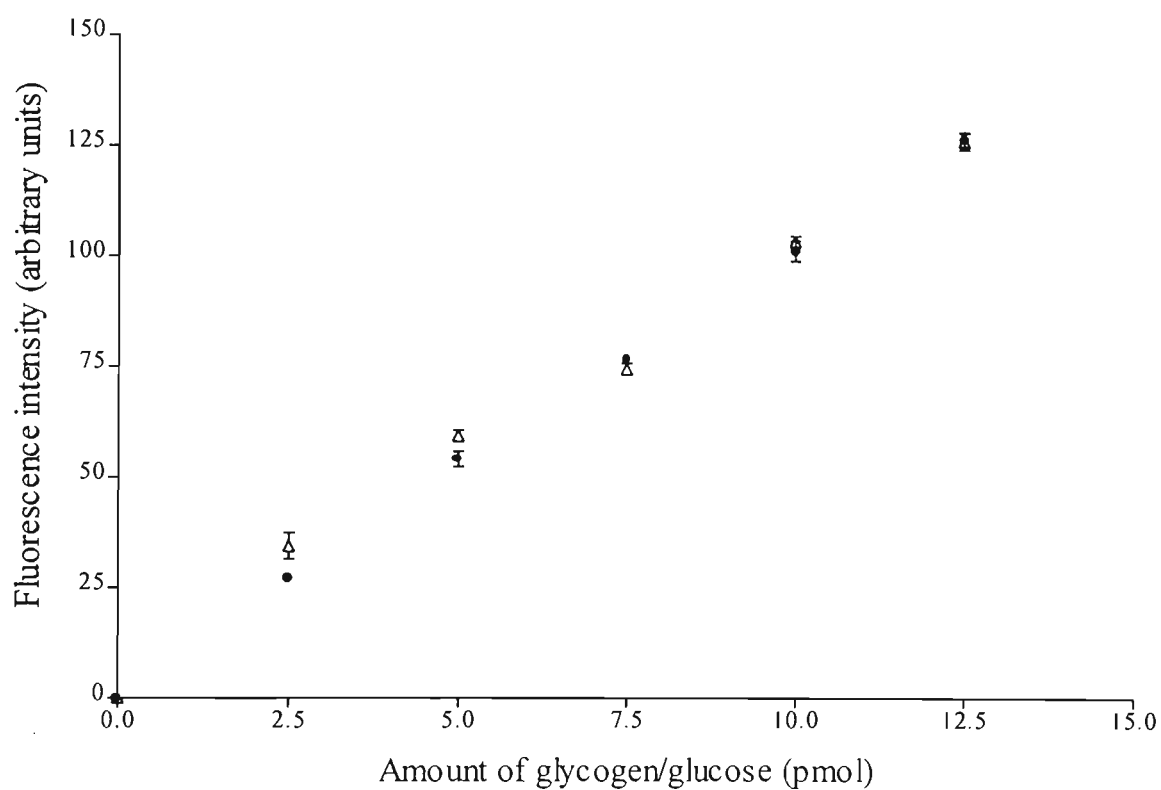


**Figure 2.11B** Comparison of the fluorescence signals produced by a series equivalent amounts of glycogen (as anhydrous glucosyl units) (●) ( $S_{y,x} = 2.864$ , slope = 10.42) and glucose (Δ) ( $S_{y,x} = 5.902$ , slope = 10.71). Results are means  $\pm$  SE of nine separate determinations. Error bars represent 95% confidence intervals for 9 replicates.

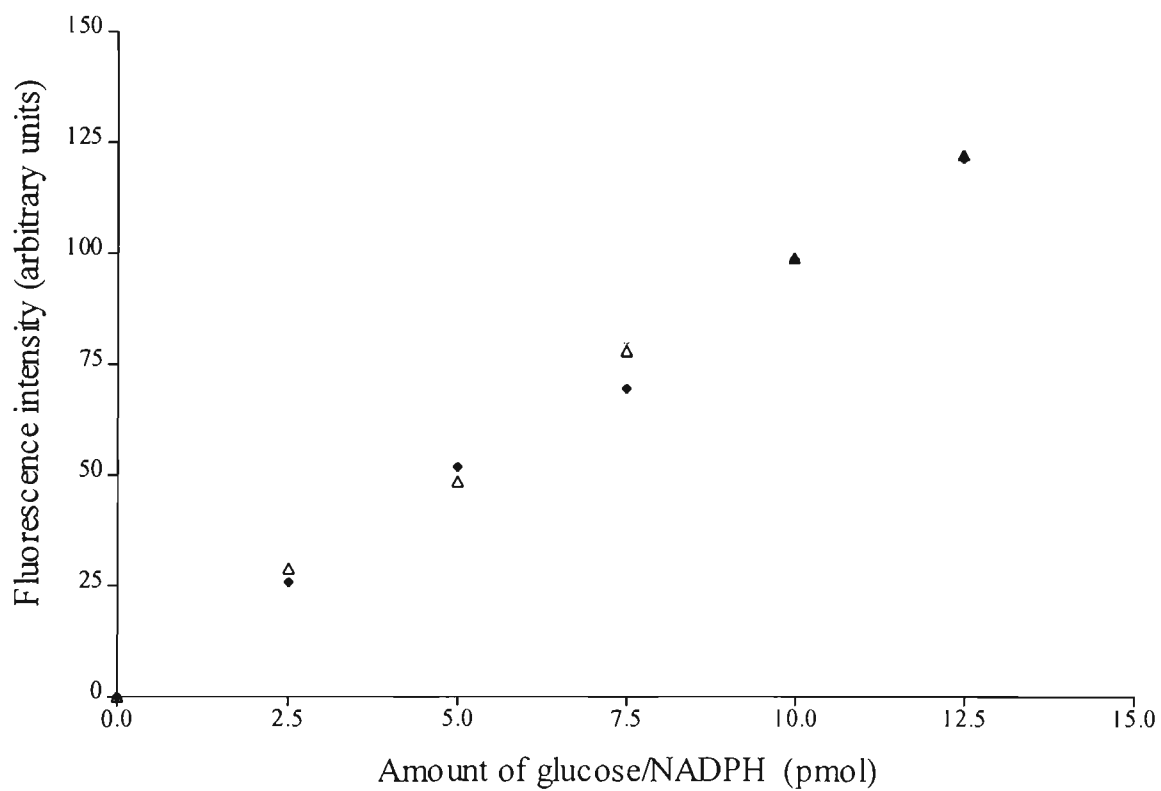


**Figure 2.11C** Standard calibration curves for commercial glucose and NADPH were constructed by a series of equivalent amounts of glucose ( $\Delta$ ) ( $S_{y,x} = 2.778$ , slope = 10.18) and NADPH ( $\blacklozenge$ ) ( $S_{y,x} = 2.281$ , slope = 9.946). Results are means  $\pm$  SE of 3 – 18 separate determinations. Error bars represent 95% confidence intervals for 3 – 18 replicates.

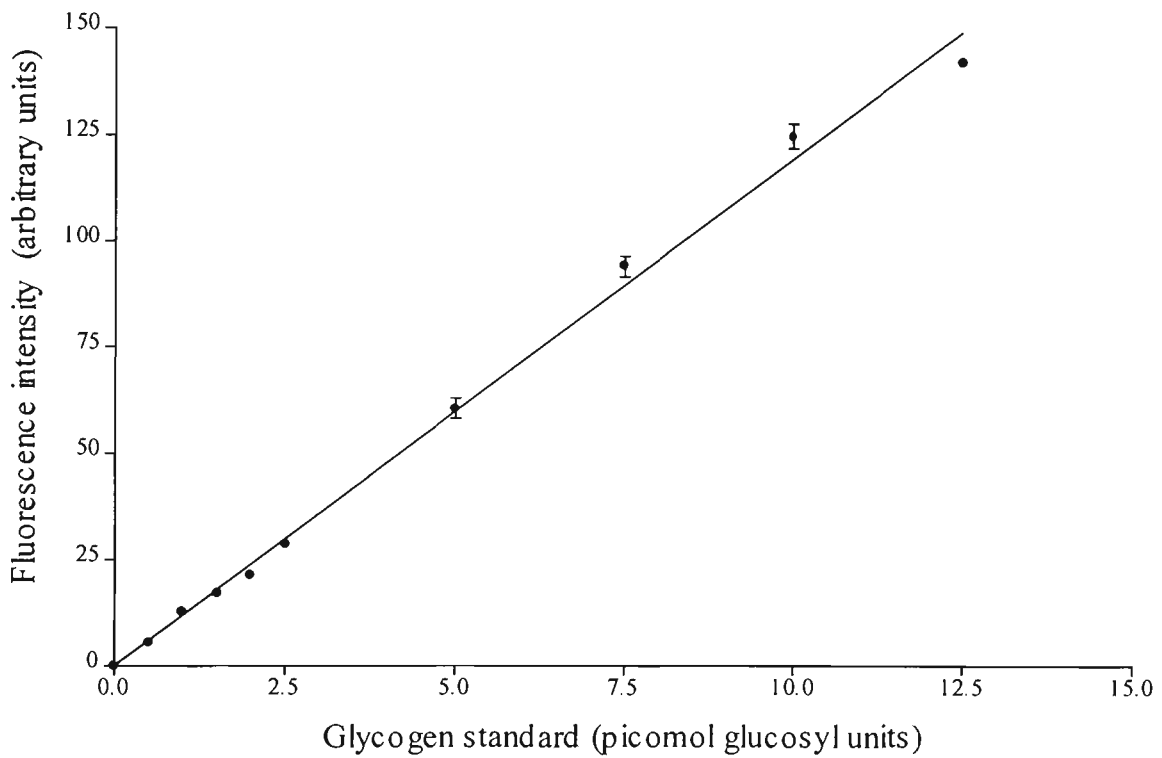


**Figure 2.11D** The linear relationship between the amount of commercial glycogen (as picomol anhydrous glucosyl units) and fluorescence intensity in the microfluorometric method ( $S_{y,x} = 6.187$ , slope = 11.25). Results are means  $\pm$  SE of 3-18 independent determinations. Error bars represent 95% confidence intervals for 3 replicates (data below 2.5 pmol) and 18 replicates (all data above 2.5 pmol).

## 2.4 DISCUSSION

The analytical method described here for measuring glycogen in solutions of commercial glycogen (rabbit liver) is a modified version of the *ultra-sensitive fluorometric* method (detection limit: 1 pmol; analytical range: 1-10 pmol) of Passonneau and colleagues (Passonneau and Lauderdale, 1974; Passonneau and Lowry, 1993).

It is important to note that the *microfluorometric* method developed in this study resembles the ultra-sensitive method of Lowry's group with respect to:

- (i) the analytical principle
- (ii) the reaction times for the two reaction steps and
- (iii) the composition of reaction cocktails.

The detection system used in the *microfluorometric* method, on the other hand, comprises an epifluorescence microscope and a photomultiplier chart recorder, instead of a conventional fluorometer. This system allows measurement of fluorescence signals produced from the illumination of a 25-nl volume of sample contained in rectangular microcells. By reducing the volume of reagents in the analytical steps to less than 10  $\mu$ l and the size of the sample used for fluorescence measurements to smaller than 1  $\mu$ l, the microfluorometric method developed in this study was capable of determining subpicomol amounts of glycogen without

amplifications of pyridine nucleotides in the final products (NADPH) through chemical or enzymatic manipulation. As a result, the whole procedure was performed in less than two and half hours. This rapid, highly sensitive microfluorometric method was subsequently used to determine glycogen concentrations in single fibres from four different skeletal muscles of the cane toad *Bufo marinus* (Chapter 3) and in single fibres tested for responsiveness to depolarisation induced activation (Chapter 4).

## CHAPTER 3

# **Microfluorometric analyses of glycogen in freshly dissected, single skeletal muscle fibres of the cane toad using a mechanically skinned fibre preparation**

### 3.1 INTRODUCTION

As already mentioned in the General Introduction, there is compelling evidence that the mechanical performance of skeletal muscles is positively correlated with the intracellular glycogen content (Fitts, 1994; Bergström *et al.*, 1967), but the molecular mechanism underlying this relationship is still unknown. Previous studies have shown that the glycogen content varies greatly between individual muscle fibres (for review see Brown, 1994). Therefore it is not possible to study the correlation between glycogen content and contractile function using multicellular preparations such as whole muscles or bundles of muscle fibres. There is also evidence that in skeletal muscle, glycogen is present in different molecular forms, which can be distinguished by solubility in acidic solutions (Jansson, 1981) or by molecular weight (Alonso *et al.*, 1995). However, no information is available about the specific roles played by these molecular forms of glycogen in muscle contractility. Clearly, the fibre-related variability in glycogen content and the

molecular heterogeneity of muscle glycogen have to be considered in any research concerned with the mechanism by which glycogen affects skeletal muscle contractility.

At the start of the present study, the most widely used method for determining glycogen (as well as other intermediate metabolites and enzymes) in single fibres of skeletal muscle was that developed and refined in Lowry's laboratory (Michel *et al.*, 1994; Hintz *et al.*, 1982; Lust *et al.*, 1981; Hintz *et al.*, 1980; Nassar-Gentina, 1978; Lowry *et al.*, 1978; Lust *et al.*, 1975). The method, as used by the author of this thesis when visiting Lowry's laboratory in 1998, involves the following steps:

- (i) the muscle, dissected in a cold chamber ( $-20^{\circ}\text{C}$ ), is rapidly freeze-clamped with aluminium tong, pre-cooled in liquid Freon-12, and immediately placed into liquid Freon-12,
- (ii) the frozen muscle is placed in a freeze dryer (30 gauge,  $-30^{\circ}\text{C}$ ) for 48 hours
- (iii) the freeze-dried muscle is cut, in a cold chamber, into 1-cm long pieces, which are then placed back in the freeze dryer for another 48 hours; when totally dry, the muscle pieces are placed in a vacuum glass cell and stored at  $-80^{\circ}\text{C}$  until used
- (iv) single fibre segments are dissected from freeze-dried muscle pieces in a room in which the temperature ( $20^{\circ}\text{C}$ ) and humidity (50%) are rigorously controlled
- (v) the linear density (mass/length) of freeze-dried single fibre segments is determined using a fish-pole balance and a microscale to weigh and measure the fibre segment, respectively

- (vi) the glycogen content in freeze-dried fibre segments is determined by the ultra-sensitive fluorometric method described in section 2.1.

The whole procedure, which includes the preparation of single fibre segments and the completion of the analytical protocol would take on average 5 days.

The broad aim of the study presented in this chapter was to apply the rapid microfluorometric method described in Chapter 2 for determining the glycogen content of freshly dissected, single skeletal muscle fibres. More specifically, it was of interest to investigate the issue of glycogen heterogeneity at a single fibre level and to quantify the glycogen content of mechanically skinned muscle fibre preparations from iliofibularis, pyriformis, cruralis and sartorius muscles of the cane toad *Bufo marinus*.

## 3.2 MATERIALS AND METHODS

### 3.2.1 ANIMALS AND CHEMICALS

#### 3.2.1.1 ANIMALS

Male and female cane toads (*Bufo marinus*) weighing 40 – 350 g, which had been collected by the supplier (Peter Krauss Ltd) at two different locations (Coastal North Queensland – summer toads; Gulf of Carpentaria – winter toads), were kept, unfed, at 16-21°C for up to four weeks before use. Toads were doubly pithed after a comatose state was induced by one hour exposure to 4°C. All experimental procedures involving toads were approved by the Animal Experimentation and Ethics Committee at Victoria University of Technology.

#### 3.2.1.2 CHEMICALS

The chemicals used in the work presented in this chapter include all those listed in Chapter 2 and HDTA (hexamethylenediamine-N,N,N',N'-tetra-acetic acid) which was purchased from Sigma-Aldrich (St.Louis, MO, USA).

### **3.2.2 PREPARATION OF MECHANICALLY SKINNED SINGLE MUSCLE FIBRE SEGMENTS**

Preparation of mechanically skinned single muscle fibres involved the following steps: (i) muscle dissection, (ii) muscle handling/storage prior to fibre isolation, (iii) isolation of single fibre segments, (iv) measurement of fibre segment dimensions and (v) mechanical skinning (removal of the plasma membrane) of fibre segments.

#### **3.2.2.1 MUSCLE DISSECTION**

The iliofibularis (IF), piriformis (PYR), cruralis (CRU) and sartorius (SAR) muscles were identified based on their anatomical appearances and locations according to Walker (1967) and Dunlap (1960) (see also in Figures 3.1A and 3.1B). Usually, in an experiment carried out to determine glycogen concentration in single fibres, only one type of muscle was used per toad due to concerns related to glycogen stability.

All procedures involved in muscle dissection were carried out at RT. The toad was immobilised on a soft wooden surface or a wax plate by pinning its limbs with surgical needles, in a position that depended on the muscle to be excised (abdomen down for IF and PYR, abdomen up for SAR and on one side for CRU). Next, a small hole was created in the skin by lifting the skin at a point corresponding to the proximal attachment of the muscle tendon and cutting it with scissors. The skin was then detached from the

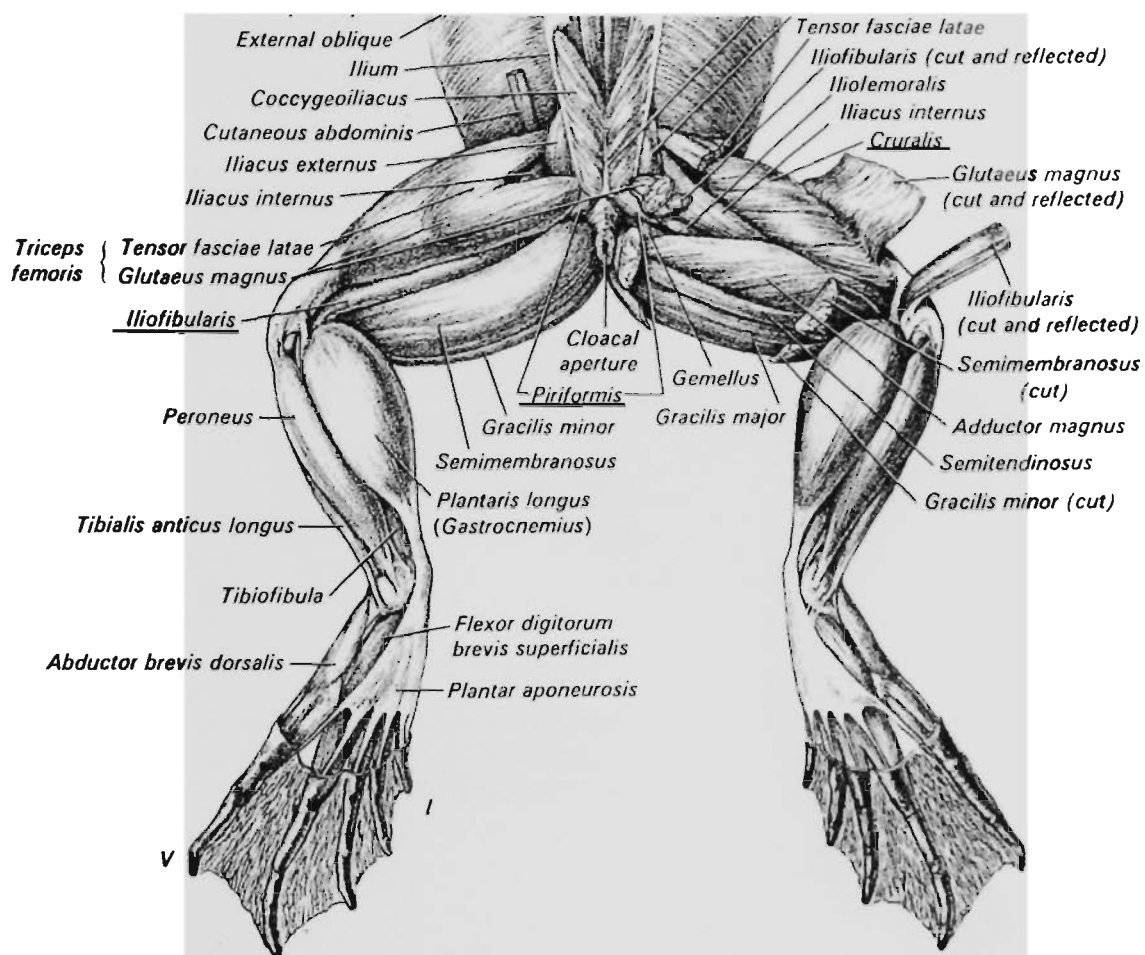


**Figure 3.1A** A dorsal view of frog muscles. Left side, superficial muscles; right side, deeper muscles (reproduced from Walker, 1967). Underlined are the muscles used in this study.

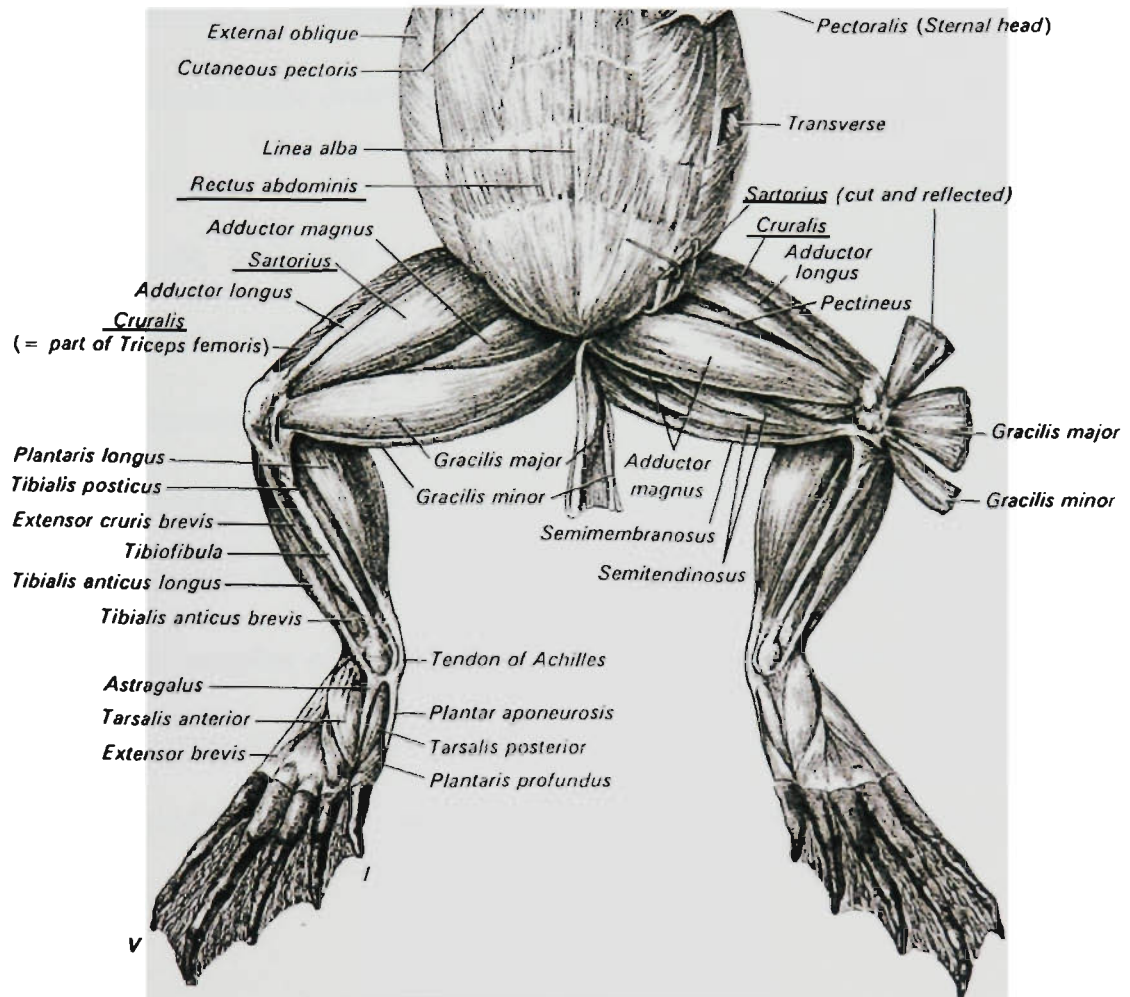


**Figure 3.1B** A ventral view of frog muscles. Left side of drawing, superficial muscles; right side, deeper muscles (reproduced from Walker 1967). Underlined are the muscles used in this study.

muscles connected to its inner surface by inserting the scissors into the hole and carefully moving them from one side to the other. After the operation field was opened, one could see the *deep fascia* - a thick, dense and opaque membrane of connective tissue that covered and held muscles together. This membrane was carefully removed without damaging the muscle tissue underneath.

*Iliofibularis muscle.* The distal tendon of the IF muscle was gently lifted up with a pair of teeth-forceps and cut (Fig.3.2A). The muscle was then gradually dissected by using scissors to cut connective tissue on either side and under the muscle until the proximal tendon was reached (Fig.3.2B). The muscle was finally removed by cutting the proximal tendon (see Fig.3.2C). When removing the iliofibularis muscle, great care was taken (i) not to disturb the complex of nerve-blood vessels lying immediately under this muscle as indicated by an arrow in the Fig.3.2C, and (ii) not to stretch or tear away the muscle, thereby stimulating the muscle contraction which would cause a breakdown of endogenous glycogen.

*Cruralis and Sartorius muscles.* The strategy used to dissect CRU and SAR muscles was similar to that described for iliofibularis muscle.

*Pyriformis muscle.* Dissection of PYR muscle was carried out essentially as described for IF except that the muscle was removed starting from the *proximal* tendon.

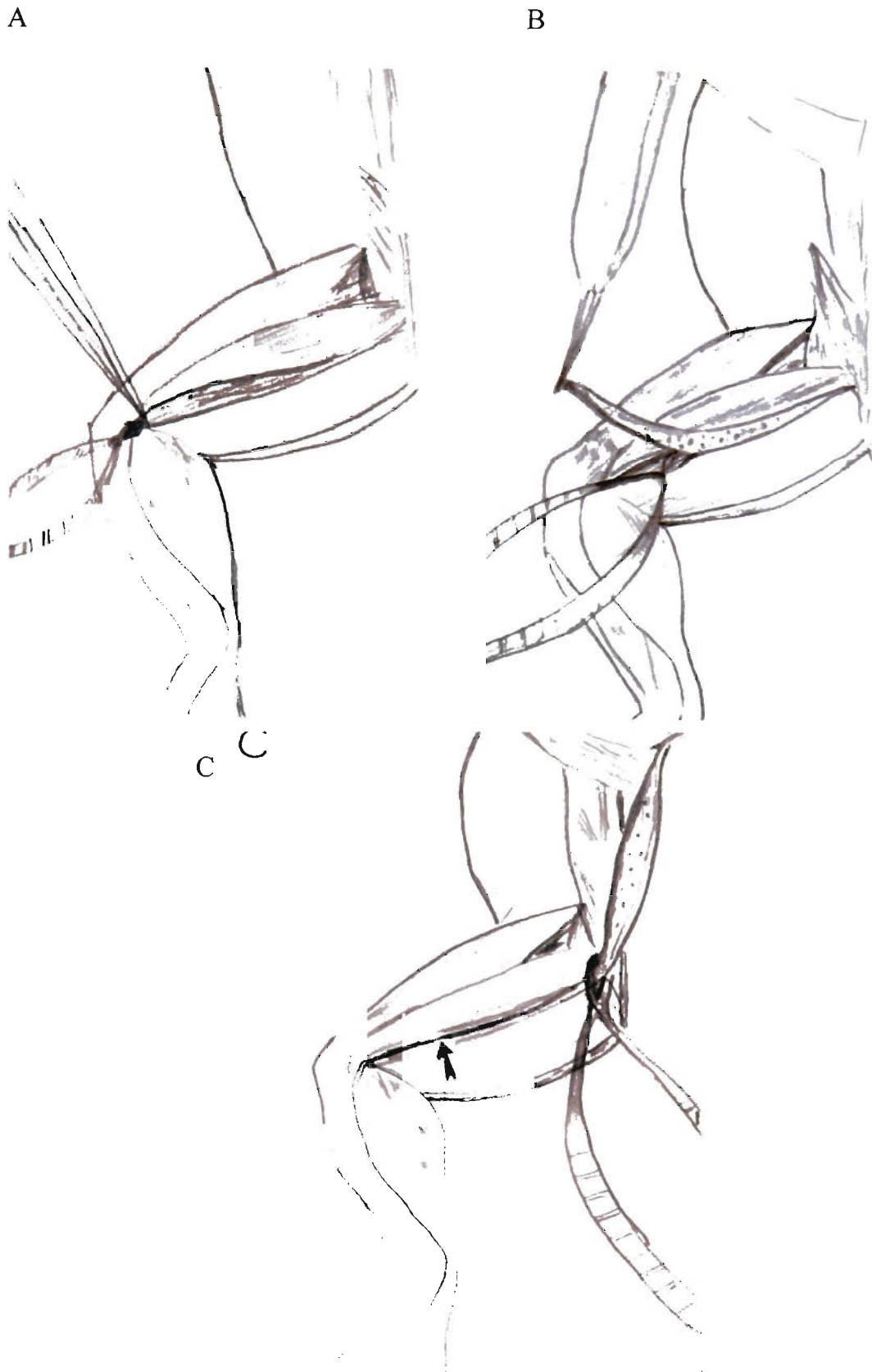


**Figure 3.2 Dissection of the IF muscle of the cane toad.**

(A) The distal tendon of the IF was gently lifted up and cut. (B) The connective tissue on either side and under the muscle were gradually cut until the proximal tendon was reached. (C) The muscle was removed by cutting the proximal tendon.

### 3.2.2.2 MUSCLE HANDLING/STORAGE PRIOR TO FIBRE ISOLATION

After dissection, the whole muscle preparation was blotted dry on Whatman No.1 filter paper and then was placed under paraffin oil in a petri dish on a 2 mm-thick layer of transparent resin (Sylgard 184; Corning, Medfield, PA, USA). The advantages of using paraffin oil when dissecting single muscle fibres are as follows: (i) it facilitates the visualisation of the single fibre by having a different refractive index, (ii) it precludes fibre swelling or fibre-water loss when fibre segments are prepared, and (iii) it confers on the fibre a quasi-circular cross-sectional area through the surface tension exerted on the fibre at the fibre/oil interface (Bortolotto *et al.*, 1999). The muscle preparation was immobilised, without stretching, onto the resin bed with entomological pins (Fig.3.3A). Unless indicated otherwise, freshly dissected muscles were kept intact under oil for 30 min to 1 hour at RT before isolating single fibres for glycogen determination. This is because it was observed that muscles contracted vigorously if fibres were isolated immediately after muscle dissection.

### 3.2.2.3 ISOLATION OF SINGLE FIBRE SEGMENTS

Isolation of single fibre segments was carried out at RT using an Olympus dissecting microscope (magnification range: 6.4 to 40 ×), jewellers' forceps No. 5 and iris scissors (Dupont, Switzerland). It was noted that IF, PYR and SAR muscles were enclosed in a very thin layer of connective tissue with scattered black pigmentation; this layer was

always removed before dissecting small bundles of fibres. For CRU muscle, some exceptions were noticed. CRU is one part of the *triceps femoris* muscle, which is anatomically divided into three parts: gluteus magnus (*vastus externus*), tensor fasciae latae (*rectus anticus*) and cruralis (*vastus internus*) (Walker, 1967). The thin connective tissue membranes that divide these three parts cannot be visualised with the naked eye but can be easily distinguished under the dissecting microscope. In the present study, to minimise muscle stimulation, the *triceps femoris* muscle was dissected as a whole and single muscle fibres were isolated from the CRU part without separating CRU from the rest of the muscle. In CRU muscle, single fibres were found to run obliquely between the proximal and distal end and terminating on the medial tendon. Because of this arrangement, the isolation of small bundles of fibres in the CRU muscle had to be started from a lateral edge of the proximal end using a similar strategy as that described for IF (see below).

Single fibres were randomly dissected from various regions of PYR, CRU and SAR muscles and from the peripheral twitch region of the IF muscle (Hoh *et al.*, 1994) as shown in Fig.3.3. The first step involved the isolation of a small bundle of about 3-5 fibres (Fig.3.3A-C); the bundle, held with a pair of forceps in the distal tendon region, at the interface between the tendon and muscle tissue (Fig.3.3A) was carefully cut and pulled away, just enough to create a bifurcation at the boundary between the bundle and the bulk of muscle (Fig.3.3B). Subsequently, the bundle was further dissected to the

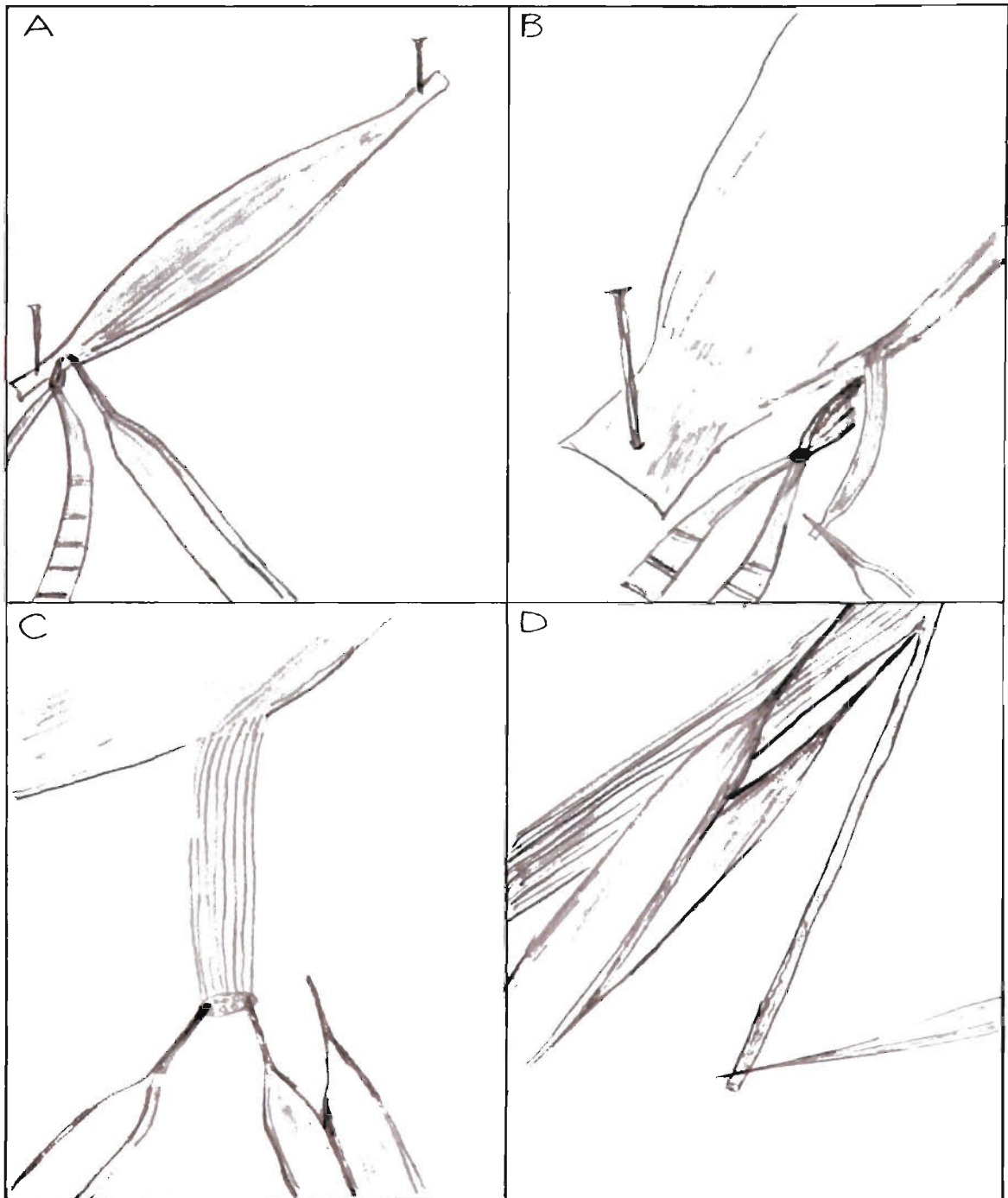


**Figure 3.3** Procedure used to dissect, under oil, single fibres from skeletal muscle of the toad.

(A-B) Small bundle of about 3-5 fibres, held with a pair of forceps, was cut between at the interface between the tendon and the muscle tissue and was pulled away. (C-D) One single fibre was then separated by using one tip of a fine jeweller's forceps to detach it from the other fibres after making a sharp cross-section.

required length using the fine scissors as shown in Fig.3.3B. When the desired length of fibre bundle was obtained, a single fibre segment was isolated from the bundle using two pair of forceps as shown in Fig.3.3C-D. Briefly, a cut was made at the free end of the bundle, at the interface between the tendon and muscle tissue; this allowed the visualisation of the boundaries between fibres. One single fibre was then separated by using one tip of the forceps to detach it from the other fibres, starting at the sharp cross-section previously made in the bundle. Normally, a single fibre could be isolated by pulling it away slowly after being detached. However, in some cases, two or even several muscle fibres were found to be connected by tiny fibres of connective tissues. In such cases, if the single muscle fibre was carelessly pulled away from the bundle, it broke at the point of attachment to the connective tissue. To avoid such breakage, the connective tissue was carefully cut while the single fibre segment was pulled away from the bundle.

In order to ensure that the dissected fibre was a single fibre, the preparation was observed under maximal magnification while being rolled over with the forceps in the dissecting dish. A single fibre would display two shining lines on either side of the preparation due to the deflection of incident light by the plasma membrane of the fibre. There was no other *sharp* or *straight* line between these two lines. If a boundary or very fine line was observed between the aforementioned lines, it was suspected that more than one fibre had been dissected. It is worth noting, however, that for large fibres from iliofibularis muscle, such as type 1 fibres, two blurred, thin and wavy lines could be very often seen between the main shining lines, even in single fibre preparations. These lines were

probably reflections of incident light from the inner surface of plasma membrane. In several instances, the edges of the plasma membrane were very thick on one or both sides. In such cases, it was suspected that at least one satellite cell was attached to the isolated fibre. These tiny, fragile satellite cells were ruptured and removed before recording the fibre dimensions. The isolated fibre was straightened (but not stretched) to allow easy measurement of fibre length and diameter.

#### 3.2.2.4. MEASUREMENT OF FIBRE SEGMENT DIMENSIONS

The fibre segment dimensions (length and diameter) were measured using a video-camera-monitor system and callipers. The length of the segment and the width of the fibre in at least three points along its length were measured with the calliper on the monitor screen at 12 × and 40 × magnification, respectively. The volume of the fibre segment, expressed as litre fibre (l fibre), was calculated assuming it to be a cylinder with a diameter equal to the mean value of the fibre width (equation 1):

$$V = \frac{1}{4}\pi d^2 h \quad (\text{Eq. 1})$$

where  $d$  = diameter,  $h$  = length of fibre segment.

In some circumstances, when the cross-section of the fibre segment had an ellipsoidal shape, the fibre volume was calculated using Equation 2:

$$V = \pi h(a + b)^2/16 \quad (\text{Eq. 2})$$

where a, b were the largest and the smallest diameter of the fibre segment (major axis and minor axis of an ellipse).

Before the volume of the fibre segment was calculated, the dimensions measured on the monitor screen as calliper units were converted to real fibre dimensions expressed in mm using the conversion factors 39.95 div/1mm and 133.5 div/1mm for 12 x and 40 x magnification, respectively. For each magnification, the conversion factor was determined by measuring a 1-mm division of a calibrated micro-scale on the monitor screen with a calliper when this calibrated micro-scale was placed under microscope.

Unless indicated otherwise, the dimensions of a single fibre segment were measured prior to the mechanical removal of its plasma membrane.

#### 3.2.2.5 MECHANICAL REMOVAL OF THE PLASMA MEMBRANE OF FIBRE SEGMENTS

Immediately after recording the dimensions of the isolated fibre segment, the fibre was mechanically skinned using a dissecting microscope, fine jewellers' forceps and iris scissors as illustrated in Fig.3.4. This strategy involved: (i) placing the petri dish such

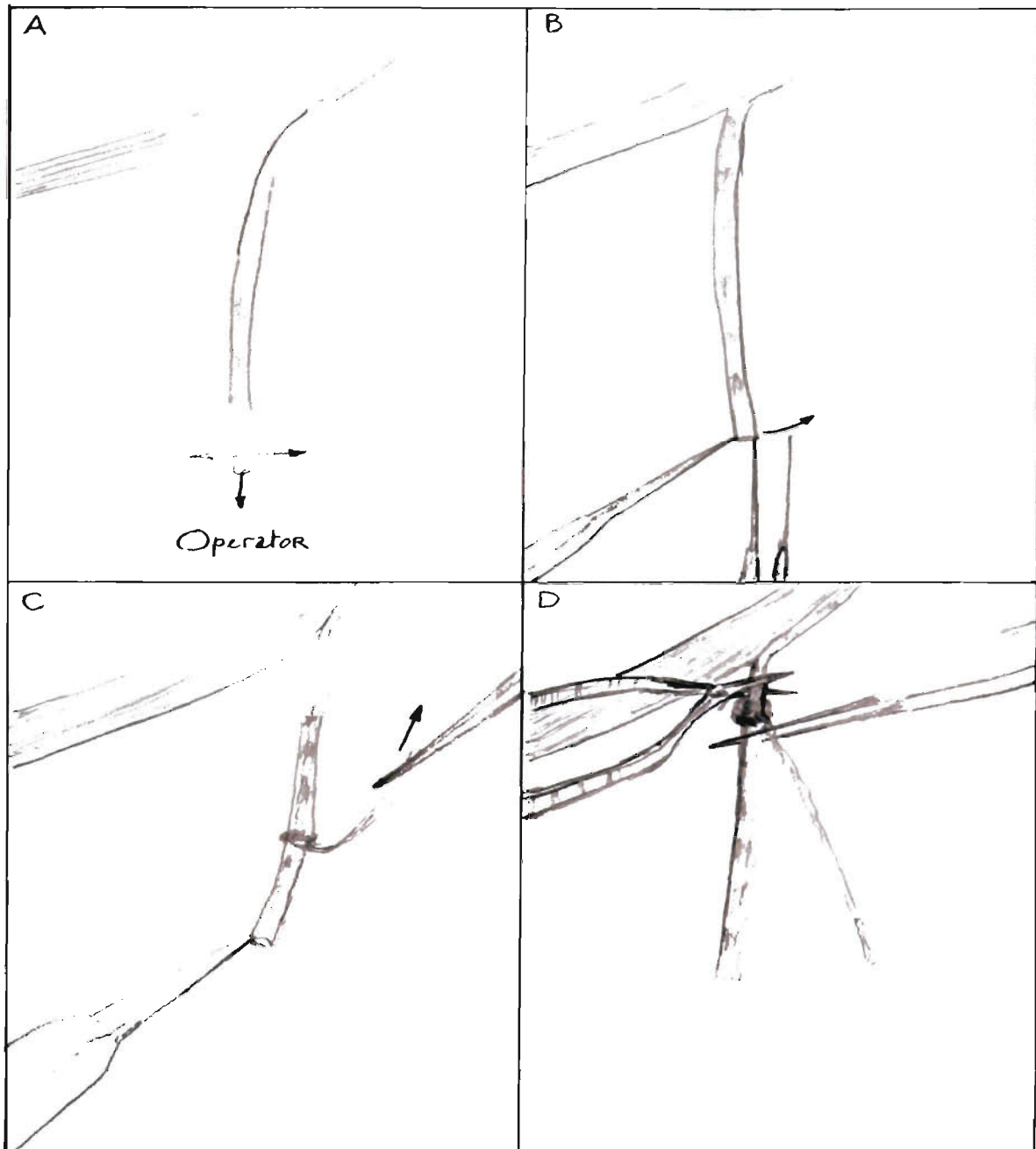


**Figure 3.4 Strategy used when mechanically skinning a single muscle fibre.**

(A) Making a sharp cross section at the free-end of the fibre. (B-C) Splitting and pulling apart of the plasma membrane along the edge of the fibre segment. (D) The process of the membrane skinning produced a split of the fibre that could be seen as two branches and a rolled-sleeve structure associated with the end of the fibre that was still connected with the muscle.

that the free end of the fibre faced the operator (Fig.3.4A), (ii) cutting a small section of the free end (the damaged end of the fibre) with the fine scissors (Fig.3.4A), and (iii) splitting and pulling apart of the plasma membrane along the edge of the fibre segment (Fig.3.4B-C). If successfully skinned, the process of the membrane skinning produced a split of the fibre that could be seen as two branches and a rolled-sleeve structure associated with the end of the fibre that was still connected with the muscle (Fig.3.4D). The fibre preparation was finally removed by holding it with forceps under the rolled-sleeve structure and cutting the fibre immediately above this structure. The skinned fibre was rapidly transferred through air into the first of a series of reaction droplets (see analytical method section 3.2.3.2), which had been prepared previously under oil in another petri dish. For glycogen determination, the preparation of a mechanically skinned fibre segment took less than five minutes and both branches of the split fibre were used.

### **3.2.3 GLYCOGEN ANALYSIS IN THE MECHANICALLY SKINNED SINGLE MUSCLE FIBRES**

In the microfluorometric method described in this study, the glycogen content in single skeletal muscle fibres was determined *in situ* by subjecting the mechanically skinned single fibre preparation to the enzymatic action of *amyl $\alpha$ -1,4- $\alpha$ -1,6-glucosidase* at RT. The volume of solutions in the analytical protocol was kept as small as possible because it was expected that the absolute amount of glycogen in single muscle fibres would be

very low. Also, in this protocol, unlike in that used for the construction of commercial glycogen standard curves, there was no transfer of samples from the step-1 mixture to the GLU reagent in step 2; instead, at the completion of the AG reaction, the GLU reagent was added directly to the step-1 mixture.

The microfluorometric method for glycogen assay in single muscle fibre segments involved three steps: (i) removal of non-glycogen fluorogenic materials (*Washing step*), (ii) enzymatic hydrolysis of fibre glycogen (*Step 1*) and (iii) conversion of glucose to G6P and then to 6-phosphogluconolactone and reduction of NADP<sup>+</sup> (*Step 2*).

### 3.2.3.1 PREPARATION OF UNDER-OIL DROPLETS FOR GLYCOGEN ANALYSIS IN MECHANICALLY SKINNED SINGLE FIBRE SEGMENTS

At the beginning of this study it was found that single muscle fibre segments contained non-glycogen fluorogenic material as well as two pools of glycogen: one of which was lost during the washing step ('washable glycogen') and another that remained associated with the washed fibre ('non-washable glycogen') (for details see section 3.2.3.4 to 3.2.3.6). Subsequent to this finding, three glycogen-related parameters were determined for each fibre segment: non-glycogen fluorogenic material (**NGlyc**), washable glycogen (**WGlyc**) and non-washable glycogen (**NWGlyc**). The droplets containing the fibre washing solution (1.5-2.5 µl) were placed in one petri dish, while those for determining

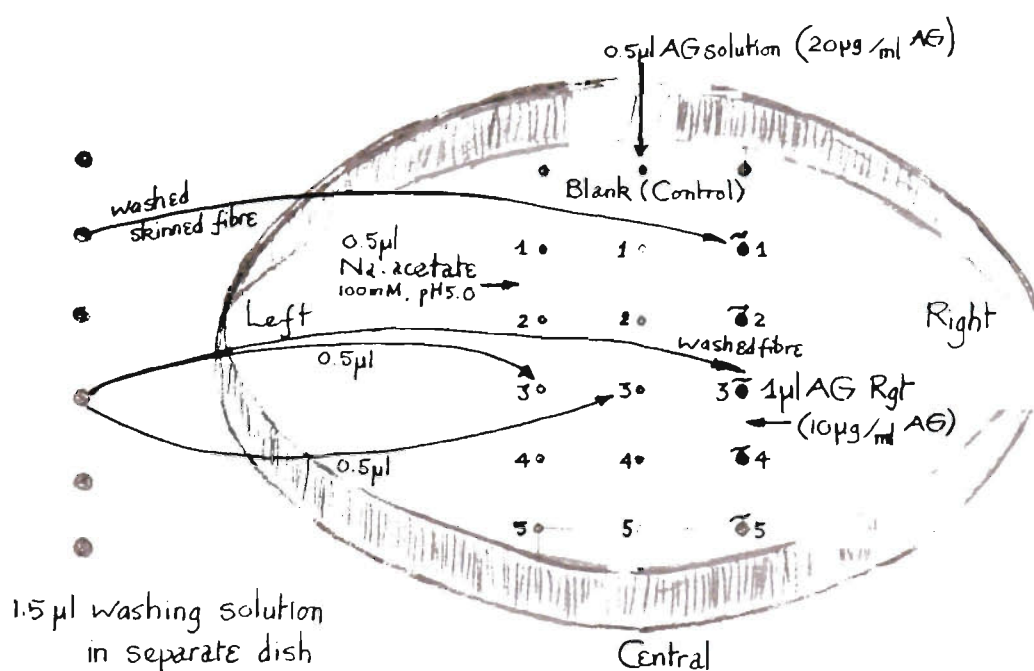


**Figure 3.5** Arrangement of reagent droplets on the bottom of the petri dish, under a layer of oil for glycogen analysis in mechanically skinned single muscle fibres (see section 3.2.3.1 for details).

Fluorescence measurements were carried out in samples aspirated from droplets in the left row (for **NGlyc**), in the centre row (for **WFluo = NGlyc + WGlyc**) and in the right row (for **NWGlyc**).

**NGlyc** (0.5  $\mu$ l 100 mM Na acetate buffer, pH 5.0), **WFluo** (0.5  $\mu$ l AG solution) and **NWGlyc** (1  $\mu$ l AG solution) were placed in a different petri dish, in three parallel rows, 1 cm apart, as illustrated in Fig.3.5. At the end of the washing period, the skinned fibre segment was rapidly transferred to the corresponding droplet on the *right-hand-side* line for the determination of **NWGlyc**. Then, two aliquots (0.5  $\mu$ l each) from the washing-solution droplet were processed as follows. One aliquot was transferred to the corresponding droplet on the *left-hand-side* line for determining **NGlyc**, while the other was transferred to the corresponding droplet on the *middle-line* for determining the washable fluorogenic material (**WFluo** = **WGlyc** + **NGlyc**). At the completion of the AG reaction (45 min), four volumes of HK/G6PDH reaction solution were added to the droplets containing the AG reaction solution.

### 3.2.3.2 THE TRANSFER OF A SKINNED FIBRE SEGMENT FROM THE MUSCLE DISSECTING-DISH TO A REACTION DROPLET

Glycogen determination in a single muscle fibre segment involved the transfer of the segment from the muscle dissecting/fibre skinning dish to the washing droplet and then from the washing droplet to the droplet containing the AG solution.

As described in section 3.2.2.5, the process of mechanical skinning created a rolled-sleeve structure at the end of the fibre still connected to the muscle. At this point in time, the fibre was ready to be cut from the muscle and transferred to the washing solution.

The fibre segment was cut above the rolled-sleeve structure with the iris scissors, while the two branches of the fibre were held down, under the structure, with the jewellers' forceps. The cut-fibre segment was held steady between the forceps in one hand, while quickly replacing, with the other hand, the muscle-dissecting dish with the petri dish containing the washing solution droplets. To introduce the fibre segment into the appropriate droplet, the forceps that held the skinned muscle fibre were brought close to the washing solution droplet without touching it, the two arms of the forceps were opened and the fibre segment was detached using one arm of another pair of forceps. As a result of these manipulations the skinned muscle fibre segment was made to rest beside the droplet of washing solution. Finally, using one arm of the forceps in one hand, the skinned muscle fibre was pushed gently toward the droplet until it touched it. As soon as the muscle fibre segment touched the washing solution in the droplet, it was automatically and rapidly sucked in due to hydrophilic forces and surface tension.

### 3.2.3.3 THE TRANSFER OF A SKINNED FIBRE SEGMENT BETWEEN TWO REAGENT DROPLETS

At the end of the washing step, the skinned muscle fibre was transferred from the washing solution droplet in one petri dish to the droplet containing the AG reagent in another petri dish. The transfer involved two steps: the removal of the fibre segment out of the first droplet and its introduction into the second droplet. The latter step was carried out as described in the previous section. The removal of the skinned fibre segment out of

the first droplet involved: (i) focusing the microscopic viewing field onto the droplet, (ii) taking hold of the fibre segment and lifting it gently out of the droplet with only one tip of the forceps, and (iii) introducing the fibre segment into the next droplet, without touching the droplet with the tip of the forceps.

The use of only one tip rather than both tips of the jewellers' forceps to remove the fibre segment from a reagent droplet served two purposes: (i) it minimised the transfer of solution (by capillarity) from one droplet to another and (ii) it minimised the danger of disturbing the dome-shape of the first droplet, which was subsequently analysed for **NGlyc** and **WFluo**.

#### 3.2.3.4 DETERMINATION OF NON-GLYCOGEN FLUOROGENIC MATERIAL (**NGlyc**)

At the beginning of this study, it was anticipated that a single muscle fibre would contain, in addition to glycogen, a number of fluorescent non-glycogen compounds (**NGlyc**), such as intracellular glucose, glucose-6-phosphate, NADH/NADPH, which would contribute to the fluorescent signal generated by the fibre at the end of the analytical protocol.

These compounds had to be removed prior to glycogen determination. Hence, the protocol used to determine glycogen in mechanically skinned muscle fibre segments involved a *washing step* which preceded the AG step.

Unless otherwise indicated, fibres were washed in 100 mM Na-acetate buffer, pH 5.0 for 5 min at RT. The volume of the washing droplet was varied according to the size of the fibre segment. The average volume of most fibres examined in this study was about 20 nl; for these fibres the volume of the washing droplet was 1.5  $\mu$ l. When fibres were larger than 29 nl the volume of washing droplet was increased to 2.0  $\mu$ l.

After the transfer of the washed fibre to the AG reagent droplet, the amount of **Nglyc** in the washing solution was determined as follows:

*Step 1.* An aliquot of 0.5  $\mu$ l of washing solution was mixed, without incubation, with a previously prepared droplet of 0.5  $\mu$ l Na-acetate buffer at RT (see Fig. 3.5).

*Step 2.* Four microlitres ( $\mu$ l) of GLU reagent was added to step 1 droplet and incubated for 20 min at RT.

At the end of incubation period, the fluorescence signal was measured as described in the section 2.2.2.1 (Chapter 2). The amount of **Nglyc** was calculated from the fluorescence signal and expressed in mmol equivalent NADPH/l fibre.

### 3.2.3.5 DETERMINATION OF WASHABLE GLYCOGEN (**Wglyc**)

In the initial stage of this study, it was observed that the fluorescence signal generated by an aliquot of the washing solution (after the removal of the skinned fibre segment) which was subjected to both reaction steps in the glycogen determination protocol

(section.2.2.2.4) was always higher than that produced by an equal aliquot subjected to *step 2* only. This indicated that the washing process removed not only the *non-glycogen fluorogenic materials* but also washed away a significant amount of glycogen which was perhaps loosely bound to intracellular structures. Henceforth, this type of diffusible glycogen will be referred to as **washable glycogen (Wglyc)** to differentiate it from the glycogen pool that remained associated with the skinned fibre segment after washing process.

The amount of **Wglyc** for given fibre segment was calculated by subtracting the amount of **Nglyc** (determined as described in the previous section) from the total amount of washable fluorogenic material present in the fibre (**Wfluo**). The amount of **Wfluo** was determined using a protocol similar to that used to determine **Nglyc** (section 3.2.3.4), except that AG reagent rather than the Na-acetate buffer was used in the first step and the AG reaction (*Step 1*) was carried out for 45 min.

### 3.2.3.6 DETERMINATION OF GLYCOGEN CONTENT IN THE WASHED FIBRE SEGMENT (**NWglyc**)

Determination of the glycogen associated with the washed skinned fibre segment (**NWglyc**) was carried out as follows:

*Step 1.* The fibre segment (average volume 20 nl) was incubated in 1  $\mu$ l of AG reagent for 45 min at RT. If the fibre volume was smaller than 10 nl or larger than 29 nl, the volume of the droplet was changed to 0.5 or 2.0  $\mu$ l, respectively.

*Step 2.* Four volumes of the GLU reagent were added directly to the *step 1* droplets and incubated at RT for 20 min. The compositions of the AG and GLU reagents were the same as those used for constructing the glycogen standard curves (section 2.2.2.4).

At the end of the incubation period, triplicate samples were aspirated into microcells and fluorescence signals were recorded as described before. The concentration of NWGlyc (mmol glucosyl units / l fibre) was calculated from fluorescence signals.

### 3.2.4 CALCULATIONS AND STATISTICAL ANALYSES

For each fibre segment analysed in this study, the following glycogen-related parameters were determined/calculated:

**NWGlyc** : measured directly as described in section 3.2.3.6

**Wglyc** = **Wfluo** (measured as described in section 3.2.3.5) – **Nglyc** (measured as described in section 3.2.3.4)

**Tfluo** (total fluorogenic materials present in a single fibre) = **Wfluo** + **NWGlyc**

**tGlyc** ( total glycogen in a single fibre) = **Wglyc** + **NWGlyc**

**NWGlyc** was measured in triplicate. Due to the very small volume ( $< 1.0 \mu\text{l}$ ) of sample available, three readings of one sample only were performed for **Wfluo** and **Nglyc**.

Unless otherwise stated, the data were expressed as means  $\pm$  SE. Student's *t*-test was used to compare two groups of data and one-way Anova (Bonferoni post-test) was used to compare several groups of data.

### 3.3 RESULTS

#### 3.3.1 INTRACELLULAR POOLS OF FLUOROGENIC MATERIAL IN SINGLE MUSCLE FIBRES

The myoplasm contains low molecular weight non-glycogen components (**NGlyc**) such as NADPH, glucose and glucose-6-phosphate, which normally contribute to the total fluorescence signal when muscle glycogen concentration is estimated by fluorometric methods. In this study, the **NGlyc** was removed by washing it out from mechanically skinned muscle fibre preparations, because the myoplasmic space was made accessible by the removal of the plasma membrane. During the washing step, which preceded the AG reaction step, segments of muscle fibres were incubated, immediately after dissection and skinning, in 1.5-2.5 $\mu$ l of buffer, and the amount of washed non-glycogen fluorogenic material was estimated from the fluorescence signal produced by an aliquot of the wash solution subjected to step 2 only (see Materials and Methods for details).

As shown in Table 3.1, the **NGlyc** component in fibre segments washed for 5 min in 100 mM Na-acetate buffer, pH 5.0, 100 mM Na-acetate buffer, pH 7.0, or HDTA/KOH, pH 5.0, represents  $9.33 \pm 1.29\%$ ,  $13.02 \pm 2.04\%$  and  $11.24 \pm 1.07\%$ , respectively, of the total fluorogenic material. These values are not statistically different from each other ( $P > 0.05$ ) indicating that any of these three buffers can be used in the washing step to remove the **NGlyc** component from mechanically skinned muscle fibres. The amount of

fluorogenic material detected in the Na-acetate buffer as **Nglyc** did not increase significantly after 15 min, but doubled after a 40 min wash (Table 3.1) suggesting that prolonged incubation of skinned muscle fibre preparation in acetate buffer pH 5.0 causes a gradual breakdown of fibre glycogen.

**Table 3.1.** The effect of the washing buffer and time of fibre washing on the proportion of total fluorogenic material (tFluo) detected as non-glycogen (Nglyc), total glycogen (tGlyc), washable-glycogen (Wglyc), and non-washable glycogen (NWGlyc) components in single fibres of iliofibularis muscle of the cane toad (*Bufo marinus*).

Washing buffer and time	n	Nglyc (%tFluo)	tGlyc (%tFluo)	Wglyc (%tGlyc)	NWGlyc (%tGlyc)	Ratio Wglyc/NWGlyc
<i>100 mM Na acetate buffer, pH 5.0</i>						
5 min	11	9.33 ± 1.29	90.67 ± 1.29	19.45 ± 2.18	80.55 ± 2.18	0.25 ± 0.03
10 min	7	11.50 ± 2.04	88.50 ± 2.04	23.51 ± 3.02	76.49 ± 3.02	0.26 ± 0.05
15 min	7	13.64 ± 1.17	86.36 ± 1.17	22.43 ± 5.36	77.57 ± 5.36	0.27 ± 0.09
40 min	7	19.24 ± 2.84*	80.76 ± 2.84*	26.03 ± 4.49	73.97 ± 4.49	0.38 ± 0.08
<i>100 mM Na acetate buffer, pH 7.0</i>						
5 min	8	13.02 ± 2.40	86.98 ± 2.40	23.84 ± 3.96	76.16 ± 3.96	0.34 ± 0.08
<i>75 mM HDTA KOH buffer, pH 5.0</i>						
5 min	34	11.24 ± 1.07	88.76 ± 1.07	15.21 ± 2.93	84.79 ± 2.93	0.25 ± 0.06

Note: Values are mean ± SE. \*  $P < 0.05$  vs values for 5 min wash.

The proportion of glycogen washed from fibres (**WGlyc**) incubated for 5 min in Na-acetate buffer pH 5.0 ( $19.45 \pm 2.18\%$ ), Na acetate buffer pH 7.0 ( $23.84 \pm 3.96\%$ ), or HDTA/KOH, pH 5.0 ( $15.21 \pm 2.93\%$ ) are not statistically different from each other (Table 3.1). Also there was no significant difference between the values for the ratio of washed glycogen/non-washed glycogen (**WGlyc/NGlyc**) calculated for Na-acetate buffer pH 5.0 ( $0.25 \pm 0.03$ ), Na-acetate buffer pH 7.0 ( $0.34 \pm 0.8$ ) and HDTA/KOH, pH 5.0 ( $0.25 \pm 0.06$ ). Extending the washing time in Na-acetate buffer pH 5.0 to 40 min did not cause a statistically significant increase in the amount of glycogen removed from the fibre, strongly indicating that the two pools of glycogen separated by the washing strategy represent two molecular forms: one diffusible, the other non-diffusible, probably trapped by or associated with intracellular structures.

### **3.3.2 TIME COURSE OF ENZYMATIC REACTIONS IN THE ANALYTICAL PROTOCOL FOR GLYCOGEN DETERMINATION**

At the end of the washing period, the mechanically skinned muscle fibre preparation was transferred to the AG reaction mixture (reaction step 1), in which the non-washed glycogen was broken down *in situ* by AG. The time course of this reaction (see Fig. 3.6) indicates that, under our conditions, the breakdown of fibre glycogen by the exogenous glucosidase is completed by 45 min. This time value was confirmed by the finding that a second incubation with AG of fibres that had been subjected to reaction step 1 did not result in more detectable glucose. In contrast, the hydrolysis of the commercial glycogen

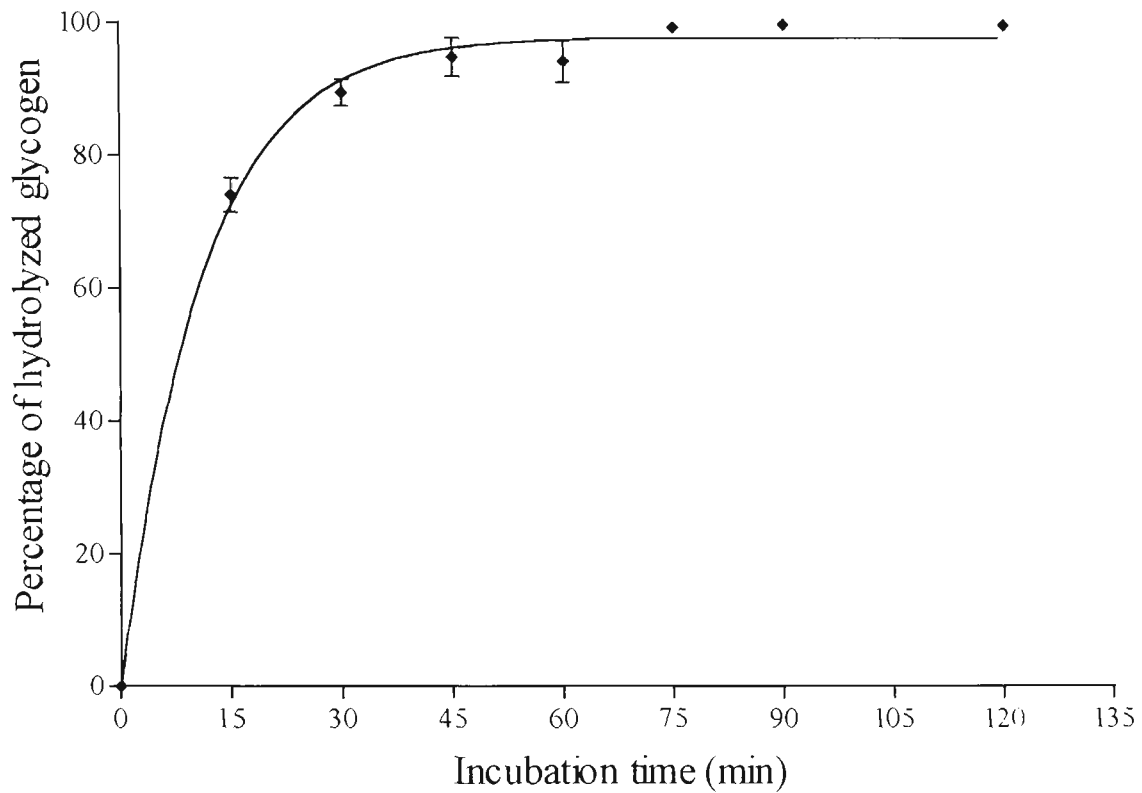


**Figure 3.6** The time course of endogenous fibre glycogen hydrolysis by exogenous amyloglucosidase.

After washing period, the mechanically skinned muscle fibre preparation was incubated in 1.5  $\mu\text{l}$  of AG reagent. At the end of each specified incubation period, an aliquot of 0.5  $\mu\text{l}$  fibre/AG-reagent mixture was transferred into 2.0  $\mu\text{l}$  of GLU reagent and incubated for another 20 min (*Step 2*). The fluorescence signal was immediately recorded after completion of the step-2 reaction. The remaining 1.0  $\mu\text{l}$  of fibre/AG reagent was incubated for up to 120 min, then 0.5  $\mu\text{l}$  aliquot of this mixture was transferred into step-2/GLU reagent and processed as the first aliquot. The fraction between the first and the final fluorescence signals, produced by subjecting the aliquots of step-1/fibre-AG-reagent mixture to step-2 reactions, indicated the percentage of the fibre glycogen that had been hydrolysed in a specified incubation time. Results show means  $\pm$  SE from four separate single skinned fibre glycogen determinations. Error bars represent 95% confidence intervals for four replicates. The curve was fitted with measured data by one phase exponential association:  $y = 98.11(1 - e^{-Kx})$  where  $K = 0.0899$ . Goodness of fit:  $R^2 = 0.9896$ ,  $S_{y,x} = 3.398$ .

used for constructing the standard curves was completed only after 120 min (see section 2.3.1.1). This time difference can be easily explained if one considers that the commercial glycogen used in this study was rabbit liver glycogen (see section 2.2.1), and that liver glycogen has a much higher molecular weight than skeletal muscle glycogen ( $10^8$  to  $5 \times 10^9$  Da v.  $10^7$  Da) (Alonso *et al.*, 1995). The completion time of reaction step 2 for single fibres was 20 min (see section 2.3.1.2) and as expected, did not differ from that for commercial glucose standards.

In its current version, the protocol for glycogen analysis in mechanically skinned muscle fibre segments includes: (i) 5min wash of the fibre segment in 1.5µl HDTA/KOH, pH 5.0; (ii) determination of glycogen and non-glycogen components in the wash; (iii) 45 min incubation of the washed fibre segment in 1.0 µl AG reaction cocktail; and (iv) 20 min incubation of the washed fibre/AG reagent mixture with 4 µl GLU reagent. Under these conditions, the detection limit for glycogen determination in a 20 nl fibre segment was 5.1 mmol glucosyl units/l fibre.

### **3.3.3 STABILITY OF FLUOROGENIC MATERIAL IN TOAD SKELETAL MUSCLE**

In order to investigate the stability of fluorogenic material in toad iliofibularis muscle, muscles were stored, under oil, at RT for up to 6 hours or at 4°C for up to 44 hours. As

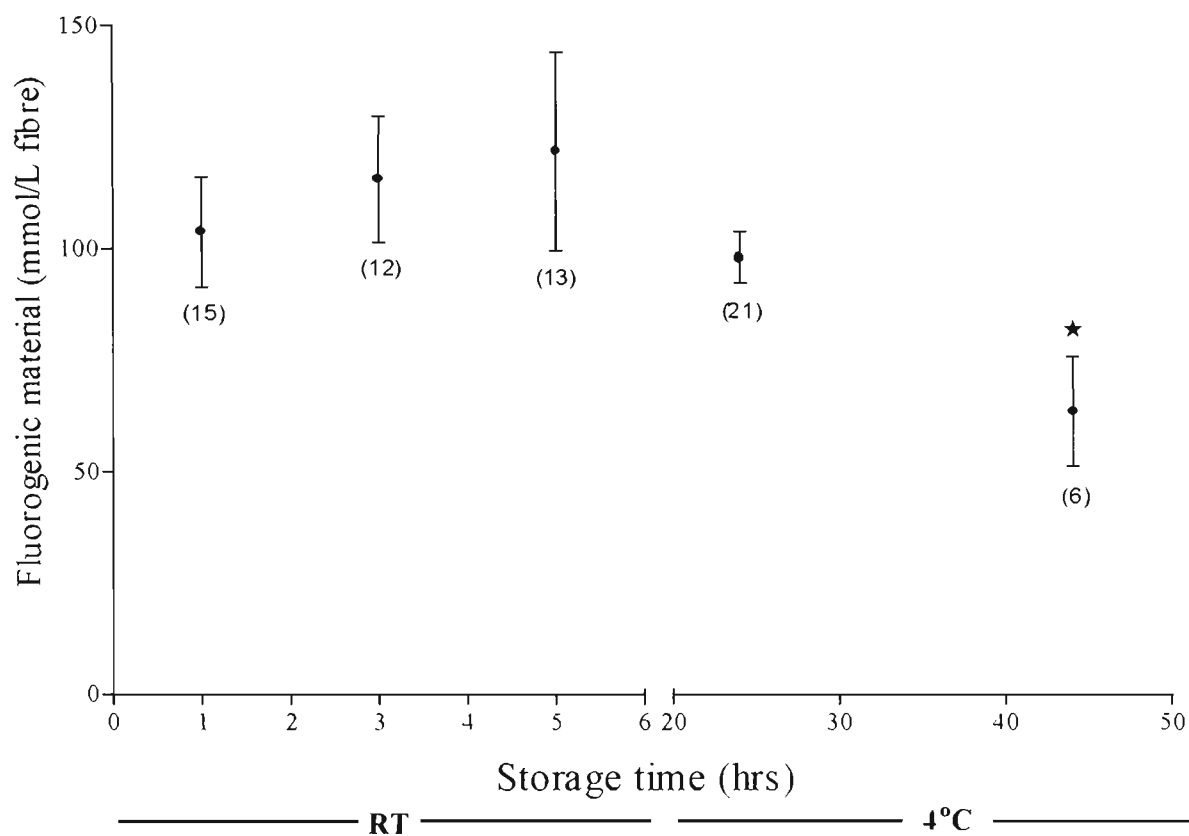


**Figure 3.7** The effect of storage conditions on the total amount of endogenous fluorogenic material (tFluo) in the mechanically skinned single muscle fibre preparations from the iliofibularis muscle of the toad.

Muscles were dry-blotted on Whatman filter paper and immediately stored under oil for a specified period of time. After a storage period elapsed, 6-21 single fibres were isolated from the peripheral twitch region of muscle and glycogen content was determined using the protocol described in the Material and Methods. Results are means of independent determinations indicated in the brackets  $\pm$  SE. (\*)  $P < 0.05$  v. the value obtained for muscles kept at RT for less than 2 h.

seen from Fig. 3.7, muscle storage under either of these conditions did not significantly affect the total amount of endogenous fluorogenic material (**tFluo**) in single fibres. A slight but significant decrease in **tFluo** was observed, however, in fibre segments isolated from a muscle that had been stored at 4°C for 44 hours.

In fibre segments isolated from muscles stored for up to 6 hours at RT and for up to 24 hours at 4°C, the **NGlyc** component represented  $8.93 \pm 1.09\%$  ( $n = 16$ ) and  $8.93 \pm 1.53\%$  ( $n = 12$ ) of the total fluorogenic material, respectively. However, the proportion of non-glycogen fluorogenic material was markedly higher ( $43.90 \pm 7.56$ ,  $n = 5$ ) in fibre segments dissected from a muscle stored at 4°C for 40 hours, indicating that during prolonged storage some of the glycogen is converted to **NGlyc** components. The data presented in this chapter were obtained with fibres isolated from freshly dissected muscles or from muscle which had been stored at 4°C for less than 24 hours.

### **3.3.4 TOTAL GLYCOGEN CONTENT IN SINGLE FIBRES FROM IF, PYR, CRU AND SAR MUSCLES OF THE CANE TOAD**

The concentration of total glycogen was determined in segments of single fibres isolated from one muscle of each type: IF (24 fibres), PYR (36 fibres), CRU (36 fibres) and SAR (36 fibres). The muscles were obtained from winter adult toads only. The average values

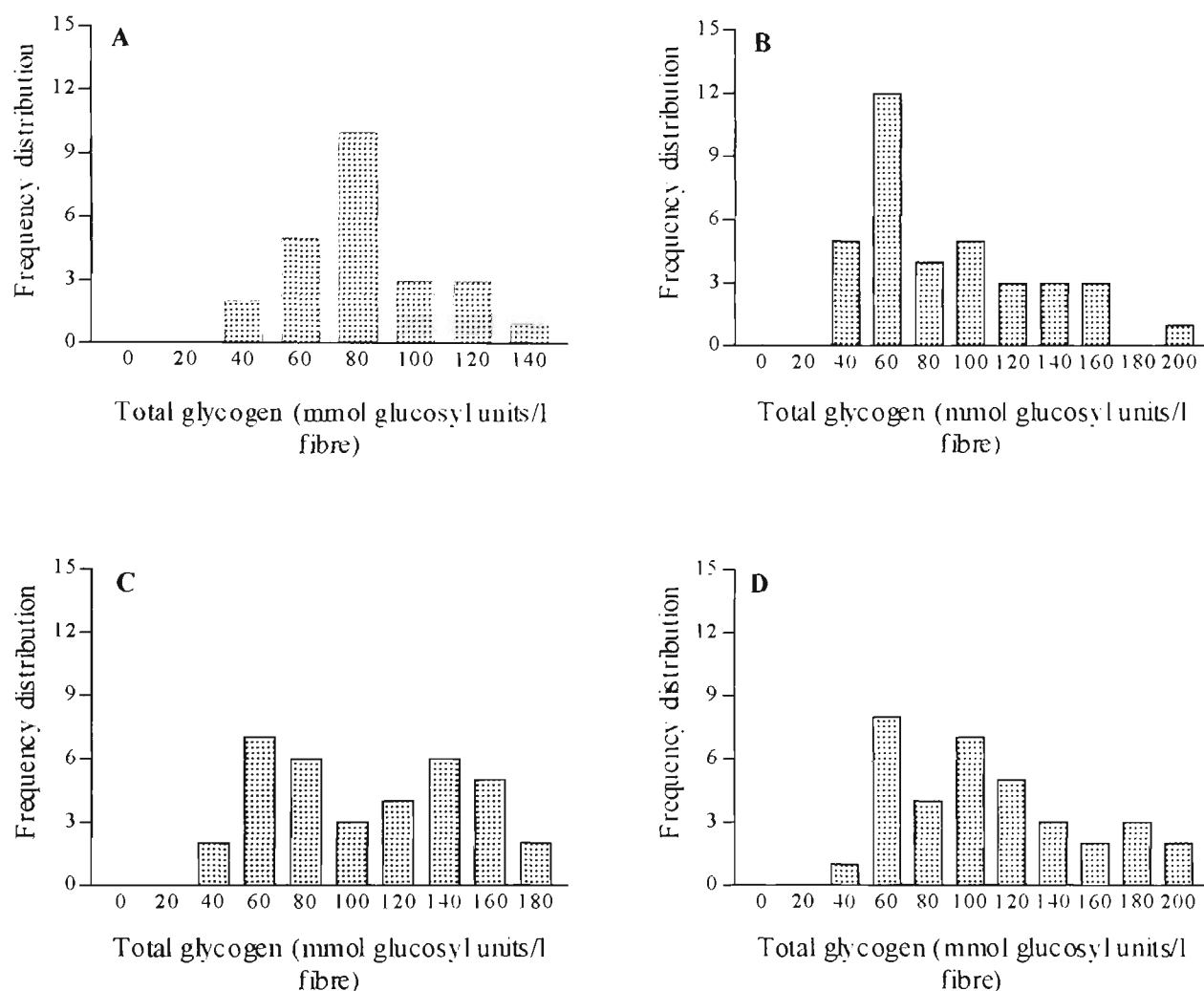


**Figure 3.8** Histogram of total glycogen (tGlyc) concentration values (as mmol of anhydrous glucosyl units per l fibre) measured in IF, PYR, CRU and SAR single fibres.

(A) 24 fibres of one IF muscle, (B) 36 fibres of one PYR muscle, (C) 35 fibres of one CRU muscle and (D) 35 fibres of one SAR muscle. All muscles were dissected from winter adult toads that had similar size (SVL = 120 – 130 mm) and body weight (~200-250g). One should note that the glycogen values obtained for one CRU muscle fibre (383.5 mmol glucosyl unit/l fibre) and for one SAR muscle fibre (367.2 mmol glucosyl unit/l fibre) were not included in the respective histograms C and D.

for glycogen content in fibres from each of the four muscles were  $84.2 \pm 5.0$  mmol glucosyl unit/l fibre (IF),  $89.3 \pm 7.0$  mmol glucosyl unit/l fibre (PYR),  $106.6 \pm 7.0$  mmol glucosyl unit/l fibre (CRU) and  $107.4 \pm 7.3$  mmol glucosyl unit/l fibre (SAR). These values were not significantly different ( $P > 0.05$ ).

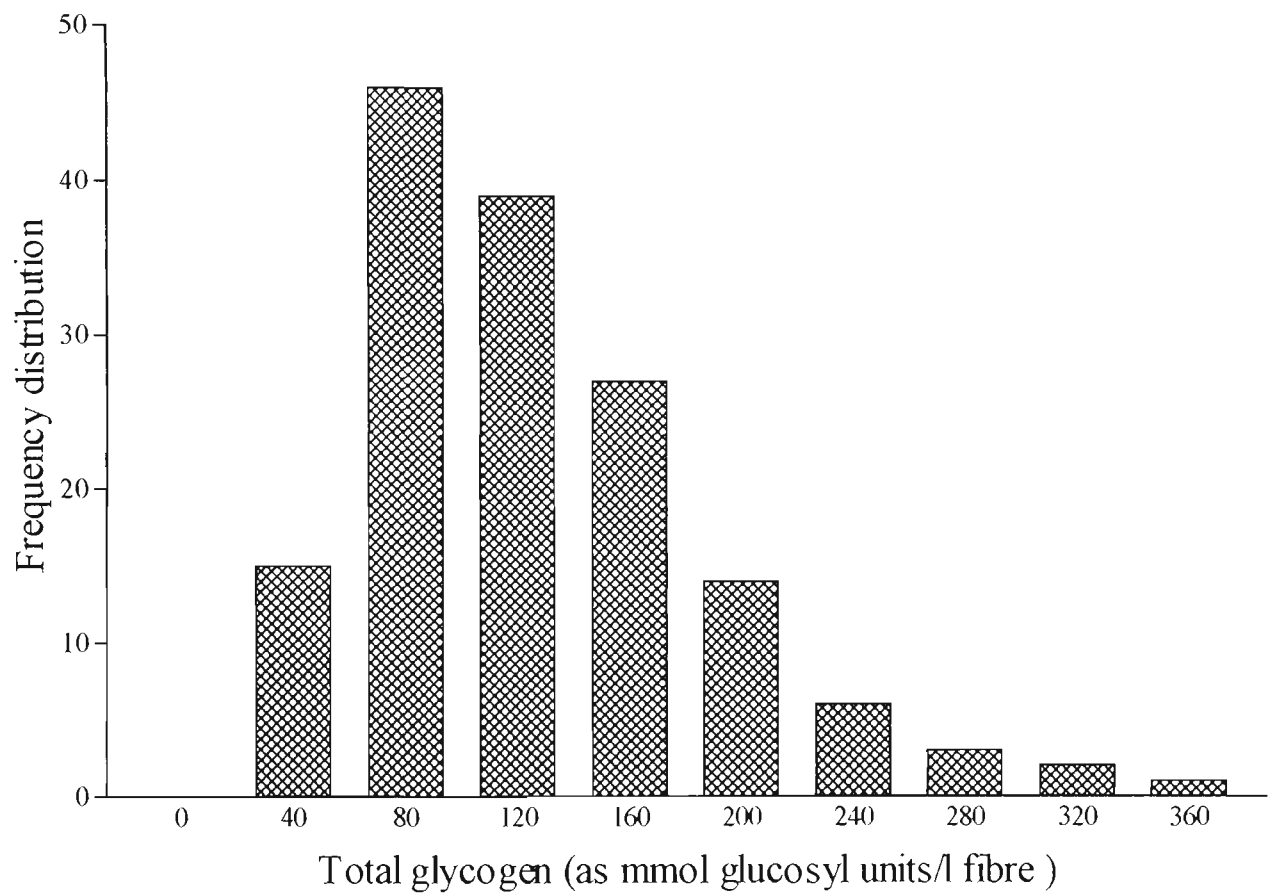
As shown in Table 3.2 and in Fig. 3.8, all four muscles displayed large inter-fibre variations with respect to fibre glycogen content. It is worth noting that while the lowest values for glycogen content observed in fibres from IF, PYR, CRU and SAR were relatively similar (33.7-46.1 mmol glucosyl unit/l fibre), the highest values found in fibres from CRU (383.5 mmol glucosyl unit/l fibre) and SAR (367 mmol glucosyl unit/l fibre) were markedly higher than the highest glycogen values found in fibres from in IF (137.8 mmol glucosyl unit/l fibre) and PYR (194.5 mmol glucosyl unit/l fibre). The total fibre glycogen data, presented as histograms in Fig. 3.8 show a similar distribution of glycogen values in PYR (panel B) and SAR (panel D) muscles with 58.3% (PYR) and 52.8% (SAR) of values falling in the 60-100 mmol glucosyl unit/l fibre range. In IF (panel A) most fibres (62.5%) contained 60-80 mmol glucosyl unit/l fibre, while in CRU (panel C) a large proportion (41.7%) of fibres contained 120-160 mmol glucosyl unit/l fibre and only 36% of values fell in the 60-80 mmol glucosyl unit/l fibre.

Fig. 3.9 shows the histogram obtained for 129 fibres isolated from the iliofibularis muscle of 14 toads. The values for total glycogen (**tGlyc**) found in this larger population of fibres ranged between 25.8 to 369 mmol glucosyl units/l fibre, with 59% of the values

falling in the 80 and 120 mmol/l fibre bins. The diameter of the fibres examined ranged between 32.2 and 122.5  $\mu\text{m}$ , but there was no correlation between fibre diameter and glycogen content. As shown in Fig. 3.10, however, the glycogen content of 30 fibres of IF muscles from four winter (August – October) toads was 38.4% lower than that of 42 fibres prepared from IF muscles of five summer (January-February) toads. There was no statistically significant difference between fibres obtained from summer toads and fibres obtained from winter toads with respect to the proportion of glycogen removed by washing.

**Table 3.2. The ranges of the glycogen concentration** (as mmol of anhydrous glucosyl units/litre fibre) **in single fibres prepared from one muscle of each type: IF, PYR, CRU and SAR.** All muscles were dissected from winter adult toads of similar size (snout-vent length, *SVL* 100-120 mm) and body weight (~200-250 g).

Muscle	<i>n</i>	Range of fibre glycogen content (as mmol glucosyl unit/l fibre)
Iliofibularis ( <b>IF</b> )	24	41.8 - 137.8
Pyramidal ( <b>PYR</b> )	36	33.7 - 194.5
Cruralis ( <b>CRU</b> )	36	46.1 - 383.5
Sartorius ( <b>SAR</b> )	36	45.1 - 367.2



**Figure 3.9** Histogram of the total glycogen concentration values determined in the 129 single fibres isolated from the iliofibularis muscles of 14 toads.

Glycogen was measured using the protocol described in the sections 3.2.3.4, 3.2.3.5, 3.2.3.6.

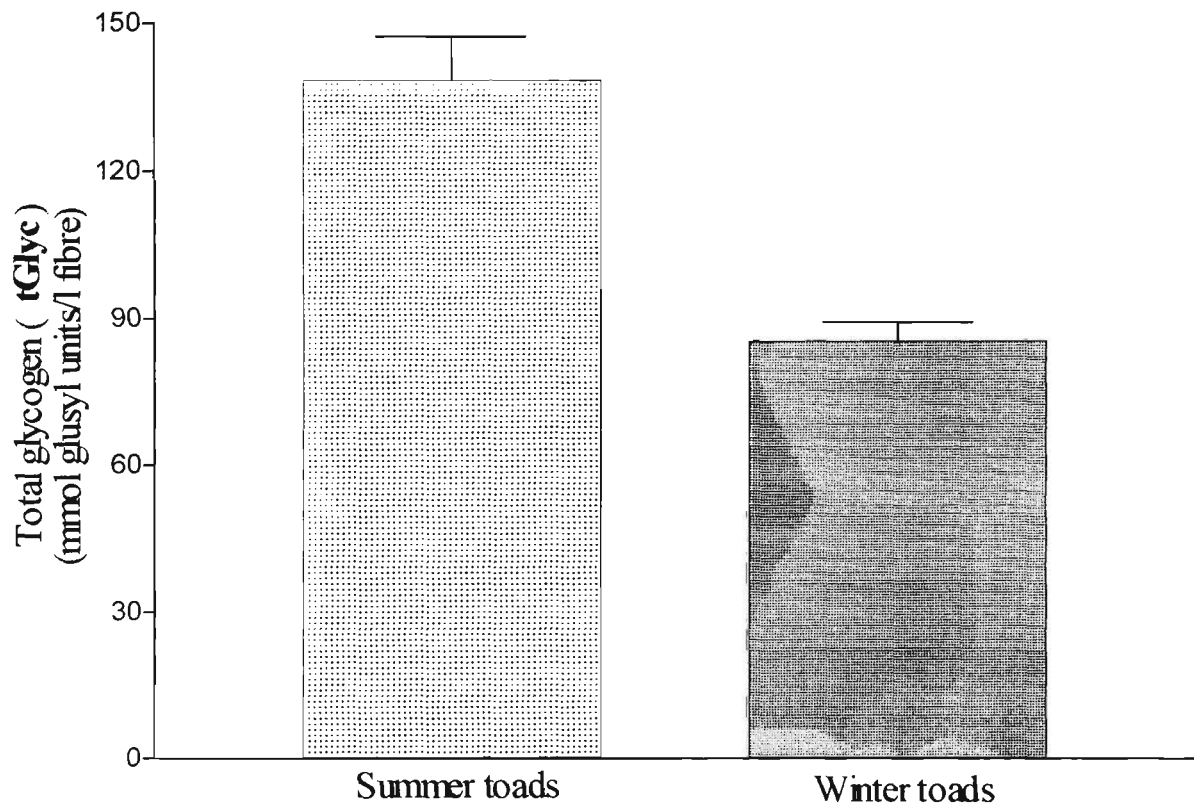


**Figure 3.10** Comparison of total glycogen concentration (as mmol of anhydrous glucosyl units/l fibre) in two fibre-populations, one comprising 30 IF muscle fibres dissected from four winter (August-October) toads and the other including 42 IF muscle fibres obtained from five summer (January-February) toads. Results are means  $\pm$  SE.  $P < 0.05$  (unpaired Student *t*-test).

### 3.4 DISCUSSION

*The muscle fibre preparation and intracellular pools of fluorogenic material.* One predictable advantage of using the mechanically skinned muscle fibre preparation for measuring glycogen concentration in single fibres is that non-glycogen fluorogenic contributors, **NGlyc**, (glucose, G6P, NADH and NADPH) to the fluorescence signal can be eliminated (washed) from the myoplasmic space prior to the analytical glycogen-hydrolysis step. This advantage is particularly relevant to studies on muscle fatigue, in which the fibres examined would contain low levels of glycogen and variable levels of the **NGlyc** contributors.

The buffer chosen initially for the washing step was sodium acetate, 100 mM, pH 5.0, which was also used in the AG reagent preparation. The slightly acidic pH of this buffer would also prevent the sarcoplasmic reticulum (SR)  $\text{Ca}^{2+}$ -release channel from opening (Lamb *et al.*, 1991). However, Na-acetate may enter the SR and release intralumenal- $\text{Ca}^{2+}$  by osmotic shock (Fryer and Stephenson, 1996). Therefore, it was of interest to examine whether using a buffer with an impermeant anion, such as 75 mM HDTA/KOH, pH 5.0 buffer, produced a different result with respect to the **NGlyc** component. As shown in Table 3.1, there was no statistically significant difference between the results obtained with the two buffers after a 5-min wash. It is important to note that when the single fibre preparation was incubated in Na-acetate buffer pH 5.0 for 40 min, the amount of **NGlyc** detected in the wash was twice as high as that detected in the 5 min wash

protocol. This indicates that prolonged washing of mechanically skinned single muscle fibre segments in an acetate solution (100 mM), pH 5.0 removed not only the endogenous non-glycogen fluorogenic material (**NGlyc**), but also brought about a gradual degradation of fibre glycogen. The breakdown of fibre glycogen may be partly caused by  $\text{Ca}^{2+}$  release from the SR and subsequent activation of the endogenous  $\text{Ca}^{2+}$ -dependent phosphorylase kinase/phosphorylase system.

An important result obtained in this study was that 5 min incubation of skinned muscle fibre segments in buffer solution (100 mM, Na-acetate, pH 5.0 or pH 7.0 or 75 mM HDTA/KOH, pH 5.0) prior to the AG reaction step washed away from the skinned muscle fibre not only the **NGlyc** component, but also a certain amount of fibre glycogen. The amount of washable glycogen (**WGlyc**) was neither buffer composition nor pH specific and ranged between 15-26% of the total glycogen (**tGlyc**). Extending the fibre washing time in acetate buffer pH 5.0 from 5 to 40 min did not give a significant shift in the amount of glycogen released, strongly indicating that the toad skeletal muscle fibre contains a proportion of glycogen that is not diffusible.

The idea that skeletal muscle cells contain more than one glycogen pool has been canvassed in the literature on glycogen in mammalian systems by three groups of studies. In one group of studies, two glycogen pools were distinguished by their different degrees of solubility in perchloric acid (Jansson, 1981); the acid soluble fraction represented 25% while the acid-insoluble fraction represented 75% of the total glycogen (when

concentration of muscle glycogen was lower than  $350 \text{ mmol kg}^{-1} \text{ d.w.}$ ). In the second group, two pools of glycogen were differentiated ultrahistochemically by their different topographical location in the muscle fibre; the largest pool was detected in the intermyofibrillar/intramyofibrillar compartment, with the highest density around the SR membrane, while the second pool was detected in the subsarcolemmal space (Friden *et al.*, 1989; see also section 1.3.1). The third and most recent study by Alonso *et al.* (1995) distinguished two glycogen pools in muscle, on the basis of their molecular weight and the role played in glycogen biogenesis. According to Alonso and co-workers (1995), 15% of the total glycogen in skeletal muscle is present as proglycogen, while 85% is present as macroglycogen. Details regarding proglycogen and macroglycogen can be found in section 1.3.2.

The identity and myoplasmic location of the two glycogen pools separated during the washing step used in this study are still unknown, and so far there is no published information about glycogen pools in amphibian muscle. However, based on the finding that the glycogen that diffused in the washing solution during 5-40 min incubation of mechanically skinned muscle fibres of the toad represents about 15-26% of the fibre glycogen, it is tempting to speculate that the washable glycogen pool (**WGlyc**) described here is related to the acid-soluble glycogen reported by Jansson (1981) and to the proglycogen species of Alonso *et al.* (1995). The fact that some glycogen diffuses out of the mechanically skinned fibre segment indicates that this form of glycogen is not bound or is only weakly bound to intracellular structures. In this context it is noteworthy that

Hoyle *et al.* (1973) described a pool of freely moving glycogen particles in barnacle muscle fibres which may be equivalent to the diffusible glycogen pool in the anuran muscle. Importantly, the fact that the bulk of the muscle glycogen in the present study does not diffuse out of the mechanically skinned fibre preparation evidently suggests that this form of glycogen is tightly associated with intracellular structures such as the sarcoplasmic reticulum membranes (Friden *et al.*, 1989).

*Inter-fibre and inter-muscle variability in glycogen content in the cane toad.* Glycogen determination in segments of 24 fibres from the twitch region of one IF muscle, 36 fibres from one CRU muscle, 36 fibres from one PYR muscle and 36 fibres from one SAR muscle clearly showed that there is a large variation in glycogen content between individual single fibres. Therefore, it is impossible to estimate the glycogen concentration of single fibres based on the average value obtained for the whole muscle.

Glycogen concentrations in segments of 129 IF fibres obtained from 14 toads produced an even larger variety of values ranging between 25.8-369 mmol glucosyl units/l fibre. The larger variability of values in this case is due to seasonal differences in fibre glycogen content. Nevertheless, 76 out of the 129 fibres (~60%) analysed had a glycogen content of 80-120 mmol glucosyl units/ l fibre (Fig. 3.9). The mean ( $\pm$  SE) of glycogen concentration for the whole fibre population ( $n = 129$ ) investigated in this study was  $128.5 \pm 5.7$  mmol glucosyl units/ l fibre or about  $109 \pm 5$  mmol glucosyl units/kg wet weight of muscle, assuming that 1 g wet weight of any of the four toad muscles examined

has the same solid and water content as that reported by Desmedt (1953) for the sartorius muscle of the frog (i.e. 0.213 g solid, 0.662 g intracellular water and 0.125 g extracellular water). This value compares well with that of Wilkie for frog (100 mmol glucosyl units/kg wet weight), cited in an earlier paper by Lüttgau (1965), but appear to be considerably higher than that obtained for single frog fibres (about 56 mmol glucosyl units per kg wet weight; converted from an average value of 315.5 mmol glucosyl units per mg protein using their factor of 5.6) by Nassar-Gentina *et al.* (1978), who used the conventional fluorometric protocol of Passonneau and Lowry (1973) and freeze-dried fibre preparations. The lower values obtained with freeze-dried fibre preparations may be caused by the partial breakdown of glycogen by  $\text{Ca}^{2+}$  released from the SR during the freeze-drying process.

*Glycogen stability in toad muscle.* The fibres used in this study were isolated from fresh (quickly dissected and not freeze-dried) muscles. As shown in Fig. 3.7, storing the toad muscle under paraffin oil at room temperature for up to 6 h or at 4°C for up to 24 h did not significantly decrease the total amount of fluorogenic material detected in single fibres. Since, with the described analytical protocol, glycogen represents at least 90% of the fluorogenic material, this result indicates a high degree of glycogen stability in the toad skeletal muscle and confirms an earlier report by Sahyun (1931) that glycogen is not rapidly hydrolysed in intact frog muscles kept at RT for 2 h.

*The analytical method.* The microfluorometric method for glycogen determination in segments of single muscle fibres described in this chapter differs from the method developed by Lowry and colleagues (Michel *et al.*, 1994; Hintz *et al.*, 1982; Lust *et al.*, 1981; Hintz *et al.*, 1980; Nassar-Gentina, 1978; Lowry *et al.*, 1978 & Lust *et al.*, 1975) with respect to (i) the strategy used to estimate the fibre size (fibre volume *vs* fibre mass) and (ii) the strategy used to prepare fibre segments for glycogen analyses (fresh fibres, mechanically skinned *vs* freeze-dried fibres).

The use of fresh rather than the freeze-dried fibre segments for glycogen determination (i) reduces substantially the time required for sample preparation (less than 1 hour *vs* more than 4 days), (ii) enables the experimenter to determine in the same fibre the glycogen and other various physiological parameters (see Chapter 4), and (iii) allows the separation and analyses of different intracellular pools of glycogen. One potential limitation of the fresh muscle fibre preparation is that endogenous glycogenolytic enzymes may break down glycogen during the time between animal sacrifice and the exposure of the skinned fibre to AG. Given the stability of glycogen in toad muscle, this has not been a problem when glycogen was determined in fibres prepared from toad skeletal muscles.

## CHAPTER 4

# **Correlation between glycogen content and responsiveness to the Na<sup>+</sup>-depolarisation of mechanically skinned muscle fibres of the cane toad *Bufo marinus***

### 4.1 INTRODUCTION

There are consistent observations that depletion of intracellular glycogen stores in muscle is associated with reduced muscle performance (Chin & Allen, 1997; Fitts, 1994; Vøllestad *et al.*, 1988; Galbo *et al.*, 1979; Bergström *et al.*, 1967), but the cellular mechanisms responsible for the glycogen depletion-related impairment of muscle function are not fully understood (Chin & Allen, 1997; Fitts 1994). So far, all studies on the role of glycogen in muscle have involved the depletion of the muscle glycogen pool by inducing a state of muscle fatigue. Therefore, from these studies it is not possible to draw unequivocal conclusions concerning the nature of the relationship between glycogen content and muscle contractility because in addition to glycogen depletion, many other factors known to affect excitation-contraction (E-C) coupling (Stephenson *et al.*, 1998; see also section 1.2.3) would have been altered in the myoplasm of the fatigued muscle fibres.

Further advances can be made if the relationship between glycogen and muscle contractility is investigated in single fibres containing different concentrations of glycogen under conditions where the ionic composition of the myoplasmic environment is kept constant and similar to that in a rested muscle. The mechanically skinned single muscle fibre preparation is particularly well suited for such a task because the ionic composition of the myoplasmic environment can be directly controlled under conditions where the normal signal transduction mechanism remains functional (Lamb & Stephenson, 1990). Furthermore, individual fibres from freshly dissected skeletal muscles exhibit a broad range of glycogen concentrations (Hintz *et al.*, 1982; see also Chapter 3) and this allows preparation of mechanically skinned single fibres with a variety of naturally occurring glycogen concentrations.

The aim of the work presented in this chapter was to use single muscle fibres from the cane toad to determine the stability of glycogen in mechanically skinned fibre preparations under various conditions used in physiological experiments and to investigate whether there is a relationship between fibre glycogen content and E-C coupling under conditions of high concentrations of ATP and creatine phosphate in the myoplasmic environment. The results show that mechanically skinned fibre preparations exposed to aqueous solutions retain a large proportion of the initial glycogen in the intact fibre for a considerable period of time, that this pool of glycogen becomes depleted when contractions are elicited by the depolarisation of the transverse tubular system (T-system), that fibre capacity to respond to T-system depolarisation is related to glycogen content and, that this relationship is not based on the role of glycogen as an energy store.

## 4.2 MATERIALS AND METHODS

### 4.2.1 ANIMALS

Summer and winter toads (*Bufo marinus*) of both genders were collected and handled as described in section 3.2.2.1.

### 4.2.2 THE MECHANICALLY SKINNED FIBRE PREPARATION

Muscles (IF) were dissected and mechanically skinned fibres were prepared and measured as described in sections 3.2.2.1, 3.2.2.3, 3.2.2.4 and 3.2.2.5. The fibres were normally divided into two segments. When no T-system depolarisation experiments were carried out, both segments of a fibre were used to determine glycogen content under various conditions as described later in the text. When force recordings were made, the first segment of a pair was quickly skinned and rapidly mounted on the force recording apparatus; the second segment was used to measure glycogen concentration at the beginning of an experiment. This value was defined as the initial glycogen content. The segment used in the Na-depolarisation experiment was tied at one end with 10.0 (Deknatel) braided silk to the arm of a Sensoror 802 force transducer whilst the other end was clamped between the tips of a fine pair of forceps (Lamb & Stephenson, 1990; Stephenson & Williams, 1981; Moiescu & Thieleczek, 1978; Ashley & Moiescu, 1977). The sensitivity of the force measuring system was normally  $5\text{V N}^{-1}$  but could be varied. The natural frequency of the system was higher than  $180\text{ s}^{-1}$ , depending on the particular stainless-steel hook attached to

the original arm of the transducer. The total drift of the force recording system after a warming-up period (30min) was below  $3 \text{ nN s}^{-1}$  and the extraneous compliance was below  $10 \text{ mm/N}$ . The maximal forces recorded with this system were in the range  $0.1 - 1 \text{ mN}$  (Stephenson & Williams, 1981). All experiments were performed at a temperature of  $23 - 25^\circ\text{C}$ .

### 4.2.3 T-SYSTEM DEPOLARISATION EXPERIMENTS

*(These experiments were performed in collaboration with D. G. Stephenson)*

In the mechanically skinned muscle fibre, the T-system seals off uniformly along the entire length of the preparation (Lamb *et al.*, 1995). Under the action of the  $\text{Na}^+/\text{K}^+$  pump, normal  $\text{K}^+$  and  $\text{Na}^+$  gradients are re-established across the T-system when the preparation is bathed in the K-HDTA repriming solution (Table 4.1) and the sealed T-system becomes polarised like in an intact muscle fibre at rest (Lamb & Stephenson, 1990). The T-system can then be rapidly depolarised by transferring the fibre segment to a similar solution where all  $\text{K}^+$  is replaced by  $\text{Na}^+$  (depolarising solution, Table 4.1). Since the SR is almost equally permeable to  $\text{Na}^+$  and  $\text{K}^+$ , it is not expected that any significant swelling of the SR compartment would take place when switching from a  $\text{K}^+$ -based repriming solution to a  $\text{Na}^+$ -based depolarising solution (Lamb & Stephenson, 1990). The depolarisation of the sealed T-system in a skinned fibre preparation initiates the normal sequence of events occurring in E-C coupling and elicits a transient force response (Fig. 4.1) analogous to a  $\text{K}^+$ -contracture in an intact muscle fibre (Lamb & Stephenson, 1990). In all T-system depolarisation experiments, the skinned fibre segments were initially adjusted to slack length and

then were stretched by 20% to provide optimum conditions for observation of force responses (Lamb & Stephenson, 1990).

**Table 4.1. Composition of solutions used in physiological experiments (mM)**

	K	Na	Mg <sup>2+</sup>	HDTA	EGTA <sub>total</sub>	Ca <sup>2+</sup>
Repriming Solution	117	36	1	49.95	0.05	0.0002
T-system Depolarising Solution	-	153	1	49.95	0.05	0.0002
Relaxing Solution	117	36	1	-	50	< 10 <sup>-6</sup>
Maximum Ca <sup>2+</sup> -Activating Solution	117	36	1	-	50	0.03
Low Mg <sup>2+</sup> Solution	117	36	0.015	49.95	0.05	0.0001

All solutions also contained 8 mM ATP, 10 mM creatine phosphate and 60 mM HEPES pH buffer (pH 7.10 ± 0.01). Note that even without specific addition of inorganic phosphate to solutions, there was contaminating inorganic phosphate in solutions estimated at about 0.15 mM and that this concentration increases to 0.3 mM in maximally Ca<sup>2+</sup>-activated fibres (Fryer *et al.*, 1995).

HDTA = hexamethylenediamine N, N, N', N'-tetraacetic acid

EGTA = ethyleneglycol bis(β-aminoethyl ether)-N, N'-tetraacetic acid

The preparations were then equilibrated for 2 min in the repriming solution before being subjected to the series of successive cycles of depolarisation-repolarisation of the T-system. Prior to depolarisation of the T-system, the preparations were incubated in the repriming solution for a sufficiently long period of time (normally 1 min) to ensure that the peak amplitude of response was not dependent on the time in the repriming solution. Note that after a certain number of T-system depolarisation-induced responses, the E-C coupling mechanism becomes impaired and the size of the T-system depolarisation-induced force responses declines. This is known as fibre 'run-down' and cannot be reversed (Lamb & Stephenson, 1990). As illustrated in Fig. 4.1.

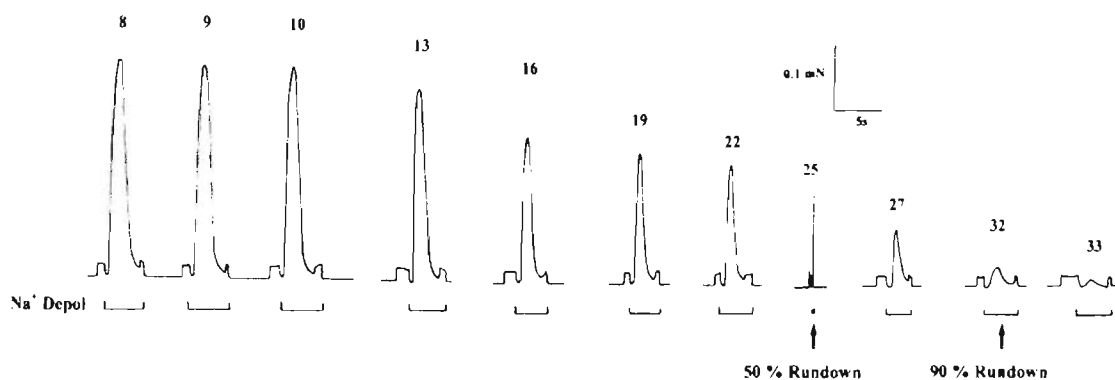


**Fig. 4.1** The ‘run-down’ of force responses induced by the depolarisation of the sealed T-system in a mechanically skinned muscle fibre segment.

The preparation was successively equilibrated in the ‘Repriming Solution’ to ensure maximal repriming of the voltage sensors in the T-system and then was transferred to the ‘Depolarising Solution’. This caused T-system depolarisation by ionic substitution, activation of the voltage sensors,  $\text{Ca}^{2+}$  release from the SR and activation of the contractile apparatus followed by voltage sensor inactivation,  $\text{Ca}^{2+}$  re-uptake by the SR and force relaxation (see Lamb & Stephenson, 1990). In the fibre shown, 50% and 90% run-down occurred after the 25<sup>th</sup> and the 32<sup>nd</sup> response to T-system depolarisation, respectively. The fibre segment diameter was 57.7  $\mu\text{m}$  and the initial glycogen concentration estimated from the paired segment (see text) was 96 mmol glucosyl units/l fibre. The 5 s time scale applies for the time in the  $\text{Na}^+$  depolarisation solution as indicated by the bars under traces, with the exception of the 25<sup>th</sup> response where the time scale was 75s. Numbers above traces refer to response number. Note that the ‘fibre capacity to T-tubule depolarisation’ was estimated to be 12.2 in this fibre (see text).

50% run-down is reached when the T-system depolarisation-induced force response becomes less than 50% of the maximum depolarisation-induced force response in that preparation and similarly, 90% run-down is attained when the response to T-system depolarisation decreases below 10% of the maximum depolarisation-induced response.

The most important parameter determining the loss of capacity to respond to T-system depolarisation is the preceding number of T-system depolarisation-induced responses and it has been suggested that the 'run-down' is caused by the use-dependent loss of some factor from the preparation (Lamb & Stephenson, 1990). In this study, *fibre response capacity* to T-system depolarisation is defined as the equivalent number of maximum  $\text{Ca}^{2+}$ -activated force responses that can be elicited in that preparation by successive T-system depolarisation until the response declines to 50% of its highest level. This parameter is obtained by dividing the sum of amplitudes of the depolarisation-induced force responses to 50% 'run-down' by the maximum  $\text{Ca}^{2+}$ -activated force response normally obtained at the end of an experiment. Therefore, *fibre response capacity* is always smaller than the number of depolarisation-induced responses to 'run-down'. Note that the ability of the contractile apparatus to develop maximum  $\text{Ca}^{2+}$ -activated force decreases only marginally for the duration of an experiment. Control experiments with three freshly dissected mechanically skinned muscle fibres activated successively by rapidly raising  $[\text{Ca}^{2+}]$  to 4  $\mu\text{M}$  and then decreasing it to below 0.1  $\mu\text{M}$  (Moiescu & Thieleczek, 1978; Moiescu, 1976) have shown that the maximal  $\text{Ca}^{2+}$ -activated force obtained at 30  $\mu\text{M}$   $[\text{Ca}^{2+}]$  decreased by only  $6.6 \pm 0.2\%$  after 35 activation-relaxation cycles lasting 4-6 s where the average

force response was  $85.5 \pm 3.0$  % of the maximum  $\text{Ca}^{2+}$ -activated force. Both the duration of the activation and the force level attained during activation were considerably higher than the corresponding averages for the depolarisation-induced force responses to 50% 'run-down'. Therefore, no specific correction was made to take into consideration the rather small deterioration in the ability of the skinned fibre to develop maximum  $\text{Ca}^{2+}$ -activated force that may be caused by successive depolarisation-induced responses.

The method used for expressing *fibre response capacity* takes into consideration the integrity of the coupling mechanism upon T-system depolarisation in a particular fibre segment until the 50% 'run-down' is reached, because it is based on the premise that full coupling should result in sufficient  $\text{Ca}^{2+}$  release from the SR to elicit near maximal  $\text{Ca}^{2+}$ -activated force responses (see for example Lamb & Stephenson, 1990).

#### **4.2.4 GLYCOGEN ANALYSIS**

##### **4.2.4.1 GLYCOGEN DETERMINATION IN CONTROL SEGMENTS**

The procedures used to determine total glycogen in control segments were carried out as described in chapters 2 and 3. They involved the determination of washable glycogen (**WGlyc**, section 3.2.3.5) in the washing solution and non-washable fibre glycogen (**NWGlyc**, 3.2.3.6). In this study the skinned fibre segments were washed in the 'repriming solution' (see Table 4.1) for 2 min in order to determine **WGlyc**.

#### 4.2.4.2 GLYCOGEN ANALYSIS IN FIBRES MOUNTED IN THE FORCE RECORDING APPARATUS

The method of fibre segment attachment to the force recording apparatus (which involves tying one end of the fibre segment to the force transducer and clamping the other end between platform forceps) prevents about 30% of the volume of the fibre segment used for force recording from being accessible to the bathing solutions.

Therefore, a correction can be made to estimate the glycogen concentration in the part of the fibre segment that was exposed to solutions. In performing this correction it was assumed that all glycogen lost from the fibre segment originated from 70% of the fibre volume and that the glycogen concentration in the remaining 30% of the fibre volume, which was not accessible to the bathing solution, was equal to the initial glycogen concentration, measured in its paired 'control' segment.

#### 4.2.5 ANALYSIS OF MUSCLE PROTEINS BY SODIUM DODECYL SULFATE – POLYACRYLAMIDE GEL ELECTROPHORESIS (*SDS- PAGE*)

Muscle proteins in single fibre segments or solutions in which single fibre segments were incubated for various periods of time, were solubilized at RT (19-25°C) for 24 hours in 10 to 20 µl solubilizing buffer (80 mM Tris, 2.3% w/v SDS, 710 mM β-mercaptoethanol, 10 mM dithiothreitol, 12.5% v/v glycerol, 13.6% w/v sucrose, 0.01% w/v Bromophenol Blue, 0.1 mM PMSF, 0.002 mM leupeptin and 0.001 mM pepstatin). The samples were subsequently boiled for 3 min (Chrambach, 1985) and

cooled down to RT before being subjected to SDS-PAGE or were stored at  $-85^{\circ}\text{C}$  until use.

**Table 4.2. Recipe for preparing the GLYCINE-SDS separating gels used in analyses of low molecular weight muscle proteins.**

Total volume is 12 ml (for casting two separating gels).

Stock solutions	Volume (ml)	Final concentration
Acrylamide and Bis stock, T=36%; C=2.6%	4.000	T=12%; C=2.6%
Tris-HCl separating gel buffer; 3 M, pH=9.3	3.000	750 mM
Distilled water (double deionised)	2.418	---
Glycerol	2.400	20% (v/v)
SDS 10% (w/v)	0.120	0.1% (w/v)
Ammonium persulfate 10% (w/v)	0.048	0.04% (w/v)
TEMED, concentrated solution (14.2 M)	0.014	0.116% (v/v)

*Acrylamide-bisacrylamide stock solution; T = 36%, C = 2.6%:* 35.064 g of acrylamide and 0.936 g of bisacrylamide were dissolved in total volume of 100 ml of distilled water and stored at  $4^{\circ}\text{C}$ . Due to acrylamide monomer being hydrolysed into acrylic acid and ammonia upon prolonged storage (Hames and Rickwood, 1990), only enough acrylamide/bisacrylamide stock solution for use within one month was prepared to ensure reproducibility of data.

*Separating gel buffer 3 M Tris-HCl, pH 9.3:* 36.41 g of Tris and 30 ml of 1 M HCl were mixed and vigorously stirred until all Tris was dissolved and then the pH of the mixture was adjusted to the desired value. This buffer was stored and used over several months.

Low molecular weight ( $< 45$  kDa) myofibrillar proteins were separated on Glycine-SDS-PAGE using acrylamide/bisacrylamide separating gels (see Table 4.2 for composition) and the Hoefer Mighty Small II SE 260 Mini-Vertical Gel

Electrophoresis Unit (Pharmacia Biotech, San Francisco, USA). The gels, covered with running buffer, were allowed to set at RT overnight (see Table 4.2).

**Table 4.3. Recipe for preparing the stacking gels used in the GLYCINE-SDS-PAGE system.** Total volume is 6 ml.

Stock solutions	Volume (ml)	Final concentration
Acrylamide and Bis stock, T=10%; C=4.76%	2.400	T = 4%; C = 4.76%
Tris-HCl separating gel buffer, 0.5 M, pH=6.8	1.500	125 mM
Distilled water (double deionised)	1.374	---
Glycerol	0.600	10% (v/v)
SDS 10% (w/v)	0.060	0.1% (v/v)
Ammonium persulfate 10% (w/v)	0.060	0.1% (v/v)
TEMED, concentrated solution (14.2 M)	0.006	0.1% (v/v)

*Acrylamide-bisacrylamide stock solution; T = 10%, C = 4.76%:* 10.00 g of acrylamide and 0.5 g of bisacrylamide are dissolved in total volume of 100 ml of distilled water and stored at 4°C.

*Stacking gel buffer 0.5 M Tris-HCl, pH 6.8:* 6.181 g of Tris and 30 ml of 0.5 M HCl are mixed and vigorously stirred until all Tris is dissolved. adjusted to desired pH and made up to 100 ml with distilled water.

The composition of the stacking gels used in this study is presented in Table 4.3.

Stacking gels were allowed to set at RT for 30 min.

The running buffer contained SDS 0.1% w/v, 50 mM Tris and 380 mM glycine and gels were run at constant current (10 mA/gel) for 4.5 h at RT. A 10 µl sample aliquot containing 4 nl fibre volume or a volume of solution in which a 4 nl fibre segment

was washed/incubated for an appropriate time was loaded for each electrophoretic well. The gels were stained using the Hoefer silver staining protocol and protein bands corresponding to major muscle proteins (such as myosin heavy chain and light chains, tropomyosin, actin, creatine kinase and parvalbumin) were identified based on their migration velocity using commercially purified rabbit muscle proteins as references.

#### **4.2.6 DATA PRESENTATION AND STATISTICAL ANALYSES**

All data are presented as means  $\pm$  SE and statistical significance was assessed with Student's paired and unpaired *t*-test, as appropriate. Linear regression analysis was done using the software package GraphPad Prism.

## 4.3 RESULTS

### 4.3.1 GLYCOGEN STABILITY IN MECHANICALLY SKINNED MUSCLE FIBRE PREPARATIONS

In Chapter 3 it was shown that toad skeletal muscle fibres contain a washable and a non-washable glycogen pool. The non-washable glycogen pool, representing about 74 to 85% of the total glycogen in intact fibres, did not decline in mechanically skinned muscle fibre segments after exposure to a solution lacking MgATP at pH 5.0 for up to 40 min. Raising the pH to more physiological levels (pH 7.0) produced similar results to those obtained at pH 5.0. Thus, after 30 min exposure to 100 mM Na-acetate solution of pH 7.0 without added calcium or MgATP, the fraction of initial total glycogen remaining in the fibre was  $83.9 \pm 3.3\%$  and this value was not significantly different from the fraction of glycogen remaining in the skinned fibre preparation after only 5 min wash (Fig. 4.2). These results were obtained with paired segments from the same fibre whereby the first segment was used to estimate the total initial glycogen concentration in the fibre (5 min washed in acetate buffer pH 5.0) and the second segment was used to estimate the glycogen remaining in the fibre after the respective period of incubation in the various rigor solutions. By using paired segments from the same fibre, where one segment acted as control, it was possible to avoid the large variability in glycogen concentration between fibres in the same muscle and between fibres in different toads (see Chapter 3).

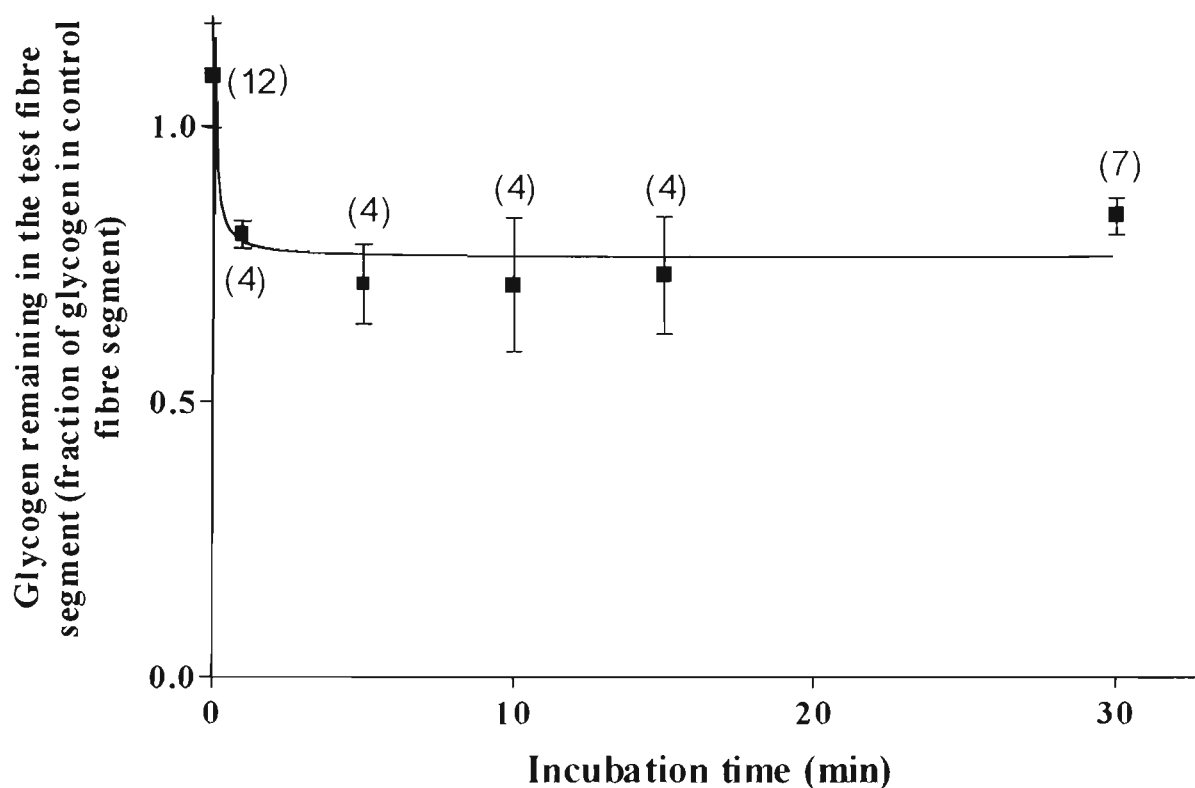


**Figure. 4.2.** Fraction of total glycogen remaining in mechanically skinned fibres after exposure to a rigor solution containing 100 mM Na-acetate at pH 7.0.

The results were obtained with paired segments from the same fibre, where the first segment was used to estimate total initial glycogen in the fibre and the second segment was used to estimate the glycogen concentration remaining in the fibre after the respective period of incubation. Numbers above data points indicate the number of pairs of fibre segments used. The data point at time zero was obtained from total glycogen measurements in 12 pairs of segments which were not exposed to the rigor solution. The points were fitted by a hyperbola.

The experimental point for zero wash time in Figure 4.2 was obtained by measuring the total glycogen concentration in 12 pairs of fibre segments which were not exposed to the rigor solution and by calculating the ratio between total glycogen concentrations in the second and the first segment belonging to a pair. This ratio ( $1.09 \pm 0.09$ ,  $n = 12$ ) was not statistically significantly different from 1.00.

The high retention of glycogen in skinned fibres exposed to non-MgATP solutions could be due to the formation of rigor cross-bridges between myofilaments, rendering the myofibrils rather stiff, which would prevent glycogen particles from being washed away from the preparation under rigor conditions. Therefore, for the present study it was important to examine the fate of the glycogen pool in mechanically skinned fibre segments to a relaxing solution, which mimics the intracellular ionic composition of the myoplasmic environment when the fibre is at rest. Such a solution is the 'repriming' solution (Table 4.1) used in the T-system depolarisation-induced responses and results obtained with this solution are shown in Fig. 4.3. All results in Fig. 4.3 were obtained with paired segments from the same fibre. In these experiments the 'control' segment in each pair was washed for 2 min in the 'repriming' solution to resemble the conditions used in the T-system depolarisation-induced experiments where the skinned fibre segments are incubated for 2 min in the 'repriming' solution prior to being subjected to the first depolarisation. The 'test' segment was also initially incubated for 2 min in the 'repriming' solution and this was normally followed by further treatment. No further treatment of the 'test' segment was necessary for the zero time wash where the data point represents the ratio between fibre glycogen in 12 'test' segments and their paired 'control' segments when

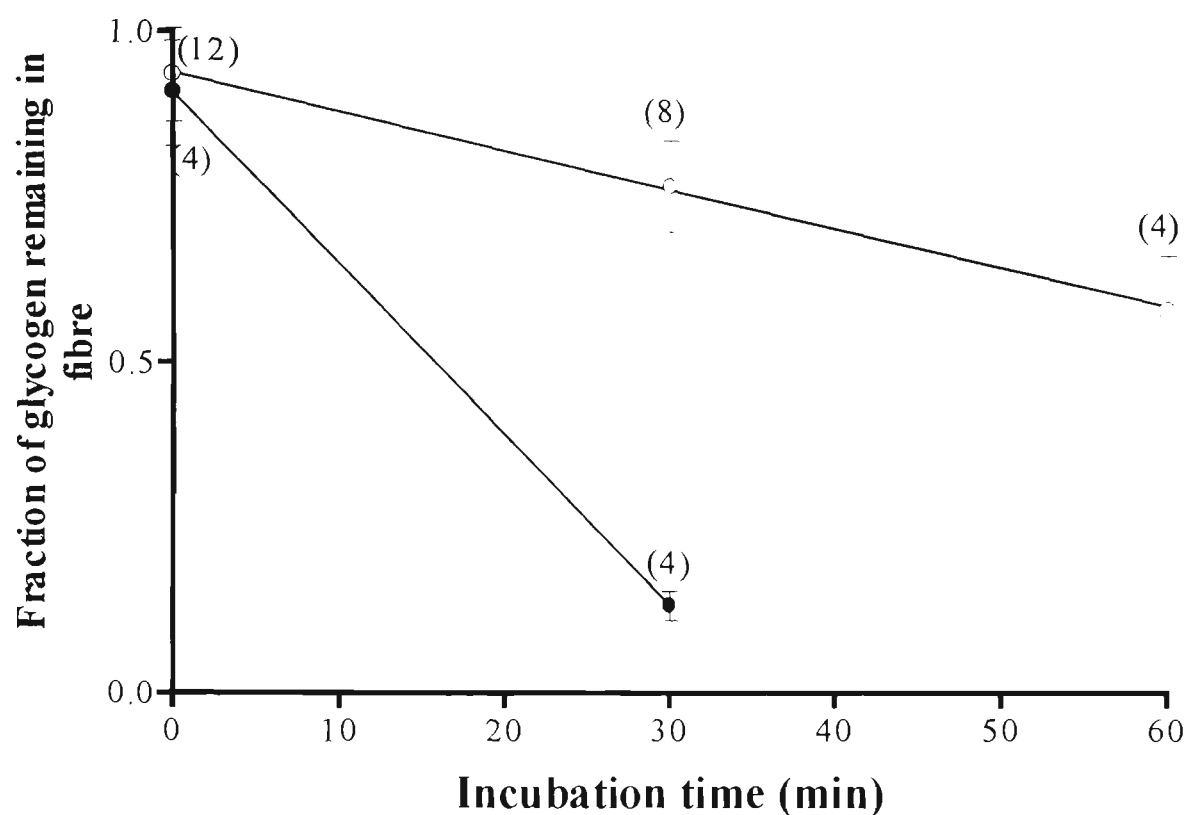


**Figure. 4.3.** Time course of fibre glycogen loss from mechanically skinned fibre segments exposed to a solution mimicking the intracellular ionic environment when the muscle fibre is at rest (repriming solution in Table 4.1) (O) and to a solution containing  $30 \mu\text{M Ca}^{2+}$  (Maximum  $\text{Ca}^{2+}$ -Activating Solution in Table I) (●).

The results were obtained with paired segments from the same fibre where both segments ('control' and 'test') were initially washed for 2 min in the repriming solution. Results are expressed as fraction of glycogen concentration in the 'test' segment/ glycogen concentration in the 'control' segment after the 2 min wash in the repriming solution. Numbers above data points indicate the number of pairs of fibre segments used. The data point at time zero was obtained from glycogen measurements in 12 pairs of segments which were exposed for 2 min to the repriming solution. The mean value of glycogen in the individual fibres used in this experiment after the 2 min wash in the repriming solution was  $81.2 \pm 4.3$  mmol glucosyl units/l fibre volume ( $n=32$ ). The slopes of the lines of best fit  $0.0059 \pm 0.0020 \text{ min}^{-1}$  for (O) and  $0.0266 \pm 0.0038 \text{ min}^{-1}$  for (●).

both were washed for 2 min in the 'repriming' solution. As illustrated in Figure 4.3, exposure of the 'test' skinned fibre segments to 'repriming' solution caused a steady, time-dependent loss of fibre glycogen at a rate of  $0.59 \pm 0.20\%$  fibre glycogen  $\text{min}^{-1}$ . Thus, after 30 min exposure to this solution, the fibre glycogen content was  $76.7 \pm 7.0\%$  of that in the control segment ( $n = 8$ ). Analysis of glycogen in the relaxing solutions in which the skinned fibre segments were incubated, indicated that this glycogen pool could account for all fibre glycogen lost from the fibre under such conditions (ratio between glycogen present in the bathing solution and estimated glycogen lost from the 'test' fibre segment was  $1.14 \pm 0.36$ ,  $n = 8$ , where the amount of glycogen lost was calculated by subtracting the concentration of glycogen remaining in the 'test' fibre segment from that in the 'control' fibre segment and by multiplying by the volume of the 'test' fibre segment). Hence, in a relaxing solution, fibre glycogen does not appear to be degraded to simple sugar molecules before being lost into the bathing solution. This is fully consistent with the fact that glycogenolysis does not occur at low  $[\text{Ca}^{2+}]$  and in the absence of inorganic phosphate.

In order to determine whether the rate of glycogen loss from the mechanically skinned fibre is  $[\text{Ca}^{2+}]$  dependent, the preparation was activated in the presence of  $30 \mu\text{M Ca}^{2+}$  (maximally activating  $\text{Ca}^{2+}$  solution, Table 4.1) and the fraction of glycogen lost was estimated both in the fibre segment and in the washing solution. The results from such an experiment using paired segments from the same fibre are also shown in Figure 4.3. The data point for 10 second exposure to the maximally activating  $\text{Ca}^{2+}$  solution was not statistically different from the data point for no exposure to the  $30 \mu\text{M Ca}^{2+}$  solution ( $90.7 \pm 8.0\%$ ,  $n = 4$  vs  $93.6 \pm 7.0$ ,  $n = 12$ ). However, after 30 min

exposure to the 30  $\mu\text{M}$   $\text{Ca}^{2+}$  solution,  $86.7 \pm 2.2\%$  ( $n = 4$ ) of the initial fibre glycogen was lost. The average rate of glycogen loss was  $2.66 \pm 0.38\% \text{ min}^{-1}$  which is 4.5 fold greater than the rate of glycogen loss in the 'repriming' solution. Moreover, analysis of the 30 min-wash solution indicated that only a very small fraction of fibre glycogen was lost as glycogen (0 to 6%,  $n = 4$ ) or glucose ( $18.6 \pm 3.8\%$ ,  $n = 4$ ) and that the majority of glycogen (about 80%) was lost in a form that was not detected with the method used. Since the end product of  $\text{Ca}^{2+}$ -activated phosphorolysis is G1P (see section 1.3.3 for details on muscle glycogen catabolism) which was not detectable by the fluorogenic analysis used in this study (due to absence of the enzyme *phosphoglucomutase* that helps to convert G1P to G6P), this result strongly indicates that the mechanically skinned fibre segments retain an active phosphorylase kinase/glycogen phosphorylase system. This is not surprising considering that phosphorylase, its modulating enzymes and glycogen particles are part of a tightly integrated system which is regulated by  $\text{Ca}^{2+}$  (Entman *et al.*, 1980). Note that even without specific addition of inorganic phosphate to solutions, the ATP and creatine phosphate solutions contained about 0.15 mM inorganic phosphate and in the maximally activated fibre this concentration is expected to increase up to 0.3 mM (Fryer *et al.*, 1995).

Considering that fibre glycogen was lost by prolonged exposure to 30  $\mu\text{M}$   $\text{Ca}^{2+}$  solution, it was of great interest to find out whether glycogen could also be lost from the fibre segment by T-system depolarisation-induced  $\text{Ca}^{2+}$  release from the SR loaded at endogenous levels. In this experiment the skinned fibre preparation was successively activated by depolarisation of the sealed T-system (Figure 4.1) until the

preparation was 90% 'run-down' (the depolarisation-induced force response was reduced to 10% of its maximum level and remained below 10% of its maximum level after one more depolarisation). Under these conditions, the fibre glycogen content in the 90% run-down fibre segment decreased by  $53 \pm 9\%$  ( $n = 4$ ) compared with that in the control segment. The control segment from the same fibre was incubated for 2 min in the 'repriming' solution before being analysed for glycogen. The average time to 90% run-down was  $26 \pm 4$  min for the four pairs of fibre segments used in this experiment and the fraction of fibre glycogen at the end of the T-system depolarisation-induced sequence of force responses ( $47 \pm 9\%$ ,  $n = 4$ ) was significantly reduced ( $P = 0.016$ ) compared with that following incubation without depolarisation in the 'repriming' solution for 30 min ( $76.7 \pm 7.0$ ,  $n = 8$ , Fig. 4.3). Furthermore, if a correction was made for solution inaccessibility to part of the fibre volume due to the method of fibre attachment to the force recording apparatus (see Methods), one could estimate that the glycogen concentration in the part of the fibre segment which was exposed to solutions, would have decreased to less than 25% of the initial value ( $24.3 \pm 12.9\%$ ,  $n = 4$ ). Regardless of whether the correction was applied or not, these results clearly demonstrate that glycogen depletion occurred in the mechanically skinned fibre when  $\text{Ca}^{2+}$  was released from the SR by the depolarisation of the T-system.

In order to estimate the rate of glycogen loss from the fibre during T-system depolarisation-induced responses one could consider that the average number of depolarisation-induced responses to 90% run-down was  $21.3 \pm 4.7$  ( $n = 4$ ) and that the average duration of a response measured at the base was about 2 s (see Fig. 4.1).

Therefore, one could argue that, on average, the preparations were activated by T-system depolarisation for 42.6 s and this caused a depletion of fibre glycogen by 29.7% without correction for restricted access of 30% fibre segment volume to the bathing solution (76.7 – 47%) and 52.4% (76.7 – 24.3%) when the correction was applied. With these values, the rate of glycogen loss caused by T-system depolarisation-induced responses was estimated to be 41.8 and 73.8% min<sup>-1</sup> without and with restricted volume correction, respectively. In either case, this rate is at least one order of magnitude greater than that measured in the fibre segment exposed to the maximum Ca<sup>2+</sup>-activating solution.

#### **4.3.2 CORRELATION BETWEEN FIBRE RESPONSIVENESS TO T-SYSTEM DEPOLARISATION AND GLYCOGEN CONTENT**

As seen in Fig. 4.1, after a certain number of T-system depolarisation-induced responses are elicited in a mechanically skinned fibre preparation, the E-C coupling mechanism becomes impaired as indicated by the decline in the size of the T-system depolarisation-induced responses. This loss of fibre response capacity to T-system depolarisation cannot be reversed and its onset shows a great deal of variability between fibres (Lamb & Stephenson, 1990).

The major goal of this study was to assess whether there is a correlation between fibre response capacity to T-system depolarisation and fibre glycogen concentration under conditions where the concentrations of ATP and creatine phosphate in the myoplasm were high and not altered. In order to determine the fibre response capacity to T-

system depolarisation for individual fibre segments, the sealed T-system network of the mechanically skinned fibre preparation was successively depolarised as shown in Fig. 4.1 until the depolarisation induced response decreased to 50% of the maximum Na-depolarisation-induced force response and this was then followed by brief activation (less than 10s) in the maximum  $\text{Ca}^{2+}$ -activating solution of  $30 \mu\text{M Ca}^{2+}$ . Several preparations were briefly exposed to a low  $[\text{Mg}^{2+}]$ -solution ( $0.015 \text{ mM}$ ) immediately after the 'run-down' to check the pool of SR releasable  $\text{Ca}^{2+}$ . The glycogen concentration in the fibre segment at the start of the series of successive depolarisations (initial glycogen) was assessed from measurements of glycogen concentration in its paired segment that was incubated in the repriming solution for 2 min. This is the normal incubation period in the repriming solution prior to subjecting a fibre segment to successive depolarisation-repolarisation cycles.

In order to ensure that the fibre population tested had a broad range of glycogen concentrations, iliofibularis muscles were obtained from toads collected throughout the year since it had been previously shown that fibre glycogen content varies greatly with the seasons when the toads were collected (see Chapter 3).

The results obtained with 22 pairs of fibre segments from 7 toads collected in summer (3), spring (1), autumn (1) and winter (2), are displayed in Fig. 4.4 and a statistical analysis of the data indicates that there is a highly significant linear correlation ( $P < 0.0001$ ) between fibre response capacity expressed as equivalent number of maximum  $\text{Ca}^{2+}$ -activated force responses that can be elicited by successive T-system depolarisation until 50% run-down and initial fibre glycogen concentration. No fibre

which had a low initial glycogen content (Fig. 4.4) displayed a high fibre response capacity to T-system depolarisation. This clearly shows that the presence of a significant pool of fibre glycogen is necessary to ensure a high capacity for fibre excitability.

Note that in order to convert the number of depolarisation-induced responses to *fibre response capacity*, the sum of the amplitudes of the depolarisation-induced responses was divided by the maximum  $\text{Ca}^{2+}$ -activated response in that fibre (see Methods). For the fibre whose results are shown in Fig. 4.1, the maximum  $\text{Ca}^{2+}$ -activated response was not measured because the fibre segment could not be exposed to high  $[\text{Ca}^{2+}]$  before measuring the glycogen content. However, based on the fibre cross-sectional area the maximum  $\text{Ca}^{2+}$ -activated force could be estimated and it would have been about 1.5 fold the size of the largest depolarisation-induced response. Based on this estimation, the fibre response capacity would have been 12.2 and this is within the range of the data points shown in Fig. 4.4. The slope of the line of best fit in Fig. 4.4 indicates that each mmol glucosyl/l fibre unit of *initial* glycogen confers on the fibre the capacity to produce a T-system depolarisation-induced response. The intercept of the line of best fit with the X-axis is close to and not significantly different from zero suggesting a direct proportionality between initial glycogen content and fibre response capacity to T-system depolarisation.

In order to verify that in the run-down fibres the SR was functional and loaded with enough  $\text{Ca}^{2+}$  to elicit near maximal contractions, the inhibition exerted by the 1mM

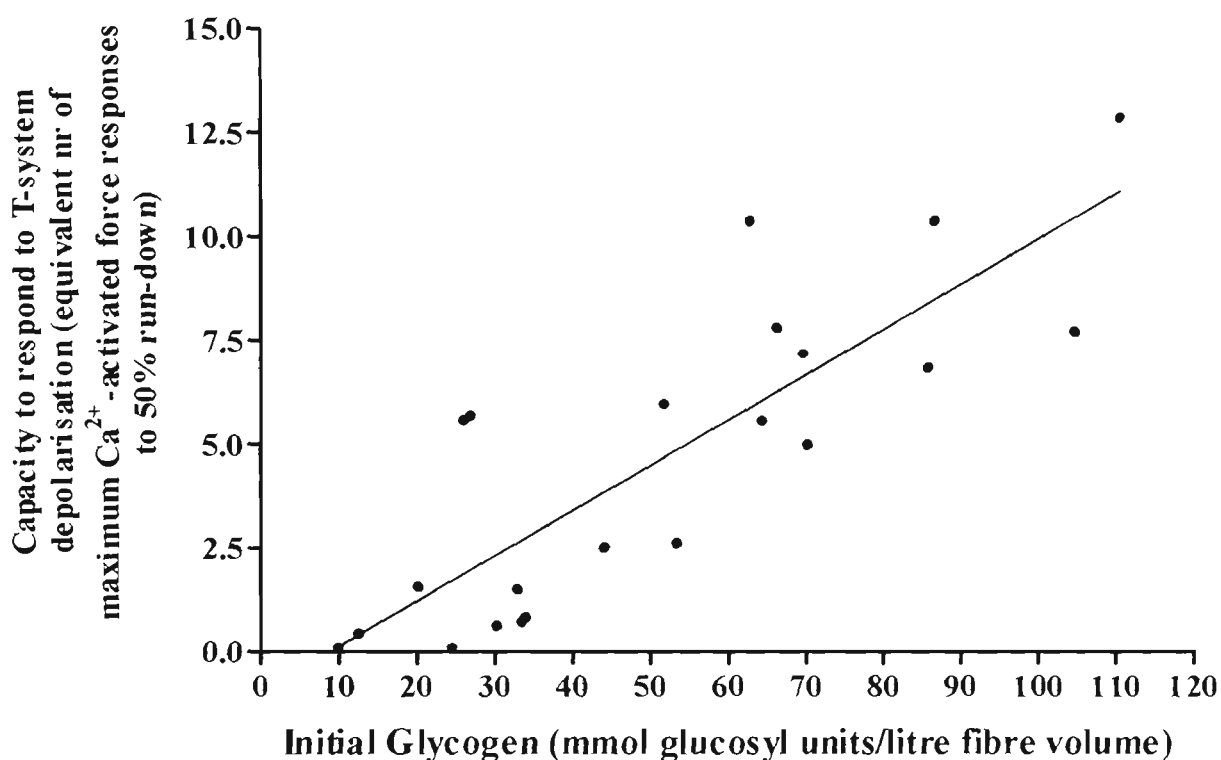


**Figure 4.4.** Correlation between capacity of fibre to respond to T-system depolarisation and glycogen concentration in the fibre at the beginning of the series of depolarisation, measured in paired segments from the same fibres.

The fibre response capacity to T-system depolarisation is expressed in equivalent number of maximum  $\text{Ca}^{2+}$ -activated force responses that can be elicited in that preparation by successive T-system depolarisations until the response declined to 50% of its highest level (50% run-down, see text). Correlation factor  $r = 0.83$ ; slope  $0.109 \pm 0.016$  maximum  $\text{Ca}^{2+}$ -activated responses per mmol glucosyl unit of initial fibre glycogen (95% confidence intervals 0.075 to 0.144;  $P < 0.0001$  that slope is zero). Y axis intercept:  $-0.93 \pm 0.95$ .

$Mg^{2-}$  on the SR  $Ca^{2+}$  release channels was removed by exposing six 'run-down' preparations to a low  $Mg^{2+}$  (0.015 mM) solution (Table 4.1). In all instances, near maximal  $Ca^{2+}$ -activated force responses were obtained, demonstrating that the SR was functional and that a large pool of releasable  $Ca^{2+}$  was available in the SR at that time. Since neither the contractile apparatus nor the SR function appear to be impaired in 'run-down' fibres (Lamb & Stephenson, 1990), it follows that the 'run-down' must be caused by impairment of an earlier event in the E-C coupling process. It has been already shown that T-system depolarisation induced contraction is accompanied by marked glycogen loss. To determine the level of depolarisation-induced force response (expressed as percent of the maximum  $Ca^{2+}$ -activated force) that leads to the depletion of 1 mmol glucosyl unit/l fibre, estimates were made of the glycogen concentration lost ( $Glyc_{lost}$ ) and the equivalent number of maximum  $Ca^{2+}$ -activated force responses induced by depolarisation in 17 fibre segments after they were activated to 50% run-down and then briefly (less than 10s) maximally activated in the 30  $\mu M$   $Ca^{2+}$  solution.  $Glyc_{lost}$  was calculated by subtracting the glycogen concentration in the 50% run-down fibre segments (correction for solution inaccessibility to 30% of the fibre volume due to constraints associated with the fibre attachment to the force recording apparatus; see Methods) from the 'initial' glycogen concentration measured in the paired segments (corrected for the incubation-related loss of glycogen in the HDTA repriming solution; see Fig. 4.3). No correction was made with respect to the brief exposure to the maximum  $Ca^{2+}$ -activating solution because, as shown in Fig. 4.3, exposure for 10s to the 30  $\mu M$   $Ca^{2+}$  solution would have reduced the fibre glycogen concentration by less than 1%.

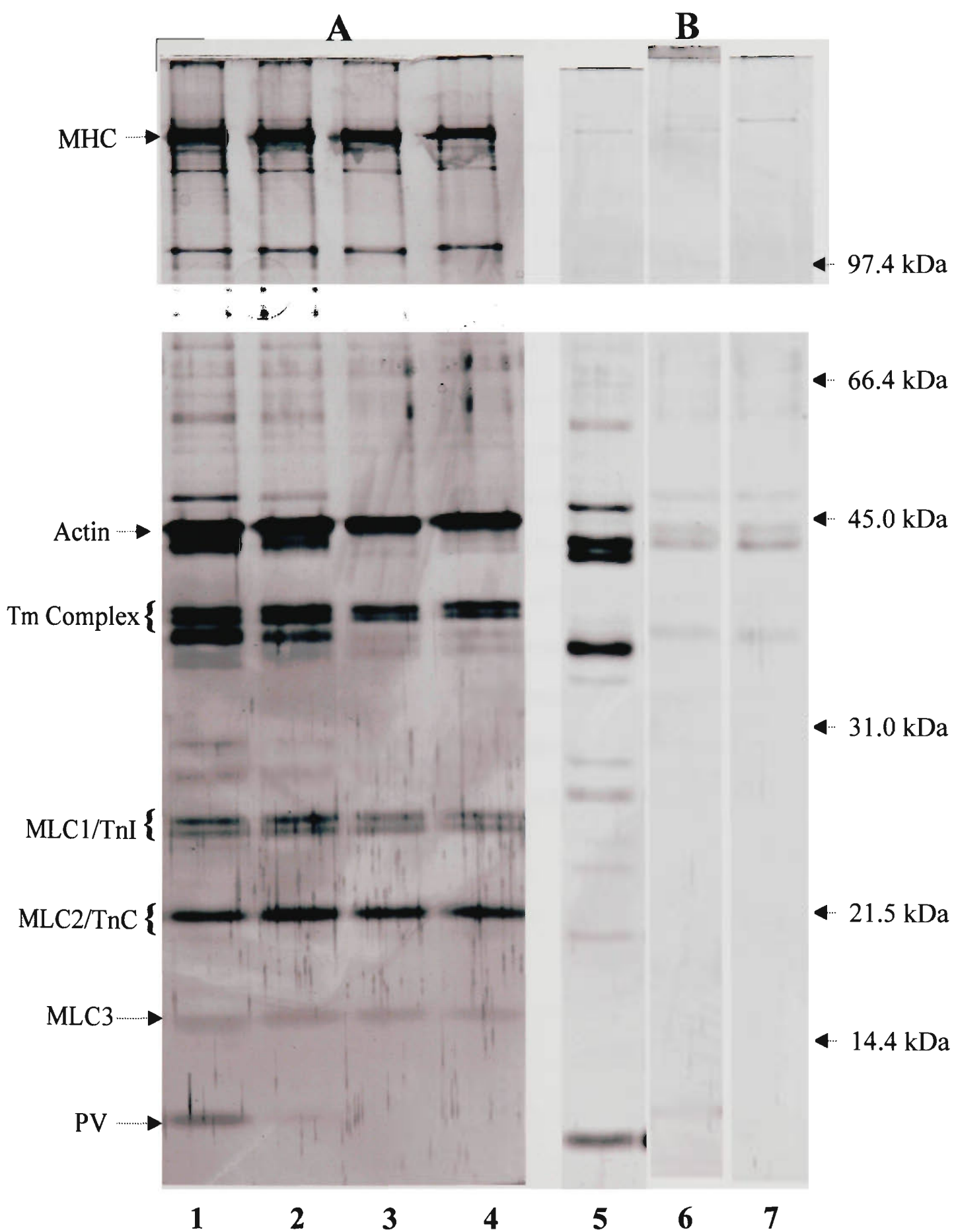
A value of  $8.6 \pm 3.5\%$  of the maximum  $\text{Ca}^{2+}$ -activated force induced by T-system depolarisation per 1 mmol glucosyl unit of *lost* fibre glycogen/l fibre was obtained from the linear regression analysis of the data. This value was close to and not statistically different from the 'response capacity' to T-system depolarisation conferred on the fibre by 1 mmol glucosyl unit of *initial* fibre glycogen/l fibre ( $10.9 \pm 1.6\%$  maximum  $\text{Ca}^{2+}$ -activated force), suggesting a causal relationship between the depolarisation-induced fibre glycogen loss and the use-dependent reduction in the capacity of the fibre to respond to T-system depolarisation. Addition of glycogen (100 mmol glucosyl units/ml) to solutions did not prevent fibre run-down and did not restore to any degree the ability of the 'run-down' fibres to respond to sealed T-system depolarisation.

#### **4.3.3 PROTEIN PROFILE OF FIBRE SEGMENTS AND WASH-OUT/INCUBATION SOLUTIONS**

Many different types of molecular species are docked to glycogen particles and therefore are expected to be lost from a mechanically skinned fibre preparation when glycogen is broken down. If some of these molecules, such as kinases and phosphatases, are necessary in E-C coupling, then E-C coupling would become impaired when glycogen is broken down. The extent of protein loss was assessed from the freshly skinned fibre preparation incubated under conditions where the glycogen pool becomes depleted (high  $[\text{Ca}^{2+}]$ ) and where the glycogen pool is only marginally affected (low  $[\text{Ca}^{2+}]$ ).



**Figure 4.5.** Silver stained electrophoretogram of muscle proteins from segments of single muscle fibres (A) and from the solutions (see Table 1 for the composition of solutions) to which single fibre segments were exposed for various lengths of time (B). Samples shown are as follows: Lane 1: freshly dissected fibre; Lane 2: fibre segment after 2 min incubation in the low  $[Ca^{2+}]$  repriming solution containing 100  $\mu$ M total EGTA (washed fibre); Lane 3: washed segment after additional 30 min incubation in the low  $Ca^{2+}$  repriming solution; Lane 4: washed fibre segment after 30 min incubation in the maximum  $Ca^{2+}$ -activating solution; Lane 5: the low  $Ca^{2+}$  repriming solution in which the fibre segment was incubated/washed for 2 min; Lane 6: the low  $Ca^{2+}$  repriming solution in which the fibre segment was incubated for 30 min; Lane 7: the maximum  $Ca^{2+}$ -activating solution in which a washed fibre segment was incubated for 30 min. Sample size for single fibre segment: 4nl fibre volume; sample for solution: the whole volume of washing/incubating solution in which a 4 nl fibre segment was washed/incubated for the appropriate time. Results in lanes 3, 4, 6 and 7 were obtained with paired segments of one fibre. MHC: myosin heavy chain; Tm: tropomyosin; MLC: myosin light chain; TnI: troponin I; TnC: troponin C; PV: parvalbumin.



In Fig. 4.5A are shown the protein profiles of freshly skinned segments before exposure to an aqueous solution (lane 1), after 2 min wash in the low  $[Ca^{2-}]$  solution (repriming solution with 100  $\mu$ M total EGTA; lane 2), after another 30 min in the low  $[Ca^{2-}]$  solution (lane 3), where the glycogen pool remains largely intact (see Fig. 4.3) and after 30 min exposure to the maximum  $Ca^{2-}$ -activating solution (lane 4), when the glycogen pool is greatly diminished (see Fig. 4.3). The results show that there was essentially no loss of any of the major protein components in the muscle fibre such as myosin heavy chains and actin after any of the treatments described above. The protein profile in the wash-out/ incubation solutions was also examined and the results are also shown in Fig. 4.5B. From the silver stained SDS-PAGE analysis one can see that there are at least 11 proteins varying in molecular weight between 10 and 80 kDa which are lost after 2 min wash (lane 5). Further incubation of the skinned fibre segments for 30 min in either the low  $[Ca^{2-}]$  or high  $[Ca^{2-}]$  solution apparently caused only further wash-out of the same protein species which were lost after 2 min in the low  $[Ca^{2+}]$  'repriming' solution but did not result in the obvious removal of extra protein components (lane 6&7). Similar results demonstrate that the amount of protein that is tightly and specifically bound to the fibre glycogen is below the limit of detection with our quite sensitive technique.

#### 4.4 DISCUSSION

This study demonstrates that the mechanically skinned fibre preparation is very well suited to investigate the relationship between fibre glycogen and muscle contractility under conditions where the composition of the intracellular environment can be carefully controlled.

The most important result from this investigation refers to the finding that, under conditions where the concentrations of ATP (8 mM) and creatine phosphate (10 mM) were maintained high and constant, the capacity of the skinned muscle fibre to respond to T-system depolarisation was strongly positively correlated with the concentration of the glycogen pool in the fibre (Fig. 4.4). Moreover, successive force responses induced by T-system depolarisation were shown to be the major factor responsible for the depletion of the glycogen pool in the skinned fibre preparation. In turn, the depolarisation-induced depletion of fibre glycogen markedly diminished the capacity of the skinned fibre preparation to respond to T-system depolarisation. These results represent the strongest indication so far that the presence of non-washable glycogen in skeletal muscle fibres is a pre-requisite for normal E-C coupling and that this protective role exerted by glycogen does not relate to its role of energy store in the fibre. Recently, Chin and Allen (1997) reported that the mean values for myoplasmic  $[Ca^{2+}]$  during tetanic stimulation in mammalian skeletal muscle fibres were positively correlated with the relative glycogen concentration in the intact fibres and there is a large body of information, particularly for mammalian skeletal muscle, that associates the presence of glycogen above a critical level with the ability of the

muscle to contract (Chin & Allen, 1997; Fitts, 1994; Vollestad *et al.*, 1988; Galbo *et al.*, 1979; Bergström *et al.*, 1967). Some have argued recently that glycogen depletion may lead to local shortages in ATP (8 mM) and creatine phosphate (10 mM) in the myoplasmic environment. In the present experiments the provision of 8 mM ATP and 10 mM creatine phosphate should have prevented any local shortage of ATP. The high activity of creatine phosphokinase associated with the SR membranes (see for example Rossi *et al.*, 1990) would have further prevented any significant local depletion of ATP and accumulation of ADP in the vicinity of the SR. Previous observations with mechanically skinned fibre segments indicated that it was necessary to decrease the [ATP] in the bathing solution to 2 mM or less in order to reduce the amount of Ca<sup>2+</sup> release from the SR by T-system-induced depolarisation (Owen *et al.*, 1997). Therefore, the experiments reported here provide strong evidence against any variant of an energy limitation hypothesis for the protective role played by glycogen in muscle contractility. This conclusion is in agreement with Vollestad *et al.*, (1988) who argued against the energy limitation hypothesis on the basis that there was a significant amount of ATP that remained available in the myoplasm, even under conditions of extreme fatigue. However, under those conditions one could argue that locally, the free energy from the hydrolysis of ATP could have been significantly reduced due to accumulation of inorganic phosphate and ADP.

The results from this study demonstrate that in mechanically skinned fibres, the glycogen pool is very stable under rigor conditions and relatively stable in relaxing solutions. The pool of glycogen in mechanically skinned fibres is likely to be represented by glycogen particles tightly attached to the SR membranes (Entman *et al.*, 1980) since any glycogen which was not tightly attached to intracellular structures

should be able to diffuse out from the preparation in the relaxing solution. The enhanced stability of the glycogen pool in the rigor preparation can be explained by further trapping of glycogen particles between rigid myofibrils in rigor. The slow loss of glycogen in the relaxing solution appears to be in the form of glycogen rather than as a result of glycogenolysis, suggesting that some glycogen particles are able to diffuse slowly from the relaxed muscle.

Importantly, the rate of loss of glycogen was markedly increased by a factor of 4.5 when the ionised  $[Ca^{2+}]$  in the preparation was increased from 0.2 to 30  $\mu M$  and under these conditions glycogen was broken down rather than simply diffusing out of the preparation. The observations indicate that  $Ca^{2+}$ -dependent glycogenolysis by phosphorolysis occurs in the mechanically skinned fibre preparation, as would be expected if the SR-glycogenolytic complex (Entman *et al.*, 1980) remained functional in this preparation. It is particularly important to note that the rate of glycogen loss from the skinned fibre preparation appeared greater by at least one order of magnitude following T-system depolarisation-induced force responses. This could be due either to a more efficient activation of the SR-glycogenolytic complex by physiological  $Ca^{2+}$  release from the SR (Entman *et al.*, 1980; Danforth & Helmreich, 1964) than by exogenous  $Ca^{2+}$  or to a considerably longer period of activation of the SR-glycogenolytic complex than the duration of the force response (which was used to calculate this rate) or both. Nevertheless, it was estimated that about 9 – 12 mmol glucosyl units/l fibre (the reciprocal values of 10.9% and 8.6% of maximum  $Ca^{2+}$ -activated force per mmol glucosyl units/l fibre; see Results) are lost with each equivalent maximum  $Ca^{2+}$ -activated response induced by depolarisation. This is

equivalent with 14 – 18 mmol phosphate/l fibre water (assuming that 1 litre fibre contains about 0.65 l water; see Baylor *et al.*, 1983) being used in glycogen phosphorolysis for each equivalent maximum  $\text{Ca}^{2+}$ -activated response. Undoubtedly, this represents a sizeable sink for inorganic phosphate which is an important fatiguing factor (see reviews by Stephenson *et al.*, 1998; Fitts, 1994). The prevention of phosphate accumulation in the fibre by glycogen phosphorolysis could provide a simple physiological mechanism by which the presence and degradation of glycogen opposes fatigue. However, this mechanism is not able to explain the tight correlation between glycogen concentration and capacity of the fibre to respond to T-system depolarisation under our conditions, where the phosphate generated by the SR and myofibrillar ATPases was allowed to diffuse freely into the bathing solutions.

In this study, it was not possible to determine whether the protective role mechanism exerted by the presence of endogenous glycogen is due to glycogen *per se* or to the many different types of molecular species that are either docked to the glycogen particles or are functionally coupled via endogenous glycogen particles associated with the SR membranes (Entman *et al.*, 1980). The failure of exogenous glycogen to revert or prevent loss of fibre capacity to respond to T-system depolarisation cannot be taken as strong evidence against a specific role of endogenous glycogen particles *per se* in E-C coupling simply because it is highly unlikely that exogenous and endogenous glycogen will occupy the same location in the fibre and will have the same three-dimensional structure. Furthermore, the inability to detect loss of specific molecular species associated with the loss of glycogen from the fibre (Figure 4.5), despite the use of highly sensitive analyses, cannot be taken as strong evidence against

the possibility that molecular species associated with glycogen particles may be implicated in the E-C coupling process (see review by Stephenson *et al.*, 1995). Species such as kinases and phosphatases would be expected to lose their local distribution and/or become functionally uncoupled when the glycogen particles diminish below a critical size.

Results from this study may provide an explanation for the 'run-down' phenomenon described earlier in this preparation (Lamb & Stephenson, 1990) because in this study, the 'run-down' was correlated with glycogen depletion in the fibre. Thus, fibre 'run-down' occurs not only after successive T-system depolarisation-induced responses, but also after prolonged exposure (45-60 min) to a repriming solution (Lamb & Stephenson, 1990). In this study it was shown that, in both situations, the loss of fibre excitability is paralleled by loss of glycogen content. In this context, skinned fibre 'run-down' under the conditions used in this study can be viewed as a type of muscle 'fibre fatigue' associated with glycogen depletion.

It is worthwhile to point out that whilst glycogen may be an important factor implicated in the 'run-down' phenomenon observed in mechanically skinned fibres under the conditions used here and in other studies (Lamb & Stephenson, 1990), there are also other factors which can cause different types of 'run-down'. For example, a rise in  $[Ca^{2+}]$  above 10  $\mu M$  for several seconds causes complete uncoupling in toad skeletal muscle fibres (Lamb *et al.*, 1995), but according to Fig. 4.3, this type of uncoupling is unlikely to be associated with glycogen depletion. Also, interference

with the FK506 binding protein can cause loss of fibre excitability (Lamb & Stephenson, 1996).

Results presented in this study conclusively show that (i) the largest pool of muscle fibre glycogen is not freely diffusible from the freshly mechanically skinned fibre preparation when exposed to an aqueous environment, (ii) this glycogen pool becomes depleted in mechanically skinned fibre preparations when T-system depolarisation-induced contractions are elicited, (iii) fibre excitability is related either directly or indirectly to the presence of endogenous glycogen, and (iv) this process is not related to the role of glycogen as an energy store.

## CHAPTER 5

# **An electrophoretic study of myosin heavy chain expression in skeletal muscles and in single muscle fibres of the toad *Bufo marinus***

### 5.1 INTRODUCTION

As already emphasised in the General Introduction, there is overwhelming evidence that myosin heavy chain (MHC) isoform composition plays a major role in determining the contractile characteristics of skeletal muscle (Moss *et al.*, 1995). Much of the evidence regarding the functional significance and the variability of MHC isoform expression has been obtained from studies in which MHC isoforms from mammalian skeletal muscles were resolved and analysed by polyacrylamide gel electrophoresis under denaturing conditions (SDS-PAGE; Pette & Staron, 1997; Hämäläinen & Pette, 1995). For example, it is now widely accepted that (i) hindlimb mammalian skeletal muscles contain at least four MHC isoforms (one slow-twitch and three fast-twitch), (ii) these isoforms possess slightly different electrophoretic mobilities and different ATPase activities (Moss *et al.*, 1995), (iii) a mammalian single fibre may contain as many as three different MHC isoforms (hybrid fibre), and (iv) the MHC isoform composition of a given mammalian muscle is modulated by developmental, physiological and pathological factors (Pette & Staron, 1997).

Amphibian skeletal muscles such as iliofibularis (IF), pyriformis (PYR), cruralis (CRU) and sartorius (SAR) have played a central role in muscle research by providing a large proportion of the mechanical and energetics data used to develop the current theories of muscle contraction (Huxley, 1974). According to studies using light microscopy (Lännergren and Smith, 1966), mATPase- or succinate dehydrogenase (SDH)-based histochemistry (Smith & Ovalle, 1973; Lännergren & Smith, 1966), MHC isoform-based immunohistochemistry (Rowlerson & Spurway, 1988&1985), pyrophosphate gel electrophoresis of myosin isoenzymes (Lännergren & Hoh, 1984) and SDS-PAGE of myosin light chains (Martyn *et al.*, 1993), amphibian muscle is also a heterogenous tissue comprising several fibre types that differ with respect to morphologic, metabolic and functional properties.

The general consensus, so far, is that amphibian skeletal muscles contain 5 types of fibres: types 1-3 ('pure' twitch fibres where type 1 fibres are the fastest and type 3 fibres are the slowest), type 4 (intermediate fibres with mixed tonic and twitch characteristics) and type 5/tonic (slow fibres with 'pure' tonic characteristics). The fibre type composition of amphibian skeletal muscles, like that of mammalian muscle, appears to be both species/strain and muscle specific. For example, the adult IF muscle has been reported to contain all 5 fibre types in the *Xenopus laevis* (Smith & Ovalle, 1973 and Lännergren & Smith, 1966), but only 4 fibre types (type 1, 2, 3 and tonic) in the cane toad *Bufo marinus* (Hoh *et al.*, 1994). Also, SAR muscle from the adult *Xenopus laevis* appears to contain only two twitch-fibre types, types 1 and 2 (Smith & Ovalle, 1973). It is interesting to note that amphibian muscles are not only

heterogeneous but also plastic as has been suggested by the finding that the fibre type composition of toad IF muscles varies with ontogenetic growth (Hoh *et al.*, 1994).

If one adopts the frequently expressed view, which is supported by research in mammalian systems, that each pure fibre type contains a unique MHC isoform (Lutz *et al.*, 1998a&b and Hoh *et al.*, 1994), the number of MHC protein bands produced by a separating method such as SDS-PAGE for a given muscle must not be smaller than the number of fibre types identified by other methods. A survey of the literature reveals, however, that in the only two studies published so far on amphibian skeletal muscle that involved the use of SDS-PAGE (Lutz *et al.*, 1998a,b), the number of MHC isoforms (three) detected by the authors was smaller than the number of fibre types (four) that had been predicted by other methods for the species and muscles considered. The reason behind this discrepancy is that the methodological protocol used in the aforementioned studies failed to separate two MHC isoform bands (identified by Lutz *et al.*, 1998a and/or b, as types 1 and tonic).

SDS-PAGE is a relatively low-cost, but effective method for protein separation that has proven to be extremely valuable in research on mammalian muscle heterogeneity and plasticity, especially because of its ability to identify hybrid fibres. If an experimental protocol which is able to resolve all MHC isoforms expressed in amphibian muscles were to be found, SDS-PAGE could be equally valuable in research on the variability, plasticity and functional significance of MHC isoform expression in amphibian muscle.

The main aim of the present study was to establish an SDS-PAGE method, which allows the effective separation and visualisation of MHC isoforms in amphibian muscle. The method was used to examine MHC isoform expression in IF, PYR, CRU, and SAR muscles at different stages of ontogenetic growth and the MHC composition of single fibre segments from *Rectus abdominis* (RA) muscle in the cane toad (*Bufo marinus*).

## 5.2 MATERIALS AND METHODS

### 5.2.1 CHEMICALS

Acrylamide, *N, N'*-methylene bisacrylamide (*Bis*) (both ultra-pure grade) and *N, N, N', N'*-tetramethylethylenediamine (TEMED) were purchased from Bio-Rad (Hercules, CA, USA). Alanine (98% purity), ammonium persulphate, pepstatin, leupeptin, PMSF (phenylmethylsulphonyl fluoride), sodium azide ( $\text{NaN}_3$ ), EGTA [ethyleneglycol bis( $\beta$ -aminoethyl ether)-*N, N'*-tetraacetic acid], ATP (adenosine-5-triphosphate, Grade I), HEPES [N-(2-Hydroxyethyl)piperazine-N'-(2-ethanesulfonic acid)], sodium dodecyl sulphate (SDS), benzamidine, dithiothreitol (DTT), potassium phosphate mono- and di-basic ( $\text{KH}_2\text{PO}_4$  and  $\text{K}_2\text{HPO}_4$ , ultra-pure), and Bradford reagent were supplied by Sigma (St. Louis, Missouri, USA). Glycerol was obtained from ICN (USA). All other chemicals were analytical grade.

### 5.2.2 ANIMALS AND MUSCLES

Winter and summer cane toads (*Bufo marinus*) of both genders, supplied by Peter Krauss Ltd (Queensland, Australia), were kept at 16-21°C, and fed minced beef once a week for a maximum of six week before use.

In order to examine the correlation between MHC isoform composition in skeletal muscles of the toad and developmental stages, toads ranging in body weight between 0.3 and 450 g were used in this study. The toads were allocated into five groups

(metamorphlings, juveniles, juniors, young adults and old adults) according to body weight and snout vent length (SVL). The physical characteristics and the number of animals from each group used for this part of the study are shown in Table 5.1.

MHC composition in whole tissue homogenates and single fibre segments of RA muscles was examined in 8 old adult and 4 juvenile toads. The toads were kept at 16-25°C and fed crickets twice a week for up to four weeks before experimentation.

All toads were doubly pithed after a one-hour exposure to 4°C to induce a comatose state in accordance with procedures approved by the Animal Experimentation and Ethics Committee at Victoria University of Technology.

**Table 5.1 Age/size-related classification and physical characteristics of the toads used in the study of MHC expression in IF, PYR, CRU and SAR.**

Age/size group	Body weight (g, bw)	Snout-vent length (mm, SVL)
<i>Metamorphlings, n = 8</i>	0.3 – 0.5	1 – 1.5
<i>Juveniles, n = 4</i>	12 – 14	40 – 60
<i>Juniors (small adults), n = 3</i>	30 - 50	80 – 100
<i>Young (medium size) adults, n=3</i>	100 - 150	100 - 120
<i>Old (very large) adults, n = 3</i>	200 - 450	120 - 150

The four skeletal muscles used for identifying MHC isoforms and investigating age-related changes in MHC composition in skeletal muscles of the toad include

iliofibularis (IF), a predominantly twitch muscle containing a small tonic region (Hoh *et al.*, 1994); pyriformis (PYR), a muscle which in *Xenopus laevis* contains about 70% tonic/slow fibres (Orkand *et al.*, 1978); cruralis (CRU), a predominantly fast twitch muscle used for jumping (Lutz *et al.*, 1998b) and sartorius (SAR), a 'pure' twitch muscle (Hoh *et al.*, 1994; Smith & Ovalle, 1973). All these muscles have been widely used in physiological studies. The muscles, obtained from summer and winter toads and identified according to anatomical location, were rapidly and carefully dissected out as described in detail in section 3.2.2.1. IF muscles were obtained from animals of all five developmental groups listed in Table 5.1 (metamorphlings, juveniles, juniors, young adults and old adults toads), while PYR, CRU and SAR muscles were obtained only from four groups (juveniles, juniors, young adults and old adults toads).

MHC composition in single muscle fibre segments was examined using fibres dissected from the RA muscle, because in this muscle tonic and twitch regions are relatively easy to locate (Uhrík & Schmidt, 1973). The muscles were dissected from juvenile and old adult, summer toads as follows. The toads were immobilised, abdomen up, on the dissection plate and a skin incision was made on the median line of the abdominal cavity running from the sternum down to the tail end of the body. Immediately underneath the skin incision is the white line (*linea alba*)-a tough, fibrous band that extends from the xiphoid process of the sternum to the symphysis of the pelvis. This is a structure formed by the convergence at the midline of aponeuroses from the external oblique, internal oblique, and transverse abdominis muscles. The RA muscle, identified from the hypogastric region on the ventral side of the toad (see Fig. 3.1B, in Chapter 3), was dissected rapidly and carefully to

minimise muscle stimulation. Each of the two RA muscles running in parallel on either side of the linea alba, was interrupted by three transverse fibrous bands of tissue called *tendinous intersections* that divide the RA muscle into four sections: one thoracic, two abdominal, and one pelvic. Because there are no nerves or blood vessels in the linea alba, nor in the tendinous intersection or in the aponeuroses, the isolation of one part of RA muscle, achieved by cutting through the tendinous intersection bands, left the muscle virtually intact. In this study, only pelvic sections of the RA muscle were selected for dissection

### **5.2.3 PREPARATION OF MUSCLE HOMOGENATES AND MYOSIN EXTRACTS**

#### **5.2.3.1 PREPARATION OF MUSCLE HOMOGENATES**

Immediately after dissection, muscles were cleaned of connective tissue, weighed and cut into small pieces. The muscle pieces were then homogenised manually with a glass tissue homogeniser (Kontes Glass Co. DUALL, NJ, USA) in 6 volumes of relaxing solution containing (mmol/l): HEPES, 90; EGTA, 50;  $Mg_{total}$ , 10.3 ( $Mg^{2-}$ , 1);  $NaN_3$ , 1; ATP, 8; creatine phosphate, 10; pH 7.1 and protease inhibitors: leupeptin, 0.002; pepstatin, 0.001 and PMSF, 0.1. Tissue homogenisation was carried out on ice and the homogenates were stored at  $-85^{\circ}C$  until used.

### 5.2.3.2 PREPARATION OF MYOSIN EXTRACTS

Myosin was extracted from freshly dissected muscles according to Rossini *et al.* (1995). All procedures were carried out at 2-4°C. Briefly, connective tissue was carefully trimmed and discarded and muscles were homogenised in a medium containing (mmol/l): KCl, 50; EGTA, 10; pH 7.0-7.2; pepstatin, 0.03; leupeptin, 0.02; PMSF, 0.012 and benzamidine, 0.001 (solution A). The muscle homogenate was first left on ice for 10 min and then centrifuged at  $800 \times g$  for 10 min. The pellet was washed several times until the supernatant was clear.

The washed pellet was then extracted for at least 1 hour in 10 vol of a high ionic strength solution (solution B) containing (mmol/l): KCl, 300;  $K_2HPO_4$ , 150; magnesium acetate, 10; EGTA, 10; pH 6.5; pepstatin, 0.03; leupeptin, 0.012; benzamidine, 0.001 and ATP, 10 (added immediately before use). The myosin fraction was obtained by subjecting the extract to a 2-step centrifugation protocol in a pre-programmed Ultra-centrifuge (Becker): (i)  $20\,000 \times g$  for 20 min and (ii)  $120\,000 \times g$  for 2 hours.

The post- $120\,000 \times g$  supernatant was collected and dialysed overnight at 4°C against a solution containing (mmol/l): Tris-HCl, 1; EGTA, 5; pH 7.2; KCl, 10 and DTT, 0.1 (solution C).

#### **5.2.4 PROTEIN DETERMINATION IN MUSCLE HOMOGENATE AND MYOSIN EXTRACT**

The protein concentration in muscle homogenates and myosin extracts was determined using BSA (bovine serum albumin) as protein standard and the Bradford protein assay (Bradford, 1976).

#### **5.2.5 PREPARATION OF SINGLE MUSCLE FIBRE SEGMENTS FOR ELECTROPHORETIC ANALYSIS OF MHC ISOFORM COMPOSITION**

The protocols used to isolate and measure single fibre segments from RA muscles were the same as those used for IF fibres (see sections 3.2.2.3 and 3.2.2.4). The fibre segments were tied in the middle with a single knot of braided silk and the silk thread was cut such that a section of about 3 mm remained attached to the fibre. This minute piece of silk associated with the fibre segment allowed for better visualisation and easier handling of the single fibre during its transfer from the dissecting dish to the Eppendorf tube containing solubilizing buffer. An important point to make here is that fibre segments dissected under oil retain a tiny droplet of oil when taken out of the dissecting dish. If not removed, this droplet of oil can prevent the effective solubilisation of proteins in the fibre and the quality of electrophoretic analysis. The oil droplet attached to the fibre segment was gently and carefully removed with a small piece of Whatman filter paper.

## 5.2.6 ANALYSIS OF MHC ISOFORMS BY ALANINE-SDS PAGE

### 5.2.6.1 SAMPLE PREPARATION

MHC isoform analyses were performed on whole muscle homogenates, myosin extracts and single muscle fibre segments. For muscle homogenates and myosin extracts, myofibrillar proteins were solubilized by incubating the sample at RT in 10 volumes of solubilizing buffer (see section 4.2.5 for details of the composition) for 24 hours and then boiling the mixture for 3 min; an aliquot of 6  $\mu$ l (containing 200-240 ng protein) was applied per electrophoretic well. Solubilisation of myofibrillar proteins in single fibre segments was carried out as described in section 4.2.5; a 6  $\mu$ l sample containing the equivalent of 0.4 nl fibre was applied per electrophoretic well.

### 5.2.6.2 PREPARATION OF ALANINE-SDS-POLYACRYLAMIDE GEL

MHC isoforms in whole muscle homogenates, myosin extracts and in single muscle fibres were analysed on 0.75 mm thick slab gels using the ALANINE-SDS-PAGE method and the Mini-Vertical Gel Electrophoresis Unit (model Mighty Small II SE 260, Hoefer, Pharmacia Biotech, San Francisco, USA).

*The separating gel.* Details of the composition of separating gels are given in Table 5.2. Gels were allowed to polymerise at RT for 2 – 4 hours. Longer polymerisation times (up to 12 hours) did not increase the effectiveness of the gel system to resolve high molecular weight proteins from toad muscle.

**Table 5.2. Recipe for preparing the separating gels used in the ALANINE-SDS-PAGE method.** Total volume is 12 ml.

Stock solutions	Volume (ml)	Final concentration
Acrylamide and Bis stock, T=30%; C=1.2%	3.040	T=7.6%; C=1.2%
Tris-HCl separating gel buffer; 3 M, pH=8.8	1.700	425 mM
Alanine 1M	0.900	75 mM
Distilled water (double deionised)	1.128	---
Glycerol	4.800	40% (v/v)
SDS 10% (w/v)	0.360	0.3% (w/v)
Ammonium persulfate 10% (w/v)	0.060	0.05% (w/v)
TEMED, concentrated solution (14.2 M)	0.012	0.1% (v/v)

*Acrylamide-bisacrylamide stock solution: T = 30%. C = 1.2%:* 29.64 g acrylamide and 0.36 g bisacrylamide were dissolved in a total volume of 100 ml of distilled water and stored at 4°C. To ensure reproducibility of data, acrylamide/bisacrylamide stock solutions were used within a month from preparation, because it has been reported that upon prolonged storage acrylamide monomer solutions accumulate acrylic acid and ammonia (Hames and Rickwood, 1990).

*Separating gel buffer 3 M Tris-HCl, pH 8.8:* 36.41 g of Tris and 30 ml of 1 M HCl were mixed and vigorously stirred until all Tris was dissolved and then the pH of the mixture was adjusted to the desired value. This buffer was stored and used over several months.

*Alanine 1 M:* 9.10 g alanine were dissolved with vigorous stirring in a total volume of 100 ml of distilled water. The solution was stored at 4°C for up to three months. Alanine has relatively low solubility in water; therefore stock solutions of higher concentration could not be made.

*The stacking gel.* The composition of stacking gels in the ALANINE-SDS-PAGE method is presented in Table 5.3. Stacking gels were allowed to set at RT for 40 min.

The running buffer, containing 0.1% SDS, 25 mM Tris and 175 mM alanine, was freshly prepared and pre-cooled at 4° C for 2 hours before use.

**Table 5.3. Recipe for preparing stacking gels in the ALANINE-SDS-PAGE method.**

Total volume is 6 ml.

Stock solutions	Volume (ml)	Final concentration
Acrylamide and Bis stock, T=30%; C=2.6%	0.8	T = 4%; C = 2.6%
Tris-HCl separating gel buffer; 0.5 M, pH=6.8	1.5	125 mM
EDTA 80 mM	0.3	4 mM
Distilled water (double deionised)	0.757	—
Glycerol	2.4	40% (v/v)
SDS 10% (w/v)	0.180	0.3% (w/v)
Ammonium persulfate 10% (w/v)	0.060	0.1% (w/v)
TEMED, concentrated solution (14.2 M)	0.003	0.05% (v/v)

*Acrylamide-bisacrylamide stock solution; T = 30%, C = 2.6%:* 14.61 g of acrylamide and 0.39 g of bisacrylamide were dissolved in a total volume of 50 ml of distilled water and stored at 4°C for one month.

*Stacking gel buffer 0.5 M Tris-HCl, pH 6.8:* 6.181 g of Tris and 30 ml of 0.5 M HCl were mixed and vigorously stirred until all Tris was dissolved. adjusted to desired pH and made up to 100 ml with distilled water.

*EDTA 80 mM* was prepared and stored at RT for up to 1 year.

All ALANINE-SDS-PAGE gels were run at constant voltage (150 V) for 30 hours at 4° C and then were stained with Bio-Rad Silver Stain Plus (Bio-Rad, Hercules, CA, USA).

For determining the relative proportion of MHC isoforms in muscle homogenates and single muscle fibre segments, the stained gels were scanned, while still wet, with a

Molecular Dynamics Personal Densitometer (Molecular Dynamics, Sunnyvale, CA, USA) and the protein bands of interest were analysed with ImageQuaNT software version 4.1 (Molecular Dynamics) using the volume integration option.

### **5.2.7 DATA PRESENTATION AND STATISTICAL ANALYSES**

To minimise errors related to the electrophoretic method, each muscle sample was electrophoresed under identical conditions at least three times. The densitometric data are presented as means  $\pm$  standard error of the mean (SE) and statistical comparisons were performed on groups using a two-way analysis of variance followed by the Bonferroni test. Statistical significance was accepted at  $P < 0.05$ .

## 5.3 RESULTS

### 5.3.1 DEVELOPMENT OF AN SDS-PAGE METHOD FOR SEPARATING MYOSIN ISOFORMS IN TOAD SKELETAL MUSCLE

#### 5.3.1.1 REPLACEMENT OF GLYCINE WITH ALANINE IN SDS-PAGE

In the initial stages of this study, attempts were made to separate the MHC isoforms in IF, PYR, CRU and SAR muscles of the cane toad *Bufo marinus* by SDS-PAGE using several laboratory modifications of the Laemmli gel system (Laemmli, 1970). The gel shown in Fig. 5.1, shows that several of these attempts separated effectively the four adult MHC isoforms (MHCIIa, MHCII<sub>d/x</sub>, MHCIIb and MHCII<sub>β</sub>) in the rat skeletal marker (lane 5), but failed to resolve the MHC isoforms in the toad muscles (lane 1 - 4).

Recently, Talmadge & Roy (1993) described an electrophoretic method for the separation of fast MHC isoforms in rat skeletal muscles which involves the use of the trailing ion glycine both in the running buffer and in separating gel. In this study, the original Talmadge & Roy gel system failed to resolve the MHC isoforms in toad muscles. However, by altering several parameters in their protocol, two gel systems were generated: one which resolved the skeletal muscle MHC isoforms in the rat (Fig. 5.2A, lane 5), but not in the toad (Fig. 5.2A, lane 1 - 4), and another which resolved skeletal muscle MHC isoforms in the toad (Fig. 5.2B, lane 1) but not in the rat (Fig. 5.2B, lane 2).

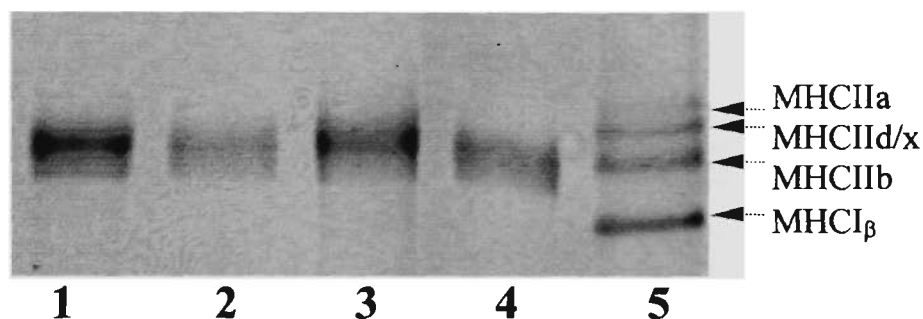


**Figure 5.1** Electrophoretogram of whole tissue homogenates prepared from IF (lane 1), PYR (lane 2), CRU (lane 3) and SAR (lane 4) muscles of young adult cane toads and of a complete rat marker (lane 5) containing the four MHC isoforms (MHC $\beta$ , fast MHCIIb, fast MHCIIId/x and fast MHCIIa) known to be expressed by adult rat hindlimb skeletal muscles.

Details of the gel system used, a modified version of Laemmli's gel system (1970), are as follows:

*Separating gel:* T = 8%, C = 1.2%, 425 mM Tris-HCl, pH 8.8, 40% (v/v) glycerol, 0.3% (w/v) SDS, 0.05% (w/v) ammonium persulfate, 0.75% (v/v) TEMED.

*Stacking gel:* T = 4%, C = 2.6%, 125 mM Tris-HCl, pH 6.8, 40% (v/v) glycerol, 0.3% (w/v) SDS, 0.1% (w/v) ammonium persulfate, 0.06% (v/v) TEMED.

*Running buffer:* 192 mM glycine, 25 mM Tris, 0.1% (w/v) SDS.

*Running conditions:*  $V_{\text{constant}} = 120\text{V}$ , water cooling, 24 hours.

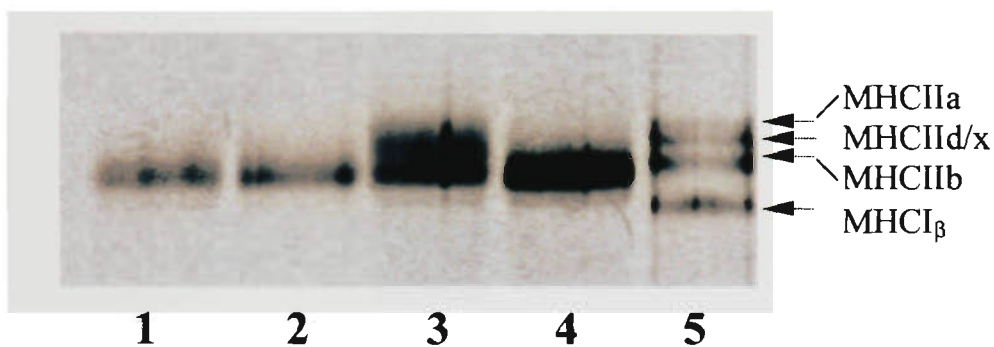


**Figure 5.2A** Electrophoretogram of whole tissue homogenates prepared from IF (lane 1), PYR (lane 2), CRU (lane 3) and SAR (lane 4) muscles of young adult cane toads and of a complete rat marker (lane 5).

Details of the gel system, a intensively modified version of the Talmadge & Roy (1993) protocol, are as follows:

*Separating gel:* T = 8%, C = 2%, 375 mM Tris-HCl, pH 8.8, 100 mM glycine, 40% (v/v) glycerol, 0.4% (w/v) SDS, 0.1% (w/v) ammonium persulfate, 0.05% (v/v) TEMED.

*Stacking gel:* T = 4%, C = 2.6%, 125 mM Tris-HCl, pH 6.8, 4 mM EDTA, 40% (v/v) glycerol, 0.4% (w/v) SDS, 0.1% (w/v) ammonium persulfate, 0.05% (v/v) TEMED.

*Running buffer:* 200 mM glycine, 26 mM Tris, 0.1% (w/v) SDS.

*Running conditions:*  $V_{\text{constant}} = 150\text{V}$ ;  $4^{\circ}\text{C}$ ; 24 hours.

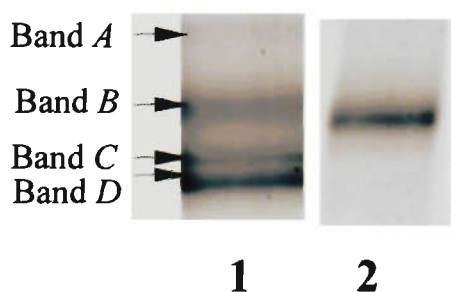


**Figure 5.2B** Electrophoretogram of whole tissue homogenates prepared from cane toad PYR (lane 1) and rat EDL (lane 2) muscles.

Details of the gel system (Glycine-SDS-PAGE) are as follows:

*Separating gel:* T = 7.6%, C = 1.2%, 425 mM Tris-HCl, pH 8.8, 100 mM glycine, 40% (v/v) glycerol, 0.3% (w/v) SDS, 0.05% (w/v) ammonium persulfate, 0.1% (w/w) TEMED.

*Stacking gel:* T = 4%, C = 2.6%, 125 mM Tris-HCl, pH 6.8, 4 mM EDTA, 40% (v/v) glycerol, 0.4% (w/v) SDS, 0.1% (w/v) ammonium persulfate, 0.05% (v/v) TEMED.

*Running buffer:* 288 mM glycine, 32.5 mM Tris, 0.1% (w/v) SDS.

*Running conditions:*  $V_{\text{constant}} = 150\text{V}$ ;  $4^{\circ}\text{C}$ ; 30 hours.

Even though the Glycine gel system described in the legend for Fig. 5.2B (Glycine-SDS-gel) separated four toad MHC isoform bands with acceptable sharpness, it displayed a very low degree of reproducibility (only two good gels for about 50 gels tested). Replacing ammonium persulfate and SDS with potassium persulfate and lithium dodecyl sulfate, and running the gel at low temperature, as suggested by Chrambach (1985), or replacing the crosslinker bisacrylamide with diacrylylpiperazine (Hochstrasser *et al*, 1988) did not improve either resolution or the reproducibility of Glycine-SDS gels. However, substitution of glycine with alanine, both in the separating gel and in the running buffer, yielded an electrophoretic system (Alanine-SDS-PAGE) which provided good resolution of the four protein bands (*A*, *B*, *C* and *D*) in the toad skeletal muscle (Fig. 5.2C, lane 1) and displayed a high degree (~75%) of reproducibility. Like the Glycine-SDS gel system, the Alanine-SDS-PAGE system failed to separate the rat muscle fast-twitch MHC isoforms (Fig. 5.2C, lane 2).

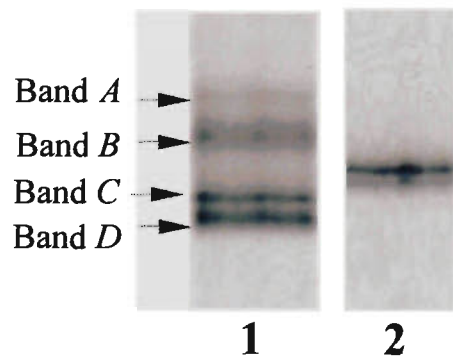


**Figure 5.2C** Representative electrophoretogram of whole tissue homogenates prepared from cane toad PYR (lane 1) and rat EDL (lane 2) muscles.

Details of the gel system (Alanine-SDS-PAGE) are given in section 5.2.6.2.

### 5.3.1.2 OPTIMIZATION OF THE ALANINE-SDS-PAGE SYSTEM

Initially, the alanine concentration used in the separating gel was identical with that of glycine in the Glycine-SDS protocol (i.e 100 mM). Subsequently, a series of experiments was carried out in which the concentration of alanine was varied, first in the separating gel and then in the running buffer, while all other parameters were kept the same as those used for the Glycine-SDS gels.

As seen Fig. 5.3A, increasing the concentration of alanine in the separating gel from 25 to 100 mM did not markedly affect the separation of protein bands *B*, *C* and *D*. Nevertheless, gels containing 75 mM alanine (lane 3), and to lesser extent those containing 100 mM alanine (lane 4), appeared to be more effective with respect to the separation and visualisation of the slowest migrating species (band *A*) and to the sharpness of bands *B*, *C* and *D*. As a result, all Alanine-SDS separating gels used in this study contained 75 mM alanine.

The concentrations of glycine (288 mM) and Tris (32.5 mM) used in the running buffer of the Glycine-SDS gel system described in Fig. 5.2B were 1.5 and 1.3 fold of those used by Laemmli in his original gel system (192 mM glycine and 25 mM Tris). Considering the relatively high cost of alanine, it was decided to examine whether lowering the concentration of alanine in the running buffer would reduce the ability of the Alanine-SDS-PAGE system to separate the high molecular weight protein bands detected in toad muscle homogenate.

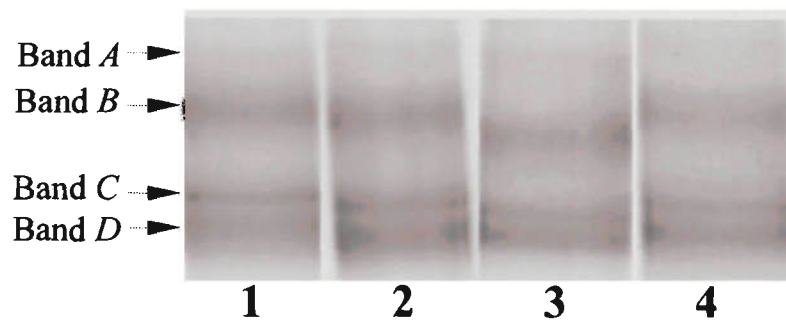


**Figure 5.3A** Electrophoretic profile of MHC isoforms in PYR muscle homogenate at different concentrations of alanine in the separating gel.

All other components were as described in section 5.2.6.2.

Lane 1: 25 mM; lane 2: 50 mM alanine; lane 3: 75 mM; lane 4: 100 mM alanine

As shown in Fig. 5.3B, decreasing the concentration of alanine in the running buffer from 288 mM to 100 mM, while maintaining the Tris concentration constant (25 mM) markedly affected the separation and sharpness of the bands *A*, *B*, *C* and *D*, such that at 175 mM alanine (lane 4) the bands were sharper and more intense than at lower (e.g. 100 mM, lane 1) or higher concentrations (e.g. 288 mM, lane 6) of alanine. Based on these data, 175 mM alanine was used in the running buffer of the optimised version of the Alanine-SDS-PAGE system.

Glycerol concentration in the separating gel has been shown to play an important role in the separation of MHC- $\alpha$  and MHC- $\beta$  isoforms in myocardial samples from different species (Reiser & Kline, 1998). As seen in Fig. 5.3C, increasing the glycerol concentration in the separating gel from 30 to 40% (v/v) (lane 1 – 5) improved markedly the resolution of protein bands *A*, *B*, *C* and *D*. In Alanine-SDS gels containing 45% and 50% glycerol (lane 6 & 7), nevertheless, bands *A*, *B*, *C* and *D* co-migrated as one band, with a similar electrophoretic mobility to that of band *D*. Therefore all separating gels used for analysing MHC expression in toad skeletal muscles contained 40% (v/v) glycerol.

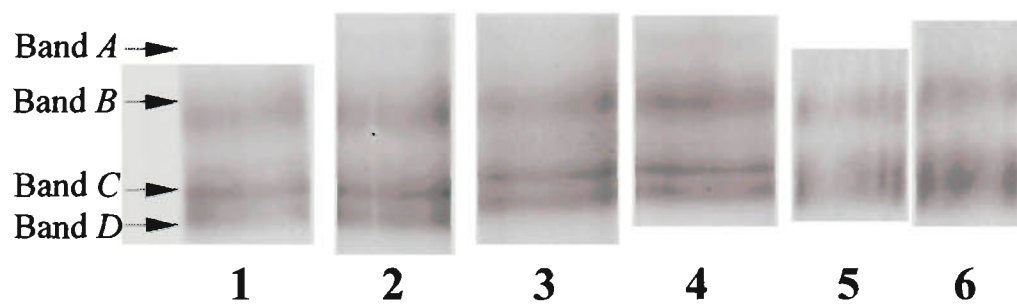


**Figure 5.3B** Electrophoretic profile of MHC isoforms in a PYR muscle homogenate at different concentration of alanine in the running buffer.

All other components were kept constant at the concentrations given in section 5.2.6.2.

Lane 1: 100 mM; lane 2: 125 mM; lane 3: 150 mM; lane 4: 175 mM; lane 5: 192 mM and lane 6: 288 mM.

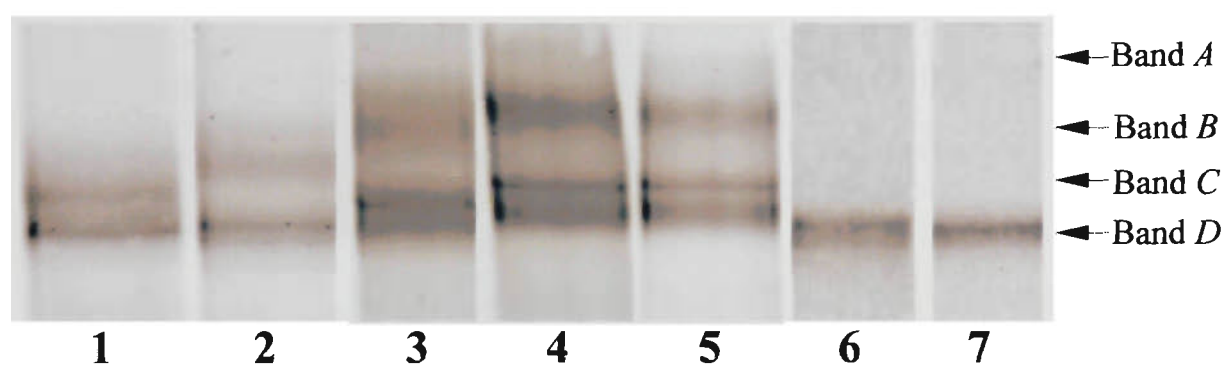


**Figure 5.3C** Electrophoretic profile of MHC isoforms in a PYR muscle homogenate at different concentration of glycerol in the separating gel.

All other components were kept constant at the concentrations given in section 5.2.6.2.

Glycerol concentration (% v/v): 30 (lane 1); 32.5 (lane 2); 35 (lane 3); 37.5 (lane 4); 40 (lane 5); 45 (lane 6) and 50 (lane 7).

### 5.3.1.3 MHC ISOFORM BANDS DETECTED IN MYOSIN EXTRACTS OF IF, PYR, CRU AND SAR ARE SIMILAR TO THE HIGH MOLECULAR WEIGHT PROTEIN BANDS DETECTED IN WHOLE MUSCLE HOMOGENATES

Alanine-SDS-PAGE analysis of homogenates prepared from adult toad IF, PYR, CRU and SAR muscles produced different electrophoretic profiles, which could be distinguished by different relative proportions of protein bands *A*, *B*, *C* and *D* (Fig. 5.4A). For example 4 bands were detected in CRU muscle (lane 3), but only three bands were detected in IF muscle (lane 1). To confirm that the bands detected in the homogenate samples were myosin heavy chain isoforms rather than other high molecular weight proteins present in the homogenates, electrophoretic analyses were also carried out on myosin extracts prepared from the contralateral muscles.

As seen in Fig. 5.4B, the electrophoretic mobility and relative proportion of the protein bands detected in myosin extracts prepared from IF, PYR, CRU and SAR muscles were very similar to those of the bands present in the homogenates (Fig. 5.4A), indicating that protein bands *A*, *B*, *C* and *D* are indeed MHC isoforms. Bands *A*, *B*, *C* and *D* were also detected in single fibre preparations (more details in section 5.4.4). Taken together, these findings validate the use of whole muscle homogenates for rapid electrophoretic analysis of MHC expression in toad skeletal muscles.

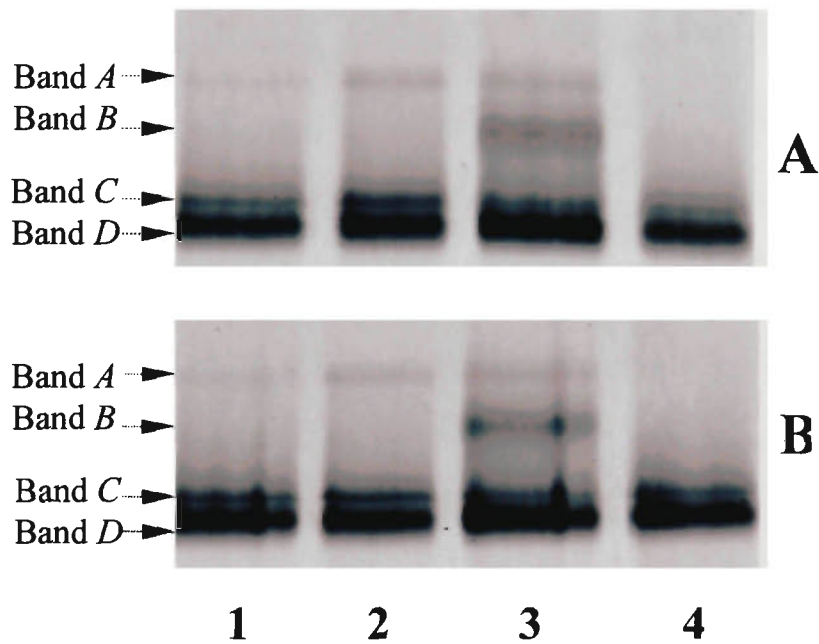


**Figure 5.4.** Alanine-SDS-PAGE analysis of adult toad IF, PYR, CRU and SAR muscle homogenates (A) and myosin extract (B) prepared from contralateral muscles.

Lane 1: IF; lane 2: PYR; lane 3: CRU; and lane 4: SAR.

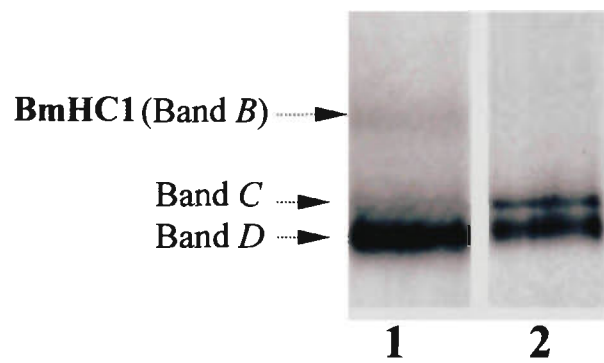
#### 5.3.1.4 IDENTIFICATION OF THE MHC ISOFORMS EXPRESSED IN IF, PYR, CRU AND SAR MUSCLES OF THE TOAD *BUFO MARINUS*

The protein bands detected on Alanine-SDS gels of whole muscle homogenates and extracts from IF, PYR, CRU and SAR were identified using previously published data on the fibre type composition of SAR and IF in the cane toad (Hoh *et al.*, 1994), of PYR in *Xenopus laevis* (Orkand *et al.*, 1978), of SAR in *Rana pipiens*, *Bufo americanus* and *Xenopus laevis* (Sperry, 1981) and of CRU in *Rana pipiens* (Gilly, 1975). Hoh *et al.* (1994) determined the fibre type composition of IF and SAR muscles of the cane toad *Bufo marinus* at different developmental stages by using ATPase-based histochemistry and MHC isoform-based immunohistochemistry. According to this study, toad SAR is a *pure* twitch muscle that contains about 2 – 4% type 1 fibres, 8% type 3 fibres, 89% type 2 fibres and no tonic fibres. As seen in Fig. 5.5A (lane 1), SAR muscle homogenates from junior toads (bw 30 – 50 g) displayed two weak bands (*B* and *C*), an intense band *D*, and no band *A*. Based on the fibre type composition data of Hoh *et al.* (1994) for toad SAR, one can tentatively identify protein bands *B*, *C* and *D*, as the twitch MHC isoforms contained in fibre type 1 or 3 (BmHC1 or BmHC3 where BmHC stands for *Bufo marinus* heavy chain), fibre type 3 or 1 (BmHC3 or BmHC1) and fibre type 2 (BmHC2), and band *A* (undetectable in SAR muscle) as tonic MHC isoform (BmHCT).

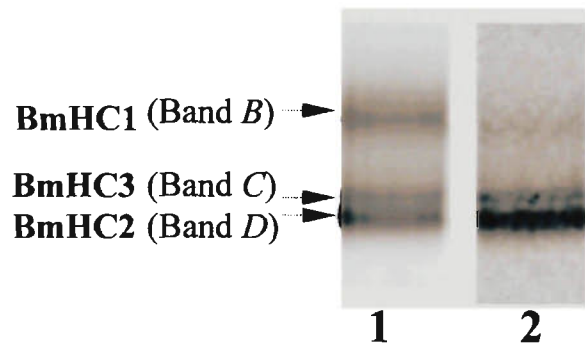
In their study, Hoh *et al.* (1994) also showed that toad maturation (as indicated by an increase in the body weight from 15 – 25 g to 180 – 200 g) was accompanied by a marked decrease in the relative proportion of type 1 fibres in SAR. As seen in

Fig. 5.5A, band *B* was present in the junior SAR (lane 1), but not in the SAR muscle homogenates from old toads (220 – 450 g; lane 2). One could therefore conclude that protein band *B* is the MHC isoform contained in fibre type 1 (BmHC1).

Further information on the identity of protein bands *B*, *C* and *D* was obtained by comparing the protein band profile of IF homogenates from juvenile (12 – 16 g) and young adult (100 – 150 g) toads observed in the present study with the fibre type composition of IF muscles from juvenile (15 – 25 g) and adult (180 – 200 g) toads, reported by Hoh *et al.* (1994). According to these authors, IF as well as SAR displayed maturation related changes in fibre type composition. These include a *fall* in the proportion of type 1 fibres (from 11% to 0%) and tonic fibres (from 5 to 3%) and a *rise* in the type 2 fibres (from 36% to 60%). The juvenile IF homogenates examined in our study contained bands *B*, *C*, *D* and a trace of band *A* which was visible on the gel but was under the detection limit of the densitometer software and therefore could not be seen in the figure (Fig. 5.5B, lane 1). The IF muscle homogenates obtained from more mature toads (young adult; 100 – 150 g), however, showed a markedly weaker band *B*, a relatively unchanged band *C* and a stronger band *D* (lane 2). Based on the same strategy for band identification as that applied for SAR, one can regard these data as further evidence for confirming that protein band *B* represents the MHC isoform contained in fibre type 1 (BmHC1) and an indication that band *D* represents the MHC isoform contained in fibre type 2 (BmHC2). Also, based on the tentative identification of band *A* as the tonic MHC isoform BmHCT, and on the identification of bands *B* and *D* as the BmHC1 and BmHC2 respectively,



**Figure 5.5A** Representative electrophoretic profile of MHC isoforms detected in SAR muscle homogenates from junior (30 – 50 g, lane 1) and old adult (200 – 450 g; lane 2) toads.



**Figure 5.5B** Representative electrophoretic profile of MHC isoforms detected in IF muscle homogenates from juvenile (12 – 14 g, lane 1) and young adult (100 – 150 g, lane 2) toads.

it is logical to suggest that band *C* is the MHC isoform contained in type 3 fibres (i.e. BmHC3).

The MHC isoform composition of the pyriformis muscle in the toad *Bufo marinus* is not yet known, but it has been reported that the PYR muscle of another amphibian, *Xenopus laevis*, contains a large proportion of slow/tonic muscle fibres (Orkand *et al.*, 1978). As shown in Fig. 5.5C, band *A* could be seen clearly on the Alanine-SDS gel of the pyriformis sample along with bands *B*, *C* and *D*. Since band *A* was not detected in the SAR muscle (pure twitch muscle) but was clearly visible in the PYR muscle, it is reasonable to suggest that band *A* is the MHC isoform contained in tonic/slow fibres (BmHCT).

Following the above tentative identification procedure, protein bands *A*, *B*, *C* and *D*, detected on Alanine-SDS-PAGE of muscle homogenates or myosin extracts from skeletal muscles of *Bufo marinus*, were referred to as **BmHCT**, **BmHC1**, **BmHC3** and **BmHC2**, respectively.

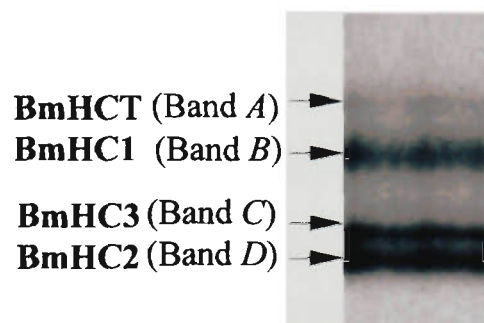


**Figure 5.5C** Representative electrophoretic profile of MHC isoforms detected in PYR muscle homogenate from young adult (100 – 150 g) toads.

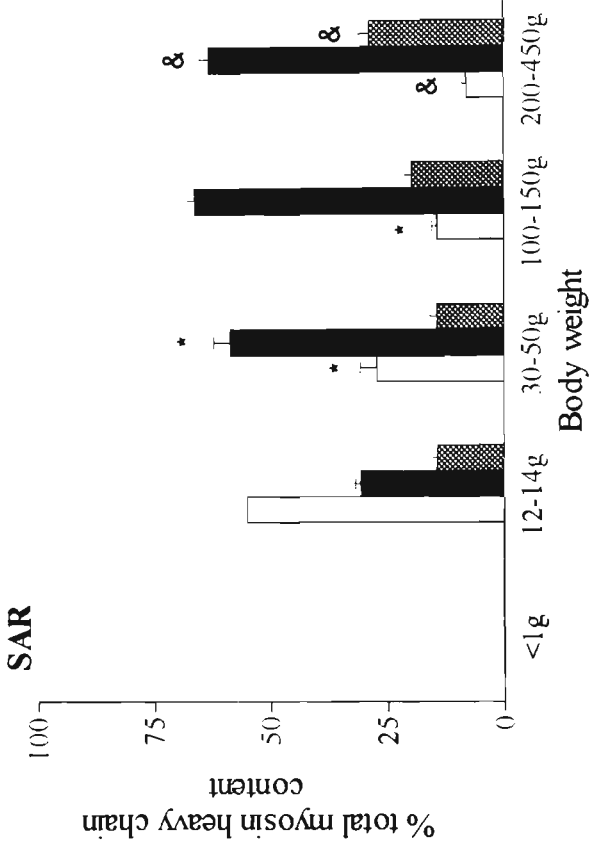
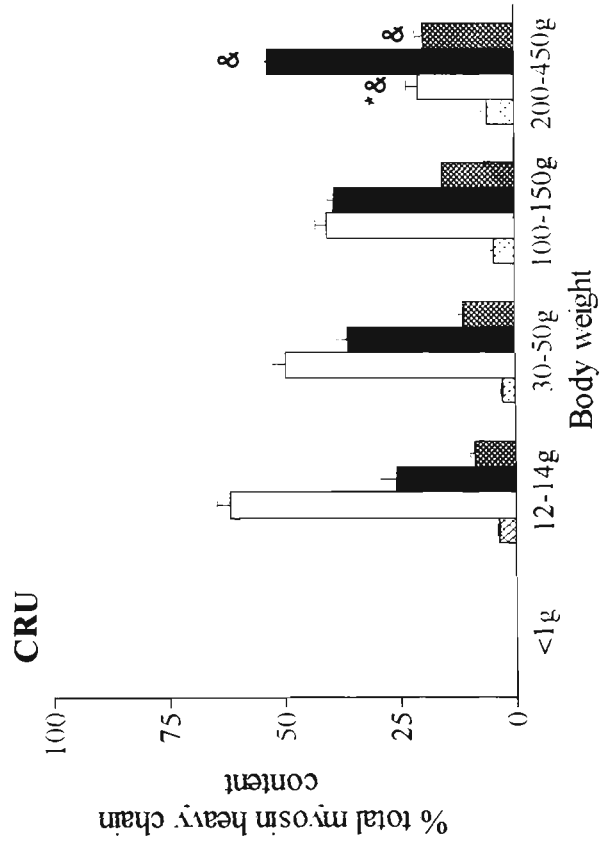
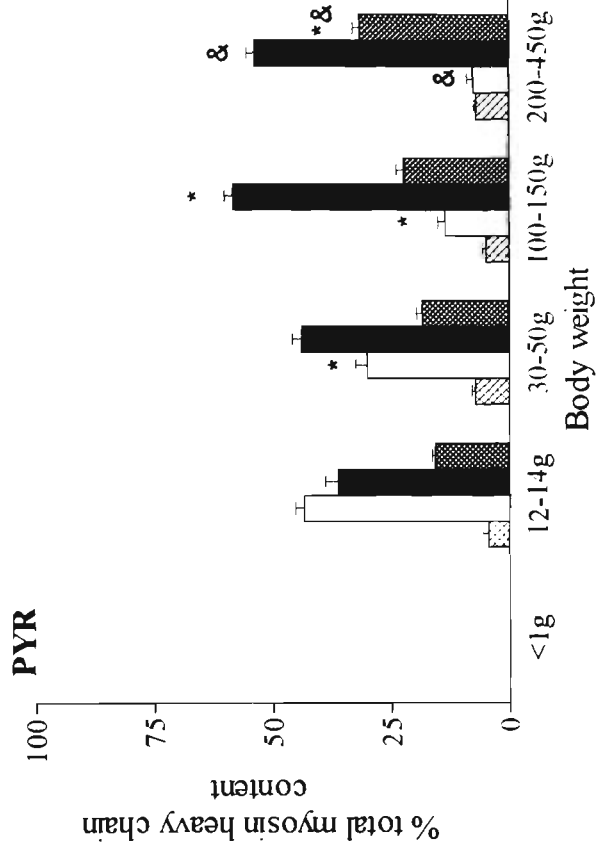
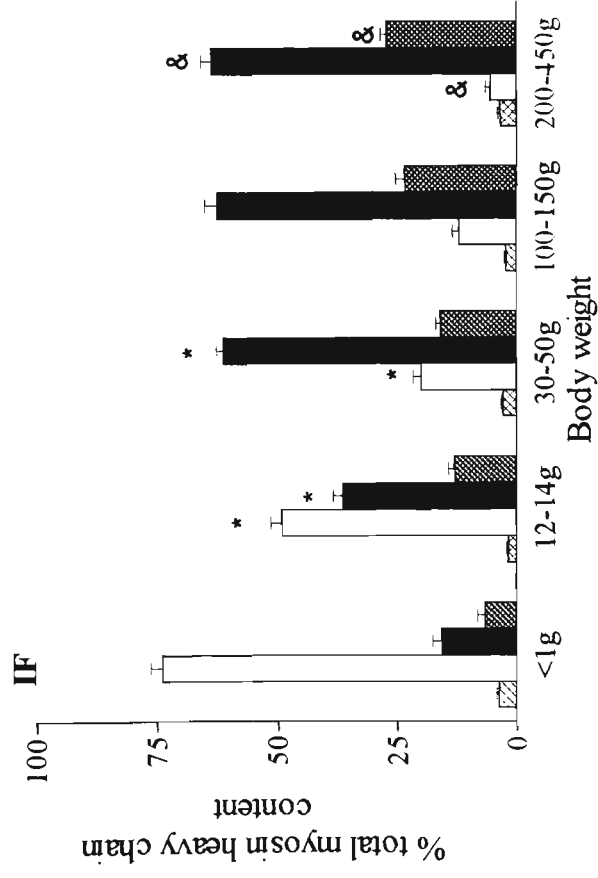
### 5.3.2 DEVELOPMENTAL CHANGES IN THE MHC COMPOSITION OF IF, PYR, CRU AND SAR MUSCLES IN *BUFO MARINUS*

In Fig. 5.6 are shown the relative proportions of MHC isoforms in the IF, PYR, CRU and SAR muscles of the cane toad at different stages of development. In all four muscles examined, at all developmental stages, BmHC1 (open bars) together with BmHC2 (black bars) represented more than 70% of the total myosin heavy chain content. Muscle-related differences in MHC isoform composition were observed between IF, PYR, CRU and SAR muscles at each of the post-metamorphic stages of development examined. For example, in 30 – 50 g toads, the ratio BmHC1/BmHC2 was 0.30 in IF, 0.68 in PYR, 1.37 in CRU and 0.46 in SAR. An increase in the body weight (and snout-vent length, SVL) of the toads from 12 – 14 g (40 – 60 mm) to 200 – 250 g (120 – 150 mm) was accompanied by a consistent *decrease* in the proportion of BmHC1 in all four muscles, but the extent of this decrease appeared to be muscle-specific. Thus, between the juvenile to the old adult stage, the proportion of BmHC1 decreased by about 8-fold in IF (49% in juvenile toads v. 6% in the old adult), but only by about 3-fold in CRU muscle (62% in juvenile vs 20% in old adult).

As also seen in Fig. 5.6, toad maturation was associated with an *increase* in the relative proportion of BmHC2 and BmHC3, but the pattern of this change was different from that observed for BmHC1. For example, the proportion of BmHC1 in IF decreased gradually from that in metamorphlings to old adult stage, while that of BmHC2 increased from 16% in metamorphlings to 61% in junior toads and then remained largely constant. A gradual increase by about a factor of 2 was also



**Figure 5.6** Bar graphs illustrating the relative proportion of MHC isoforms (BmHCT, cross-hatched bar; BmHC1, open bar; BmHC2, filled bar; BmHC3, checker board bar) in IF, PYR, CRU and SAR muscles of the cane toad at different stages of ontogenetic growth. Results are means  $\pm$  SEM. Data were obtained from 8 metamorphlings, 4 juveniles, 3 juniors, 3 young toads and 3 old toads. (\*) significantly different ( $P < 0.05$ ) from the corresponding value in the preceding developmental group. (&) significantly different ( $P < 0.05$ ) from the corresponding value in the earliest developmental group examined.



observed in each muscle for BmHC3 between the juvenile and the old toads. In contrast to twitch MHC isoforms BmHC1, BmHC2 and BmHC3, the tonic isoform BmHCT, detected only in very small proportions (less than 7% of the total MHC content) in IF, PYR and CRU and not detected in SAR muscles, did not show a definite pattern of development-related variability in terms of its expression.

### **5.3.3 MHC ISOFORM COMPOSITION OF SINGLE MUSCLE FIBRE SEGMENTS ISOLATED FROM *RECTUS ABDOMINIS***

As shown in Fig. 5.7, RA muscle homogenates prepared from juvenile toads displayed all four MHC isoforms (BmHCT, BmHC1, BmHC3 and BmHC2) identified in the PYR muscle. In adult toads, the proportion of BmHC1 decreased while the proportion of BmHC3 increased, but no marked change was detected in the relative proportions of BmHCT and BmHC2 (Fig. 5.7).

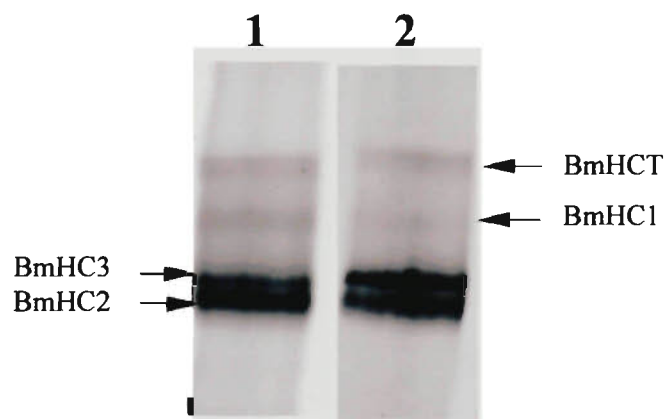
The MHC isoform composition in 136 muscle fibre segments dissected from old adult toad RA muscles was examined using the ALANINE-SDS-PAGE method and the RA homogenate sample prepared from juvenile toads as a MHC marker. Based on their MHC composition, these fibres belonged to 10 major groups: pure fibres, expressing only one MHC isoform (fibre types T, t2 and t3), 2 MHC-hybrid fibres, co-expressing two MHC isoforms (fibre types T+t1, T+t3, t1+t2 and t2+t3) and 3 MHC-hybrid fibres, co-expressing three MHC isoforms (fibre types T+t1+t3, T+t3+t2 and t1+t3+t2) (Fig. 5.8). The MHC isoforms expressed in each fibre type and the number of fibres belonging to each MHC-based fibre type group are shown in

Table 5.4. Within each group of hybrids, fibres that co-expressed the same combination of MHC isoforms could differ quite markedly with respect to their relative proportion (see for example the two hybrid fibres t2+t3 shown in Fig. 5.9).

It is interesting to note that the population of fibres examined in this work (136 fibres dissected from RA muscles of old adult toads) comprised 30% pure fibres, twice as many (66%) 2MHC-hybrid fibres and only 4% 3 MHC-hybrid fibres. No pure type 1 (t1) fibres, hybrid T+t2, hybrid t1+t3, hybrid T+t1+t2 fibres or 4 MHC-hybrid fibres were observed in this study. The relative proportion of each fibre type classified on the basis of MHC composition is presented in Fig. 5.10.

**Table 5.4. The MHC isoform composition of each fibre type group in RA muscle.**

<b>Fibre type</b>	<i>n</i>	<b>MHC composition</b>
T	6	BmHCT
t2	12	BmHC2
t3	23	BmHC3
<i>2 MHC-hybrid group</i>		
T+t1	18	BmHCT + BmHC1
T+t3	4	BmHCT+BmHC3
t1+t2	19	BmHC1+BmHC2
t2+t3	49	BmHC2+BmHC3
<i>3 MHC- hybrid group</i>		
T+t1+t3	1	BmHCT+BmHC1+BmHC3
T+t3+t2	1	BmHCT+BmHC3+BmHC2
t1+t3+t2	3	BmHC1+BmHC3+BmHC2



**Figure 5.7** Representative electrophoretic profile of MHC isoforms detected in RA muscle homogenates.

Lane 1: juvenile toads (11-14 g); lane 2: old adult toads (200-450 g).

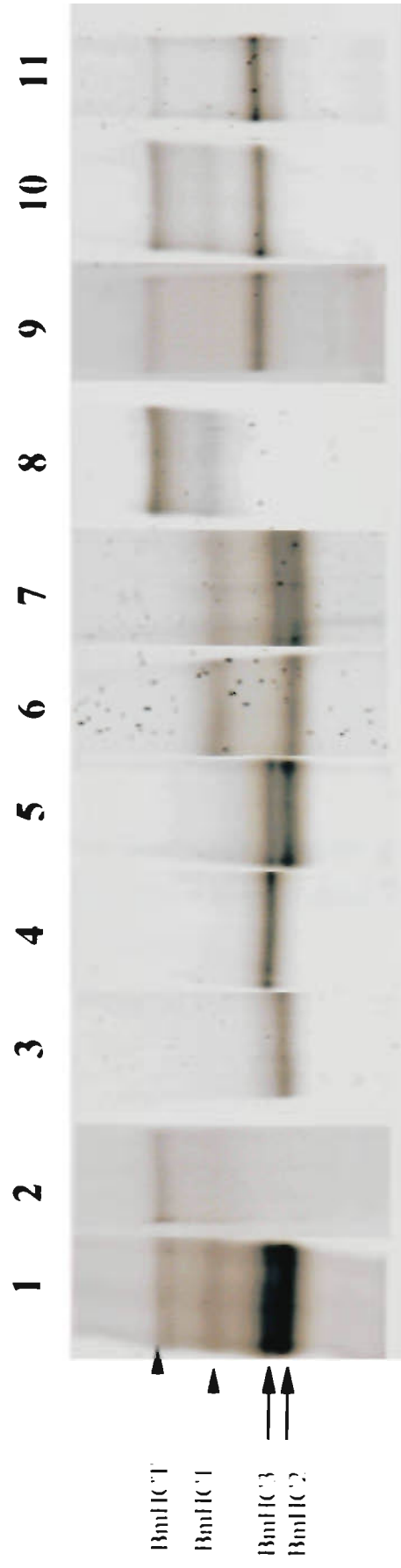


**Figure 5.8** Representative electrophoretic profile of MHC isoforms in 10 discrete fibre type populations identified among 136 fibres of RA muscles.

Lane 1: MHC isoform composition of muscle homogenate from juvenile toad containing 4 different MHC isoforms BmlHC1, BmlHC1, BmlHC3 and BmlHC2. Lane 2: type T fibre; lane 3: type 2 fibre; lane 4: type 3 fibre; lane 5: type (13)(2) fibre; lane 6: type (11)(2) fibre; lane 7: type (11)(3)(2) fibre; lane 8: type (T)(1) fibre; lane 9: type (T)(1)(3) fibre and lane 10: type (T)(1)(3)(2) fibre.

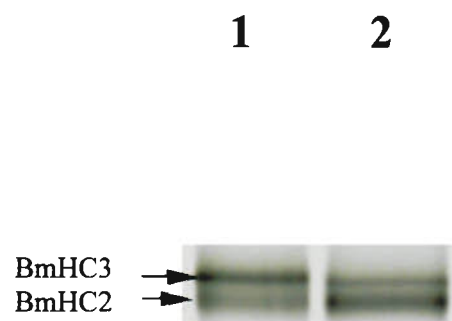
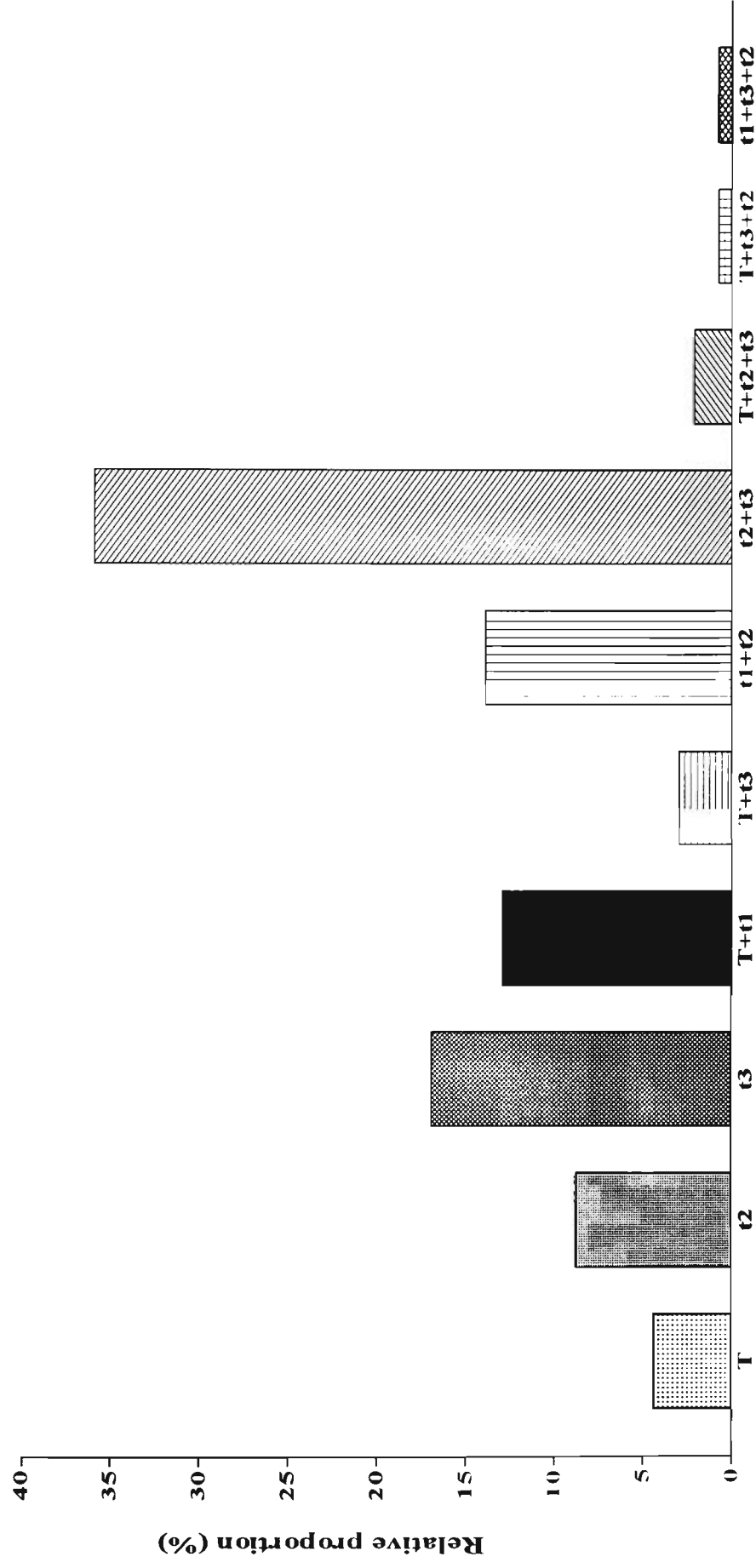


**Figure 5.9** Electrophoretogram of MHC composition expressed in t2+t3 hybrid fibres. Lane 1: t3+t2 hybrid fibre in which BmHC3 is dominant. Lane 2: t2+t3 hybrid fibre in which BmHC2 is dominant.



Fibre type based on MHC isoform composition

**Figure 5.10** Bar graph illustrating the relative proportion of 10 different fibre type populations classified based on MHC isoform composition.

**T:** pure tonic fibre; **t2:** pure type 2 fibre; **t3:** pure type 3 fibre; 2MHC isoform hybrid fibres: **T+t1**, **T+t3**, **t1+t2**, **t2+t3**; 3MHC isoform hybrid fibres: **T+t1+t3**, **T+t3+t2**, **t1+t3+t2**. The MHC isoform composition of these fibre types is given in Table 5.4.

## 5.4 DISCUSSION

### 5.4.1 SEPARATION OF MHC ISOFORMS IN TOAD SKELETAL MUSCLES BY A NOVEL ALANINE-SDS-PAGE METHOD

The most significant finding of the present study is that the number of MHC isoforms in IF and SAR muscles from *Bufo marinus* detected by a novel Alanine-SDS-PAGE method is equal to the number of fibre types determined earlier by Hoh *et al.* (1994) using conventional histochemical and immuno-histochemical methods. This strongly suggests that the Alanine-SDS-PAGE protocol described here is more effective in separating amphibian MHC isoforms than that used by Lutz *et al.* (1998a&b) in two recent studies of MHC expression in *Rana pipiens*, because the latter protocol distinguished only three MHC isoform bands for muscles known to contain four immuno-identified fibre types and also four MHC cDNAs.

In their studies on MHC expression in skeletal muscles of *Rana pipiens*, Lutz *et al.* (1998a&b) used the SDS-PAGE protocol of Talmadge & Roy (1993), a heavily modified version of Laemmli's discontinuous gel system (1970). One of the most notable characteristics of the Talmadge & Roy's electrophoretic procedure is its use of the trailing ion glycine in the separating gel as well as in the running buffer. In my research experiments, the original protocol of Talmadge & Roy was highly unsatisfactory. However, after a number of minor modifications, one electrophoretic protocol which separated four protein bands in a PYR muscle homogenate was obtained but showed a very low level of reproducibility. The reproducibility of the

gel system was greatly increased, without notable loss of resolving power, following the replacement of glycine with alanine (which has identical  $pK_a$  and  $pI$  values, but a slightly higher molecular size than glycine) both in the running buffer and in the separating gel. The effectiveness of the Alanine-SDS-PAGE system to produce well separated, well visualized and relatively sharp MHC bands was further increased through the systematic optimisation of alanine concentration in the separating gel and the running buffer and of glycerol concentration in the separating gel.

All protein bands detected by the Alanine-SDS-PAGE system in the IF, PYR, CRU and SAR muscle homogenates of the cane toad were deemed to be MHC isoform bands rather than other high molecular weight proteins with an electrophoretic mobility similar to myosin, because they were also detected in myosin extracts prepared from the contralateral muscle and in single muscle fibres from RA. It was not possible to compare the electrophoretic mobilities of all cane toad and all rat MHC isoforms on the same gel system, because the gels that separated well all MHC isoforms of rat muscles did not resolve all MHC isoforms of cane toad muscles and vice versa. Despite their limitations, these gels were good enough, however, for one to observe that toad and rat MHC isoforms have different electrophoretic mobilities on SDS-PAGE.

#### *5.4.2 IDENTIFICATION OF MHC ISOFORMS EXPRESSED IN IF, PYR, CRU AND SAR*

To establish the identities of the MHC bands detected in homogenates and myosin extracts prepared from cane toad skeletal muscles, I used the previously published

information on the fibre type composition of PYR muscle from *Xenopus laevis* (Orkand *et al.*, 1978) and on the fibre type composition of IF and SAR muscles from *Bufo marinus* at different stages of post-metamorphic growth (Hoh *et al.*, 1994). For example, the band with the lowest electrophoretic mobility on Alanine-SDS-PAGE gels (initially referred to as band A) was identified as the tonic MHC isoform (BmHCT) because it was detected in PYR (a muscle which in *Xenopus laevis* contains a sizeable proportion of tonic fibres), but was not detected in SAR (a muscle reported to lack tonic fibres in all amphibian muscles examined so far). Following a similar reasoning strategy, the MHC band which in IF displayed a decrease in the relative proportion with animal maturation was identified as BmHC1 because, according to Hoh *et al.* (1994), IF muscles in large, adult cane toads contain a much lower proportion of type 1 fibres than in very young toads.

On Alanine-SDS-PAGE, the MHC isoforms (BmHC1, BmHC2, BmHC3 and BmHCT) detected in the cane toad skeletal muscles migrated in the order BmHCT < BmHC1 < BmHC3 < BmHC2. In contrast, the MHC isoforms detected in frog skeletal muscles by Lutz *et al.* (1998a&b), using Talmadge & Roy's gel system, migrated in the order type 2 < type 1 + tonic < type 3. This discrepancy in the relative mobility of MHC isoforms between the present study and that of Lutz *et al.* could be due to interspecies-related differences in the structure of functionally similar proteins, to misidentification of protein bands, or to gel-system-related differences in the migration of structurally similar proteins. In this context, it is worth noting that the relative mobility of cardiac MHC isoforms from several mammalian species (Reiser & Kline, 1998) was found to be markedly affected by the SDS-PAGE system.

#### 5.4.3 DEVELOPMENTAL CHANGES IN THE MHC COMPOSITION OF IF, PYR, CRU AND SAR MUSCLES

Quantitative analysis of fibre type composition in the IF muscle of the cane toad, which was carried out by Hoh *et al.* (1994) at four different stages of post-metamorphic growth (15 – 25 g; 25 – 30 g; 70 – 85 g and 180 – 200 g), has shown a consistent decrease in the proportion of type 1 fibres and an increase in the type 2 fibres with animal maturation. This change was regarded by the authors as evidence of the developmental transformation of type 1 into type 2 fibres. In agreement with the data of Hoh *et al.* (1994), it was found that the growth of the cane toad from an early post-metamorphic stage (bw < 1 g) to a very large size (220 – 250 g) was accompanied, in IF muscles, by a significant decrease in the proportion of the BmHC1 isoform and an increase in the proportion of the BmHC2 isoform. Interestingly, a similar change in the relative proportion of BmHC1 and BmHC2 isoforms with post-metamorphic growth was detected in the other three muscles of the cane toad examined in the present study, viz PYR, CRU and SAR. However, the rate of change in the relative proportion of the two isoforms during the transition of the toad from the juvenile stage (12 – 14 g) to the junior stage (30 – 50 g) was higher in IF and SAR than in PYR and CRU. This difference in the rate of change is noteworthy if one considers that the aforementioned transition has been related to a change from the moist, juvenile habitat to the dry adult habitat (Freeland & Kerin, 1991), because it indicates that the responsiveness of MHC isoform gene expression to environmental influences is muscle-specific. The third MHC isoform, BmHC3 was present in small proportions in all muscles examined here, but the tonic fibre (BmHCT) was detected

only in IF, PYR, and CRU. Post-metamorphic growth was also accompanied by small increase in the proportion of the BmHC3 isoform in all four muscles, but did not affect consistently the proportion of BmHCT. Taken together, these data indicate that in the skeletal muscle of the cane toad, the degree of development-related plasticity of MHC isoform expression is isoform-specific with the molecular forms contained in faster twitch fibres being more prone to structural change than those contained in the slower twitch and tonic fibres.

#### 5.4.4 MHC ISOFORM COMPOSITION OF SINGLE MUSCLE FIBRE SEGMENTS

Using a battery of specific antibodies raised against myosins, Hoh *et al.* (1994) distinguished in hindlimb skeletal muscles of the cane toad five different fibre types: types 1, 2 and 3 (twitch fibres), type 1/2 (transitional fibres having immunohistochemical characteristics of type 1 and 2 fibres) and one tonic fibre type. In the present study, it was found, using microelectrophoretic analysis of MHC isoform composition in single fibre segments, that toad *rectus abdominis*, a trunk muscle, contained at least ten different fibre types, three of which expressed only one MHC isoform and seven which co-expressed 2 or 3 MHC isoforms. The difference between the number of fibre types found in toad hindlimb muscles by Hoh *et al.* (1994) and the number of fibre types found in a toad trunk muscle in this study is more likely to be due to the different fibre typing methods used in the two studies than to major differences in the fibre type composition of the two muscles.

A large proportion of the fibres examined in this work co-expressed two or three MHC isoforms. The presence in amphibian skeletal muscles of hybrid fibres co-expressing two or three MHC isoforms has also been reported by Lutz *et al.* (1998) who studied MHC isoform composition in 76 single fibre segments microdissected from *tibialis anterior* (TA) muscles of *Rana pipiens*. Interestingly, the proportion of hybrid fibres detected by Lutz *et al.* (1998a) in the population of TA fibres (75%) was very close to that found in the population of RA fibres examined in this study (70%). Neither the studies of Lutz *et al.* (1998a&b) nor the present study revealed co-expression of four MHC isoforms.

Only three (T, t2 and t3) of the four expected pure fibre types were found among the 136 fibres dissected from RA muscles of old adult toads. The absence of pure type 1 fibres (t1) can be easily explained if one considers the very low proportion of BmHC1 isoform displayed by ALANINE-SDS gels of whole tissue homogenates.

The hybrid fibres dissected from toad RA muscles expressed only seven out of ten possible combinations MHC isoforms (6 and 4 combinations for co-expression of two MHC isoforms and three MHC isoforms, respectively). The combinations of MHC isoforms that were *not detected* in the hybrid fibres examined in this work include T+t2, t1+t3, T+t1+t2. Given that the population of hybrid fibres detected here included T+t1, T+t1+t3 and T+t3+t2 fibres, it is unlikely that the absence of T+t2, t1+t3, T+t1+t2 fibres is due to the inability of the tonic MHC isoform to be co-expressed with some twitch MHC isoform or the inability of BmHC1 to be co-expressed with BmHC3. Therefore, the most likely explanation for the absence of

T+t<sub>2</sub>, t<sub>1</sub>+t<sub>3</sub>, T+t<sub>1</sub>+t<sub>2</sub> fibre types in the RA muscle of old adult toads is that their relative proportions in this muscle was too low such that no fibre of these types was included in the population examined.

## Concluding remarks

Shortly after starting this study it became clear that neither of the two methods deemed to be essential for addressing the research questions listed in section 1.4 was available in the scientific literature. As a result, efforts were initially directed towards the development of the required methods: one that would allow determination of glycogen content and functional parameters in the same muscle fibre preparation and the other that would allow visualisation of all four MHC isoforms expected (based on published fibre type composition) to be expressed in skeletal muscles of cane toad. Details of the two methods viz. the rapid microfluorometric method for glycogen analysis in segments of freshly dissected, mechanically skinned muscle fibres and the Alanine-SDS-PAGE system for analysis of MHC isoforms in toad skeletal muscles are given in Chapters 2, 3 and 5.

Glycogen analyses in single skeletal muscle fibres of cane toad, performed with the newly developed method, have led to the following novel observations: (i) skeletal muscle fibres of the cane toad contain two pools of glycogen, distinguishable by solubility in aqueous solutions of neutral or slightly acidic pH (pH 5), (ii) mechanically skinned fibre preparations retain a large proportion (> 75%) of fibre glycogen and endogenous glycogenolytic enzymes, such that upon exposure of the preparation to high  $\text{Ca}^{2+}$  or to  $\text{SR-Ca}^{2+}$  released by chemical depolarisation of the T-system, endogenous glycogen is rapidly broken down, (iii) glycogen content varies greatly between fibres of the same muscle and between fibres from different toads. (iv) fibre glycogen content is lower in winter toads than in summer toads, (v) the

capacity of a fibre to respond to T-system depolarisation induced activation is positively correlated with the initial concentration of fibre glycogen and (vi) fibre capacity to respond to T-system depolarisation induced activation decreases dramatically in parallel with fibre glycogen breakdown despite the presence in the bathing medium of ample amounts of creatine phosphate and ATP. Two important conclusions emerging from these findings are that *the relationship between the E-C coupling capacity of an amphibian skeletal muscle fibre and its glycogen content is not based on the role of glycogen as an energy store* and that *the mechanically skinned fibre preparation is well suited to study the regulation of endogenous glycogenolytic enzymes.*

Alanine-SDS-PAGE analyses of MHC isoform composition in four skeletal muscles of the cane toad, at different stages of development, and in single muscle fibre segments dissected from one type of adult skeletal muscle, showed that: (a) the four MHC isoforms expected to be present in skeletal muscles of the cane toad (one tonic and three twitch) can be separated electrophoretically and can be visualised with available staining methods, (b) skeletal muscles of the cane toad display age-related plasticity with respect to MHC isoform expression and (c) *Rectus abdominis* muscle of the cane toad is a very heterogenous tissue, containing at least 3 types of pure fibres and 7 types of hybrid fibres. Two important conclusions, which can be drawn from this part of the study are that, *like mammalian muscles, amphibian muscles are both very heterogenous and plastic tissues*, and that *the Alanine SDS-PAGE gel system can be used in studies concerned with the physiological role of protein isoforms in amphibian muscle.*

## Bibliography

ADAMO, K. B. & GRAHAM, T. E. (1998) Comparison of traditional measurements with macroglycogen and proglycogen analysis of muscle glycogen. *J. Appl. Physiol.* **84**(3), 908-13.

ALONSO, M. D., LOMAKO, J., LOMAKO, W. M. & WHELAN, W. J. (1995) A new look at the biogenesis of glycogen. *FASEB J.* **9**, 1126-37.

ASHLEY, C. C. & MOISESCU, D. G. (1977) Effect of changing the composition of the bathing solutions upon the isometric tension-pCa relation. *J. Physiol.* **270**, 627-52.

BAGSHAW, C. R. (1993) Muscle contraction. London: Chapman & Hall, 2<sup>nd</sup> ed. pp. 31-57.

BÁRÁNY, M. (1967) ATPase activity of myosin correlated with speed of muscle shortening. *J. Gen. Physiol.* **50**, 197-218.

BAYLOR, S. M., CHANDLER, W. K. & MARSHALL, M. W. (1983) Sarcoplasmic reticulum calcium release in frog skeletal muscle fibres estimated from arsenazo III calcium transients. *J. Physiol.* **344**, 625-666.

BERGMEYER, H. U., HORDER, M. & MARKOWETZ, D. (1983) Reliability of laboratory results and practicability of procedures. In *Methods of Enzymatic Analysis* (edited by BERMEYER, H. U., BERMEYER, J. & GRABLE, M.) PP. 21-39. Weinheim: Verlag Chemie.

BERGSTRÖM, J., HERMANSEN, L., HULTMAN, E. & SALTIN, B. (1967) Diet, muscle glycogen and physical performance. *Acta Physiol. Scand.* **71**, 140-50.

BIRKS, R., HUXLEY, H. E. & KATZ, B. (1960) The fine structure of the neuromuscular junction of the frog. *J. Physiol.* **150**, 134-44.

BORTOLOTTO, S., STEPHENSON, D. G. & STEPHENSON, G. M. M. (1999) Fibre type populations and  $\text{Ca}^{2+}$ -activation properties of single fibres in soleus muscle from SHR and WKY rats. *Am. J. Physiol.* **276**, C628-637.

BRADFORD, M. (1976) A rapid and sensitive method for the quantitation of the microgram quantities of protein utilising the principle of protein-dye binding. *Anal. Biochem.* **72**, 248-58.

BROWN, D. H. (1994) Glycogen metabolism and glycolysis in muscle. In *Myology* (edited by ENGLEL, A. G. & FRANZINI-ARMSTRONG, C.) pp. 648-65. New York: McGraw Hill.

CHIN, E. R. & ALLEN, D. G. (1997) Effects of reduced muscle glycogen concentration on force,  $\text{Ca}^{2+}$  release and contractile protein function in intact mouse skeletal muscle. *J. Physiol.* **498**, 17-29.

CHRAMBACH, A. (1985) The practice of quantitative gel electrophoresis. Deerfield Beach, FL: Weiheim, p182.

CLAUSEN, T. (1996) The  $\text{Na}^+$ ,  $\text{K}^+$  pump in skeletal muscle: quantification, regulation and functional significance. *Acta. Physiol. Scand.* **156**, 227-36.

CONLEE, R. K. (1987) Muscle glycogen and exercise endurance: a twenty-year perspective. *Exer. Sport. Sci. Rev.*, **15**:1-28. Review.

CONNETT, R. J. & SAHLIN, K. (1996) Control of glycolysis and glycogen metabolism. In *Exercise: Regulation and Integration of multiple systems* (edited in

ROWELL, L. B. & SHEPHERD, J. T.). Oxford: Oxford University Press, UK., pp. 870-911.

- CRAIG, R. (1994) The structure of the contractile filaments. In *Myology* (edited by ENGLEL, A. G. & FRANZINI-ARMSTRONG, C.) pp. 134-70. New York: McGraw Hill.
- CUENDA, A., NOGUES, M., GUTIÉRREZ-MERINO, C. & de MEIS, L. (1993) Glycogen phosphorolysis can form a metabolic shuttle to support  $\text{Ca}^{2+}$  uptake by sarcoplasmic reticulum membranes in skeletal muscle. *Biochem. Biophys. Res. Com.* **196**(3), 1127-33.
- DANFORTH, W. H. & HELMREICH, E. (1964) Regulation of glycolysis in muscle I. The conversion of phosphorylase b to phosphorylase a in frog sartorius muscle. *J. Biol. Chem.* **239**, 3133-38.
- DESMEDT, J. E. (1953) Electrical activity and intracellular sodium concentration in frog muscle. *J. Physiol.* **121**, 191-205.
- DESPOPOULOS, A. & SILBERNAGL, S. (1991) Colour atlas of physiology. Stuttgart: Georg Thieme Verlag, 4<sup>th</sup> ed., p.34.
- DiMAURO, S., TROJABORG, W., GAMBETTI, P. & ROWLAND, L. P. (1971) Binding of enzymes of glycogen metabolism to glycogen in skeletal muscle. *Arch. Biochem. Biophys.* **144**, 413-22.
- DUNLAP, D. G. (1960) The comparative myology of the pelvic appendage in the salientia. *J. Morphol.* **106**, 1-76.
- EBASHI, S. & ENDO, M. (1968)  $\text{Ca}^{2+}$  ion and muscle contraction. *Progr. Biophys. Mol. Biol.* **18**, 123-83.
- EDMAN, K. A. P., REGGIANI, C., SCHIAFFINO, S. & KRONNIE, G. TE. (1988) Maximum velocity of shortening related to myosin isoform composition in frog skeletal muscle fibres. *J. Physiol.* **395**, 679-94.

ENTMAN, M. L., KESLENSKY, S. S., CHU, A. & VAN WINKLE, W. B. (1980) The sarcoplasmic reticulum-glycogenolytic complex in mammalian fast-twitch skeletal muscle. Proposed *in vitro* counterpart of the contraction-activated glycogenolytic pool. *J. Biol. Chem.* **255**, 6245-52.

FALK, G. & FATT, P. (1964) Linear electrical properties of striated muscle fibres observed with intracellular electrodes. *Proc. Roy. Soc. B*, **160**, 69-123.

FAVERO, T. G. (1999) Sarcoplasmic reticulum  $Ca^{2+}$  release and muscle fatigue. *J. Appl. Physiol.* **87**(2), 471-83.

FITTS, R. H. (1994) Cellular mechanism of muscle fatigue. *Physiol. Rev.* **74**, 49-94.

FRANZINI-ARMSTRONG, C. (1994) The sarcoplasmic reticulum and the transverse tubules. In *Myology* (edited by ENGEL, A. G. & FRANZINI-ARMSTRONG, C.). New York: McGraw Hill Inc., 2<sup>nd</sup> ed., pp. 176-99.

FRANZINI-ARMSTRONG, C. & JORGENSEN, A. O. (1994) Structure and development of E-C coupling units in skeletal muscle. *Annu. Rev. Physiol.* **56**, 509-34.

FREELAND, W. J. & KERIN, S. H. (1991) Ontogenetic alteration of activity and habitat selection by *Bufo marinus*. *Wildl. Res.* **18**, 431-43.

FRIDÉN, J., SERGER, J. & EKBLÖM, B. (1989) Topographical localisation of muscle glycogen: an ultrahistochemical study in the human vastus lateralis. *Acta Physiol. Scand.* **135**, 381-91.

FRYER, M. W. & STEPHENSON, D. G. (1996) Total and sarcoplasmic reticulum calcium contents of skinned fibres from rat skeletal muscle. *J. Physiol. (London)* **493**, 357-70.

FRYER, M. W., OWEN, V. J., LAMB, G. D. & STEPHENSON, D. G. (1995) Effects of creatine phosphate and Pi on Ca<sup>2+</sup> movements and tension development in rat skinned skeletal muscle fibres. *J. Physiol.* **482**, 123-40.

GALBO, H., HOLST, J. J. & CHRISTENSEN, H. J. (1979) The effect of different diets and of insulin on the hormonal response to prolonged exercise. *Acta Physiol. Scand.* **107**, 19-32.

GARRETT, R. H. & GRESHAM, C. M. (1995) *Biochemistry*. New York: Harcourt Brace College Publisher, Chapters 18 & 21.

GEDDES, R. & SOO PING CHOW, J. C. K. (1994) Differing pattern of carbohydrate metabolism in liver and muscle. *Carbohydrate Res.* **256**, 139-47.

GILLY, W. F. (1975) Slow fibres in the frog cruralis muscle. *Tissue & Cell*, **7**(1), 203-210.

GOLDSTEIN, M. A., MURPHY, D. L., VAN WINKLE, W. B. & ENTMAN, M. L. (1985) Cytochemical studies of a glycogen-sarcoplasmic reticulum complex. *J. Muscle. Res. Cell. Motility.* **6**, 177-87.

GRAY, E. G. (1957) The spindle and extrafusil innervation of a frog muscle. *Proc. Roy. Soc. (Lond.)*, **145**(B), 416-30.

HALKJAER-KRISTENSEN, J. & INGEMANN-HANSEN, T. (1979) Microphotometric determination of glycogen in single fibres of human quadriceps muscle. *Histochem. J.* **11**, 629-38.

HAMES, B. D. & RICKWOOD, D. (1990) *Gel Electrophoresis of Proteins – A Practical Approach*. Oxford University Press: New York, 2<sup>nd</sup> Ed, p.31.

HÄMÄLÄINEN, N. & PETTE, D. (1995) Patterns of myosin isoforms in mammalian skeletal muscle fibres. *Microsc. Res. Tech.* **30**, 381-89.

HAN, J.W., THIELECZEK, R., VARSÁNYI, M. & HEILMEYER, Jr., L. M. G. (1992) Compartmentalised ATP synthesis in skeletal muscle triads. *Biochem.* **31**, 377-84.

HEILMEYER, Jr., L. M. G., MEYER, F., HASCHKE, R. H. & FISCHER, E. H. (1970) Control of phosphorylase activity in a muscle glycogen particle. II. Activation by calcium. *J. Biol. Chem.* **245**(24), 6649-56.

HESS, A. (1970) Vertebrate slow muscle fibres. *Physiol. Rev.* **50**(1), 40-62.

HESS, A. (1960) The structure of extrafusal muscle fibres in the frog and their innervation studied by the cholinesterase technique. *Am. J. Anat.* **107**, 129-51.

HINTZ, C. S., CHI, M. M-Y., FELL, R. D., IVY, J. L., KAISER, K. K., LOWRY, C. V. & LOWRY, O. H. (1982) Metabolite changes in individual rat muscle fibres during stimulation. *Am. J. Physiol.* **242**, C218-228.

HINTZ, C. S., LOWRY, C. V., KAISER, K. K., McKEE, D. & LOWRY, O. H. (1980) Enzyme levels in individual rat muscle fibres. *Am. J. Physiol.* **239**, C58-65.

HOCHSTRASSER, D. F., PATCHONIK, A. & MERRYL, C. R. (1988) Development of polyacrylamide gels that improve the separation of proteins and their detection by silver staining. *Anal. Biochem.* **173**, 412-23.

HODGKIN, A. L. & NAKAJIMA, S. (1972) Analysis of the membrane capacity in frog muscle. *J. Physiol. (Lond.)* **221**, 121-136.

HOH, J. F. Y., WAH, M. S. Y., EVERETT, A. W. & HUGHES, S. (1994) Plasticity of twitch muscle fibres of the toads, *Bufo marinus*, during adaptation to the seasons and to post-metamorphic life. *BAM* **4**, 369-80.

- HOROWICZ, P. (1994) Excitation-Contraction coupling in skeletal muscle. In *Myology* (edited by ENGEL, A. G. & FRANZINI-ARMSTRONG, C.). New York: McGraw Hill Inc., 2<sup>nd</sup> ed., pp.423-38.
- HOYLE, G., McNEIL, P. A. & SELVERSTON, A. I. (1973) Ultrastructure of barnacle giant muscle fibres. *J. Cell. Biol.* **56**, 74-91.
- HUANG, M. T., LEE, C. F., LIN, R. F. & CHEN, R. J. (1996) The exchange between proglycogen and macroglycogen and the metabolic role of the protein-rich glycogen in rat skeletal muscle. *J. Clin. Invest.* **99**(3), 501-05.
- HUXLEY, A. F. (1974) Muscular contraction. *J. Physiol.* **243**, 1-43.
- HUXLEY, H. E. (1964) Evidence for continuity between the central elements of the triads and extracellular space in frog sartorius muscle. *Nature (Lond)*. **202**, 1067-71.
- JANSSON, E. (1981) Acid soluble and insoluble glycogen in human skeletal muscle. *Acta Physiol. Scand.* **113**, 337-40.
- KATO, T., BERGER, S. J., CARTER, J. A. & LOWRY, O. H. (1973) An enzymatic cycling method for Nicotinamide-Adenine Dinucleotide with malic and alcohol dehydrogenases. *Anal. Biochem.* **53**, 86-97.
- KELLY, A. M. & RUBINSTEIN, N. A. (1994) The diversity of muscle fibre types and its origin during development. In *Myology* (edited by ENGEL, A. G. & FRANZINI-ARMSTRONG, C.). New York: McGraw Hill Inc., 2<sup>nd</sup> ed., pp. 119-23.
- KUFFFLER, S. W. & GERARD, R. W. (1947) The small-nerve motor system to skeletal muscle. *J. Neurophysiol.* **10**, 383-94.

- KUFFFLER, S. W. & VAUGHAN WILLIAMS, E. M. (1953) Small-nerve junctional potentials. The distribution of small motor nerves to frog skeletal muscle, and the membrane characteristics of the fibres they innervate. *J. Physiol.* **121**, 289-317.
- LAEMMLI, U. K. (1970) Cleavage of structural proteins during the assembly of the head of bacteriophage T4. *Nature (London)*, **227**, 680-85.
- LAMB, G. D. & STEPHENSON, D. G. (1996) Effects of FK506 and rapamycin on excitation-contraction coupling in skeletal muscle fibres of the rat. *J. Physiol.* **494**, 569-576.
- LAMB, G. D. & STEPHENSON, D. G. (1991) Effect of  $Mg^{2-}$  on the control of  $Ca^{2-}$  release in skeletal muscle fibres of the toad. *J. Physiol.* **434**, 507-28.
- LAMB, G. D. & STEPHENSON, D. G. (1990) Calcium release in skinned muscle fibres of the toad by transverse tubule depolarisation or by direct stimulation. *J. Physiol.* **423**, 495-517.
- LAMB, G. D., JUNANKAR, P. R. & STEPHENSON, D. G. (1995) Raised intracellular  $[Ca^{2+}]$  abolished excitation-contraction coupling in skeletal muscle fibres of rat and toad. *J. Physiol.* **489**, 349-62.
- LAMB, G. D., RECUPERO, E. & STEPHENSON, D. G. (1991) Effect of myoplasmic pH on excitation-contraction coupling in skeletal muscle fibres of the toad. *J. Physiol.* **448**, 211-24.
- LÄNNERGREN, J. & HOH, J. F. Y. (1984) Myosin isoenzymes in single muscle fibres of *Xenopus laevis*: analysis of five different functional types. *Pros. R. Soc. Lond. B* **222**, 401-08.
- LÄNNERGREN, J. & SMITH, R. S. (1966) Types of muscle fibres in toad skeletal muscle. *Acta. Physiol. Scand.* **68**, 263-74.

- LEONG, P. & McLENNAN, D. H. (1998) Complex interactions between skeletal muscle ryanodine receptor and dihydropyridine receptor proteins. *Biochem. Cell. Biol.* **76**, 681-94.
- LOMAKO, J., LOMAKO, W. & WHELAN, W. (1991) Proglycogen: a low-molecular-weight form of muscle glycogen. *FEBS Lett.* **279**, 223-28.
- LOMAKO, J., LOMAKO, W., WHELAN, W., DOMBRO, R., NEARY, J. & NOREMBERG, M. (1993) Glycogen synthesis in the astrocyte: from glycogenin to proglycogen to glycogen. *FASEB J.* **7**, 1386-93.
- LOWRY, C. V., KIMMEY, J. S., FELDER, S., CHI, M. M-Y., KAISER, K. K., PASSONNEAU, P. N., KIRK, K. A. & LOWRY, O. H. (1978) Enzyme patterns in single human muscle fibres. *J. Biol. Chem.* **253**(22), 8269-77.
- LUFF, A. R. & PROSKE, U. (1976) Properties of motor units of the frog sartorius muscle. *J. Physiol.* **258**, 673-85.
- LUST, W. D., PASSONNEAU, J. V. & CRITES, S. K. (1975) The measurement of glycogen in tissues by amylo- $\alpha$ -1,4- $\alpha$ -1,6-glucosidase after the destruction of pre-existing glucose. *Anal. Biochem.* **68**, 128-131.
- LUST, W. D., FEUSSNER, G. K., BARBEHENN, E. K. & PASSONNEAU, J. V. (1981) The enzymatic measurement of adenine nucleotides and P-creatine in picomole amounts. *Anal. Biochem.* **110**, 258-66.
- LÜTTGAU, H. C. (1965) The effect of metabolic inhibitors on the fatigue of the action potential in single muscle fibres. *J. Physiol. (London)* **178**, 45-67.
- LUTZ, G. J., BREMMER, S., LAJEVARDI, N., LIEBER, R. L. & ROME, L. C. (1998a) Quantitative analysis of muscle fibre type and myosin heavy chain

distribution in the frog hindlimb: implications for locomotory design. *J. Muscle. Res. Cell. Motility*. **19**, 717-31.

LUTZ, G. J., CUIZON, D. B., RYAN, A. F. & LIEBER, R. L. (1998b) Four novel myosin heavy chain transcripts define a molecular basis for muscle fibre type in *Rana pipiens*. *J. Physiol.* **508**(3), 667-80.

MARTYN, D. A., COBY, R., HUNTSMAN, L. L. & GORDON, A. M. (1993) Force-calcium relations in skinned twitch and slow-tonic frog muscle fibres have similar sarcomere length dependencies. *J. Muscle. Res. Cell. Motility*. **14**, 65-75.

MEISSNER, G. (1994) Ryanodine receptor/ $\text{Ca}^{2+}$  release channels and their regulation by endogenous effectors. *Annu. Rev. Physiol.* **56**, 485-508.

MELÉNDEZ, R., MELÉNDEZ-HEVIA, E. & CASCANTE, M. (1997) How did glycogen structure evolve to satisfy the requirement for rapid mobilisation of glucose? A problem of physical constraints in structure building. *J. Mol. Evol.* **45**, 446-55.

MELÉNDEZ-HEVIA, E., WADDELL, T. G. & SHELTON, E. D. (1993) Optimisation of molecular design in the evolution of metabolism: the glycogen molecule. *Biochem. J.* **295**, 477-83.

MELÉNDEZ, R., MELÉNDEZ-HEVIA, E., MAS, F., MACH, J. & CASCANTE, M. (1998) Physical constraints in the synthesis of glycogen that influences its structural homogeneity: A two-dimensional approach. *Biophys. J.* **75**, 106-14.

MICHEL, R. N., COWPER, G., CHI, M. M-Y., MANCHESTER, J. K., FALTER, H. & LOWRY, O. H. (1994) Effects of tetrodotoxin-induced neural inactivation on single muscle fibre metabolic enzymes. *Am. J. Physiol.* **267**, C55-66.

MOISESCU, D. G. (1976) Kinetics of reaction in calcium-activated skinned muscle fibres. *Nat. New. Biol.* **262**, 610-13.

- MOISESCU, D. G. & THIELECZEK, R. (1978) Calcium and strontium concentration changes within skinned muscle preparations following a change in the external bathing solution. *J. Physiol.* **275**, 241-62.
- MONTERO-LOMELÍ, M. & MEIS, L. (1992) Glucose-6-phosphate and Hexokinase can be used as an ATP-regenerating system by the  $\text{Ca}^{2+}$ -ATPase of sarcoplasmic reticulum. *J. Biol. Chem.* **267**(3), 1829-33.
- MOSS, R. L., DIFFEE, G. M. & GREASER, M. L. (1995) Contractile proteins of skeletal muscle fibres in relation to myofibrillar protein isoforms. *Rev. Physiol. Biochem. Pharmacol.* **126**, 2-63.
- NASSAR-GENTINA, V., PASSONNEAU, J. V., VERGARA, J. L. & RAPAPORT, S. I. (1978) Metabolic correlates of fatigue and recovery from fatigue in single frog muscle fibres. *J. Gen. Physiol.* **72**, 593-606.
- NIELSEN, O. B. & OVERGAARD, K. (1996) Ion gradients and contractility in skeletal muscle: the role of active  $\text{Na}^+$ ,  $\text{K}^+$  transport. *Acta Physiol. Scand.* **156**, 247-56.
- NOGUES, M., CUENDA, A., HENAO, F. & GUTIÉRREZ-MERINO, C. (1996)  $\text{Ca}^{2+}$  uptake coupled to glycogen phosphorolysis in the glycogenolytic-sarcoplasmic reticulum complex from rat skeletal muscle. *J. Biosciences.* **51**, 591-98.
- OGAWA, Y., MURAYAMA, T. & KUREBAYASHI, N. (1999) Comparison of properties of  $\text{Ca}^{2+}$  release channels between rabbit and frog skeletal muscles. *Mol. Cell. Biochem.* **190**, 191-201.
- ORKAND, P. R., ORKAND, R. K. & COHEN, M. W. (1978) Distribution of acetylcholine receptors on *Xenopus laevis* slow muscle fibres determined by  $\alpha$ -bungarotoxin binding. *Neuroscience.* **3**, 435-46.

- OWEN, V. J., LAMB, G. D., STEPHENSON, D. G. & FRYER, M. W. (1997) Relationship between depolarisation-induced force responses and  $\text{Ca}^{2+}$  content in skeletal muscle fibres of rat and toad. *J. Physiol.* **498**, 571-86.
- PAGE, S. G. (1965) A comparison of the fine structure of frog slow and twitch muscle fibres. *J. Cell. Biol.* **26**, 477-97.
- PASSONNEAU, J. V. & LAUDERDALE, V. R. (1974) A comparison of three methods of glycogen measurement in tissues. *Anal. Biochem.* **60**, 405-12.
- PASSONNEAU, J. V. & LOWRY, O. H. (1993) *Enzymatic Analysis: A Practical Guide*. Totowa, NJ: Humana Press.
- PEACHEY, L. D. (1968) Muscle. *Annu. Rev. Physiol.* **30**, 401-40.
- PETTE, D. & STARON, R. S. (1997) Mammalian skeletal muscle types transitions. *Int. Rev. Cytol.* **170**, 143-223.
- PETTE, D. & STARON, R. S. (1990) Cellular and molecular diversities of mammalian skeletal muscle fibres. *Rev. Physiol. Biochem. Pharmacol.* **116**, 1-59.
- PETTE, D., PEUKER, H. & STARON, R. S. (1999) The impact of biochemical methods for single muscle fibre analysis. *Acta. Physiol. Scand.* **166**, 261-77.
- PORTER, K. R. & PALADE, G. E. (1957) Studies on the endoplasmic reticulum. III. Its form and distribution in striated muscle cells. *J. Biophys. Biochem. Cytol.* **3**, 269-300.
- REISER, P. J. & KLINE, W. O. (1998) Electrophoresis separation and quantitation of cardiac myosin heavy chain isoforms in eight mammalian species. *Am. J. Physiol.* **274**, H1048-53.

RÍOS, E. & STERN, M. D. (1997) Calcium in close quarter: Microdomain feedback in Excitation-Contraction coupling and other cell biological phenomena. *Annu. Rev. Biophys. Biomol. Struct.* **26**, 47-82.

ROSSI, A. M., EPPENBERGER, H. M., VOPLE, P., COTRUFO, R. & WALLIMANN, T. (1990) Muscle type MM creatine kinase is specifically bound to sarcoplasmic reticulum and can support  $\text{Ca}^{2+}$ -uptake and regulate ATP/ADP ratios. *J. Biol. Chem.* **265**, 5258-66.

ROSSINI, K., RIZZI, C., SANDRI, M., BRUSON, A. & CARRARO, U. (1995) High resolution sodium dodecyl sulfate-polyacrylamide gel electrophoresis and immunochemical identification of the 2X and embryonic myosin heavy chains in complex mixtures of isomyosins. *Electrophoresis*. **16**, 101-06.

ROWLERSON, A. M. & SPURWAY, N. C. (1988) Histochemical and immunohistochemical properties of skeletal muscle fibres from *Rana* and *Xenopus*. *Histochem. J.* **20**, 657-73.

ROWLERSON, A. M. & SPURWAY, N. C. (1985) How many fibre types in amphibian limb muscle? A comparison of *Rana* and *Xenopus*. *J. Physiol.* **358**, 78P.

RÜEGG, J. C. (1992) Calcium in muscle contraction: Cellular and Molecular physiology. Berlin: Spinger-Verlag, 2<sup>nd</sup> ed. pp. 3-57.

SAHYUN, M. (1931) On the carbohydrates of the muscles of the frog (*Rana pipiens*). *J. Biol. Chem.* **94**, 29-34.

SCHIAFFINO, S. & MARGRETH, A. (1969) Coordinated development of the sarcoplasmic reticulum and T-system during postnatal differentiation in rat skeletal muscle. *J. Cell. Biol.* **41**, 855-75.

SCHIAFFINO, S. & REGGIANI, C. (1996) Molecular diversity of myofibrillar proteins: gene regulation and functional significance. *Biol. Rev.* **76**(2), 371-423.

SCHIAFFINO, S. & REGGIANI, C. (1994) Myosin isoforms in mammalian skeletal muscle. *J. Appl. Physiol.* **77**(2), 493-501.

SCHIAFFINO, S. & SALVIATI, G. (1998) Molecular diversity of myofibrillar proteins: isoforms analysis at the protein and mRNA level. In *Methods in Cell Biology*, volume 52: Methods in muscle biology (edited by EMERSON, Jr., C. P. & SWEENEY, H. L.) pp 349-69. San Diego: Academic Press.

SCHNEIDER, M. F. (1994) Control of calcium release in functioning skeletal muscle fibres. *Annu. Rev. Physiol.* **56**, 463-84.

SHEARER, J., ADAMO, K., SALTIN, B., GREER, F., MARCHAND, I. & GRAHAM, T. E. (1998) Effects of exercise intensity on pro- and macroglycogen utilisation. *Can. J. Appl. Physiol.* **23**(5), 506 (Conference Proceedings).

SMITH, R. S. & OVALLE, Jr., W. K. (1973) Varieties of fast and slow extrafusal muscle fibres in amphibian hindlimb muscles. *J. Anatomy*: **116**, 1-24.

SPERRY, D. G. (1981) Fibre type composition and postmetamorphic growth of anuran hindlimb muscles. *J. Morphol.* **170**, 321-45.

STEPHENSON, D. G. (1996) Molecular cogs in *Machina carnis* (Proceedings: Australian Physiological and Pharmacological Society, September 1995). *Clin. Exp. Pharmacol. Physiol.* **23**, 898-907.

STEPHENSON, D. G. & WILLIAMS, D. A. (1981) Calcium activated force responses in fast- and slow-twitch skinned muscle fibres of the rat at different temperatures. *J. Physiol.* **317**, 281-302.

- STEPHENSON, D. G., LAMB, G. D. & STEPHENSON, G. M. M. (1998) Events of the excitation-contraction-relaxation (E-C-R) cycle in fast and slow-twitch mammalian muscle fibres relevant to muscle fatigue. *Acta Physiol. Scand.* **162**, 229-245.
- STEPHENSON, D. G., LAMB, G. D., STEPHENSON, G. M. M. & FRYER, M. W. (1995) Mechanisms of excitation-contraction coupling relevant to skeletal muscle fatigue. *Adv. Exp. Med. Biol.* **384**, 45-56.
- STETTEN, Jr., D. W. & STETTEN, M. R. (1960) Glycogen metabolism. *Physiol. Rev.* **40**, 505-37.
- STETTEN, M. R. KATZEN, H. M. & STETTEN, Jr., D. W. (1958) A comparison of the glycogens isolated by acid and alkaline procedures. *J. Biol. Chem.* **232**, 475-88.
- STRYER, L. (1995) *Biochemistry*. New York: Freeman, 3<sup>rd</sup> ed. Chapters 19 & 23.
- TALMADGE, R. J. & ROY, R. R. (1993) Electrophoresis separation of rat skeletal muscle myosin heavy chain isoforms. *J. Appl. Physiol.* **75**(5), 2337-40.
- TASAKI, I. & MIZUTANI, K. (1944) Comparative studies on the activities of the muscle evoked by two kinds of motor nerve fibres. Part I, Myographic studies. *Jap. J. Med. Sci. Biophys.* **10**, 237-44.
- TORTORA, G. J. & ANAGNOSTAKOS, N. P. (1990) *Principles of anatomy and physiology*. New York: Harper & Row Publishers, 6<sup>th</sup> ed., pp. 232-35.
- UHRÍK, B & SCHMIDT, H (1973) Distribution of slow muscle fibres in the frog *Rectus abdominis* muscle. An electron microscopical investigation. *Pflügers Arch.* **340**, 361-66.

VOET, D., VOET, J. & PRATT, C. W. (1999) *Fundamentals of Biochemistry*. New York: John Wiley & Sons Inc. 2<sup>nd</sup> ed. pp 428-34.

VOET, D. & VOET, J. (1995) *Fundamentals of Biochemistry*. New York: John Wiley & Sons Inc. 1st ed.

VØLLESTAD, N. K., SEJERSTED, O. M., BAHR, R., WOODS, J. J. & BIGLAND-RITCHIE, B. (1988) Motor drive and metabolic responses during repeated submaximal contractions in humans. *J. Appl. Physiol.* **64**, 1421-27.

WALKER, W. F. (1967) *Dissection of the frog*. San Francisco: W. H. Freeman.

WEISS, A. & LEINWAND, L. A. (1996) The mammalian myosin heavy chain gene family. *Annu. Rev. Cell Dev. Biol.* **12**, 417-39.

XU, K. Y. & BECKER, L. C. (1998) Ultrastructural localisation of glycolytic enzymes on sarcoplasmic reticulum vesicles. *J. Histochem. Cytochem.* **46**(4), 419-27.

XU, K. Y., ZWEIER, J. L. & BECKER, L. C. (1995) Functional coupling between glycolysis and sarcoplasmic reticulum Ca<sup>2+</sup> transport. *Circ. Res.* **77**, 88-97.





